

**KWAME NKURUMAH UNIVERSITY OF SCIENCE AND TECHNOLOGY,
KUMASI**

KNUST

**SHEAR STRENGTH PROPERTIES OF STRUCTURAL LIGHTWEIGHT
REINFORCED CONCRETE BEAMS AND TWO-WAY SLABS USING
PALM KERNEL SHELL COARSE AGGREGATES**

BY

ALEX ACHEAMPONG (BSc. Building Technology)

A Thesis submitted to the Department of Building Technology,
College of Art and Built Environment
in partial fulfillment of the requirements for the degree of

DOCTOR OF PHILOSOPHY in BUILDING TECHNOLOGY

NOVEMBER, 2015

DECLARATION

I hereby declare that this submission is my own work for the award of Doctor of Philosophy degree in Building Technology and that, to the best of my knowledge, it contains no materials previously published by another person or material which has been accepted for the award of any other degree of the university, except where reference has been made in the text.

Alex Acheampong
(Student)

.....
Signature Date

CERTIFIED BY:

Prof. J. Ayarkwa
(1st Supervisor)

.....
Signature Date

Prof. C. K. Kankam
(2nd Supervisor)

.....
Signature Date

Dr. B. K. Baiden
Head of Department

.....
Signature Date

ABSTRACT

In the last three decades, the use of Palm Kernel Shells (PKS) as coarse aggregate in concrete has continuously received increasing attention among researchers, especially in Africa. This is primarily due to its environmental and economic benefits. However, while considerable amount of research has been carried out to assist in understanding its concrete mix designs and associated mechanical properties, a limited amount of works have been carried out to assist in the current understanding with respect to its shear resistance. The main objective of this study was to investigate the shear strength properties of structural lightweight reinforced concrete shallow beams and two-way slabs using PKS coarse aggregates. A comparison between properties of PKS concrete and normal weight concrete (NWC) was made. The effect of types of cement on the mechanical properties of both PKS and NWC were also investigated. The materials phase of this research evaluated fresh concrete properties such as slump, and the key mechanical properties of hardened concrete, that is, compressive, flexural tensile strengths and density. The study employed a series of trial mixes, which resulted in casting and testing 216 cubes and 180 modulus of rupture beams at 7, 14, 21, 28, 56, and 90-days of curing, to obtain an optimum mix design. The third phase of the study consisted of testing 46 reinforced concrete beams to evaluate the flexural response of the reinforced PKS concrete and NWC beams, with and without shear reinforcement. The 46 beams consisted of 19 beams without shear reinforcement (15 PKS concrete and 4 NWC) and 27 beams with shear reinforcement (21 beams were cast with PKS and 6 beams were cast with granite aggregates). The variables of the third phase were the overall depth of the beams, longitudinal reinforcement, shear reinforcement, shear

span-to-depth ratio and modes of loading. The fourth phase of the study investigated the flexural response of eight two-way slabs (four slabs were cast with PKS and four were cast with granite aggregates). The main variables were concrete strength and the modes of loading. The study revealed that the physical and mechanical properties of the PKS aggregate are satisfactory for producing structural lightweight aggregate concrete. The 28day air-dry density of PKS concrete was within the range for structural LWAC. The 28day compressive strength of the concrete produced in this study was found to satisfy the minimum strength requirements of a structural concrete based on BS 8110-1 and ASTM C330. It was found that PKS concrete beams with and without shear reinforcement behaved in a similar manner to those of NWC beams based on the range of parameters tested, including the cracking modes. PKSC two-way slabs mostly failed as a result of punching shear. The study further revealed that the design equations of the British Standards Institute, American Concrete Institute and Eurocode 2 can be used to safely predict the shear capacity of PKS concrete beams with and without shear reinforcement. It is further concluded that PKS aggregates can be used in the production of LWC for structural applications in Ghana.

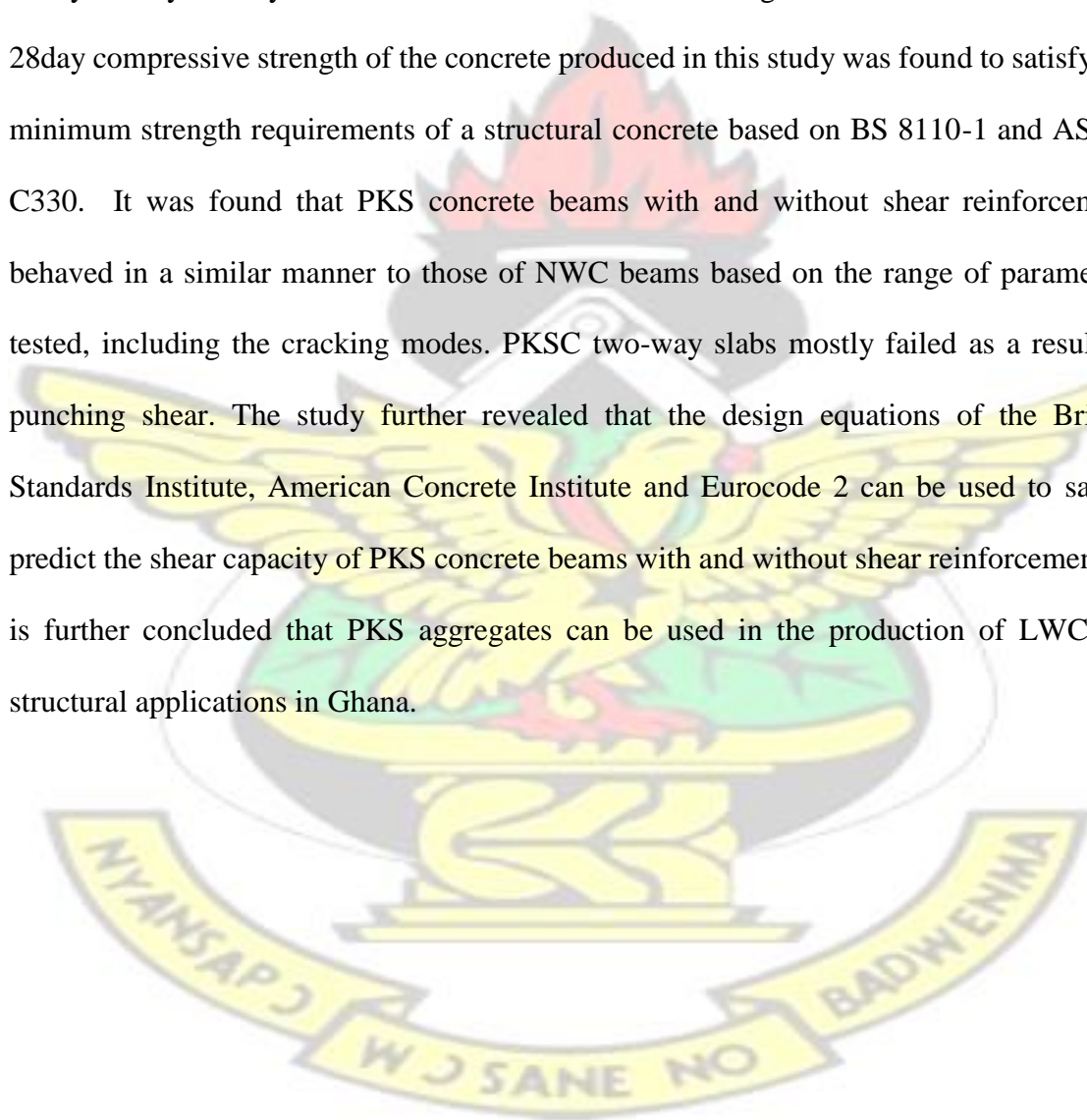


TABLE OF CONTENT

DECLARATION.....	II
ABSTRACT	III
TABLE OF CONTENT	V
LIST OF TABLES	XIII
LIST OF FIGURES	XV
NOMENCLATURE	XIX
ACKNOWLEDGEMENT	XXII
DEDICATION.....	XXIII
INTRODUCTION.....	1
1.1	1
1.2 PROPERTIES OF REINFORCED LWC	4
1.3	7
1.4 AIM	10
1.5	10
1.6 SIGNIFICANCE OF STUDY	11
1.7 OUTLINE OF THESIS	14

CHAPTER TWO

.....16

LITERATURE REVIEW

.....16

2.1	INTRODUCTION	16
2.2	DIFFERENCE BETWEEN NWC AND LWAC	16
2.3	LIGHTWEIGHT AGGREGATE CONCRETE (LWAC)	17
2.3.1	Key Hardened Properties of LWAC	18
2.3.1.1	Compressive strength	19
2.3.1.2	Tensile Strength	23
2.3.2	Constituents of Lightweight Concrete	24
2.3.2.1	Cement	25
2.3.2.2	Water	27
2.3.2.3	Admixtures	28
2.3.2.4	Aggregates	29
2.4	PROPERTIES OF LIGHTWEIGHT AGGREGATES	32
2.4.1	Shape	32
2.4.2	Flakiness and elongation indices	34
2.4.3	Texture	35
2.4.4	Grading/ Particle size distribution	36
2.4.5	Aggregate moisture content	38
2.4.6	Porosity and Water Absorption of Aggregates	40
2.5	PALM KERNEL SHELL CONCRETE	43

2.5.1 Oil Palm Tree Species	43
2.5.2 Species in Ghana	43
2.5.3 Make-up of Palm Kernel Shells	44
2.5.4 Chemical composition of PKS	48
2.5.5 Mechanical Properties of PKS Concrete	48
2.5.5.1 Compressive Strength of PKSC	48
2.5.5.2 Modulus of rupture	50
2.5.6 Structural behaviour of PKS Concrete beams	52
2.5.6.1 Flexural strength behaviour of PKS beams	52
2.5.6.2 Shear strength of PKS concrete beams	53
2.6 SHEAR TRANSFER MECHANISM IN BEAMS	55
2.6.1 Introduction	55
2.6.2 Influencing factors on the failure mechanisms	58
2.6.2.1 Effect of shear span-to-effective depth ratio, a/d	58
2.6.2.2 Effect of beam size	59
2.6.2.3 Concrete strength	60
2.6.2.4 Aggregate type	60
2.6.2.5 Percentage of Tension steel	61
2.6.3 Behaviour of Lightweight Aggregate Concrete in shear	61
2.6.4 Shear Cracking and crack width	62
2.6.5 Code Provisions against Shear Failure for lightweight concrete	64
2.6.5.1 Provisions in BS 8110 (1997)	64
2.6.5.2 Provisions in EC 2 (2004)	65
2.6.5.3 Provisions in ACI 318 – 08 (2008)	66

2.7	FLEXURAL THEORY OF RC TWO-WAY SLABS	68
2.6.6	69
	Summary	
CHAPTER THREE		
.....		70
MATERIALS AND METHODS		
.....		70
3.1	INTRODUCTION	70
3.2	TEST MATERIALS	70
3.2.1	Cement	70
3.2.2	Water	71
3.2.3	Superplasticizer	71
3.2.4	Normal weight aggregates	71
3.2.5	Palm kernel shell aggregates	72
3.3	CHEMICAL PROPERTIES OF PKS	73
3.4	PHYSICAL PROPERTIES OF THE COARSE AGGREGATES	73
3.4.1	Aggregate shape	74
3.4.2	Water absorption	74
3.4.3	Specific gravity	74
3.4.4	Aggregate impact value (AIV)	75
3.4.5	Aggregate crushing value (ACV)	75
3.3.6	Aggregate abrasion value (AAV)	76
3.5	MECHANICAL PROPERTIES	76
3.5.1	Mix Design	76

3.5.1.1	Mix	Proportions
.....	77
3.5.2	Workability of concretes	79
3.5.3	Laboratory batching and mixing	79
3.6	COMPRESSIVE STRENGTH AND DENSITY OF CONCRETE MIXES	80
3.6.1	Preparation of test Specimens	80
3.6.2	Curing of concrete cubes	81
3.6.3	Testing of concrete cubes	81
3.7	FLEXURAL TENSILE STRENGTH (MODULUS OF RUPTURE) OF PLAIN	82
.....	82
3.7.1	Preparation of test specimens	82
3.7.2	Testing of beams for flexural tensile strength	83
3.8	REINFORCED CONCRETE BEAMS	84
3.8.1	Design of the Reinforced Concrete Beam Specimens	84
3.8.2	Reinforcement details	89
3.8.3	Reinforced Concrete Specimen Identification	90
3.8.4	REINFORCED CONCRETE SPECIMEN PREPARATIONS	92
3.8.4.1	Materials	92
3.8.4.2	Reinforced Concrete Beam Preparation	93
3.8.4.3	Test Setup and instrumentation	94
3.9	REINFORCED CONCRETE TWO-WAY SLABS	95
3.9.1	Specimen details	95
3.9.2	Specimen Identification	96
3.9.3	Reinforced concrete specimen preparations	96

3.9.3.1 Materials	96
3.9.4.2 Reinforced Concrete Slab Preparation	97
3.9.4.3 Test Setup and instrumentation	98
CHAPTER FOUR	100
RESULTS AND DISCUSSION	100
4.1 INTRODUCTION	100
4.2 PHYSICAL PROPERTIES OF PKS AND NORMAL WEIGHT AGGREGATES	100
4.2.1 Particle size distribution	100
4.2.2 Aggregate shape	102
4.2.3 Water absorption	104
4.2.4 Specific gravity	104
4.2.5 Aggregate impact value (AIV)	105
4.2.6 Aggregate crushing value (ACV)	105
4.2.7 Aggregate Abrasion Value (AAV)	106
4.3 DRY DENSITY OF CONCRETES	107
4.4 EFFECT OF SUPERPLASTICIZER (SP) ON THE WORKABILITY OF PKS CONCRETE	109
4.5 COMPRESSIVE STRENGTH	113
4.5.1 Compressive strength with age of curing	113
4.5.2 Comparison of PKS-OPC and PKS-PLC concrete.....	114

4.5.3 Comparison of test results with minimum code provisions	116
4.5.4 Mode of failure of PKS concrete cubes	117
4.5.5 Compressive strength and density of the concrete cubes	120
4.6 TENSILE BEHAVIOUR OF THE CONCRETE	121
4.6.1 Tensile Failure beams	123
4.7 BEHAVIOUR OF REINFORCED CONCRETE BEAMS IN FLEXURE	124
4.7.1 Details of PKS concrete and NWC (Control) Beams	124
4.7.2 BEHAVIOUR OF BEAMS WITHOUT SHEAR REINFORCEMENT	127
4.7.2.1 General load-deflection behaviour of the beams	127
4.7.2.2 Crack Development Patterns of the Beams	131
4.7.2.3 Effect of longitudinal reinforcement, ρ_w on deflection and cracking of PKS beams	135
4.7.2.4 Effect of beam size on cracking patterns of PKS beams	141
4.7.2.5 Ultimate failure modes	143
4.7.2.6 Crack spacing and crack width	147
4.7.2.7 Shear resistance characteristics of PKSC/NWC beams	149
4.7.3 BEHAVIOUR OF BEAMS WITH SHEAR REINFORCEMENT	158
4.7.3.1 Load-deflection Characteristics of Beams with Shear Reinforcement	158
4.7.3.2 Cracking behaviour and crack width	160
4.7.3.3 Ultimate failure modes	166
4.7.3.4 Influence of shear reinforcement	169
4.7.3.5 Effect of shear span-to-effective depth ratio on deflection and cracking	

behaviour	172
4.7.3.6 Influence of parameters on reserve strength	178
4.7.3.7 Effect of loading on the behaviour of PKS beams	179
4.7.4 COMPARISON OF TEST RESULTS AND EXISTING EQUATIONS	185
4.7.4.1 Introduction	185
4.7.4.2 Beams without shear reinforcement	187
4.7.4.3 Beams with shear reinforcement	194
4.7.4.4 Serviceability Limit State	199
4.7.4.5 Summary	202
4.8 FLEXURAL BEHAVIOUR OF REINFORCED CONCRETE TWO-WAY SLABS	202
4.8.1 Introduction	202
4.8.2 MODES OF FAILURE	203
4.8.3 Load-deflection behaviour	204
4.8.4 Cracking and failure loads	205
5.6.4 Effect of Cyclic loading	206
CHAPTER FIVE	208
CONCLUSIONS AND RECOMMENDATIONS	208
5.1 SUMMARY	208
5.2 CONCLUSIONS	209
5.2.1 Physical Properties of Aggregate	209
5.2.2 Mechanical Properties of Concrete with PKS aggregates	210

5.2.3 Reinforced Concrete Beams and two-way slabs	211
5.3 RECOMMENDATIONS FOR INDUSTRY	214
5.4 RECOMMENDATIONS FOR FURTHER RESEARCH	215
5.5 LIMITATIONS OF STUDY	216

REFERENCES

.....	217
-------	-----

APPENDICES

.....	232
-------	-----

APPENDIX A: FAILURE MODES AND CRACK PATTERNS OF TEST

SPECIMENS

.....	232
-------	-----

APPENDIX B: DETERMINATION OF THEORETICAL LOADS

(SECTIONS 3.4.5.4 OF BS 8110-1 AND 5.4 OF BS 8110-2)	244
--	-----

LIST OF TABLES

		Page
Table 2.1	Compound composition of Portland cement	26
Table 2.2	Classification of particle shapes of aggregates	33
Table 2.3	Surface texture classification of aggregates	35
Table 2.4	Grading limits for lightweight aggregates	37
Table 2.5	Physical and mechanical properties of PKS aggregates	47
Table 2.6	Mechanical properties of PKS concrete at 28-days of curing	50
Table 2.7	Different approaches to shear design	67
Table 3.1	Chemical composition of PKS aggregate	73
Table 3.2	Mix proportion of the various concrete mixes	78
Table 3.3	Details of R-series beams	86
Table 3.4	Details of S-series beams	88
Table 3.5	Mix proportions of the concrete	93

Table 3.6	Details of two-way slabs	98
Table 4.1	Physical properties of aggregates	103
Table 4.2	Air dry density of various mix proportions	107
Table 4.3	Effect of SP dosage on properties of PKS concrete	112
Table 4.4	28-day mean compressive strength	115
Table 4.5	28-day compressive strength vrs density	121
Table 4.6	Properties of test beams without shear reinforcement	125
Table 4.7	Properties of test beams with shear reinforcement	126
Table 4.8	Cracking loads of beams without shear reinforcement	130
Table 4.9	Cracking behaviour of beams without shear reinforcement	133
Table 4.10	Modes of failure of beams without shear reinforcement	144
Table 4.11	Experimental cracking loads and deflections at service loads	150
Table 4.12	Normalized shear stress and reserve strength index of test beams	157
Table 4.13	Cracking details of beams with shear reinforcement	164
Table 4.14	Modes of failure of beams with shear reinforcement	167
Table 4.15	Cracking loads and ultimate deflection of beams with stirrups	177
Table 4.16	Cracking behaviour and modes of failure of cyclically loaded beams	184
Table 4.17	Experimental results of R-series beams and code predictions	191
Table 4.18	Experimental results of S-series beams and code predictions	198
Table 4.19	Normalised shear stress prediction of various design codes	201
Table 4.20	Failure crack loads and theoretical loads of two-way slabs	207

KNUST

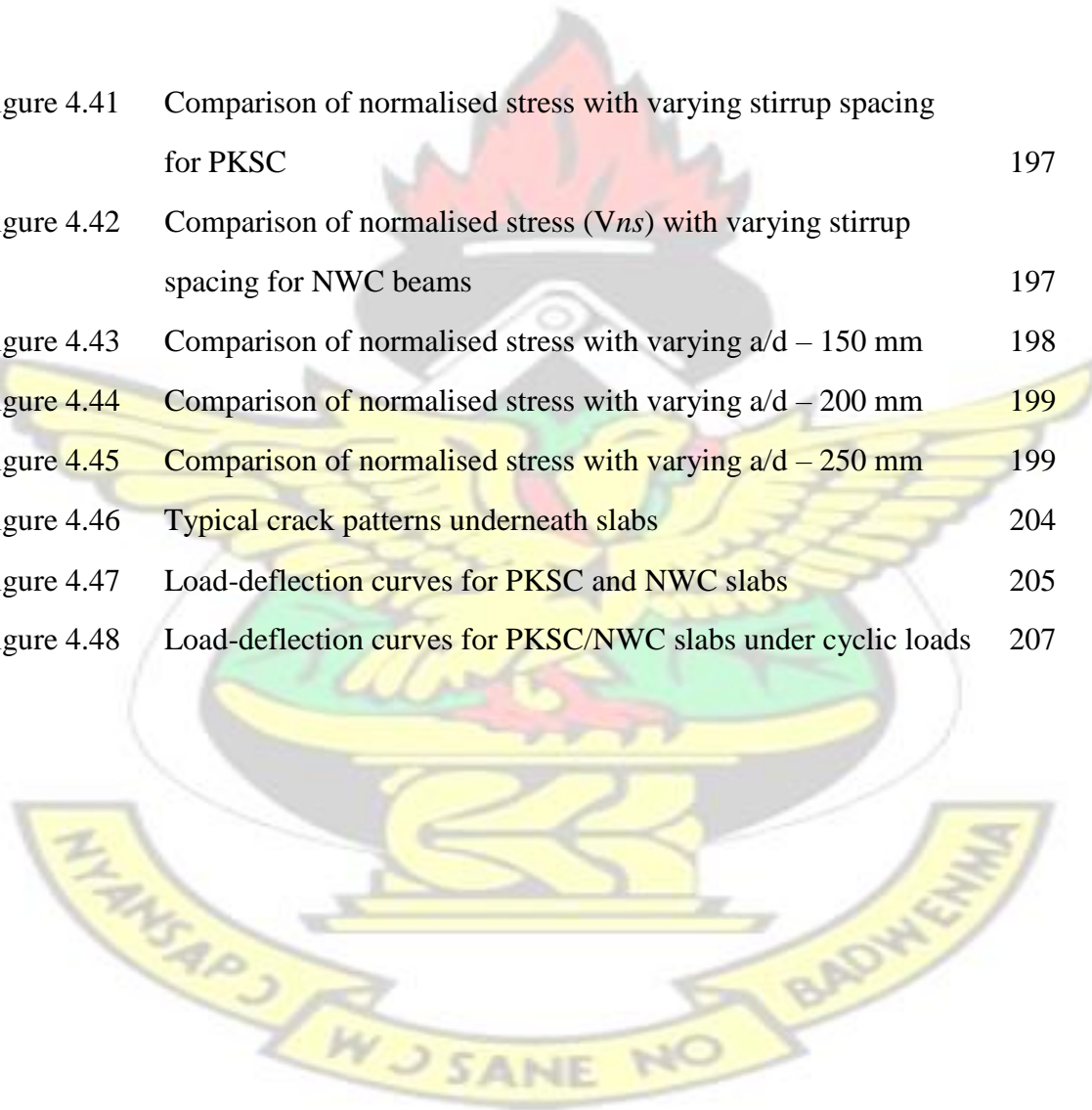
LIST OF FIGURES

	Page
Figure 1.1 Heap of Palm kernel shells	14
Figure 2.1 Effect of water cement ratio and age of curing on compressive strength of concrete	22
Figure 2.2 Effect of SP on the strength of concrete	23
Figure 2.3 Types of Aggregates by specific gravities	31
Figure 2.4 Visual assessment of particle shape from measurement of sphericity and roundness	33
Figure 2.5 Visual assessment of particle shape based on morphological observations	34
Figure 2.6 Influence of maximum size of aggregate on the 28-day compressive strength of concretes of different grades	38
Figure 2.7 Schematic representation of moisture in aggregate	40
Figure. 2.8 Internal curing at contact zone of aggregate	42
Figure 2.9 Layers of the palm fruit	43
Figure 2.10 Relationship between 28 day flexural and compressive strength	51
Figure 2.11 Shear transfer contributing to shear resistance	56
Figure 2.12 Shear at cracking and failure	59
Figure 3.1 Slump test of PKSC	79
Figure 3.2 Sample of freshly cast concrete cubes	80

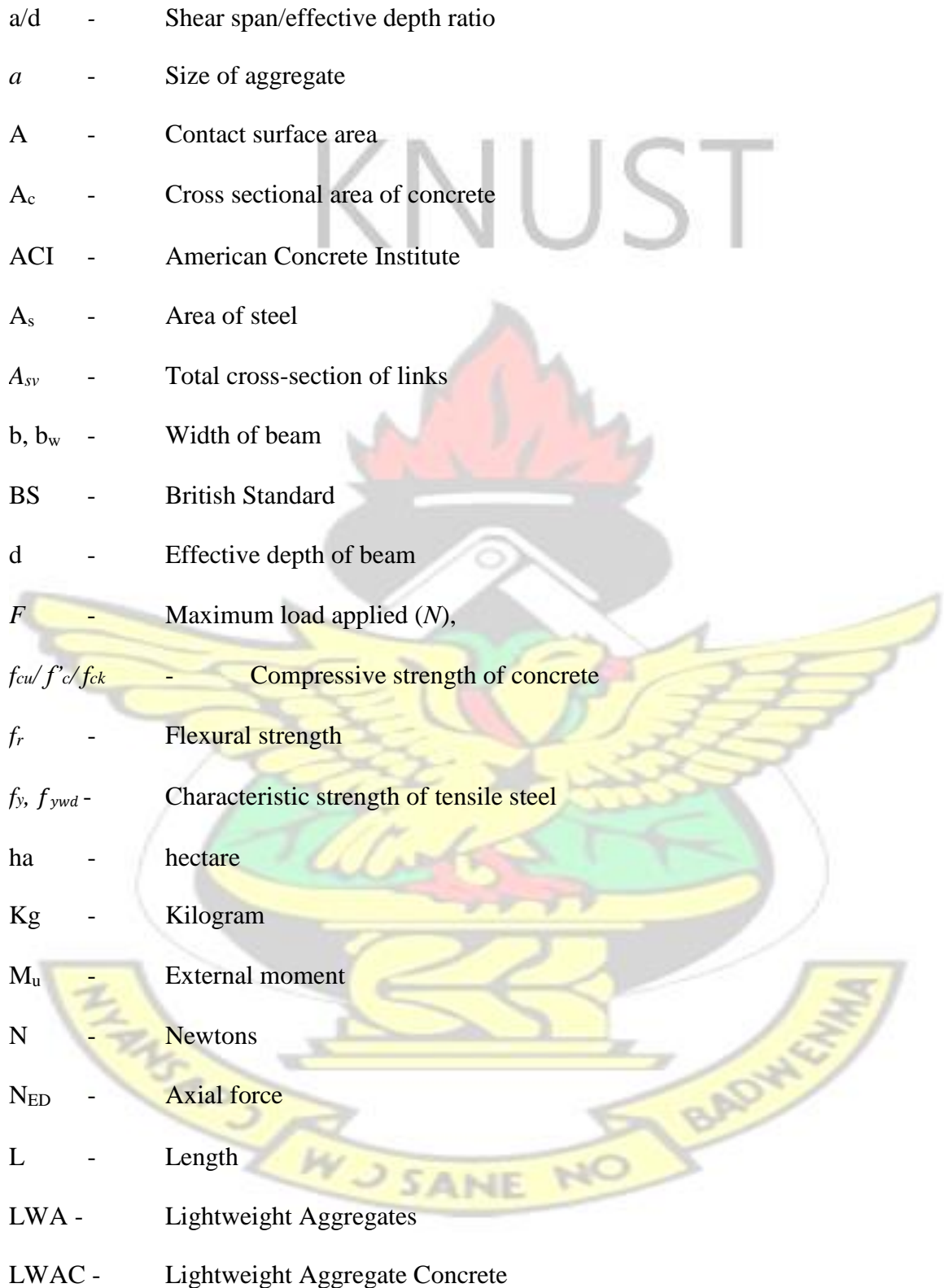
Figure 3.3	Loaded Universal Compression Testing Machine	82
Figure 3.4	Details of R-series specimens	85
Figure 3.5	Reinforcement details of beams with shear reinforcement	89
Figure 3.6	Reinforcement details of beams without shear reinforcement	90
Figure 3.7	Schematic diagram of experimental set-up	90
Figure 3.8	Samples of cast beams	93
Figure 3.9	Photograph of experimental set-up and instrumentation	95
Figure 3.10	Sample of NWC slabs	97
Figure 3.11	Sample of PKSC slabs	97
Figure 3.12	Experimental set-up of loaded slab	99
Figure 4.1	Particle size distribution of fine aggregate	101
Figure 4.2	Particle size distribution of granite aggregate	101
Figure 4.3	Particle size distribution of PKS aggregate	102
Figure 4.4	Effect of SP dosage on Slump of MPL and MOP	110
Figure 4.5	Effect of different dosage of SP on MPL	111
Figure 4.6	Effect of different dosage of SP on MOP	112
Figure 4.7	Comparison of compressive strength of PKSC with PL cement	113
Figure 4.8	Comparison of compressive strength of PKSC with OPC	114
Figure 4.9	Effect of cement types on compressive strength of PKSC	115
Figure 4.10	Schematic sketch of crack pattern of PKSC cubes	118
Figure 4.11a	Failure of PKSC cube	119
Figure 4.11b	Failure of NWC cube	119
Figure 4.12	Flexural strength of PKSC with PL cement	122
Figure 4.13	Flexural strength of PKSC with OPC	122
Figure 4.14	Load-deflection behaviour PKSC and NWC of R-series	129
Figure 4.15	Crack pattern for R-series specimens	134
Figure 4.16a-e	Load-deflection behavior of R-series beams	136

Figure 4.17a-e	Effect of ρ_w on cracking pattern of R-series beams	139
Figure 4.18a-c	Effect of beam size on load-deflection behaviour of R-series	142
Figure 4.19	Effect of increasing beam depth on shear stress	143
Figure 4.20	Typical failure modes of test beams	146
Figure 4.21	Cracking load vrs crack width curves	149
Figure 4.22	Effect of ρ_w on normalized shear strength at diagonal and ultimate load	153
Figure 4.23	Effect of Normalised shear stress on beam size	155
Figure 4.24	Influence of ρ_w on beam size and reserve strength	156
Figure 4.25	Effect of beam size ρ_w on Reserve shear strength of PKS beams	156
Figure 4.26	Applied load/ Deflection behaviour of PKSC and NWC of S-series specimens	160
Figure 4.27	Applied load versus crack width curve of PKSC and NWC of S-series specimens	163
Figure 4.28	Cracking load versus crack width curves for S-series beams	165
Figure 4.29	Crack pattern for S-series specimen beams	169
Figure 4.30	Effect of shear reinforcement on applied load vrs midspan deflection	171
Figure 4.31	Effect of normalized shear stress on stirrup spacing	172
Figure 4.32	Effect of stirrup spacing on applied loads and shear span to depth ratio	172
Figure 4.33	Applied load vrs midspan deflection for S-series beams	175
Figure 4.34	Applied load vrs span-to-depth ratio	175
Figure 4.35	Influence of shear-span-to-depth ratio on reserve strength	179
Figure 4.36	Applied load vrs Midspan deflection-first loads	182
Figure 4.37	Applied load vrs midspan deflection-service loads	183

Figure 4.38	Normalized stress (V_{ns}) at Exp. cracking and code predictions ($\rho_w = 1\%$)	193
Figure 4.39	Normalized stress (V_{ns}) at Exp. cracking and code predictions ($\rho_w = 1.5\%$)	193
Figure 4.40	Normalized stress (V_{ns}) at Exp. cracking and code predictions ($\rho_w = 2.0\%$)	194
Figure 4.41	Comparison of normalised stress with varying stirrup spacing for PKSC	197
Figure 4.42	Comparison of normalised stress (V_{ns}) with varying stirrup spacing for NWC beams	197
Figure 4.43	Comparison of normalised stress with varying a/d – 150 mm	198
Figure 4.44	Comparison of normalised stress with varying a/d – 200 mm	199
Figure 4.45	Comparison of normalised stress with varying a/d – 250 mm	199
Figure 4.46	Typical crack patterns underneath slabs	204
Figure 4.47	Load-deflection curves for PKSC and NWC slabs	205
Figure 4.48	Load-deflection curves for PKSC/NWC slabs under cyclic loads	207



NOMENCLATURE



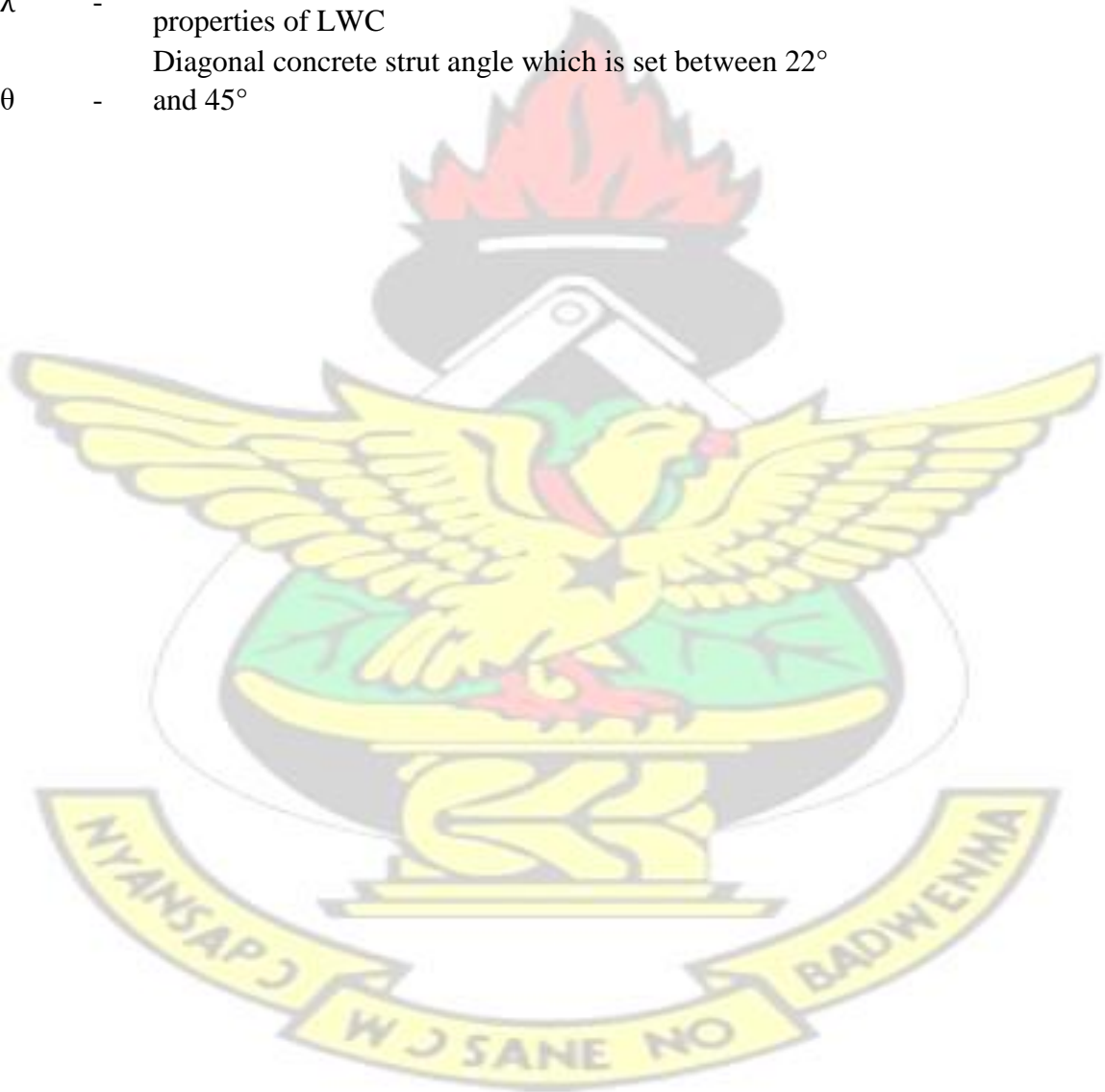
a/d	-	Shear span/effective depth ratio
a	-	Size of aggregate
A	-	Contact surface area
A_c	-	Cross sectional area of concrete
ACI	-	American Concrete Institute
A_s	-	Area of steel
A_{sv}	-	Total cross-section of links
b, b_w	-	Width of beam
BS	-	British Standard
d	-	Effective depth of beam
F	-	Maximum load applied (N),
$f_{cu}/f'_c/f_{ck}$	-	Compressive strength of concrete
f_r	-	Flexural strength
f_y, f_{ywd}	-	Characteristic strength of tensile steel
ha	-	hectare
Kg	-	Kilogram
M_u	-	External moment
N	-	Newtons
N_{ED}	-	Axial force
L	-	Length
LWA	-	Lightweight Aggregates
LWAC	-	Lightweight Aggregate Concrete

m	-	Mass of test specimen in Kg
NWA	-	Normal weight aggregate
NWC	-	Normal weight concrete
P	-	Applied load
P _f	-	First flexural crack
P _d	-	Diagonal crack
P _u	-	ultimate failure load
PKS	-	Palm Kernel Shells
SP	-	Superplasticizer
S_v	-	Spacing of links/ shear reinforcement along the beam
v	-	Volume of test specimen in m^3
V_c	-	Design concrete shear stress
V_{Exp}	-	Normalised experimental shear stress
V_n	-	Normalized shear load
V_{ns}	-	Normalized shear stress
V_s	-	Shear strength contributed by shear reinforcement.
V_{sl}	-	Service load
V_u	-	Shear force
V_{code}	-	Predicted shear force
V_{ult}	-	Predicted shear force using BS 8110
W	-	Crack width
w/c	-	Water to cement ratio
Z	-	Lever arm

KNUST



- δ_c - Ultimate deflection
- δ_{sl} - Maximum deflection at assumed service load
- γ - Partial factor of safety (taken as 1.25)
- ρ - Density of test specimen in Kg/m^3
- ρ_l, ρ_w - Longitudinal reinforcement ratio
- λ - Modification factor reflecting the reduced mechanical properties of LWC
- θ - Diagonal concrete strut angle which is set between 22° and 45°



ACKNOWLEDGEMENT

To God be all glory and honour for everything. I am highly grateful to the Almighty God for granting me the strength and knowledge to this successful end.

I wish to express profound gratitude to my supervisors; Prof. J. Ayarkwa, lecturer of the Department of Building Technology, and Prof. C. K. Kankam, a Professor of the Civil Engineering Department, KNUST. I am grateful for their guidance, encouragement, invaluable suggestions and criticisms throughout the period of this study. Their accessibility and unconditional patience are simply beyond expectations from supervisors.

I also wish to express my sincere gratitude to Prof. M. Adom-Asamoah and Dr. R. O. Afrifa, both members of the research team, for their invaluable suggestions, guidance and encouragement towards the successful completion of this project. And to all Lecturers in the Building Technology Department I say God bless you.

I am very grateful to Ghacem Company limited, Berock Ventures limited and Amoatec construction limited for the cements they donated towards ensuring the success of this project work.

I sincerely acknowledge the co-operation and assistance of the Laboratory Technicians in the Department of Civil Engineering for their assistance in the experimental works of this research.

Special thanks to Michael Dankyi, Mr. Michael Atta Gyamfi I, Mr. Obour Gyau David, Asumadu Joseph Osei and Belunuo Albert for their assistance on many occasions. To my colleagues, parents, brothers and sisters who supported me through prayers to ensure the success of this research, I say God bless you in abundance.

DEDICATION

This work is dedicated to.... my family

KNUST



CHAPTER ONE

INTRODUCTION

1.1 BACKGROUND

Many developing countries, including Ghana, are faced with the challenge of providing adequate and affordable housing. In recent times, shelter conditions have become worse; resources have remained scarce and housing demand has increased due to increase in population. Thus, the need to provide immediate practical solutions have become more urgent (Kerali, 2001). Adequate shelter is one of the most important basic human needs, yet about 25% of the world's population do not have any fixed abode, and in African cities the housing shortage ranges from 33% to 90% (Zami and Lea, 2008; Boison, 2002). Consequently, no developing country without strategies for low cost construction materials is likely to meet the growing demands of the sector (Kerali, 2001).

The construction industry relies heavily on conventional materials which include cement, crushed rock aggregate and sand or quarry dust for the production of concrete. In the United Kingdom alone, almost 146 million tonnes of sand, gravel and crushed rock aggregates were reportedly mined for construction in 2011 (Department for Communities and Local Government, 2013). To minimize the vulnerability of our building industry to the increasing costs of cement, Lim (2007) states that there is an urgent need to look for alternative materials. Previous studies on the use of affordable local construction materials for the local industry have resulted in the production of clay pozzolana as a partial substitute for ordinary Portland cement (Atiemo *et al.*, 2014; Amankwah *et al.*, 2014; Sarfo-Ansah, 2010).

Lightweight aggregate concrete is not a new invention in concrete technology; it has been used since ancient times (Shafiqh *et al.*, 2010). The demarcating line between lightweight aggregate concrete (BS EN 13055-1, 2002) and normal weight concrete (BS 8110-1, 1997) is the average density and compressive strength limits. For lightweight aggregate concrete (LWAC) production, the most popular aggregate input is lightweight aggregate (LWA) (Polat *et al.*, 2010). Manufactured lightweight aggregates have been used to produce structural concrete in developed countries for many years. Available literature shows that structural LWC with compressive strength of 25MPa can be produced with adequate economic benefits (Liu, 2005; Hossain, 2003; Haktanir and Altun, 2002; Ramazan, 2001). However, the use of lightweight aggregates from natural raw materials such as clay, slate, shale, etc., and from industrial by-products such as fly ash, PKS and slag ash have not been fully explored in developing and underdeveloped countries in Africa (Alengaram *et al.*, 2008a; Lim, 2007; Liu, 2005).

LWAC is potentially one of the most useful products for the Ghanaian construction industry because of its advantages such as reduction in cost of formwork and scaffolding, foundations, and the savings derived from the reduced cost of transportation and erection. Additionally, the reduction in the dead weight of a building through the use of lightweight aggregates in concrete could result in a decrease in the cross-section of steel reinforced columns, beams, slabs, and foundations (Yasar *et al.*, 2003; Topcu, 1997). Due to the greater fire resistance of LWC, the concrete cover to reinforcement may be reduced for the same fire rating, resulting in less volume of concrete. In addition, the reduced deadweight and lower modulus of elasticity of LWC are added advantages in the design of structures for seismic resistance. In order to build environmentally sustainable structures, the

possibility of using some agricultural wastes and industrial by-products from different industries as construction materials will be highly desirable.

LWAC also has its shortfalls in use. The porous nature of the aggregates allows water and gas to penetrate easily which is likely to affect the long-term durability of the structure. Due to the presence of air voids, steel-concrete bond is likely to be lower requiring longer development length for reinforcement, and affecting the ultimate strength in anchorage and the serviceability problem of cracking. Lower elastic modulus of LWAC means reduced stiffness and higher deflections, which may lead to serviceability problems as well. Also, there is evidence that LWAC is more brittle than NWC of equivalent strength, and failure occurs through the aggregates rather than traveling around the aggregates (Zhang and Gjrov, 1990).

However, these shortfalls may be controlled in the design of a safe and serviceable structure, even though the cost may be comparatively higher. Also, the initial cost of LWAC is usually higher than the cost of an equivalent unit of NWC, however ACI 213R03 (2003) reports that based on cost-benefit analysis, LWC outweighs NWC in many instances. Therefore, when analyzing the possibility of using LWAC for a given project, it is necessary to consider not only the cost of materials, but also the reduction in construction time, savings in handling, transportation and erection cost and, more importantly, the savings from improved buildability and functionality provided by the use of LWC. A large variety of structures including floating and offshore structures, bridges, low and high-rise buildings built around the globe, serve as examples. Many economic and innovative solutions on record would not have been possible without the use of LWC.

PKS are not common materials in the construction industry. This is either because their use for such purpose has not been well developed, or because they are not available in very large quantities as sand or gravel (Ndoke, 2006). The PKS are often dumped as waste products of the oil palm industry and sometimes used as a source of fuel for cooking (Ndoke, 2006; Omenge, 2001). However, the growing concern of resource depletion and global pollution, coupled with an escalating cost of housing has challenged many engineers to seek and develop new materials relying on renewable resources (Adewuyi and Adegoke, 2008; Teo *et al.*, 2006b). PKS, being by-products of the agricultural industry, is an abundant resource in Ghana, is cost-effective and environmentally friendly. About 80,000 tonnes of this product are generated annually in this country. The utilization of this agricultural solid waste as a lightweight aggregate in concrete could reduce the cost of construction since haulage distances would be greatly reduced, and also help resolve the problem of disposal of waste products generated at the palm oil mills.

1.2 PROPERTIES OF REINFORCED LWC

Reinforced concrete (RC) is the most common building material used in many engineering structures. The strength, stiffness and the economic advantages of reinforced concrete members, make it a suitable material for a wide range of structural applications (HyoGyoung and Filippou, 1990). Failure of the concrete is induced by initiation and propagation of cracks which are controlled by the tensile properties of the material. It is reported that the flexural strength is about 35% to 80% of direct compressive strength (Ghaffar *et al.*, 2010; Ferguson *et al.*, 1988). This disadvantage is worsened when LWC is

considered. The lower modulus of elasticity of the LWC concrete results in higher deflections, which may eventually result in serviceability challenges. Zhang and Gjrovc (1990) reports that LWC is more brittle than NWC of equivalent strength, and failure occurs through the lightweight aggregates rather than failing around the aggregates.

Shear transfer mechanisms in concrete elements are complex and difficult to predict precisely due to the complex stress redistributions that occur after cracking (Jung and Kim, 2008) and the numerous factors that influence the shear failure. Shear failure in plain concrete members is brittle in nature and consequently predisposes structures to sudden collapse without advance warning (Cho *et al.*, 2009). It is not surprising that in spite of the many decades of experimental research and the use of highly sophisticated analytical tools (Collins *et al.*, 2008; Mansour *et al.*, 2004; Teoh *et al.*, 2002; Johnson and Ramirez, 1989), the accurate prediction of shear failure still remains contentious among engineers.

The partial collapse of the Wilkins Air Force Depot warehouse in Ohio in 1955, as a result of shear failure of RC deep beams, raised further concerns about the inadequate shear design practice at that time (Oreta, 2004; Mansour *et al.*, 2004; Collins and Mitchell, 1997). This has resulted in the evolution of design code procedures which are more stringent in a bid to preventing such sudden failures. The transmission of shear forces across a crack takes place through numerous contact points between aggregate particles embedded in the crack faces, and the matrix exposed along the interface. The shearing force, V , may be resisted by the shear resistance across the compression zone, the transverse component of the force resulting from interlocking of aggregates, the transverse force induced in the main

flexural reinforcement by dowel action, and the tensile force induced in the transverse reinforcement (stirrups) (Angelakos, 1999; Ramirez and Breen, 1991).

Shear reinforcement plays a significant role in the behaviour of reinforced concrete elements of a structure. In structures without shear reinforcement, increase in crack widths results in a significant reduction in shear resistance due to aggregate interlock (Robert, 2000). Considering beams with shear reinforcement, crack widths are controlled which enhances aggregate interlock resistance (Robert, 2000). Shear reinforcement therefore increases the ultimate strength and corresponding strain due to confinement, increases ductility level of beams and prevents premature failure of beams (Maekawa and Shawky 1997; Okamura and Maekawa 1991).

Considering LWAC, the codes of practices adopt a constant fraction of normal weight concrete strength as the contribution of the concrete section at similar compressive strengths. The use of reduction factors controlling the shear behaviour of all forms of lightweight aggregate concrete is possibly an oversimplification considering the wide variety of LWA and their corresponding properties available (Juan, 2011; Regan *et al.* 2005).

Among the various factors that affect shear strength of RC concrete, the bond strength between the concrete matrix and the steel reinforcement is one of the most important aspects in structural reinforced concrete, as the bond enables the concrete and steel to act as effectively as a unit. The nature and microstructure of the interfacial zone vary depending on

the aggregate type, the surface structure of aggregate, pore structure of the aggregate, the porosity of the cement paste, and the bleeding of water beneath the aggregate (Lo *et al.*, 2004; Mehta, 1986). The aggregate interlock component of shear transfer in LWC is reported to differ significantly from its normal weight concrete counterparts. In NWC, the aggregates (usually granite) tend to be the strongest component while the interfacial transition zone between the aggregates and the cement matrix is the weakest in NWC. Thus shear cracks are found to develop around the granite aggregates. Meanwhile, shear cracks in LWC have been observed to travel through the weak lightweight aggregates (Lo *et al.*, 2004; Al-Khaiat and Haque, 1998; Zhang and Gjrrv, 1995) indicating that the lightweight aggregate is the weakest component of the concrete. This means that lightweight aggregates are not efficient crack arrestors compared to granite aggregates. Furthermore, a strong micro-structural interfacial zone improves the mechanical interlocking between the cement paste and the LWA (Lo *et al.*, 2004).

1.3 PROBLEM STATEMENT

Successful gains through research has been made on the structural performance of lightweight aggregate concrete in developed countries. However, these are mostly confined to manufactured lightweight aggregates, aggregates from industrial by-products, and naturally occurring lightweight aggregates (Teo *et al.*, 2006a). While the strength of lightweight aggregate concrete has been reported elsewhere (Lim, 2007; Chandra and Berntsson, 2002), researchers (Mannan and Ganapathy, 2001; Basri *et al.*, 1999) have focused on the mix design and other mechanical properties of PKS concrete.

A thorough literature search revealed that a limited amount of works have been carried out to assist in understanding of the structural behaviour of PKS concrete, such as bending strength (Emiero and Oyedepo, 2012; Alengaram *et al.*, 2008b; Teo *et al.*, 2006a) and the shear strength (Alengaram *et al.*, 2011a). However, owing to the high potential in the use of PKS aggregates as lightweight aggregates for structural concrete, it is imperative that more research is conducted to develop a comprehensive understanding, particularly, in the area of shear transfer mechanism for its structural elements. Additionally, there exists very little literature on the mechanical and structural properties of lightweight aggregate concretes utilizing agricultural solid wastes such as PKS in Ghana. As a result, the lack of information regarding the fresh and hardened properties, and structural performance of PKS concrete elements continues to hinder the use of this material by designers and contractors in practical applications in Ghana and other developing countries.

The shear failure of reinforced concrete beams is very complex, involving numerous parameters. Factors influencing the shear resistance capacity of beams are shear span-to-effective depth ratio (a/d), tension steel ratio (ρ), compressive strength of concrete (f_c), maximum size of coarse aggregate, density of concrete, use of fibers in concrete, size of beam, position and geometry of haunches, tensile strength of concrete, support conditions, clear span-to-effective depth ratio (L/d), number of layers of tension reinforcement, grade of tension reinforcement and end anchorage of tension reinforcement (Ghaffar *et al.*, 2010). These factors have been included in the formulation of various design codes of practice in an attempt to control the sudden failures of structural elements of normal weight concrete.

ACI-318 (1999) design procedure requires the determination of the shear-carrying capacity of beams reinforced in bending only before the addition of web reinforcement. It requires stirrups to be provided in beams once the shear at the critical section is greater than one-half the nominal shear resistance. Additionally, reinforced concrete structural elements such as slabs and foundations do not use shear reinforcement. Therefore, knowledge of the shear behaviour of reinforced concrete beams without web reinforcement is necessary in the design process of concrete beams (Rebeiz *et al.*, 2000).

Current design methods by BS 8110, ACI 318 and EC2 for shear transfer mechanism of lightweight Aggregate Concrete (LWAC) use modification factors on concrete cast using normal aggregates. Since the PKS aggregate differ from those of normal aggregates in terms of the physical properties, the shear transfer mechanism of PKS is expected to be different from those of NWC. Thus, it is apparent that, these current design procedures may not be suitable in predicting the ultimate shear resistance of the PKS concrete shallow beams and slabs. Against this background, this study seeks to provide information on the density, mechanical and structural properties of lightweight aggregate concretes utilizing PKS aggregates for structural application.

1.4 AIM

The aim of this study is to evaluate the shear behaviour of PKS lightweight aggregate concretes beams and slabs for structural application in the construction industry.

1.5 SPECIFIC OBJECTIVES

The specific objectives of the study are:

1. To determine the physical properties of PKS aggregates that make it suitable for the production of LWC. The study specifically considered aggregate impact value (AIV), water absorption, specific gravity, aggregate crushing value (ACV), Los Angeles Abrasion Value (AAV), elongation index (EI) and flakiness indices (FI).
2. To investigate the mechanical properties of PKS LWC. The mechanical properties were the compressive and the flexural tensile strengths of PKS concrete.
3. To investigate the behaviour of reinforced PKS concrete shallow beams in shear, both theoretically and experimentally, by studying the;
 - i. Effect of amount of longitudinal reinforcement on reinforced PKS concrete beams in terms of cracking and crack width, deflection, and serviceability and ultimate modes of failure of PKS beams;
 - ii. Effect of amount of shear reinforcement on the behaviour of PKS concrete beams on cracking and crack width, deflection, and serviceability and ultimate modes of failure of PKS beams;
 - iii. Size effect of reinforced PKS concrete beams in flexure and shear on cracking and crack width, deflection, and serviceability and ultimate modes of failure of PKS beams;
 - iv. Effect of loading of reinforced PKS concrete beams on cracking and crack width, deflection, and serviceability and ultimate modes of failure of PKS beams;

4. To investigate the flexural behaviour of reinforced PKS concrete two-way slabs by studying;
 - i. the effect of concrete strength on the deflection and cracking characteristics;
 - ii. the effect of loading on the ultimate strength behaviour.
5. To compare the results with the provisions of BS 8110 (1997), ACI 318-08 and EC 2 to ascertain the suitability or otherwise of the codes for predicting the shear capacity of reinforced PKS concrete beams.

1.6 SIGNIFICANCE OF STUDY

In Ghana the use of granite, river stones and quartzite as coarse aggregates in construction is a common practice and has resulted in increased cost of these construction materials. The major challenge to the use of these aggregates has been their economic and environmental sustainability. The increasing demand for concrete using crushed rock aggregates drastically reduces the natural stone deposits which eventually damages the environment, thereby causing ecological imbalance (Alengaram *et al.*, 2008b; Short and Kinniburgh, 1978). Thus, there is the urgent need to explore and identify suitable replacement materials to the natural stone. Recent concerns of major stakeholders of the construction industry has been the sourcing, development and the use of other nonconventional local construction materials including industrial and agricultural wastes (Olanipekun *et al.*, 2006). Recent studies have identified phyllite aggregates as one such substitute to crushed rock aggregates as coarse aggregates in concrete production (AdomAsamoah and Afrifa, 2013; Adom-Asamoah *et al.*, 2012; Afrifa *et al.*, 2012; Adom-

Asamoah and Afrifa, 2011; Adom-Asamoah and Afrifa, 2010).

PKS are waste by-products of the palm oil industry, often stockpiled in the vicinity of the factories. These stockpiled waste materials in the open fields have negative impacts on the environment. In Ghana, it is estimated that over 243,852 tons of oil palm fruits are produced annually of which the shells form almost 30% (Danyo, 2013; Fold and Whitefield, 2012; Teo *et al.*, 2006b; Agbodeka, 1992). The improper disposal of the shells has raised environmental concerns such as environmental pollution and environmental degradation, a typical example is shown in Figure 1.1. In addition to the sustainable disposal of the PKS, the aggregates are renewable and lends itself to sustainable use. The use of PKS as aggregates for concrete production has a strong potential of attracting investors into the oil palm production sector. This will lead to increased palm oil production which will aid in expanding the economy as a whole.

One of the sustainable ways of disposing these wastes would be the utilization as a replacement of crushed rock aggregates and river gravel. This will also help to prevent the depletion of natural resources and to maintain ecological balance (Teo *et al.*, 2006a). The use of PKS as lightweight aggregates in the production of concrete is important to the local construction industry because it has the potential of increasing the size of the economy by attracting investors into the local palm oil sector. Additionally, PKS are environmentally friendly and cost-effective. As the availability and cost of aggregate is directly related to haulage distance (Adom-Asamoah and Afrifa, 2010), the use of PKS as a substitute to crushed rock aggregates for low-cost houses, especially in areas where the oil palm mills are located

will result in cost effective construction. By substituting PKS concrete for normal weight concrete, a saving on self-weight of up to 42 percent can be realized (Olanipekun *et al.*, 2006).

In spite of the numerous advantages outlined, there is inadequate experimental data on the use of PKS aggregates in concrete production to increase the confidence of designers. While numerous research efforts have focused on developing appropriate mix designs for the PKS concrete, information on the shear behaviour of the material has remained scanty. Since no design rules have been provided in the current codes of practice (BS 8110, ACI 318-08 and EC 2), it is essential for a research investigation to be conducted to assist in the current understanding on shear transfer mechanisms of PKS concrete beams, both cast with and without shear reinforcements. Additionally, the structural response of PKS concrete two-slabs is necessary to increase designers' confidence in the use of the material. The main objective of this study is thus, to provide information on the physical properties of PKS as aggregates such as density, mechanical properties and structural behaviour of PKS concrete beams for structural application. This is to encourage the use of these by-products as construction materials in low-cost housing and reduce the environmental problems caused by the indiscriminate disposal of the PKS and the depletion of natural stones.



Fig. 1.1 Heap of Palm kernel shells

1.7 OUTLINE OF THESIS

This thesis is divided into five chapters:

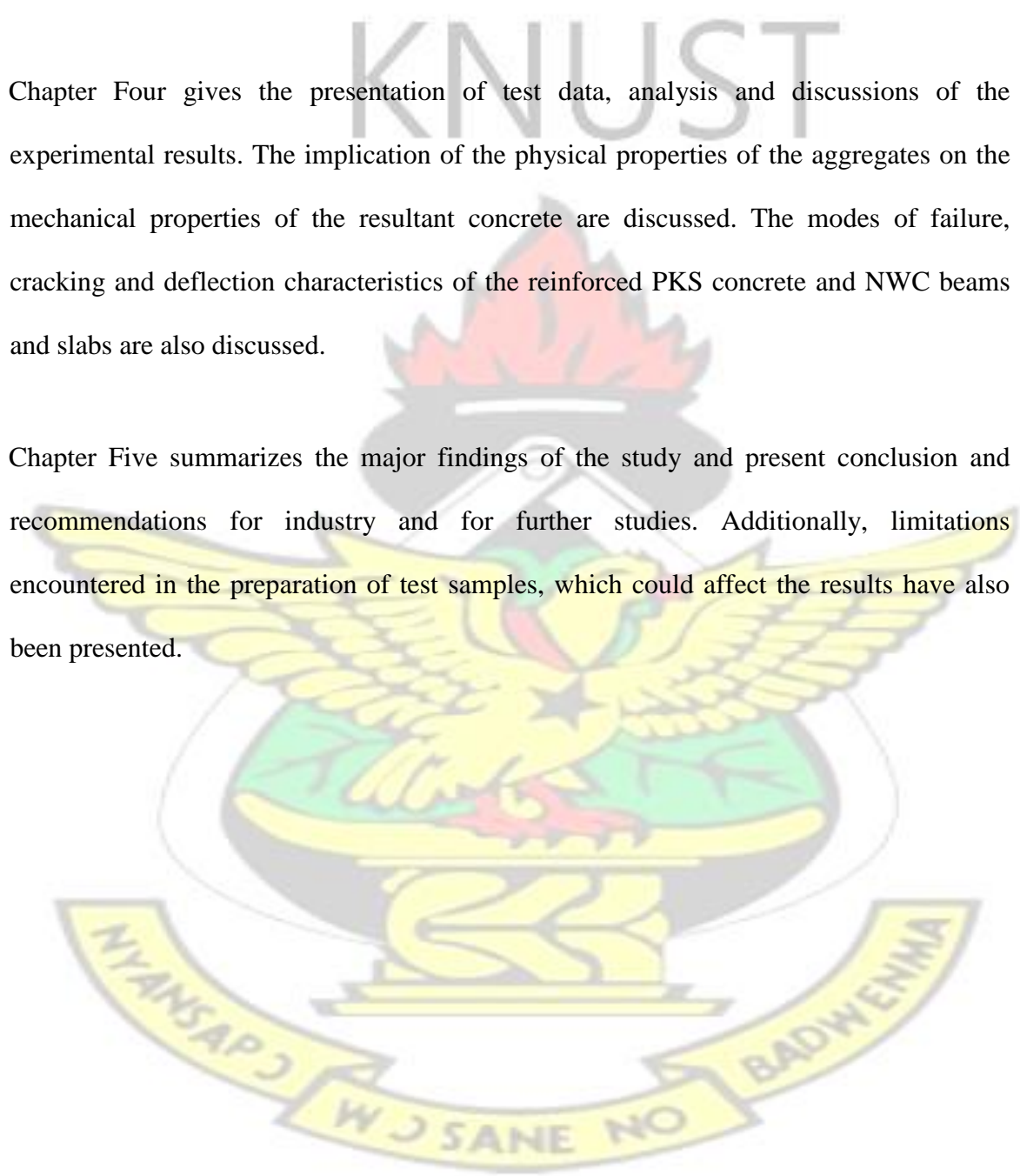
Chapter One introduces the background to the study, aim and objectives of this study. The significance of this research is also emphasized in this chapter.

Chapter Two presents a literature review on past and recent studies which focus on the study area. The difference between lightweight and normal weight concrete is established. The definition and classification of lightweight aggregates were also reviewed. Aggregate properties such as aggregate shape, texture, particle size distribution, moisture content, specific gravity, porosity and water absorption are thoroughly reviewed. Related literature on PKS concrete and the behaviour of reinforced LWC beams in shear are presented.

Chapter Three highlights the experimental procedure for the determination of the physical and mechanical properties of PKS concrete. Details of the reinforced concrete beam preparation and instrumentation are also described.

Chapter Four gives the presentation of test data, analysis and discussions of the experimental results. The implication of the physical properties of the aggregates on the mechanical properties of the resultant concrete are discussed. The modes of failure, cracking and deflection characteristics of the reinforced PKS concrete and NWC beams and slabs are also discussed.

Chapter Five summarizes the major findings of the study and present conclusion and recommendations for industry and for further studies. Additionally, limitations encountered in the preparation of test samples, which could affect the results have also been presented.



CHAPTER TWO

LITERATURE REVIEW

2.1 INTRODUCTION

Concrete is generally produced on site by mixing cement, water, aggregates and if required admixtures and additives. Considerable research work has been carried out on normal weight concrete (NWC) and artificial lightweight aggregate concrete (LWAC). Lightweight aggregates are produced in a very wide range of densities varying from 50 kg/m³ for expanded perlite to 1000 kg/m³ for clinkers (Chandra and Berntsson, 2002). With these aggregates and high range water reducers, it is possible to make LWAC of 80MPa cube compressive strength (Lim, 2007). Considering the practical advantages of LWAC, it has become an important structural material leading to the increasing demand for the material.

Knowledge of the difference between LWAC and NWC is helpful for the study of structural PKS concrete. In this chapter, the difference between LWAC and NWC is presented. The classification and properties of LWA, and studies on PKS aggregate concrete is reviewed. Additionally, the structural behaviour of reinforced LWAC in shear is presented.

2.2 DIFFERENCE BETWEEN NWC AND LWAC

Concrete is an artificial stone-like material produced with an excellent resistance to compressive stresses. It is usually cast in place in a plastic condition which subsequently

dries. The properties of concrete are determined by the properties of the constituent materials, which are the binding materials (e.g. cement), fine aggregates, coarse aggregate (e.g. gravel) and water which on mixing, hardens to form the shape of the desired structure. Normal weight concrete, predominantly used worldwide, has a density of 2240 to 2400 kg/m³ (Nawy, 2008). The heavy self-weight makes it an uneconomical structural material compared to the low self-weight of other lightweight aggregate concrete (Shanmugasundaram *et al.*, 2010). The distinguishing feature of LWAC is its lower density as compared to NWC. It is recognized that high self-weight is the major impediment in the use of structural concrete for high-rise buildings and long span bridges. In fact, the decrease in the unit weight of LWAC is obtained by the presence of voids, either in the aggregate or in the mortar or in the interstices between the coarse aggregate particles (Neville and Brooks, 2008). In structural lightweight aggregate concretes, the high strength of the mortar compensates for the low strength values of the aggregate, and the bond between the aggregates and the cement paste is much stronger compared to the bond in normal weight concrete (Chandra and Berntsson, 2002). This is because the cement paste penetrates inside the aggregates due to their porous nature, with very little interfacial transition zone between the aggregates and the matrix.

2.3 LIGHTWEIGHT AGGREGATE CONCRETE (LWAC)

LWAC has been successfully used since the ancient Roman times and it has gained its popularity due to its low density and superior thermal insulation properties. LWAC is a type of concrete with aggregates of low specific gravity or high porosity which results in a lessened dead weight of the structure.

Using lightweight aggregate concrete, when the dead load/total load is high, substantial economy is achieved on material (concrete as well as steel). This also leads to saving in the frame, foundation design, substructure and cladding of a building. From the Federation Internationale de la Precontrainte (FIP) manual of lightweight aggregate concrete (1983), LWAC has shown to have many advantages such as: lower dead load, heat insulation capacity, anti-condensation properties, reduction in use of resources, reduced energy demand, and quicker production potential. It is lighter than the conventional concrete with a dry density of about 300 kg/m³ up to 2000 kg/m³ (Neville and Brooks, 2008; BS EN 13055, 2002; ASTM C330, 1999). EuroLightCon (1998) reported that LWAC is defined by many codes as concrete having an oven-dry density of less than 2000 kg/m³ and can be produced within a range of 300 to 2000 kg/m³. The use of LWAC permits greater design flexibility and substantial cost savings, reduced dead load, longer spans, better fire ratings, smaller sections, smaller sizes of structural members, less reinforcing steel, and reduced foundation costs (Chen and Liu, 2005; Balendran *et al.*, 2002; Gao *et al.*, 1997). Bai *et al.* (2004) produced LWAC with densities in the range of 1560 and 1960 kg/m³ and having a 28-day compressive strength in the range of 20 to 40 MPa.

2.3.1 Key Hardened Properties of LWAC

The hardened properties of concrete are important since these are inextricably connected with the design and long-term performance of concrete structures. The hardened properties of LWAC differ significantly from those of normal weight concrete, mainly attributed to high porosity of LWA, which causes high water absorption rate and smaller modulus of elasticity of concrete thus made. In recent years, development of lightweight foamed

concrete (LWFC) with high compressive strength of 40 MPa and fresh density of 1600 kg/m³ and above have been developed (Lim, 2007). The high strength LWAC is basically produced using low water to cement or cementitious materials ratio and air in the form of preformed foam. Yasar *et al.* (2003) studied the strength properties of LWAC made with crushed basaltic pumice (scoria) and fly ash. LWAC with average density of 1863 kg/m³ was produced. It was concluded that scoria lightweight aggregates can be used in the production of structural LWAC. It was possible to produce a LWAC with a compressive strength of 25 N/mm² using fly ash.

Kilic *et al.* (2009) examined the effect of scoria and the pumice aggregates on the strengths and unit weights of LWAC. Four different aggregate sizes of 8-16 mm, 4-8 mm, 2-4 mm and 0-2 mm were used in their study. The study found that with a density range of 1368 to 1997 kg/m³, cylinder compressive strengths of 15.8 MPa to 44.1 MPa could be achieved. It was concluded that aggregate type influenced the unit weight, compressive strength and flexural tensile strength of corresponding concrete. Kilic *et al.* (2009) further concluded that it was possible to produce concrete of satisfactory strength grades which satisfy the strength requirement for load bearing structural elements.

2.3.1.1 Compressive strength

Compressive strength is the most important mechanical property of concrete. Both normal concrete and LWAC can be considered as consisting of cement paste, aggregates and transition zone at the interface between the aggregates and the cement paste. The compressive strength of LWAC is determined by the characteristics of the lightweight

aggregate, compared to the strength of NWC which depends on the characteristics of the paste. Each of the three constituents affects the properties of concrete although their significance varies to a great extent. For a given set of cement and aggregates, under the same conditions of curing and testing, the compressive strength of a concrete primarily depends on water/cement ratio, mix proportions, and consistency, and degree of compaction. LWAC needs more cement than conventional concrete in order to obtain the same strength. Weaker LWA therefore requires even stronger mortars and higher cement contents to achieve a given strength as compared to conventional concrete (Newman, 2005). The presence of voids in lightweight aggregates and/or in the matrix makes lightweight aggregates weaker in strength, stiffness and ductility, and these weaknesses reflect in the properties of the resulting concrete (Lim, 2007).

2.3.1.1.2 Effect of water/cement ratio on compressive strength

Water-cement ratio is the most important parameter in determining the compressive strength of concrete, consistence and durability (Waziri *et al.*, 2011; Adeagbo, 1999). Water/cement ratio influences the porosity of the cement matrix within the hardened concrete, which itself heavily influences concrete durability.

Waziri *et al.* (2011) studied the effect of water/cement ratio on the strength properties of quarry-sand concrete with two normal mix proportions of 1:2:4 and 1:3:6 (cement: sand: gravel). The water/cement ratios were 0.50, 0.55 and 0.60. It was reported that the compressive strength of all mixes decreased with increasing water/cement ratio. The mix with a water/cement ratio of 0.60 obtained the least compressive strength. This inverse

relationship between water-cement ratio and compressive strength of concrete was first articulated by Abrams (1927). This is now referred to as the water-cement ratio rule;

$$f_{cu} = \frac{k_1}{k_2^{w/c}} \quad (2.1)$$

where f_{cu} represents the compressive strength, w/c represents the water-cement ratio of the concrete mixture and k_1 and k_2 are empirical constants.

Typical curves illustrating the relationship between water-cement ratio and compressive strength at a given moist curing age are shown in Fig. 2.1 (Ksenija *et al.*, 2011; Mehta and Monteiro, 2006).

The factors that contribute to the strength of hydrated cement paste and the effect of increasing the water-cement ratio on porosity at a given level of cement hydration helps to understand the w/c ratio relationship in concrete as the natural consequence of a progressive weakening of the cement matrix (Ksenija *et al.*, 2011; Colak, 2006). This is caused by the increase in porosity of the concrete as a result of increasing the water-cement ratio. The effect of water-cement ratio on compressive strength of concrete usually depends on the properties of the mix constituents: sands, gravels and cements (Jo *et al.*, 2007).

Water/cement ratio has the same effect on the strength of LWAC as on normal weight concrete. According to Newman (2005) the reduction in effective water/cement ratio due to the higher water absorption of lightweight aggregate is difficult to predict, measure and verify. For a given type and quantity of aggregate and cement, the compressive strength f_c depends exclusively on the w/c ratio (Xuan *et al.*, 2009). Shamsai *et al.* (2012) report that

reducing the water-cement ratio from 0.50 to 0.33 increases the compressive strength of nano silica concrete from 34.4% to 35.2 %.

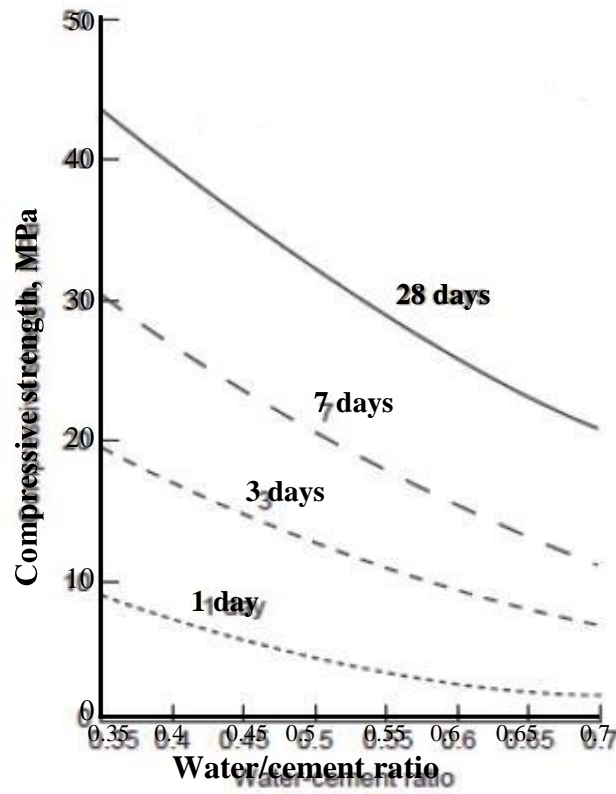


Fig. 2.1 Effect of water cement ratio and age of curing on compressive strength of concrete

Good workability of concrete, however, cannot be achieved with a water to cement ratio below 0.40 without the use of superplasticizer (Neville, 2006). To achieve high strength LWAC at a given workability, the use of a superplasticizer can result in a water reduction of 25-35% (Fig. 2.2) (Neville and Brooks, 2008). Currently, newly developed superplasticizers allow the use of low water-cement ratio in order to achieve very high strength concrete without loss of workability (Halit, 2008).

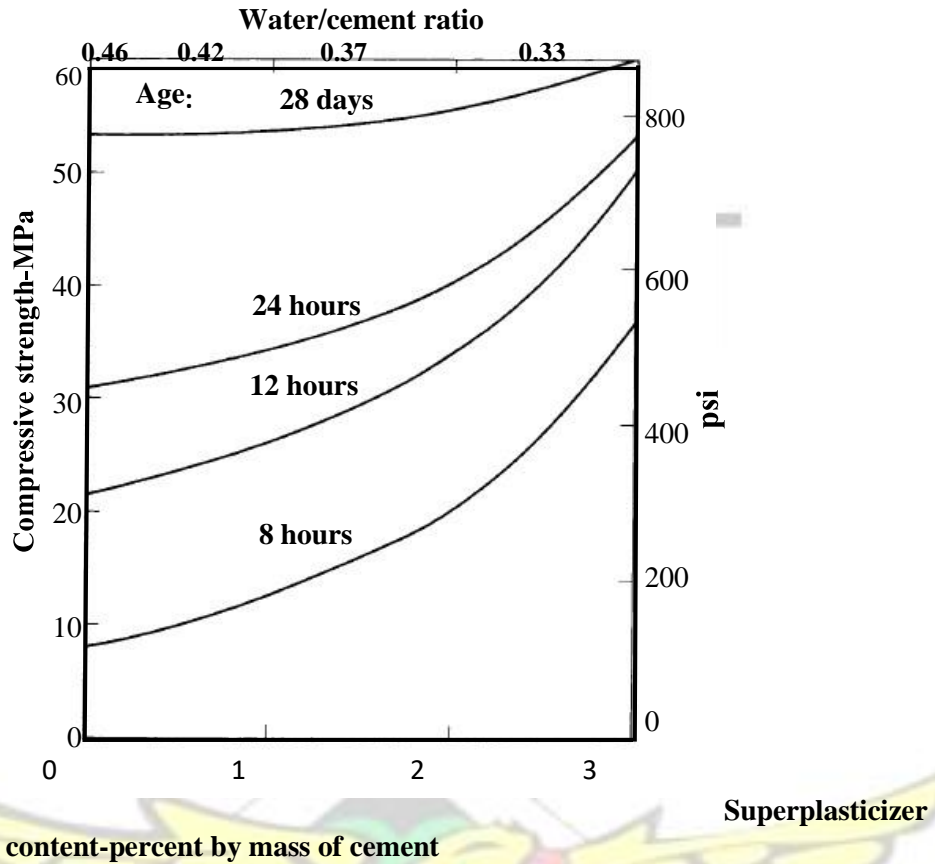


Fig. 2.2 Effect of SP on the strength of concrete (Neville and Brooks, 2008)

2.3.1.2 Tensile Strength

Flexural tensile strength (modulus of rupture) is an important property in concrete design since it affects shear strength, flexural cracking, bond strength and brittleness ratio of the concrete. The concept of flexural strength is based on the elastic beam theory and is defined as the maximum normal stress in an un-reinforced beam calculated from the maximum bending moment M_u assuming that the beam behaves elastically (Novak *et al.*, 2002). Traditionally, tensile strength has been defined as a function of compressive strength. However, this is known to be only a first approximation that does not reflect aggregate particle strength, surface properties, or the concrete's moisture content and distribution

(ACI 213R, 2003). For most lightweight aggregates, the tensile strength limit may be reached earlier than the compressive strength ceiling.

LWAC generally has lower tensile strength compared to that of normal weight concrete with similar compressive strength due to their lower modulus of elasticity (Zhang and Gjorv, 1995). Lim (2007) found that flexural tensile strength of lightweight foamed concrete is higher than that of other lightweight aggregate concretes such as PKS and expanded shale concretes. The relationship between the tensile strength and compressive strength for pumice and leca lightweight aggregate concrete was established in the form of equation 2.2

$$f_r = 0.73\sqrt{f_{cu}} \quad (2.2)$$

Where f_{cu} is the compressive strength of concrete; f_r is the flexural tensile strength

Alengaram *et al.* (2010b) reasoned that failure of concrete in tension occurs as a result of breakdown of bond between the cement matrix and the surface of the aggregate or by fracture of the matrix itself, and not as a result of fracture of the aggregate. However, for weak lightweight aggregates, the fracture of the concrete is as a result of the fracture of the aggregates itself.

2.3.2 Constituents of Lightweight Concrete

The essential components in LWAC are similar to that of NWC, aside the difference in coarse aggregate. These components are described in detail under the following sub sections.

2.3.2.1 Cement

The most commonly used cement is ordinary Portland cement (OPC), but other supplementary materials such as pozzolana, silica fume and fly ash can also be included as long as their acceptance has been demonstrated. The manufacture of Portland cement consists of ingredients mainly lime, silica, alumina and iron oxide from limestone and clay/shale which react together on firing to form a series of more complex products. The relative proportions of these oxide compositions are responsible for influencing the various properties of particular cements; in addition to the rate of cooling and fineness of grading which affects the strength of the cement. In many structural applications, the choice of cement has a lesser influence on the long-term performance of concrete than the practical aspects of mix control, cement content, water content, aggregate quality, compaction, finishing and curing (Newman and Choo, 2003).

ACI 213R-03 (2003) states that, the same criteria for choosing type of cement for normal weight concrete (NWC) applies to LWAC. BS EN 197-1 (2000) recommends the use of Portland cement which conforms to the respective strength classifications for all forms of structural applications. Cement content less than 250 kg/m^3 should not be used in structural concrete so that the durability of the concrete will not be compromised (Liu, 2005). In modern codes, there is a trend to focus more on the effective water/binder ratio than on the cement content or strength grade while formulating requirements for durability.

2.3.2.1.1 Types of Cement

It is recognized that different types of cements have different properties and performance. The choice of cement, especially the type and/or strength class, based on the requirements

for durability depends largely on the exposure and type of construction in which it is incorporated (BS EN 197-1, 2000). BS EN 197-1 (2000) classifies cements into five main types depending on its constituents. These are: Portland cement (CEM I), Portland composite cement (CEM II), Blastfurnace cement (CEM III), Pozzolanic cement (CEM IV), and Composite cement (CEM V).

2.3.2.1.2 Chemical Compounds of cement

Four main compounds are considered as the major constituents of cement and these compounds are presented in Table 2.1. The compositions of Portland cement is based on the 'Bogue composition' which are given in the equations below.

$$C_3S = 4.07(CaO) - 7.60(SiO_2) - 6.72(Al_2O_3) - 1.43(Fe_2O_3) - 2.85(SO_3) \quad (2.3)$$

$$C_2S = 2.87(SiO_2) - 0.754(3CaO \cdot SiO_2) \quad (2.4)$$

$$C_3A = 2.65(Al_2O_3) - 1.69(Fe_2O_3) \quad (2.5)$$

$$C_4AF = 3.04(Fe_2O_3) \quad (2.6)$$

Table 2.1 Compound composition and its contribution to hydration of Portland cement

Chemical formula	Shorthand notation	Weight percent	Reaction rate	Contribution to strength
3CaO. SiO ₂	C ₃ S	50	Moderate	High
2CaO. SiO ₂	C ₂ S	25	Slow	Low initially and high later
3CaO. Al ₂ O ₃	C ₃ A	12	Fast	Low
4CaO. Al ₂ O ₃ . Fe ₂ O ₃	C ₄ AF	08	moderate	Low

(Nawy, 2008; Neville and Brooks, 2008)

It is seen that the principal products of the

hydration reactions, which primarily account for the strength of concrete, are the calcium

silicate hydrates (C_3S and C_2S) that make up most of the hydrated cement (Nawy, 2008). These silicates are the most important compounds responsible for the strength of hydrated cement paste and are formed from the reactions between the two calcium silicates and water.

KNUST

2.3.2.2 Water

In general, potable water is safe for use in concrete. Water containing harmful substances such as salts, silts, suspended particles, organic matter, oil, or sugar can unfavorably affect the strength and setting properties of cement, and disrupt the affinity between aggregate and cement paste (Nawy, 2008). Therefore, the suitability of water should be examined before use. As a rule, any water with silt content below 2000 mg/L is suitable for use in concrete (Shetty, 2005). Due to the high water absorption of lightweight aggregates, the effect of water-to-cement ratio in LWAC mixes is not directly comparable to NWC. However, the effect of free water in the mix is similar to that in normal weight concrete.

Generally, the compressive strength of LWAC reduces as free water increases (Chandra and Berntsson, 2002). De-Pauw *et al.* (1995) defined different types of water in lightweight aggregates, and established a relationship between them. The authors stated that when working with lightweight aggregates, the following quantities are to be considered:

W_{tot} = Total amount of water in concrete mix,

W_{agg} = Amount of water initially present in the aggregate,

W_{abs} = Amount of water absorbed by the aggregate during mixing of the concrete,

W_{free} = Amount of water available in the cement paste when mixing the concrete,

W_{add} = Amount of water added when mixing the concrete.

Therefore, the following relationships are considered to be valid:

$$W_{tot} = W_{agg} + W_{abs} + W_{free} \quad (2.7) \text{ and}$$

$$W_{add} = W_{abs} + W_{free} \quad (2.8)$$

2.3.2.3 Admixtures

Superplasticizers (SP) are used to improve workability (flowability and homogeneity) of fresh concrete and to produce high performance concretes. The effect of superplasticizer on LWAC is similar to that of using them in NWC (Popovic, 1992).

The mechanism of superplasticizer is to give the cement particles highly negative charge so that they repel each other (deflocculating) due to the same electrostatic charges. As a result of deflocculation of the cement particles, more water will be provided for mixing the concrete (Alsadey, 2012). That notwithstanding, the improved workability produced by the superplasticizer is of a short period and thus there is a high rate of slump loss after 30 to 90 minutes (Neville and Brooks, 2008). The absorption of a part of the free water with the dissolved admixture will decrease the effectiveness of the admixture (FIP manual, 1983). ACI 304.5R (1991) recommends the use of soaked LWA to avoid absorption of the admixture into the LWA.

Alsadey (2012) investigated the influence of superplasticizer (SP) on the strength of concrete. The study focused on normal concrete with characteristic strength of 30 N/mm² at 28 days, using ordinary Portland cement as binder and Sikament R2002 as the superplasticizer. The

author prepared four mixes using admixture dosages of 600 ml/100kg, 800 ml/100kg, 1000 ml/100kg and 1200 ml/100kg of cement. The authors report of concrete strength of 55 MPa with an optimum superplasticizer dosage of 1% of the weight of cement. The study reports of a direct relationship between the workability and the amount of SP. That notwithstanding, very high dosages of SP impaired the cohesiveness of the concrete. Similarly, the author observed that increasing the amount of SP improved the compressive strength significantly when compared to the control mix without SP. However, the direct relationship between the compressive strength and the amount of SP only existed up to an optimum limit up to 1%. Beyond this limit, increase in the dosage of SP reduced the compressive strength of the concrete (Alsadey, 2012).

Prior to the above study, Collepradi (1995) commented on several factors through which SP affects the various properties of concrete in both fresh and hardened states. Amongst the various processes are reduction in interfacial tension, multi-layered adsorption and release of water trapped among the cement particles, retarding effect of cement hydration and change in morphology of hydrated cement.

2.3.2.4 Aggregates

Aggregates were originally viewed by Troxell *et al.* (1968) as being inert and dispersed throughout the cement paste in concrete, largely due to economic reasons, that is, as a fill material. Studies have shown that fine and coarse aggregates are very important in concrete because aggregates occupy 60% to 75% of the concrete volume and strongly influence the concrete's freshly mixed and hardened properties, mix proportions, and economy (Neville and Brooks, 2008; Alexander and Mindness, 2005; Quiroga and Fowler, 2004; Andaleeb,

2005; Kosmatka *et al*, 2003; Galloway, 1994). The essential requirement of an aggregate for concrete is that it remains stable within the concrete (both in the fresh and hardened states) and in any given environment, throughout the design life of the concrete (Smith and Collis, 2001).

KNUST

2.3.2.4.1 Classification of Aggregate

Aggregates can be classified in several different ways: whether they are natural or manufactured; whether they are crushed or naturally processed; whether they are inert or reactive; based on their specific gravity; and based on the sizes of their particles. Based on the specific gravities, three categories as normal weight aggregates, lightweight aggregates, and heavyweight aggregates (Fig. 2.3) can be produced (Neville and Brooks, 2008; Andaleeb, 2005; Kosmatka *et al*, 2003). On the basis of size, one can distinguish between fine aggregates, consisting mostly of small materials passing No. 4 sieve (3/16 in.) and retained on No. 200 sieve and coarse aggregates, mostly consists of large particles retained on the 4.75-mm (No.4) sieve (ASTM C125-07, 2007).

On the basis of source classification, aggregates can be natural or artificial. Natural aggregates are formed from weathering and abrasion process, or by crushing a larger parent rock artificially. In this case, the properties of the aggregates including chemical and mineral composition, specific gravity, strength, chemical stability, colour and pore structure, largely depend on the properties of the aggregates of the parent rock (Neville and Brooks, 2008). These properties influence the quality of concrete in the fresh and hardened states. Meanwhile the properties of artificial aggregates largely depend on the

manufacturing process. PKS aggregates are renewable lightweight natural aggregates. The particle size distribution largely depends on the cracking method of the palm kernels.

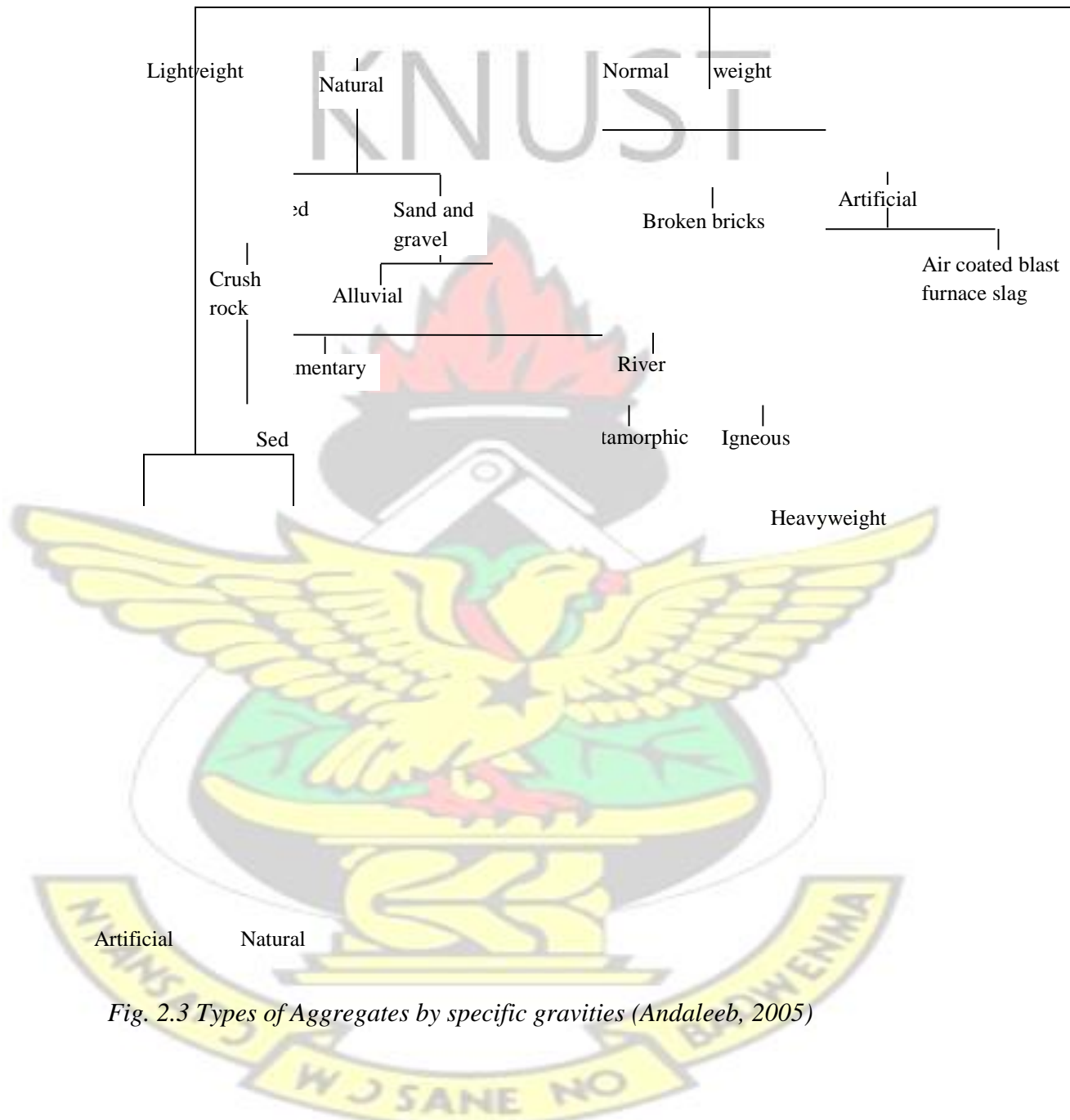


Fig. 2.3 Types of Aggregates by specific gravities (Andaleeb, 2005)

There are many types of aggregates available that are classified as lightweight, with a wide range of properties. Some examples of LWA used to produce structural LWAC include leca, pumice, perlite, vermiculite, diatomite, scoria, shale, clay and slate, sintering grate,

expanded shale, clay, fly ash and palm oil shells (Neville and Brooks, 2008; Kosmatka *et al.*, 2003; BS EN 13055, 2002; Chandra and Berntsson, 2002; ACI 213R-03, 2003). It is also worth noting that research in the use of organic natural aggregates in the form of PKS has advanced in other African countries in the past few decades (Alengaram *et al.*, 2008a; Olanipekun *et al.*, 2006; Teo *et al.*, 2006b; Mannan and Ganapathy, 2004; Basri *et al.*, 1999).

2.3.2.4.2 Lightweight Aggregates, LWA

Lightweight aggregates are the basic ingredients for making lightweight aggregate concrete. There are two sources of lightweight aggregates: aggregates from natural sources and aggregates from artificial sources. Pumice, scoria, tuff, PKS and other materials of volcanic origin are lightweight aggregates from a natural source. Expanded blast-furnace slag, clinker, fly ash, vermiculite and expanded perlite, which are the by-products of industrial processes, are man-made lightweight aggregates (Chandra and Berntsson, 2002; Owens, 1993; Popovics, 1992). The main characteristic of lightweight aggregate is its high porosity, which eventually results in a lower specific gravity. In recent years, due to the numerous advantages of the use of lightweight aggregate concrete in construction, there has been an increasing interest in the production and also investigation of properties of this material (Shafigh *et al.*, 2011; Kan and Demirbog, 2009; Subasi, 2009; Kilic *et al.*, 2009).

2.4 PROPERTIES OF LIGHTWEIGHT AGGREGATES

2.4.1 Shape

Shape refers to the geometry of the aggregate. Shape is related to sphericity, form, angularity, and roundness (Quiroga and Fowler, 2004; Galloway, 1994). The shape of aggregate particles influences paste demand, placement characteristics such as workability,

strength, void content, packing density and cost (Rached *et al.*, 2009; O’Flynn, 2000). For the same amount of paste, a mixture with round or cubical shaped aggregate will have better workability than a mixture with flaky and elongated aggregates. The ideal aggregate particle is one that is angular and irregular in shape.

Table 2.2 Classification of particle shapes of aggregates (Neville and Brooks, 2008)

Classification	Description
Rounded	Fully water-worn or completely shaped by wearing
Irregular	Naturally irregular or partly shaped by attrition and having rounded edges
Flaky	Materials of small thickness relative to the other two dimensions
Angular	Possessing well-defined edges formed at the intersection of roughly planar faces
Elongated	Materials in which the length is considerably larger than the other two dimensions
Flaky and elongated	Materials having the length considerably larger than the width and the width considerably larger than the thickness

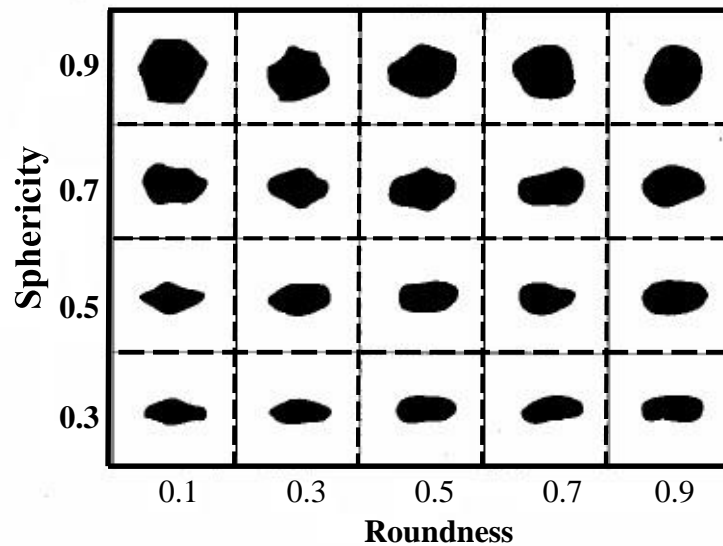


Fig. 2.4 Visual assessment of particle shape derived from measurement of sphericity and roundness (Quiroga and Fowler, 2004)

Two important aspects of shape which are desirable for concrete production are roundness and sphericity. While the roundness describes the relative sharpness of the edges and corners of a particle (Quiroga and Fowler, 2004), the sphericity measures the ratio of the surface area of the particle to its volume. A broad classification of shapes of coarse and fine aggregates are given in Table 2.2. Ahn (2000) provides two comparable charts for visual assessment of particle shape. These charts are shown in Fig. 2.4 and Fig. 2.5.

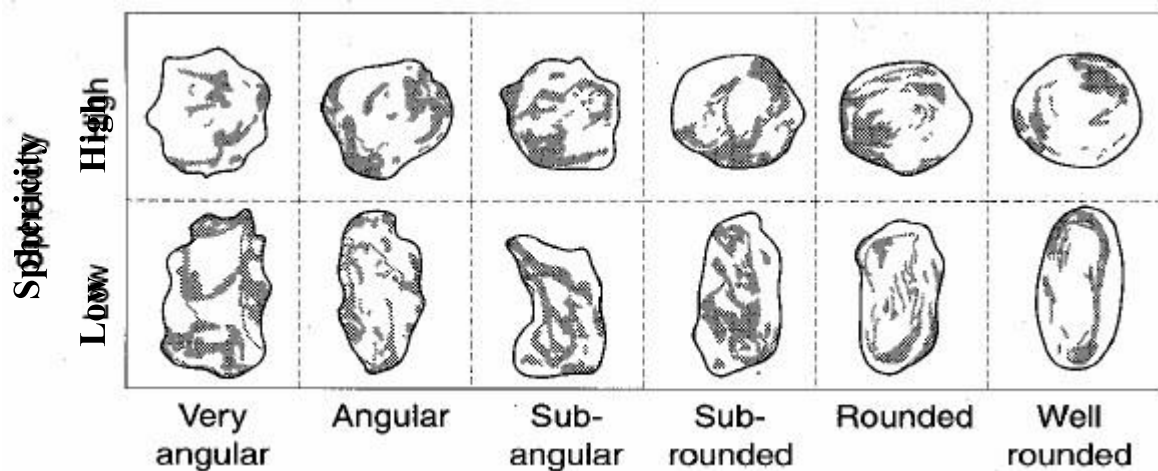


Fig. 2.5 Visual assessment of particle shape based on morphological observations (Quiroga and Fowler, 2004)

2.4.2 Flakiness and elongation indices

According to Legg (1998), flaky and elongated particles tend to produce harsh mixes and affect the extent to which concrete products can be finished. Flaky and elongated aggregates, principally those of intermediate sizes (9.5mm and 2.36 mm), can affect the mobility of aggregates and contributes to harshness (Shilstone, 1990). Excessive use of poorly shaped particles reduces the strength of concrete through increase in water demand. Additionally, flat particles can be oriented in such a way that they could weaken the

strength and durability of the concrete. During concrete production, water accumulates below elongated and flaky particles which reduce the bond between the paste and the aggregates in general (Shetty, 2005). Flakiness and elongation influence aggregate gradation, reduces interlocking characteristics, and some specifications limit the amount of flaky and elongated particles (Bambang *et al.*, 2005; Quiroga and Fowler, 2004). For example, the BS 882 (1992) allows not more than 50 percent of flaky particles for uncrushed gravel and not more than 40 percent of flaky particles for crushed gravels.

2.4.3 Texture

Graves (2006) defines surface texture of an aggregate as the degree to which the surface may be either rough or smooth, or coarse grained or fine grained. Surface texture plays an important role in developing the bond between an aggregate particle and a binding material. A rough surface texture gives the binding material something to grip, thereby producing a stronger bond (Ahn and Fowler, 2001). Roughly-textured angular grains produce better bond with the cement paste to generate higher tensile strengths (O’Flynn, 2000).

Table 2.3 Surface texture classification of aggregates (Neville and Brooks, 2008)

Surface texture	Characteristics
Glassy	Conchoidal fracture (well-shaped fracture surfaces)
Smooth	Water-worn, or smooth due to fracture of laminated or finegrained rock
Granular	Fracture showing more or less uniform rounded grains
Rough	Rough fracture of fine or medium-grained rock containing no easily visible crystalline constituents

Crystalline	Containing easily visible crystalline constituents
honeycombed	Contains visible pores and cavities

Natural aggregates have a smooth surface while the surface properties of LWAs can vary considerably from rough and porous to smooth and dense depending on the raw material and manufacturing processes (Lamond and Pielert, 2006). For manufactured lightweight aggregates, the shape and surface texture depend to a large extent on the manufacturing process (Concrete Society of UK, 1987). The classification of surface texture is based on the degree to which the particle surfaces are polished or dull, smooth or rough (Table 2.3).

2.4.4 Grading/ Particle size distribution

Concrete is produced with coarse aggregates that range from 5 mm to 50 mm size with 20 mm being very common. The grading of an aggregate is defined as the frequency of distribution of the particle sizes of a particular aggregate (Rached *et al.*, 2009; Lamond and Pielert, 2006). Particle size distribution significantly affects some properties of concrete like packing density and voids contents. Consequently, the workability, segregation, durability and some other characteristics of concrete are greatly affected (Karthik *et al.* 2007).

Past researchers have it that uniformly distributed mixtures produce better workability than gap-graded mixtures (Chandra and Berntsson, 2002; Golterman *et al.*, 1997; Glavind *et al.*, 1993), and is desirable for the efficient utilization of the matrix. Uniformly distributed aggregates lead to higher packing, which result in concrete with higher density and less

permeability (Golterman *et al*, 1997 and Glavind *et al*, 1993), and improved abrasion resistance (Mehta and Monteiro, 1993).

Table 2.4 Grading limits for lightweight aggregates (ASTM C330)

Nominal size designation	Percentage (mass) passing sieves having square openings									
	25.0 mm	19.0m m	12.5m m	9.5 mm	4.75 mm	2.36 mm	1.18 mm	300 μm	150 μm	75 μm
Fine aggregate:										
4.75 mm to 0	--	--	--	100	85-100	--	40-80	10-35	5-25	--
Coarse aggregate:										
25.0 to 4.75 mm	95-100	--	25-60	--	0-10	--	--	--	--	0-10
19.0 to 4.75 mm	100	90-100	--	10-50	0-15	--	--	--	--	0-10
12.5 to 4.75 mm	--	100	90-100	40-80	0-20	0-10	--	--	--	0-10
9.5 mm to 2.36 mm	--	--	100	80-100	5-40	0-20	0-10	--	--	0-10
Combined fine and coarse aggregates:										
12.5 mm to 0	--	100	95-100	--	50-80	--	--	5-20	2-15	0-10
9.5 mm to 0	--	--	100	90-100	65-90	35-65	--	10-25	5-15	0-10

A uniform grading requirement for coarse lightweight aggregates specified by ASTM C330 (1999) is presented in Table 2.4. According to Quiroga and Fowler (2004), size distribution divides aggregates in three categories as coarse aggregates, fine aggregates and microfines. The exclusion or inadequacy of any size fraction could result in poor workability and durability of the concrete (Shilstone, 1990). Excessive coarse aggregate can produce concrete with poor abrasion resistance while excessive sand can produce mixes requiring increased water for effective finishing. Smaller nominal maximum size of aggregate has a larger surface area compared to larger nominal size of aggregates. This results in a high

bonding strength at the interface zone around the smaller aggregate particles when concrete is under loading (Neville, 1997).

Yaqub and Bukhari (2006) studied the effect of size of coarse aggregate on compressive strength of high strength concrete. The study concluded that aggregate sizes of 10mm and 5mm showed higher strength than all other sizes of aggregates. In a separate study, Bhikshma and Annie (2013) reported of improved workability of concrete as the size of aggregates increased from 10 mm to 20 mm. Figure 2.6, taken from Neville and Brooks (2008), shows a relationship between the maximum sizes of aggregate on the 28-day compressive strength of concrete of different richness. The decrease in strength arise from the lower bond area created by the very large particles.

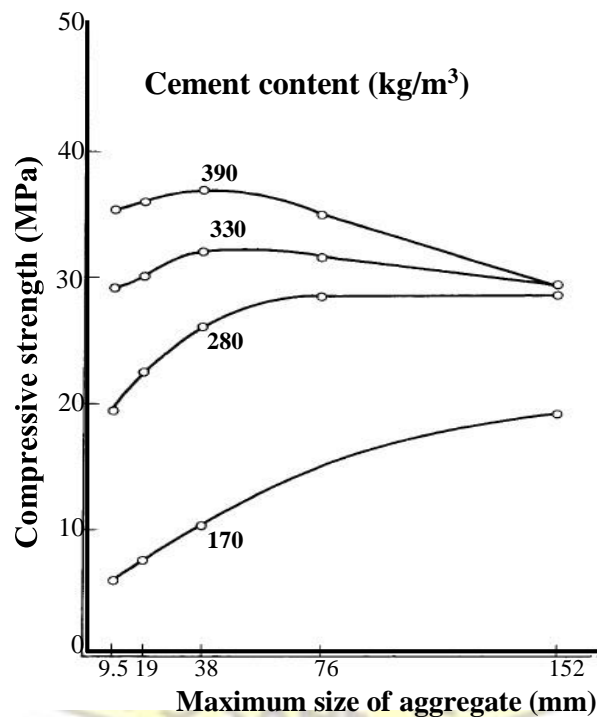


Fig. 2.6 Influence of maximum size of aggregate on the 28-day compressive strength of concretes of different grades (Higginson et al., 1963 cited in Neville and Brooks (2008))

2.4.5 Aggregate moisture content

Moisture content is the water contained in an aggregate in excess of saturated and surfacedry conditions. Since aggregates contain some voids, it is possible for water to be absorbed into the particle. Additionally, water can be retained on the surface of the particle as a film of moisture. Four moisture states of the aggregate can be defined as follows (ASTM C12707, 2007):

- i. Oven Dry (OD): aggregates are dried by heating in an oven at 110 °C for sufficient time to reach a constant mass.
- ii. Air Dry (AD): all moisture is removed from the surface, but internal pores can be partially full.
- iii. Saturated Surface Dry (SSD): permeable pores of aggregate particles are filled with water to the extent achieved by submerging in water for the prescribed period of time, but without free water on the surface of the particles.
- iv. Wet/moist: All pores are completely filled with water with film of water on the surface. These four states of aggregates are shown diagrammatically in Fig. 2.7.

Newman and Choo (2003) state that the reduction of free water/cement ratio due to the water absorption of lightweight aggregate is difficult to predict and thus the specification of effective water/cement ratio for mixes is not practicable since it is difficult to measure and verify. Free water contents of lightweight aggregates are the same as for normal weight concrete (about 180–200 l/m³). However, lightweight aggregate absorption requires higher total water contents of about 250–300 l/m³ (Newman and Choo, 2003).

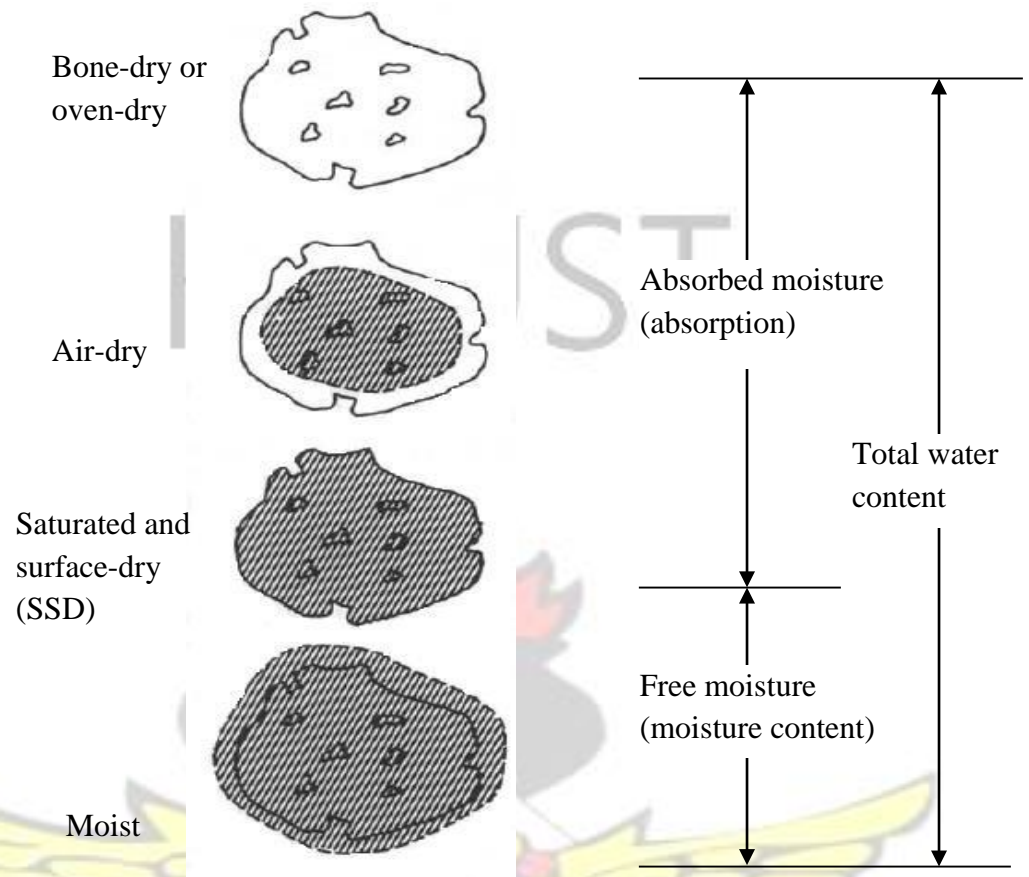


Fig. 2.7 Schematic representation of moisture in aggregate (Neville and Brooks, 2008)

2.4.6 Porosity and Water Absorption of Aggregates

BS EN 1097-6 (2000) and ASTM C127-07 (1993) define water absorption of an aggregate as the increase in the weight of the aggregate due to water being absorbed into the pores of the material during a prescribed time, but not including the water adhered to the surface of the aggregate. Aggregates with low absorption tend to reduce the amount of shrinkage and creep (Washa, 1998). The internal structure of lightweight aggregates consists of interconnected voids of varying size and shape which amounts to about 40% of the volume (Saha, 1999). Due to the open surfaces texture coupled with the large interconnecting pore structure, lightweight aggregates (LWA) absorb more water than normal weight

aggregates. The rate and total amount of water absorption depends on the pore volume, structure of the pore (whether connected or disconnected), pore distribution, characteristic of particle surface, and the initial moisture content (Clarke, 1993; Kayali and Haque, 1999). The size, number, and the continuity of the pores through an aggregate particle affect the strength of the aggregate, surface texture, specific gravity, bonding capabilities, abrasion resistance, and others.

For most LWAs the water absorption varies from 5% to 25% (Shafigh *et al.*, 2010; Newman and Choo, 2003; Concrete Society of UK, 1987). For example, the water absorption of LWAC such as expanded polystyrene concrete and pumice aggregate concrete is in the range of 3%–6% (Babu and Babu, 2003) and 14%–22% (Guduz and Ugur, 2005) respectively. Both aggregates show higher water absorption than that of NWC which is less than 1% (Newman and Choo, 2003). The water absorbed by the LWA have significant effect on the properties of freshly mixed concrete, the effective water/cement ratio and the hydration of cement. One important effect of the aggregate absorption on the freshly mixed concrete is the loss of concrete workability at the mixing stage (Liu, 2005; Punkki and Gjorv, 1995). This leads to incomplete hydration of the cement paste, lowering the strength of the hardened concrete (Lo *et al.*, 2004). Thus, the rate of initial absorption is important to foresee the loss of workability of the fresh mix (Neville and Brooks, 2008) as well as the effective water/cement ratio (ACI 211.2, 2004).

In the long term, there is more improvement in the quality of concrete containing pre-wet lightweight aggregate than with ordinary concrete (Lo *et al.*, 2004). This is due to the

improved hydration of the cement provided by the moisture available from the slowly released reservoir of absorbed water within the pores of the lightweight aggregate as illustrated in Fig. 2.8 (Ries *et al.*, 2010). The fact that absorbed moisture in the lightweight is available for internal curing has been known for more than five decades. Pioneering work on improved long term strength gains made possible by the use of saturated normal weight aggregates, was reported by Klieger (1957), who reported on the role of absorbed water in lightweight aggregates for extended internal curing. Ries *et al.* (2010) also documented the benefits of using pre-wet LWA at the time of batching and confirmed that availability of absorbed moisture within the LWA produced a higher strength concrete that was less sensitive to poor field-curing conditions.

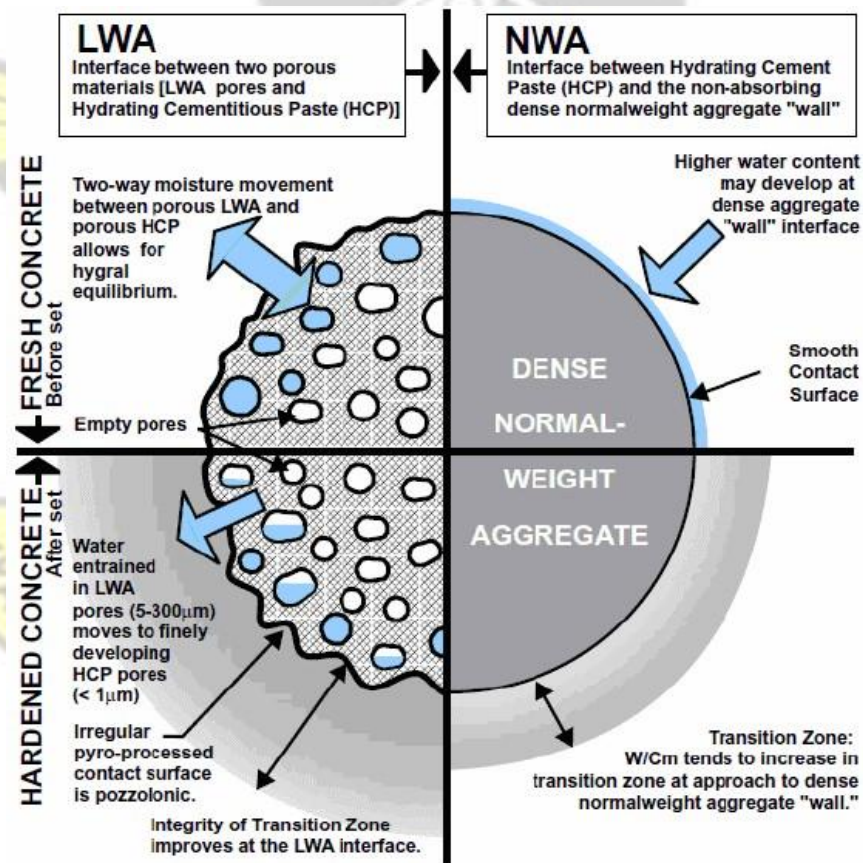


Fig. 2.8 Internal Curing at Contact Zone of aggregate (Ries *et al.*, 2010)

2.5 PALM KERNEL SHELL CONCRETE

2.5.1 Oil Palm Tree Species

The oil palm tree is a monocotyledon belonging to the genus *Elaeis*. The palm crop has two distinct parts: the fleshy mesocarp which produces palm oil, and the kernel which produces palm kernel oil (Fig 2.9). According to Sundram *et al.* (2003) the genus *Elaeis* comprises two species, namely *Elaeis guineensis* (*E. guineensis*) and *Elaeis oleifera* (*E. oleifera*). The *E. guineensis* originates from West Africa whilst *E. oleifera* is a stumpy plant of South American origin. Following the preceding background, the oil palm trees in Ghana are derived from the *Elaeis guineensis* specie. It is found mostly in the southern parts of Ghana and Nigeria. It however grows in plantations in equatorial tropics in Southeast Asia and South America in different varieties (Adzimah and Seckley, 2009; Hartman *et al.*, 1993).

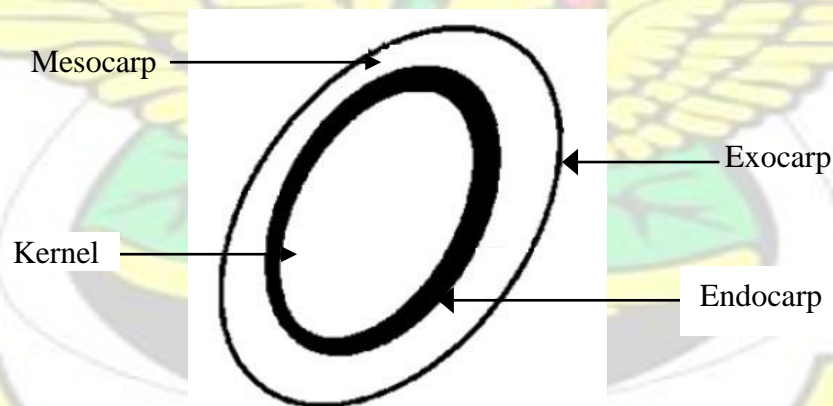


Figure 2.9 Layers of the palm fruit (Adzimah and Seckley, 2009)

2.5.2 Species in Ghana

Currently, three main species of oil palm (*E. Guineensis*) trees are found in Ghana (Adzimah and Seckley, 2009; Poku, 2002). These are:

- i. ***Dura***: This specie has a thick shell, ranging from 4-8 mm thick, separating the pulp from the kernel. The mesocarp is very thin while the kernel constitutes about 7% to 20% of the volume of the fruit. It is the most common specie used in large scale plantations in Ghana. The PKS comprises approximately 10% to 50% of the total composition of the palm oil fruitlet (Teo *et al.*, 2006b).
- ii. ***Pisifera***: This specie has virtually no shell to the kernel and is frequently female sterile. Due to marked tendency to female sterility, the *pisifera* palms are not used for commercial plantations.
- iii. ***Tenera***: This has a thinner shell of about 0.5-3 mm between the pulp and the kernel, with a fibrous layer which rounds the nut. The kernel is relatively small, comprising about 3% to 15% of fruit weight.

2.5.3 Make-up of Palm Kernel Shells

PKS are hard endocarps of the palm kernel fruit that surround the palm seeds. During palm oil processing, six stages can clearly be identified: sterilization, threshing, pressing, depericarping, separation of kernel and shell and clarification (Abdullah, 1996). PKS is obtained as crushed pieces, the sizes of which vary from fine aggregates to coarse aggregates, after the crushing of palm kernel to remove the seed, which is used in the production of palm kernel oil (Olutoge, 2010). The colour of the shells ranges from dark grey to black with a variety of shapes, such as curved, flaky, angular, polygonal, elongated, roughly parabolic, and other irregular shapes, depending on the breaking pattern of the nut (Teo *et al.*, 2006b).

The surfaces of the shells are fairly smooth for both the concave and convex faces with rough and spiky broken edges. PKS are hard in nature and do not deteriorate easily when used for concrete and therefore, does not contaminate or leach to produce toxic substances (Basri *et al.*, 1999). The thickness varies and depends on the specie of palm tree from which the palm nut is obtained and ranges from 0.15 – 8mm (Shafigh *et al.*, 2010; Teo *et al.*, 2006b; Basri *et al.*, 1999; Okpala, 1990).

PKS possess similar characteristics as coarse aggregates which encourage their use as replacement for conventional granite aggregates and the properties are summarized in Table 2.5. PKS aggregate has a unit weight of between 500 and 620 kg/m³ (Teo *et al.*, 2006b; Mannan and Ganapathy, 2001) and this is approximately 60% lighter than conventional granite aggregates. The shell has a porosity of 37% with loose and compacted bulk densities of 545 and 595 kg/m³ respectively (Mannan and Ganapathy, 2001; Okpala, 1990). This implies that the material is within the range of bulk densities for lightweight aggregate (300 to 1100 kg/m³) (Neville and Brooks, 2008). Consequently, the resulting concrete will be lightweight. The densities of fresh PKS concrete are found to be in the range of 1753–1763 kg/m³ (Okafor, 1988) depending on the mix proportions, the use of river sand and the water-cement ratio.

Okpala (1990) reported that the crushing strength of PKS aggregate as deduced from the Bache and Nepper (1998) is 12.10 N/mm² compared to a compressive strength of 181 N/mm² for granite aggregates. The slump and compacting factor values of the PKS concrete is reported to increase with increase in water/cement ratio, and decreases with increased

aggregate content (Okpala, 1990). It has been found that PKS LWC has a good thermal conductivity for low cost housing (Harimi *et al.*, 2007). This advantageous property of a good thermal performance is due to the high porosity, which results in low specific gravity as indicated in Table 2.5.

KNUST

Alengaram *et al.* (2008a) improved the mechanical properties of PKS concrete by incorporating 10% silica fume and 5% of fly ash by weight of cement. The authors used a ratio of 1: 1.2: 0.8: 0.35 (cement: sand: aggregate: water) and a cement content of 510 Kg/m³. The superplasticizer used was 1% of the weight of cement. The fresh density of the PKS concrete was found to be approximately 1880 Kg/m³ which was about 20% less than the density of NWC. Additionally, measured slump values for PKS concrete averaged 65 mm. This showed that the PKS concrete had a good consistency (moderate workability).



Shafiqh <i>et al.</i> , 2012	18.73 (10.20)	1.22	-	-	-	-	5.72	-	-	-
---------------------------------	---------------	------	---	---	---	---	------	---	---	---



2.5.4 Chemical composition of PKS

Teo *et al.* (2007) found in their study that PKS are chemically made of Nitrogen, Sulphur, Calcium (as CaO), Magnesium (as MgO), Sodium (as Na₂O), Potassium (as K₂O), Aluminium (as Al₂O₃), Iron (as Fe₂O₃), Silica (as SiO₂) and Chloride (Cl⁻). Of all the chemical components of the shells, the sulphur is a threat to the durability of PKS concrete. The attack of sulphuric acid on hydrated Portland cement could cause crack formation and disintegration of concrete. Chandra and Berntsson (2002) report that with 5% sulphuric acid, the amount of deterioration of lightweight aggregate concrete is more severe than that of normal weight aggregate concrete. Given the relatively small quantity of sulphur in the PKS (about 0.00783%) (Teo *et al.*, 2007), its effect on hydrated cement is insignificant. It is noted by Zayed *et al.* (2004) that a sulphur trioxide content beyond 3% increases drying shrinkage and strength loss for mortar. Given the relatively small quantity of sulphur in the shells, it could be concluded that the presence of the sulphur will have an insignificant effect on the strength properties of PKS concrete. Moreover, the PKS do not contaminate or leach out to produce toxic chemical substances once they are bound in concrete matrix (Basri *et al.*, 1999).

2.5.5 Mechanical Properties of PKS Concrete

2.5.5.1 Compressive Strength of PKSC

The compressive strength of concrete is the most desirable property. Earlier investigations show that PKS can be used as aggregate for producing structural LWAC (Teo *et al.*, 2007; Teo *et al.*, 2006b; Mannan and Ganapathy, 2004; Mannan and Ganapathy, 2001; Basri *et al.*, 1999; Abdullah, 1996; Okpala, 1990; Okafor, 1988). Other researchers (Alengaram *et al.*, 2008a; Olanipekun *et al.*, 2006; Mannan and Ganapathy, 2002; Okpala, 1990) have investigated the physical, mechanical and flexural properties of PKS concrete and have shown its behaviour to be

similar to that of normal weight concrete (NWC). Okafor's (1988) study on the use of PKS, found that similar to normal weight concrete (NWC), water to cement (w/c) ratio affects the mechanical properties (such as compressive strength) of PKS concrete.

Abdullah (1996) obtained a compressive strength (f_{cu}) of 20 N/mm² with a water-cement ratio of 0.4, for LWC using PKS as aggregates. Using the ACI method of mix design, Mannan and Ganapathy (2001) reported that the compressive strength of PKS concrete was 13.65 N/mm² instead of a target strength of 28 N/mm². Mannan and Ganapathy (2002) demonstrated that by using 480 kg/m³ cement, a water to cement ratio of 0.41 and mix proportion of 1:1.71:0.77 by weight (cement: sand: PKS aggregate), the 28-day compressive strength of PKS concrete was between 20 and 24 N/mm² depending on the curing condition without any additive. These results show that PKSC attain the strength of more than 17 N/mm², which is a requirement for structural LWC as per ASTM C330 (Kosmatka *et al.*, 2003).

In a recent study, Mannan *et al.* (2006) improved the quality of PKS aggregates and decreased the water absorption of PKS aggregates by about 82% to obtain a compressive strength of 39.2 N/mm². The study improved the quality of PKS by pre-treating the PKS aggregates with 20% poly vinyl alcohol and thus improved the bond between the PKS and cement paste. Some of the mechanical properties of PKS concrete, reported by various researchers, are summarized in Table 2.6.

Table 2.6 Mechanical properties of PKS concrete at 28-days of curing

Author (s) (year)	w/c ratio	Mix proportions	Slump (mm)	Compressive strength (N/mm ²)	Tensile strength (N/mm ²)
Okafor (1988)	0.48	1:1.7:2.08	8	23	6.20
	0.54	1.188:2.18	28	22	5.50
	0.65	1.21:1.12	50	16	4.30
Okpala (1990)	0.50	1:1:2	30	22.2 19.8	2.81
	0.60		63	16.5	2.53
	0.70		Collapse	14.9	2.30
	0.80		collapse		2.13
Mannan and Ganapathy (2001)	0.53	1:2.73:0.85	0	13.65	-
Mannan and Ganapathy (2002)	0.41	1:1.71:0.77	-	24.22	4.00
Olanipekun <i>et al.</i> (2006)	0.50	1:1:2	-	17.5	-
Teo <i>et al.</i> (2007)	0.38	1:1.66:0.60	60	28	-
Mahmud <i>et al.</i> (2009)	0.35	1:1:0.8	160	26.98	2.79
Alengaram <i>et al.</i> , (2011)	0.300.35	1:0.8:1 (5% fly ash;	-		-
	0.35	10% silica fume) 1:1.0/1.2/1.6:0.8 (5% fly ash; 10% silica fume)			
Shafigh <i>et al.</i> , (2011)	0.38	1:1.74:0.72 (steel fibres)	-	39.34-44.95	5.42-7.09
Alengaram <i>et al.</i> (2010)	0.35	1:1.2:0.80	105	37.41	3.70
				25.8 – 30.30	

2.5.5.2 Modulus of rupture

The modulus of rupture (MOR) of PKS concrete is reported to be in the range of 4.3 N/mm² to 6.2 N/mm² (Shafigh *et al.*, 2011; Mannan and Ganapathy, 2002; Okafor, 1988). Figure 2.9 shows a relationship between modulus of rupture and the compressive strength of PKSC and expanded

clay lightweight aggregate concrete at 28 days as reported by Shafigh *et al.* (2010). Mathematically, it was established that the flexural tensile strength (f_r) of PKSC could be calculated using equation 2.9.

$$f_r = 0.33 \left(\sqrt[3]{f_{cu}^2} \right) \quad (2.9)$$

A study by Mahmud *et al.* (2009) confirmed that the relationship between the flexural tensile strength and the compressive strength of PKS concrete could be presented by equation 2.10.

$$f_r = 0.3 \left(\sqrt[3]{f_{cu}^2} \right) \quad (2.10)$$

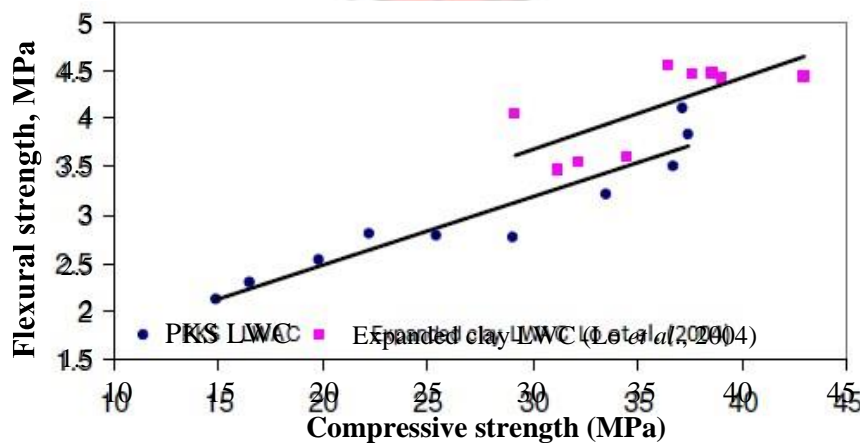


Fig. 2.10 Relationship between 28 day flexural and compressive strength (Shafigh *et al.*, 2010)

Lo *et al.* (2004) and the FIP manual (1977) give the relationship between the flexural tensile strength and the compressive strength of LWC, made with expanded shale and clay aggregates, by equations 2.11 and 2.12 respectively.

$$f_r = 0.69 \sqrt{f_{cu}} \quad (2.11)$$

$$f_r = 0.46 \left(\sqrt[3]{f_{cu}^2} \right) \quad (2.12)$$

The above equations (2.9 to 2.12), show that the flexural tensile strength of PKS LWC is generally lower than that of LWC made with artificial lightweight aggregates (Shafigh *et al.*, 2010).

2.5.6 Structural behaviour of PKS Concrete beams

2.5.6.1 Flexural strength behaviour of PKS beams

The flexural behaviour of reinforced PKS concrete beams was reported by Alengaram *et al.* (2008b) and Teo *et al.* (2006a). Three singly and doubly reinforced beams with different amount of reinforcement ratios were tested by the four-point load method (Teo *et al.*, 2006a). All the PKS beam specimens showed typical structural behaviour in flexure and yielding of the tension steel occurred before crushing of the compression concrete in the pure bending zone (Alengaram *et al.*, 2013). For beam specimens up to a reinforcement percentage of 3.14%, the experimental ultimate loads were 4% to 35% higher compared to the prediction by BS 8110. The experimental ultimate load obtained was 6% lower compared to the predicted BS 8110 load for PKS beam specimens with reinforcement of 3.9 percent. Vertical flexural cracks were observed in the pure moment zone and final failure occurred due to crushing of the concrete in the compression zone with significant amount of deflection at failure. Since all the beams were under-reinforced, it was reported that yielding of the tensile reinforcement occurred before crushing of the concrete in the pure bending zone. A comparison between the experimental moments (M_{ult}) and the theoretical design moments (M_{exp}) revealed a closer relationship for doubly reinforced beams than singly reinforced ones (Alengaram *et al.*, 2013; Teo *et al.*, 2006a).

Alengaram *et al.* (2011a) also compared grade 30 PKSC beams with normal weight concrete beams in relation to their mechanical and structural properties. Both PKSC and NWC beams demonstrated flexural failure associated with yielding of the longitudinal reinforcement before crushing of concrete in compression zone. Flexural cracks were observed and extended to the neutral axis for both types of concrete. Meanwhile the PKSC beams failed in a ductile manner which allowed sufficient warning compared to the brittle failure mode of the NWC beams. It was

further noted that experimental moments in PKSC beams were slightly higher than NWC beams. The experimental deflections obtained at service stage were all close to the deflections predicted by BS 8110 code compared to the ACI code and were within the allowable limit of 8.4 mm as stipulated by the BS8110 code for structural use. The study concluded that reinforced PKS concrete beams showed higher ultimate shear-strength-to-density ratio than that of normal weight concrete. It was concluded that ACI 318-08 (2008) and BS 8110-1 (1997) underestimate the shear capacity of PKS concrete.

Pull-out tests on PKS concrete to study the bond strength of PKS concrete and reinforcing steel was conducted by Teo *et al.* (2007, 2006b). The study found that depending on the curing condition and size of bar, the 28-day bond strength for plain and deformed bars varied from 3.0 – 5.59 N/mm² and 6.32 – 9.36 N/mm² respectively. It was further reported that the bond compression failure at earlier ages of the samples (3 to 28 days) could be attributed to the failure of the bond between aggregate and the cement matrix, where the crack paths propagated around the aggregates. On the other hand, compression failure at latter ages (56-180 days) was observed to occur through the PKS aggregates. Alengaram *et al.* (2010b) found that the bond strength of PKSC was about 86% of NWC of grade 30 N/mm². However, the ultimate experimental bond strength was found to be about 2.5 times higher than the theoretical values calculated using BS 8110.

2.5.6.2 Shear strength of PKS concrete beams

Alengaram *et al.* (2011a) reported on the shear behaviour of reinforced PKS concrete beams and NWC beams. The concrete compressive strength was 30 N/mm². The authors employed four beams without shear reinforcement and four beams with shear reinforcement. The authors

concluded that ultimate shear strength-to-density ratios obtained for the beams with and without shear reinforcement were 49% and 22% higher than corresponding NWC beams respectively. Additionally, the shear strength ratios between the experimental and predicted values based on the BS8110, ACI and EC2 code of practice ranged from 1.57 to 2.83. Thus, all the three codes underestimated the actual shear strength of PKSC and NWC beams with and without shear reinforcement. This was attributed to the good aggregate interlock mechanism suggested by Jumaat *et al.* (2009).

Jumaat *et al.* (2009) reported on an experimental study carried out to compare the shear strength of oil palm shell foamed concrete (OPSFC) beams and normal weight concrete (NWC) beams with a compressive strength of 20 N/mm². The study employed a total of eight specimen beams with four beams with and without shear reinforcement each. It was reported that the shear strength of OPSFC beam specimens without shear reinforcement performed better than corresponding NWC beam specimens by about 10%. It was further reported that beams with shear reinforcement exhibited “zig-zag” shear cracks on both sides of the beam specimens. Further examination of the OPSFC beam specimens showed rougher shear failure surfaces than those of NWC beam specimens. This was attributed to the convex nature of the PKS which contributed to good aggregate interlock and a subsequent higher shear resistance. It was further reported that the convex portion of the PKS contributed to good bonding with the cement mortar, and hence, provided a higher resistance against bond failure between the PKS and cement matrix, else a lower shear resistance would have resulted.

2.6 SHEAR TRANSFER MECHANISM IN BEAMS

2.6.1 Introduction

The behaviour of reinforced concrete (RC) elements in flexure has been well established such that their flexural strengths can be predicted with reasonable accuracy. Contrary to the flexural behaviour of structural members, sophisticated approaches have been proposed based on fracture mechanics, Artificial Neural Network (ANN), physical models of structural failure, and finite element analyses (Song *et al.*, 2010; Oreta, 2004) to predict the behaviour of beams in shear. Experiments have been conducted to understand shear failure of RC beams with and without stirrups for a wide range of concrete strengths, longitudinal reinforcement ratios, effective depths, and span lengths subjected to both concentrated and distributed loads (Oreta, 2004). That notwithstanding, no single theory is available for estimating the precise shear strength of reinforced concrete elements. This problem has been attributed to the complex nature of the shear transfer mechanisms, especially after cracks are initiated (Song *et al.*, 2010). The major difficulties in developing a theoretical expression for the shear strength of RC beams are due primarily to the indeterminacy of the internal force system of a cracked reinforced member, the non-homogeneity of concrete, and the nonlinearity of its stress–strain diagram (Oreta, 2004).

Research has shown that the resistance of reinforced concrete members to shear is the summation of several internal shear transfer mechanisms (Hawkins *et al.*, 2005). The various shear transfer mechanisms in accordance with the report by a joint ASCE-ACI Committee 426 (1973) and ASCE-ACI Committee 445 (1998) is illustrated in Fig. 2.11

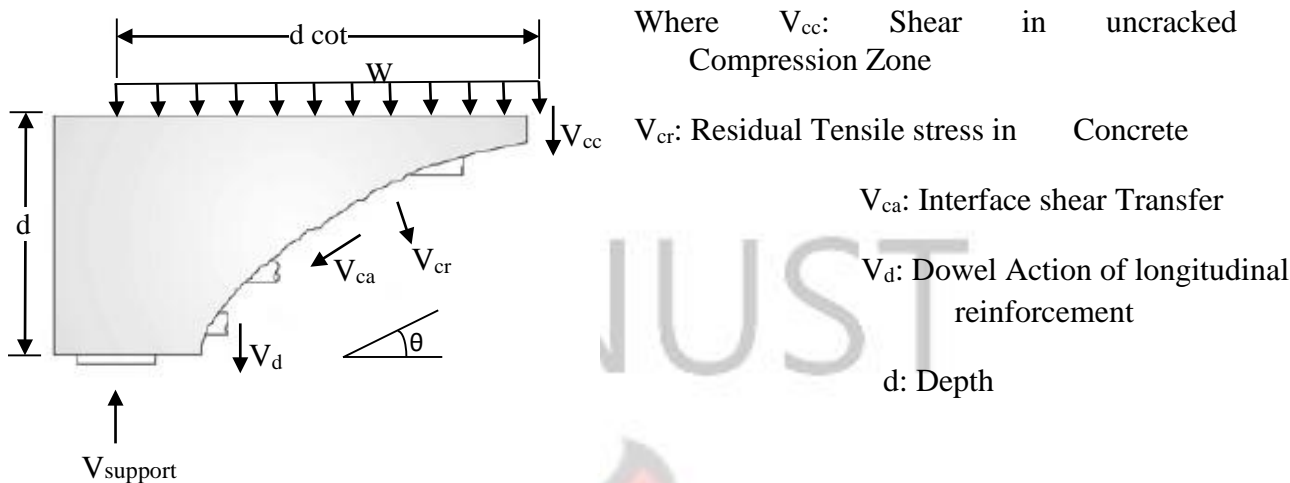


Fig. 2.11 Shear transfer contributing to shear resistance (Jung and Kim, 2008)

These transfer mechanisms include shear in the uncracked compression zone (20%-40%), vertical component of aggregate interlock or interface shear transfer (35%-50%), dowel action of the longitudinal reinforcement (15%-25%) (Adom-Asamoah and Afrifa, 2013; Alengaram *et al.*, 2011b), residual tensile stresses across the crack, and the tensile stresses induced in the shear reinforcement (Jung and Kim, 2008). This shows that a major component of the shear transfer in the fractured interface is generated from the frictional forces that develop across the diagonal shear cracks due to “aggregate interlock” which provides resistance against slip (Hassan *et al.*, 2008).

Shear transfer mechanism through aggregate interlock is complex due to the several mechanisms involved in the interaction between normal and shear stresses at a cracked section. The fracture mode of the concrete is a very important aspect of interface shear transfer. In NWC members, cracks usually travel around the aggregates which result in protruding aggregate particles on the crack face to provide resistance against slip (Slobe, 2012). In most lightweight and high strength concrete members, cracks travel through the aggregates. This results in smooth crack surfaces

with corresponding reduction in shear transfer across the crack. Secondly, the size of aggregate a , the crack width w and the compressive strength f_c' are important aspects of interface shear transfer. The shear stress on the crack, v_{ci} can be determined using the modified compression field theory that which combines these parameters as follows (Benz *et al.*, 2006):

$$v_{ci} \leq \frac{0.18\sqrt{f_c'}}{0.31 + \frac{24w}{a+16}} \quad (2.13)$$

Considering beams with shear reinforcement, the truss model used for predicting the shear strength of members is known to provide reliable results. This model assumes that a cracked reinforced concrete beam acts like a truss with parallel longitudinal chords, a web composed of diagonal concrete struts, and transverse steel ties. This ensures that when a force is applied to the truss, the force component in each section of the member (both compression and tensile zones) could be determined by statics.

Shear stresses in the uncracked compression zone of the concrete contribute to the shear resistance in a concrete member. The magnitude of the transferring shear force depends on the depth of the compression zone (Slobe, 2012). In over-reinforced concrete members where there is a relative reduction in the effective depth of the concrete section, the contribution of the compression zone becomes minor. In a slender beam without axial compression, the shear force in the compression zone has a minor contribution to the shear capacity, because of a relatively small depth of the compression zone.

2.6.2 Influencing factors on the failure mechanisms

Kong and Evans (1998) summarized a host variable's contributions towards ultimate shear failure of normal weight concrete beams without shear reinforcement. The influences of the most

dominant variables are concrete strength, size effect, span-to-effective depth ratio, longitudinal reinforcement ratio, axial force, and several other influencing parameters such as support conditions, loading points, etc. However, the truss model ignores the compressive force in the uncracked compression zone of the concrete which makes it over-conservative (Waner *et al.*, 1999). The effect of the major influencing factors have been explained below.

2.6.2.1 Effect of shear span-to-effective depth ratio, a/d

The cracking behaviour of a reinforced concrete beam without shear reinforcement after cracking depends mainly on the shear span-to-depth ratio (a/d). Kani (1967) revealed that the shear span-to-depth ratio (a/d) of 2.5 marks the transition between different failure modes and is the same for different member sizes and longitudinal reinforcement ratios. In short span beams (a/d smaller than 2.5) the beam develops a compression arch which increases the beams' ability to transfer significant loads after diagonal cracking. Failure usually occurs with accompanied concrete crushing of the compression zone.

Considering a simply supported beam with symmetrical two-point loading without shear reinforcement, the shear at flexure failure, shear failure and for inclined cracking with a constant depth is plotted in Figure 2.12.

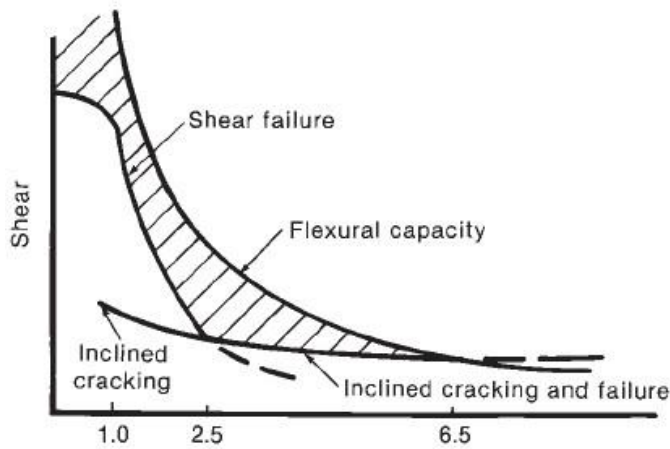


Fig. 2.12 Shear at cracking and failure (adapted from Wight and Macgregor, 2012)

From Figure 2.12, for slender beams ($2.5 < a/d < 6.5$) a brittle diagonal-tension failure occurs shortly after the formation of a dominant diagonal crack (Slobe, 2012; Ghannoum, 1998). This is because the compression strut which is required for arching action does not form due to the long shear span distances (Yap, 2012). Stresses are unable to be distributed from the point of loading to the supports and will therefore fail once the beam action precipitates. Meanwhile, very slender beams with a/d greater than 6.6, the beam will fail by flexure before any inclined cracking is developed. The developed diagonal crack propagates quickly after initiation and is usually accompanied by concrete spalling along the tension reinforcement. However, this transition point becomes more critical in over-reinforced beams and almost disappears in specimens with lower reinforcement ratios.

2.6.2.2 Effect of beam size

The size of a beam is an important factor affecting the shear strength of reinforced concrete beams. Size effect occurs in normal weight concrete beams with and without shear reinforcement (Bazant and Kim, 1984; Bazant and Sun, 1987). The shear strength of reinforced concrete beams without shear reinforcement decreases as the member depth increases, which is called the “size effect” in

shear. Tests by Kani (1967) on size effect first demonstrated this effect. The main reason for this size effect is the result of larger width of diagonal cracks in larger beams which reduce the residual stresses and the ability to transmit crack interface shear stresses (Slobe *et al.*, 2012). Bazant and Sun (1987) have revealed that the failure of concrete is primarily due to the release of strain energy from the beam into the cracking zone as the cracking zone extends; the larger the structure, the greater is the energy release. According to the theory of fracture mechanics, concrete exhibits size effects of two different modes. First is the size effect in failures occurring at macro-crack initiation, which is typical of plain concrete while the second is the size effect in failures occurring after large stable crack growth, which is typical of reinforced concrete beams. The latter is caused by the release of energy associated with stress redistribution caused by a large crack (Qiang and Bazant, 2011).

2.6.2.3 Concrete strength

The increase in concrete strength results in increase of the dowel action capacity, the aggregate interlock capacity and the compression zone capacity. This results in a corresponding increase in the shear capacity of the concrete. In many design codes this relation is directly included in the formulas for shear strength (Slobe, 2012). It is known that the bond strength between the tension reinforcement and concrete increases as the concrete strength is increased.

2.6.2.4 Aggregate type

The type of aggregate influences the aggregate interlock mechanism with different aggregate crushing strength, impact strength and abrasion strength, which in turn affects the shear strength of the concrete beam. Depending on the type of aggregate and the resulting bond between the aggregate and the paste, fracture through the aggregate results in smoother crack surfaces which

reduces the shear transfer through aggregate interlock (Sagaseta and Vollum, 2011). While studies by Walraven and Stroband reports that aggregate fracture reduced the shear strength of high strength concrete push-off specimens, no significant reduction in shear strength was noticed in LWAC with stirrups by Walraven and Al-Zubi (1995). In a separate study, Hamadi and Regan (1980) revealed that the shear strength of expanded clay LWAC beams with shear reinforcement decreased through aggregate fracture.

2.6.2.5 Percentage of Tension steel

The shear strength is affected by the percentage of tension reinforcement as lower percentage of tension steel results in the reduction of shear strength. This is because of the decreased dowel shear capacity and increased crack widths, which reduce the aggregate interlock capacity of the section. Beams with a relatively low percentage of longitudinal reinforcement may fail at very low shear stresses. This reduction of shear capacity can be attributed to the fact that a lower amount of reinforcement generally results in an increased crack width, which leads to lower interface stresses and residual stresses (Slobe, 2012). Also the dowel action is reduced when the longitudinal reinforcement ratio decreases.

2.6.3 Behaviour of Lightweight Aggregate Concrete in shear

Generally, it is assumed that LWC is weak in shear due to its lower tensile strength. Considering shear and diagonal tension, these properties are completely different to require design modifications. Attempts to address this issue in codes of practice have generally resulted in imposing reduction factors to normal weight concrete equations (Juan, 2011). This is because although LWC has higher material tensile strength, under air drying which is the case in practice,

it will generally have a lower tensile strength than normal weight concrete of equal compressive strength.

The simplest approach to predicting the shear strength of a reinforced concrete section without shear reinforcement has been to relate the average shear stress at failure to the tensile strength of the concrete (Vecchio and Collins, 1988) and this is still the basis of the ACI Building Code and other international codes of practice (ASCE-ACI, Committee 445). Woo and White (1991) have reasoned that a non-uniform shear stress distribution at the outermost flexural crack as a result of a concentration of bond stresses and a reduction of the internal lever arm due to arch action in the flexurally cracked zone is the reason for the low average stress at flexure-shear cracking (Juan, 2011).

In RC structures, the provision of minimum shear reinforcement is mandatory in most design codes of practice primarily to prevent sudden brittle failure after reaching the first diagonal cracking load and to control widening of cracks at service loads. In members with shear reinforcement, the shear strength is assumed to be provided by the concrete (V_c) and the remainder by the shear reinforcement (V_s). The shear reinforcement significantly enhances the shear strength of beams, primarily due to the formation of compression strut inclined at 45° , provides a better dowel action, restrains crack propagation and minimizes bond splitting failures at tension steel levels.

2.6.4 Shear cracking and crack width

When reinforced concrete beams are subjected to shear forces, shear cracks form diagonally with an inclination towards the neutral axis of the beam (Zakaria *et al.*, 2009). The width of a crack in

a reinforced concrete member is partly contributed by the elastic recovery of the concrete at the formation of the crack and partly by relative slip between steel and concrete. As the concrete reaches its flexural strength, primary cracks form. The width of cracks generally depends on the spacing of cracks; the more the number of cracks within a given length, the smaller will be the crack width. With increasing use of high strength materials, both steel and concrete, exploitation of various types of LWC, and the employment of ultimate strength design.

The number and the length of cracks also depend on the size and placement of the reinforcing steel (Hyo-Gyoung and Filippou, 1990). Upon the initiation of the primary cracks the concrete stress reduces to zero and the steel carries the entire bending stress. The concrete between the cracks, however, still carries some bending stresses, which decreases as the magnitude of applied load increases (Hyo-Gyoung and Filippou, 1990). This reduction in concrete bending stress with increasing load is associated with the breakdown of bond between reinforcing steel and concrete. A secondary system of internal cracks develops around the reinforcing steel, which begins to slip in relation to the surrounding concrete (Hyo-Gyoung and Filippou, 1990).

After cracking, shear is resisted by aggregate interlock, dowel action of the main reinforcing bars and the resistance of the uncracked concrete in the compression zone of the beam. If the cracks are wider, the aggregate interlock mechanism will fail and be rendered ineffective. Also, as the concrete strength increases the crack surfaces become smoother and consequently more dowel action is required. Thus the shear capacity of lightly reinforced members may not increase for higher concrete strengths unless the cracks are contained, either by the addition of stirrups, for example, or increasing the percentage of longitudinal reinforcement.

The shear behavior of reinforced lightweight pumice concrete and lightweight foamed concrete (LWFC) were studied by Lim (2007). The compressive strength of the lightweight aggregate concrete was between 20 to 90 MPa and density ranged from about 1500 to 2000 kg/m³. The study concluded that, the cracking performance of a LWC beam with respect to the number of cracks and maximum crack width at anticipated service load was marginally better than its normal weight concrete counterparts.

2.6.5 Code provisions against shear failure for lightweight concrete

Provisions for design of reinforced concrete members in shear appear in majority of international standards of concrete design. Most of these codes of practice use sectional methods for the design of conventional beams under shear. However, in all codes of practice, the shear strength is based on an average shear stress on the overall effective cross section ($b_w d$). In members without shear reinforcement, shear is assumed to be transmitted by the concrete web (V_c). In members with shear reinforcement, a portion of the shear strength is assumed to be resisted by the concrete (V_c) and the shear reinforcement (V_s). The shear strength provided by concrete is assumed to be same for beams with and without shear reinforcement and is considered as the shear causing significant diagonal shear crack. These assumptions are similar for most Standards but there exist some variations in influencing factors considered in determining the values of V_s and V_c , thereby resulting in different results (Table 2.7). Provision of some of the more well-known standards for beams without shear reinforcement are reviewed in this section.

2.6.5.1 Provisions in BS 8110 (1997)

Failure of a concrete beam is brittle in nature and if shear reinforcement is not provided, failure could occur without warning. To avoid brittle failure, the British Code BS 8110 (1997) (section

3.4.5.4 and Table 3.8) considers major factors which affect the shear strengths of reinforced concrete elements. Flexural reinforcement ratios are considered by the term in the first parenthesis

$$\left(\frac{100A_s}{b_v d}\right) < 3\%$$

, while shear span-to-effective depth ratios are simplified into the term in the second parenthesis $\left(\frac{400}{d} \geq 1\right)$. The characteristic compressive strength of the concrete is considered for concrete strengths ranging from 25 MPa to a maximum of 40 MPa in the third

parenthesis $\left(\frac{f_{cu}}{25}\right)^{1/3}$. The code further introduces a factor of $2\frac{d}{a}$ to account for the effect of shear span-to-effective depth ratios up to 2.0. The code imposes a factor of 0.8 for LWC of strength ranging from 25 MPa to 40 MPa. Clarke (1987) suggested that for beams without shear reinforcement, the factor can be increased to 0.9. The code however provides an alternative Table based on the longitudinal reinforcement for concrete strengths below 25 MPa. For design purposes, a material partial safety factor, $\gamma = 1.15$ for steel and 1.5 for concrete, is included in the equation (Table 2.7).

2.6.5.2 Provisions in EC 2 (2004)

The section 6.2 of the Eurocode 2 adopts a semi-empirical equation for members which do not require shear reinforcement. A general equation is given with values $C_{Rd,c}$, k_1 and k subject to variations specified in national annexes of countries within the CEN. The equation considers the cylinder concrete strength (f_{ck}), longitudinal reinforcement ratio ($\rho \leq 0.02$), effective depth of the member (d) and shear span to effective depth ratio (a/d) in the shear strength prediction for normal weight concrete beams without shear reinforcement. The recommended value of $C_{Rd,c}$ is provided as $0.18/\gamma_c$ for NWC while the factor is reduced to $C_{Rd,c} = 0.15/\gamma_c$ for LWC. Another reduction factor which depends on the density of the lightweight aggregate concrete is also adopted in the

general equation. The coefficient is taken as 60% of the normal weight concrete by the ratio of the upper limit of the appropriate density class to the density of normal weight aggregate concrete (2200 kg/m³). The reduction factor becomes $\eta_1 = 0.40 + \frac{0.60\rho}{2200}$. The final equation incorporating these factors has been simplified into equation 2.14 for members not requiring shear reinforcement.

$$V_{RD,C} = [C_{IRD} C_{N1} k(100\rho_1 f_{ck})^{1/3 + k_1 \sigma_{cp}}] bwd \quad (2.14)$$

For members with shear reinforcement, the code predicts the shear strength, $V_{Rd,s}$ based on equation 2.15

$$V_{Rd,s} = \frac{A_{sw}}{s} Z f_{ywd} \cot\theta \quad (2.15)$$

2.6.5.3 Provisions in ACI 318 – 08 (2008)

The ACI 318-08 (2008) code also defines the critical shear strength, V_c of a concrete beam as the stress at the occurrence of the first critical inclined crack. The critical diagonal stress responsible for the crack propagation is the result of the shear stress due to the externally factored shear force, V_u and the horizontal flexural stress due to external bending moment M_u . The code adopts a reduction factor of 0.85 for sand-lightweight aggregate concrete while a factor of 0.75 is assumed for all-lightweight aggregate concrete (Section 11.2 of ACI 318-08). $\lambda\sqrt{f'_c}$ measures the concrete tensile strength while ρ_w defines the effect of longitudinal ratio. The quantity $V_u d / M_u$ shall not be greater than 1.0 in computing V_c . The shear span to depth ratio, a/d , is often replaced by the quantity $M_u = V_u d$. ACI-ASCE Committee 426 reports that the equation overestimates the influence of f'_c and underestimates the influence of ρ_w and $V_u d / M_u$. Hence, the sensitivity of

failure shear stress to size and reinforcement ratio was not recognized (Oreta, 2004). Many other researchers have raised imperfections with this equation since it underestimates the effects of the shear span-to-depth ratio and the tensile reinforcement ratio on the shear strength, overestimates the effect of the compressive strength and only predicts the cracking shear strength (Sarsam and Al-Musawi, 1992; Mphonde and Frantz, 1984). Additionally, the equation does not properly account for the difference in behaviour between the arch action of short beams and the beam action of long, slender beams principally due to the underestimation of the shear span to depth ratio.

The design of shear reinforcement is based on a modified truss analogy that the total shear is carried by shear reinforcement. However, considerable research has indicated that shear reinforcement needs to be designed to carry only the shear exceeding that which causes inclined cracking, provided the diagonal members in the truss are assumed to be inclined at 45 degrees (ACI 318-08). When the factored shear force V_u exceeds the shear strength provided by the concrete (ϕV_c), shear reinforcement should be provided to transmit the excess shear. The contribution of the shear reinforcement is calculated as:

$$V_S = \frac{A_v f_{yt} d}{s} \leq 0.66 \sqrt{f'_c} b_w d \quad (2.16)$$

Table 2.7 Different approaches to Shear Design

Approach	Shear Strength due to concrete, V_c	Shear Strength due to stirrup, V_s
BS 8110 - 97	$V_c = \frac{0.79}{\gamma} \left[\left(\frac{100 A_s}{b_v d} \right)^{1/3} \times \left(\frac{400}{d} \right)^{1/4} \times \left(\frac{f_{cu}}{25} \right)^{1/3} \right] b d$	$V_s = \frac{A_{sv}}{S_v} \times 0.95 f_y d$
EC 2 - 2004	$V_{RD,C} = \left[0.12 \left(1 + \sqrt{200/d} \right) (100 \rho_1 f_{ck})^{1/3} + \frac{0.1 N_{ED}}{A_c} \right] b d$	$V_{RD,S} = \frac{A_{sw}}{S} Z f_{ywd} \cot \theta$

$$V_c = \left[0.16\lambda\sqrt{f'_c} + 17\rho_w \frac{V_u d}{M_u} \right] b_w d$$

$$V_s = \frac{A_v f_{yt} d}{S}$$

V_c : Shear strength provided by concrete; f'_c : Concrete compressive strength; b_w : Web width; d : Effective depth; V_u : Shear force; M_u : External moment; ρ_1, ρ_w : Longitudinal reinforcement ratio; N_{ED} : Axial force; A_c : Cross sectional area of concrete; λ : modification factor reflecting the reduced mechanical properties of lightweight concrete; Z : Lever arm; f_y : tensile strength of longitudinal reinforcement; V_s : shear strength contributed by shear reinforcement.

2.7 FLEXURAL THEORY OF RC TWO-WAY SLABS

Reinforced concrete slabs on columns are used for construction because of their simplicity (simple formwork and reinforcement, flat soffit allowing an easy placement of equipment, and installation underneath the slab) (Muttoni, 2008). The design of slab-column connection is considered as the most critical point in the design of slabs, because of the concentration of shear stresses around this area that can lead to punching (Sacramento *et al.*, 2012). Punching failure is a localized failure mode that can occur without significant warnings and may subsequently lead the whole structure to ruin through the progressive collapse (Sacramento *et al.*, 2012). For a twoway slab simply supported along its four edges, and loaded concentrically, the ultimate moment of resistance based on the yield line method of analysis may result in one of two failure mechanisms (Adom-Asamoah and Kankam, 2008), namely:

(a) Diagonal yield line pattern ($P_{ult} = 8 M_{ult}$)

(b) Circular fan pattern ($P_{ult} = 2\pi M_{ult}$)

Theoretically, punching shear strength is estimated to be made up of the concrete section alone and the combined action of both concrete section and tension reinforcement (BS 8110-1, 1997).

The critical section is considered based on a perimeter distant $1.5h$ from the boundary of the loaded area where ' h ' is the overall slab thickness. Considering a loading platen of diameter 127 mm, the length of the critical perimeter, L is given by equation 2.17.

$$L = (127 + 1.5h)\pi \quad 2.17$$

The effective area, A , over which shear is critical is given by $A = L \times d$

2.6.6 Summary

It is clear that LWC brings many advantages as a structural material both in practice and as a medium for research to further unravel the mechanisms of shear resistance. The properties of aggregates for structural concrete production are very essential in the production of quality structural concrete from concrete materials. However, PKS aggregates are still emerging agricultural by-product for concrete production. Thus, the current understanding about the shear resistance of PKSC beams with and without shear reinforcement are still lacking and only a limited study (Jumaat *et al.*, 2009; Alengaram *et al.*, 2011a) has been carried out in spite of the nearly three decades of research. In addition, the design provisions for design against shear failures in beams with and without shear reinforcement have not been fully explored in the codes of practice. The investigations carried out have not been covered adequately to validate that the design code provision for normal weight concrete beams is completely suitable to be adopted for the shear strength predictions of PKS concrete beams. Therefore, it is considered that there is a need for an experimental study to understand the shear strength of PKS concrete beams with and without shear reinforcement, and to determine whether the current design codes for normal weight concrete beams are applicable for PKS concrete beams.

CHAPTER THREE

MATERIALS AND METHODS

3.1 INTRODUCTION

The primary objectives of the study were to investigate the physical properties of PKS aggregates, the mechanical properties of PKS concrete (LWAC), the behaviour of reinforced PKS concrete beams and the behaviour of PKS reinforced concrete two-way slabs. Therefore, the physical properties of PKS aggregates, the mix compositions, and the mechanical properties of hardened concretes that affect the short-term structural response of PKSC beams are discussed. The materials used in the preparation of the concrete are discussed under each objective. The methodologies involved in the determination of concrete properties, namely density, compressive strength and flexural strength are also discussed. Beam preparations and specifications, with the objective of investigating the complete response of reinforced PKS concrete short span and long span beams are discussed. Additionally, the methodologies involved in the preparation of the PKS reinforced concrete two-way slabs have also been discussed.

3.2 TEST MATERIALS

3.2.1 Cement

The cement types used in this study were Portland-limestone cement (CEM II/B-L) and ordinary Portland Cement (OPC) conforming to BS EN 197-1 (2000). The CEM II/B-L and OPC conform to strength classes 32.5R and 42.5N respectively as specified in BS EN 197-1 (2000). Both types of cement are readily available for producing concrete both in the laboratory, and on the market for other construction activities.

3.2.2 Water

Water is required in the production of concrete for hydration of cement, to wet the aggregate, and to lubricate the mixture for easy workability. Contaminated water is destructive to the strength and setting properties of cement. It can also disrupt the affinity between the aggregate and the

cement paste which can adversely affect the workability of a mixture (Nawy, 2008). In this study, clean water conforming to BS 1348-2 (1980) was used for mixing the materials and curing the concrete samples.

3.2.3 Superplasticizer

Superplasticizers are admixtures that are used as ingredients in concrete to improve the workability of the mixture, and to produce a high strength concrete, using very low water/cement ratio (Neville and Brooks, 2008). The selection of the type of superplasticizer (SP) and its dosage are very important to improving the workability of fresh PKS concrete. In this study, Sikament visocrete, a high range water-reducer and slump retention concrete admixture, complying with ASTM C494 type A (1999), was used to achieve the required workability. The superplasticizer contents were measured as a percentage of the weight of the cement content based on the manufacturers' recommendation. The proportion of superplasticizer used in this study were 0%, 0.8%, 1%, 1.5% and 1.8% of the weight of cement content.

3.2.4 Normal weight aggregates

River sand with maximum aggregates size of 4.75 mm, specific gravity of 2.66, moisture content of 4% and a fineness modulus of 2.71 was used throughout the study. The coarse aggregate used for control samples was crushed granite of maximum size of 12 mm.

3.2.5 Palm kernel shell aggregates

The PKS used as aggregates were obtained from a palm kernel oil production site at Ayigya in the Kumasi Metropolis. PKS aggregates have two distinct surfaces: smooth concave and convex surfaces. The convex surfaces (outer face) have fibres, the amount of which depends on the amount of time it has been exposed to the weather. This face can be smooth or rough depending

on the extraction method (Okpala, 1990). Fresh shells contain a lot of fibres (about 50% by volume) and oil film coating. These fibres increase demand for water and interfere with the aggregate-cement bond (Shafiqh *et al.*, 2011). The concave surface (inner face) is the face from which the palm kernel nuts are removed. This face is relatively smooth with no fibres. Usually, the PKS contain impurities such as oil, dirt and fibres, depending on the method of production. It is therefore necessary to clean the palm kernels shells before use. This can be achieved through various methods such as weathering, boiling in water, and washing with detergent (Shafiqh *et al.*, 2011; Olutoge, 2010; Teo *et al.*, 2006b).

In this investigation, weathered PKS, specifically *Dura* and *Tenera* species, were flushed with portable water to remove dirt, oil film coating and other impurities which could be detrimental to the concrete. They were dried indoors under laboratory conditions for four months. The PKS were in various irregular shapes and varying sizes. The aggregates were oven dried and the physical properties were determined in accordance with BS 812 (1990). Due to the high water absorption capacity of the PKS aggregates, they were pre-soaked in water for 24 hours and subsequently air dried to saturated surface dry condition (Teo *et al.*, 2006b; Mannan *et al.*, 2002) before they were used for concrete production. Particles with sizes less than 2.36 mm were rejected due to the relatively large surface area which could affect the concrete properties. When the pre-soaked aggregates are used in concrete, it is reported that internal curing from the reservoir of water absorbed by the aggregates enhances cementitious hydration (Teo *et al.*, 2010; Lo *et al.*, 2004).

This has been shown in other researches.

3.1 CHEMICAL PROPERTIES OF PKS

Palm kernel shell is an organic material which makes its chemical composition different from other lightweight aggregates. Table 3.1 presents the chemical properties of PKS given by Teo *et al.*, (2007).

Table 3.1 Chemical composition of PKS aggregate (Teo *et al.*, 2007)

Elements	Chemical composition (%)
Nitrogen, N	0.41
Sulphur, S	0.000783
Calcium (as CaO)	0.0765
Magnesium (as MgO)	0.0352
Sodium (as Na ₂ O)	0.00156
Potassium (as K ₂ O)	0.00042
Aluminium (as Al ₂ O ₃)	0.130
Iron (as Fe ₂ O ₃)	0.0333
Silica (as SiO ₂)	0.0146
Chloride (as Cl)	0.00072
Loss on Ignition	98.5
Ash	1.53

3.4.1 Aggregate shape

Flakiness and elongation indices describe the shape of a given aggregate. The PKS and granite aggregates used in the study were sampled from portions passing 14 mm sieve size and retained

¹ .4 PHYSICAL PROPERTIES OF THE COARSE AGGREGATES

The physical properties of the coarse aggregates studied were aggregate impact value (AIV), water absorption, specific gravity, aggregate crushing value (ACV), Los Angeles Abrasion Value (AAV), elongation index (EI) and flakiness index (FI). The methods involved in determining these properties are described subsequently.

on the 10 mm sieve size. The flakiness of both PKS and granite were determined by separating the flaky particles using a metal thickness gauge and expressing the mass of aggregates passing as a percentage of the mass of the sample tested (BS 812, 1990). Similarly, the elongation of both PKS and granite were determined by separating elongated particles using a metal length gauge and expressing the mass of aggregates passing as a percentage of the mass of the sample tested (BS 812, 1990).

3.4.2 Water absorption

The water absorption of the PKS and granite aggregates was determined in accordance with the recommendations for testing aggregates in BS 812 (1990). A test specimen was immersed in water in a glass vessel for 24 hours. After immersion, entrapped air was removed by gently agitating the soaked specimen. After 24 hours, the sample was placed on a dry cloth and gently surface-dried with the cloth and then weighed to obtain a surface dry weight. The sample was then placed in an oven at a constant temperature of $105 \pm 5^{\circ}\text{C}$ for 24 hours and subsequently cooled and weighed. The water absorption was determined as the ratio of the decrease in mass of the surface dry sample to the mass of the oven-dry sample, expressed as a percentage.

3.4.3 Specific gravity

The specific gravity of both aggregates was determined in accordance with the American Standard for Testing Materials, ASTM C127-07 (1993). The test specimen was immersed in water in a glass vessel for 24 hours. Subsequently, the vessel was overfilled with water and covered with a glass disc to ensure no air was trapped in the vessel. Subsequently, the test specimen was weighed while still submerged in water. The test specimen was removed from the water, dried gently with a cloth and weighed to obtain a saturated surface dry weight. The specimen was finally dried in

an oven for 24 hours at a constant temperature of $105 \pm 5^\circ\text{C}$ and subsequently cooled and dried. The Specific gravity was determined from the ratio of the weight of the aggregates to the weight of equal volume of water using the vessel.

3.4.4 Aggregate impact value (AIV)

The AIV of the PKS and granite aggregates was determined in accordance with BS 812 (1990). A standard test with aggregates passing a 14 mm test sieve but retained on a 10 mm test sieve was used. A test specimen was compacted by 25 strokes with a tamping rod into an open steel cup of an aggregate impact test machine. The specimen was subjected to a total of 15 blows from a height of 380 mm above the upper surface of the aggregates in the cup. After the 15th blow, the whole specimen was sieved on a 2.36 mm test sieve. The aggregate impact value was determined by measuring the ratio of the mass of fine particles passing the 2.36 mm test sieve to the total mass of the test specimen, expressed as a percentage. The degree to which the impacted samples broke depend on the impact resistance of the material.

3.4.5 Aggregate crushing value (ACV)

The ACV of the PKS and granite aggregates was determined in accordance with provisions in BS 812 (1990). Aggregates passing a 14 mm test sieve but retained on a 10 mm test sieve was used for this test. A cylinder of the test apparatus was placed on a base plate and the test specimen was compacted in three layers of approximately equal depth. Each layer was subjected to 25 strokes from a tamping rod of cross-section 16 mm, distributed evenly over the surface of the layer. The test specimen was leveled in the steel cylinder and subsequently fitted with a freely moving plunger. The specimen was subjected to a load of 400 kN applied through the plunger in 10 minutes. After crushing, the test specimen was sieved on a 2.36 mm test sieve. The aggregate

crushing value was then determined as a percentage of the mass of fine particles passing the 2.36 mm test sieve to the total mass of the test specimen.

3.3.6 Aggregate abrasion value (AAV)

The AAV for the PKS and granite aggregates was determined in accordance with BS 812 (1990). Two specimens from a test portion with their centre points opposite to each other were placed in an abrasion machine. The lap was turned through 500 revolutions at a speed of 28 revolutions per minute with abrasive charges fed onto it. On completion of 500 revolutions, the aggregate abrasion value was determined by measuring the difference in mass of the aggregates before and after the abrasion. The result was expressed as a percentage by weight of the test sample.

3.5 MECHANICAL PROPERTIES

3.5.1 Mix Design

Concrete mix design is the process of choosing suitable ingredients of concrete and determining their relative quantities with the objective of producing the most economical concrete while retaining the specified minimum properties such as strength, durability, and consistency (Neville and Brooks, 2008). To date, proper guidelines for mix proportioning of LWC are scarce and those available are also not specific (Abdullahi *et al.*, 2009). Accurate determination of mix proportion of concrete ingredients becomes more difficult when lightweight aggregates from organic sources are used because of the water absorption problems associated with most lightweight aggregates.

The UK's Department of Environment's, DOE, (1998) mix design method is for normal weight concrete. The method specified by Shetty (2005) is used for lightweight aggregates. The PKS aggregate is an organic material and its properties are different from other lightweight aggregates such as leca, foamed slag, aglite and lytag (Mannan and Ganapathy, 2001). Therefore, to achieve

a desired strength and workability using PKS aggregate, trial mixes were required to achieve an optimum mix. A target 28-day compressive strength of 30 N/mm² was designed using the UK's Department of Environment's (1988) mix design method for the normal weight concrete due to its simplicity and the varieties of aggregate properties considered in the design process.

3.5.1.1 Mix Proportions

Water to cement ratios (w/c) of 0.40 and 0.35 were selected for the various mix proportions. The low water/cement ratios were selected to ensure low permeable concrete of adequate strength (Neville and Brooks, 2008). Decreasing the w/c ratio implies decreasing the workability and increasing the target 28-day compressive strength. Considering the relatively low w/c ratio (below 0.4), superplasticizers were used to obtain the required workability (Neville and Brooks, 2008). However, the effectiveness of a given dosage of superplasticizer depends on the w/c ratio and the type of cement. Decreasing the w/c ratio increases the effectiveness of the superplasticizer (Alsadey, 2012). Thus to maintain a consistent medium workability, the amount of superplasticizer was adjusted in relation to the w/c ratio. The dosages of superplasticizer were 0%, 0.8%, 1%, 1.5% and 1.8% of the mass of cement to improve the workability of the PKS concrete. The dosage of superplasticizer was determined based on the recommendations of the manufacturer; the appropriate quantity of superplasticizer should be determined from trial mixes. However, the maximum quantity should be limited to 1.8% of the weight of the cement. According to ACI 213R-03 (2003), the absolute volume of LWA should normally take up 40 % ± 5 % of the concrete and can be adjusted to achieve the required density. Based on the mass per unit volume of concrete constituents, the concrete mix proportions used (cement: sand: PKS: water-cement ratio) are presented in Table 3.2, including basic details of all the mixes.

Table 3.2 Mix proportions of the various concrete mixes

Type of concrete	Mix no.	Cement, Kg/m ³	Sand: cement ratio	w/c	Mix proportions (By weight)	SP (%)	Air dry Density (Kg/m ³)
PKS with PL cement	MPL-1	500	1.3	0.40	1:1.3:0.7	0	1946
	MPL-2	500	1.5	0.35	1:1.5:0.6	0.8	1912
	MPL-3	500	1.4	0.35	1:1.4:0.8	1.0	1870
	MPL-4	500	1.3	0.40	1:1.3:0.7	1.5	1968
	MPL-5	500	1.6	0.35	1:1.6:0.5	1.8	1964
PKS concrete with OPC	MOP-1	500	1.3	0.40	1:1.3:0.7	0	1913
	MOP-2	500	1.5	0.35	1:1.5:0.6	0.8	1980
	MOP-3	500	1.4	0.35	1:1.4:0.8	1.0	1947
	MOP-4	500	1.3	0.40	1:1.3:0.7	1.5	1915
	MOP-5	500	1.6	0.35	1:1.6:0.5	1.8	1969
NWC	NPL	440	1.7	0.45	1:1.7:2.5	0	2377
	NOP	440	1.7	0.45	1:1.7:2.5	0	2376

Where SP is superplasticizer

For the mix identity number, the first letter identifies the type of aggregate, 'M' for PKS concrete and 'N' for normal weight concrete. The next two letters denote the type of cement used in the study, where 'PL' denotes Portland-limestone cement and 'OP' for ordinary Portland cement; the last numbers denote the amount of superplasticizer used in the study. The number '1' denotes zero percent (0%), '2' denotes 0.8%, '3' denotes 1.0%, '4' denotes 1.5% and '5' denotes 1.8% of cement weight. For example, MPL-1 denotes Portland-limestone cement concrete with zero percent (0%) superplasticizer using PKS.

3.5.2 Workability of concretes

The workability of PKSC was measured by the “slump test” (Fig. 3.1). During the mixing, a disproportionate amount of superplasticizer had to be added in order to achieve the desired workability. That notwithstanding, while slump was moderate, most of the mixes were stiff, making it difficult to place. Concrete mix with identity MOP-5 experienced bleeding and segregation which resulted in delayed initial set time.



Fig. 3.1 Slump test of PKS concrete

3.5.3 Laboratory batching and mixing

Thorough mixing of aggregates for concrete is essential for the production of homogeneous and consistent concrete. Weight batching was adopted to determine the proportions of materials for each mix. A uniform concrete mix was achieved by hand mixing in a pan in the laboratory. The measured quantities of sand and coarse aggregates were carefully poured into the mixing pan to ensure no loss of particles. The required quantity of cement was then added and subsequently mixed thoroughly until a uniform and homogenous mix was obtained. Two thirds of the water were pre-mixed with the superplasticizer before it was added to the aggregate and cement mix. The ingredients were then thoroughly mixed to obtain a uniform concrete before placing in the

moulds. Each mixing cycle took approximately 10 minutes while slumps were measured for each mixing cycle to ensure consistency.

3.6 COMPRESSIVE STRENGTH AND DENSITY OF CONCRETE MIXES

3.6.1 Preparation of test Specimens

The mean compressive strength was determined by testing three 150 x 150 x 150 mm concrete cubes in accordance with BS EN 12390-3 (2009). Cube steel moulds of dimensions 150 x 150 x 150 mm conforming to BS EN 12390-1 (2000) were used. The steel moulds were cleaned thoroughly before placing the concrete. Freshly mixed concrete was placed and compacted, each layer in 30 seconds with a vibrating table, in three layers into the steel moulds. The concrete was compacted using an electric table vibrator to ensure minimum amount of voids. After compaction, the concrete was leveled to obtain a smooth surface (Fig 3.2). Each set of specimens, comprising three (3) cubes were identified using the mix identifications in Section 3.5.1.1. A total of 216 cubes were cast and tested.



Fig. 3.2 Sample of freshly cast concrete cubes

3.6.2 Curing of concrete cubes

After casting, the concrete cube specimens were covered using a moist hessian mat for 24 hours. This ensured minimum loss of moisture from the surface of the concrete during the early stage of curing (Orchard, 1979). The specimens were de-moulded and totally immersed in water, of average temperature of 21°C in a curing tank to ensure complete hydration as recommended in BS EN 12390-2 (2009). Long period of moist curing has also been found to reduce the incidence of cracking (Kong and Evans, 1998). On each day of testing, excess moisture was wiped from the surfaces of the cube specimens and subsequently left in the open air for about 30 minutes before crushing at 7 days, 14 days, 21 days, 28 days, 56 days and 90 days. This ensured that the test specimens were air-dried before crushing.

3.6.3 Testing of concrete cubes

Three concrete cubes were tested at each age for each concrete mix. The compressive strength of the concrete cubes was tested at the Civil Engineering Laboratory of the Kwame Nkrumah University of Science and Technology (KNUST), Kumasi, using a Universal Compression Testing Machine of maximum capacity of 1000 kN (Fig. 3.3). The load was applied perpendicular to the direction of casting (BS EN 12390-3, 2002) without shock to the concrete specimen. Each specimen was crushed within 15 minutes. The compressive strength of each specimen was obtained by dividing the maximum crushing load applied by contact surface area.

$$f_{cu} = (F/A) \quad (3.1)$$

where f_{cu} = compressive strength of test specimen (N/mm^2), F = the failure load applied (N), A = contact surface area of test specimen (mm^2).



Fig. 3.3 Loaded Universal Compression Testing Machine

3.7 FLEXURAL TENSILE STRENGTH (MODULUS OF RUPTURE) OF PLAIN CONCRETE

3.7.1 Preparation of test specimens

In the test for flexural tensile strength (modulus of rupture), 100 mm × 100 mm × 500 mm timber moulds were used in conformity with BS 12390-1 (2000). Concrete designed to the same mix proportions for the compressive strength tests were used for the flexural tensile strength tests. The fresh concrete was placed and compacted, each layer in 30 seconds with a vibrating table, in two layers into the timber moulds. The concrete was compacted using an electric table vibrator to ensure minimum amount of voids. After compaction, the concrete was leveled to obtain a smooth surface and subsequently identified as explained in section 3.5.1.1. A total of 180 modulus of rupture beams were cast and tested.

3.7.2 Testing of beams for flexural tensile strength

Excess moisture was wiped from the surfaces of the specimens and subsequently left in the open air for about 30 minutes before testing at 7, 14, 28, 56 and 90 days. The specimens were subjected to four-point loading in accordance with BS EN 12390-5 (2000). The Universal Flexural Testing Machine with a 220 kN capacity was used for the application of loads. A constant loading rate of 0.2kN/s was maintained throughout the test programme. The loads were positioned within the middle third of the specimen. The loading span was maintained at 450 mm throughout the test programme. The flexural tensile strength (MOR) was determined using the formula

$$f_r = \left(\frac{F \times L}{b \times d^2} \right) \quad (3.2)$$

where f_r = flexural strength of test specimen (N/mm^2), F = the maximum load (N), L = the distance between the supporting rollers (mm), b is the breadth and d is the depth of the cross section (BS EN 12390-5, 2000).

3.8 REINFORCED CONCRETE BEAMS

The objective of this part of the study was to investigate the effect of the amount of longitudinal reinforcement, effect of the amount of shear reinforcement, effect of varying size of beams, effect of loading and shear span/effective depth ratio on the structural behaviour of reinforced PKS concrete beams in shear. These were assessed by means of the measurement of shear capacity, deflection, cracking, and modes of failure.

3.8.1 Design of the Reinforced Concrete Beam Specimens

A total of forty-six (46) reinforced concrete beam specimens, rectangular in cross-section, were designed for testing. The beams were grouped under two broad categories: beams without shear reinforcement (R-series) and beams with shear reinforcement (S-series). Beams in the S-series are required by design codes to contain a minimum prescribed amount of transverse reinforcement such that shear forces are resisted by both the transverse reinforcement and the concrete. Beams in the R-series were necessary since design codes of practice were largely developed based on information obtained from beams tested without shear reinforcement. In this case, the concrete section plays a major role in resisting the shear forces imposed on such members through different transfer mechanisms (Jung and Kim, 2008; Hassan *et al.*, 2008). Details of the test programme have been summarized in Table 3.3 and 3.4 for the R-series and S-series respectively.

Specimens in the R-series consisted of nineteen beams with two groups of shear span to effective depth ratios of 2.07, 2.50 and 3.11: representing short span (2.07 and 2.5) and slender (3.11) beams. The PKSC beams were 17 while the NWC beams were 2 in number. The beams were designed having a width of 120 mm or 110 mm, and varying depths of 150 mm, 200 mm, 225 mm, 250 mm and 300 mm. Each beam category contained three amounts of longitudinal reinforcement (ρ_w) ratios of 1.0%, 1.5% and 2.0%. The reinforcement details have been presented in Figure 3.4a-c.

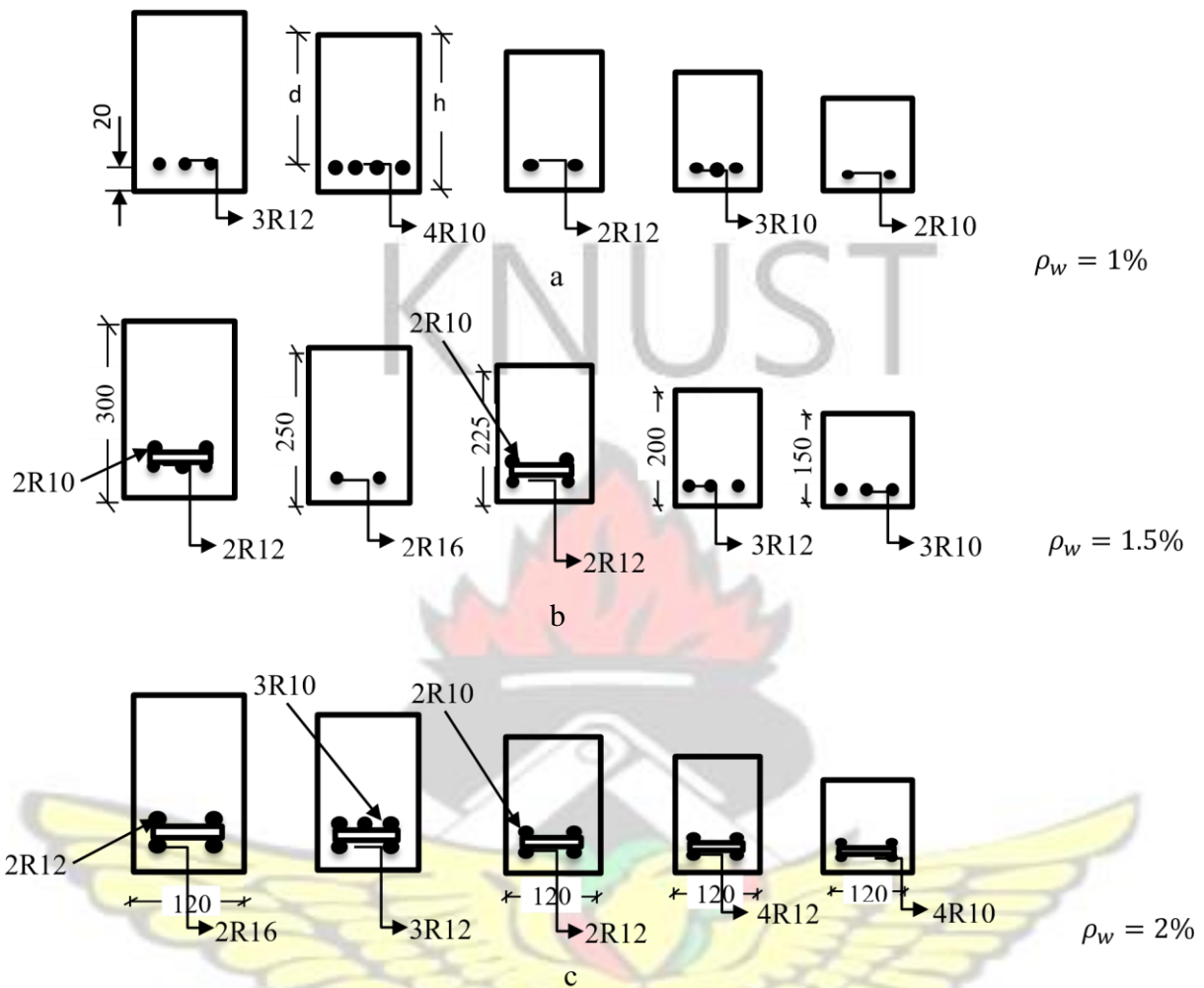


Fig. 3.4(a-c) Details of R-series specimens

Thus three groups of beams for each depth category could be identified. The slender beams consisted of two identical reinforced concrete beams of constant cross section of 110 mm wide by 225 mm depth. The reinforced NWC and PKSC specimens were designed in accordance with the provisions in BS 8110-1 (1997) and BS 8110-2 (1985) respectively.

Table 3.3 Details of R-series beams (Beams without shear reinforcement)

Beam ID	Cross section	Length mm			Percentage of tension steel	As provided (mm ²)

	B mm	D mm		Shear span/ eff. depth ratio, a_v/d_{eff}	Shear reinforcement spacing (mm)	(%)	
1 P 150	120	150	1000	2.5	Non	1.0	2-R10
1.5 P 150	120			2.5	Non	1.5	3-R10
2 P 150	120			2.5	Non	2.0	4-R10
1 P 200	120	200	1500	2.5	Non	1.0	2-R12
1.5 P 200	120			2.5	Non	1.5	3-R12
2 P 200	120			2.5	Non	2.0	4-R12
1 P 225	120	225	1700	2.5	Non	1.0	3-R12
1.5 P 225	120			2.5	Non	1.5	2-R12, 2-R10
2 P 225	120			2.5	Non	2.0	3-R12, 2-R10
1 P 250	120	250	2000	2.5	Non	1.0	4-R10
1.5 P 250	120			2.5	Non	1.5	2R16
2 P 250	120			2.5	Non	2.0	3-R12,3R10
1 P 300	120	300	2400	2.5	Non	1.0	3-R12
1.5 P 300	120			2.5	Non	1.5	3-R12, 2-R10
2 P 300	120			2.5	Non	2.0	2-R16, 2-R12
2.44 P 225a	110	225	1500	2.07	Non	2.44	3-R16
2.44 P 225b	110	225	2000	3.11	Non	2.44	3-R16
2.44 N 225a	110	225	1500	2.07	Non	2.44	3-R16
2.44 N 225b	110	225	2000	3.11	Non	2.44	3-R16

Specimens in the S-series consisted of 27 beams comprising 24 PKS concrete beams and 3 NWC beams. The shear span-to- effective depth ratios varied from 1.5 to 3.11, representing short span

and slender beams respectively. The short span beams were further grouped under beams subjected to monotonic and cyclic loadings, and designed with a constant width of 120 mm and 250 mm deep. Considering the beams subjected to monotonic loading, three varying amounts of shear reinforcement ratios of 0.38, 0.28 and 0.23, for 150 mm, 200 mm and 250 mm shear reinforcement spacing respectively, were used in the study. Thus three groups of beams for each a_v/d category could be identified in relation to the shear reinforcement spacings (150 mm, 200 mm and 250 mm). In terms of shear span-to-effective depth ratios, five distinct ratios could be identified as $a_v/d_{eff} = 1.5, 2.0, 2.5, 3.0$ and 3.11 for the monotonically loaded beams. For the short span beams subjected to cyclic loading, eight (8) beams with four varying amounts of shear reinforcement were used. The shear reinforcement spacings were 150 mm, 200 mm, 250 mm and 300 mm. However, all the beams had a constant $a_v/d_{eff} = 2.5$. All beams were subjected to twenty (20) cycles of loading and unloading at both first crack (4 beams) and service loads (4 beams).

The slender beams consisted of $a_v/d_{eff} = 3.0$ (three in number) and $a_v/d_{eff} = 3.11$ (six in number for both NWC and PKS concrete beams). The slender beams also comprised varying shear spacings of 150 mm, 200 mm and 250 mm. All beams of NWC and PKS concrete specimens were designed in accordance with the provisions in BS 8110-1 (1997) and BS 8110-2 (1985) respectively.

Table 3.4 Details of S-series (Beams with shear reinforcement)

Beam ID	Cross section	Length (mm)			Percentage of	As provided

	B (mm)	D (mm)		Shear span/ eff. depth ratio, a_v/d_{eff}	Shear reinforcement spacing (mm)	Tension steel (%)	(mm ²)
2P 150 A	120	250	2000	1.5	150	2.0	3-R12,3R10 (576)
2P 200 A	120	1.5		200			
2P 250 A	120	1.5		250			
2P 150 B	120	250	2000	2.0	150	2.0	3-R12,3R10 (576)
2P 200 B	120	2.0		200			
2P 250 B	120	2.0		250			
2P 150 C	120	250	2000	2.5	150	2.0	3-R12,3R10 (576)
2P 200 C	120	2.5		200			
2P 250 C	120	2.5		250			
2P 300 C	120	2.5		300			
2P 150 D	120	250	2000	3.0	150	2.0	3-R12,3R10 (576)
2P 200 D	120	3.0		200			
2P 250 D	120	3.0		250			
2.44P 200 E	110	225	2000	3.11	200	2.44	3-R16
2.44P 250 E	110	225		3.11	250		
2.44P 300 E	110	225		3.11	300		
2.44N 200 E	110	225	2000	3.11	200	2.44	3-R16
2.44N 250 E	110	225		3.11	250		
2.44N 300 E	110	225		3.11	300		
2P150Cf	120	250	2000	2.5	150	2.0	3-R12,3R10
2P200Cf	120	250	2000	2.5	200	2.0	3-R12,3R10
2P250Cf	120	250	2000	2.5	250	2.0	3-R12,3R10

Table 3.4 Details of S-series beams cont'd

2P300Cf	120	250	2000	2.5	300	2.0	3-R12,3R10
2P150Cg	120	250	2000	2.5	150	2.0	3-R12,3R10
2P200Cg	120	250	2000	2.5	200	2.0	3-R12,3R10
2P250Cg	120	250	2000	2.5	250	2.0	3-R12,3R10
2P300Cg	120	250	2000	2.5	300	2.0	3-R12,3R10

3.8.2 Reinforcement details

Deformed mild steel bars (characteristic strength of 270 N/mm^2) were used for the main tension reinforcement and shear reinforcement (stirrups). Each specimen was reinforced with varying amount of mild steel bars as tension reinforcement. No compression reinforcement was provided. However, 2R6 hanger bars were used to support the shear and tension reinforcements in position. The tension reinforcement had concrete cover of 20 mm to meet at least one-hour fire resistance and a mild condition of exposure in accordance with the provisions in BS 8110-1 (1997). In addition to these provisions, clause 3.3.1.2 of BS 8110-1 (1997) requires that cover to all reinforcement should not be less than the size of the main bar. Thus 20mm cover to the reinforcement was considered adequate. Shear reinforcement used for the twenty-seven (27) beams were R6 smooth mild steel bars, bent into closed links. The specimen reinforcement details are shown in Figures. 3.5, 3.6 and 3.7.

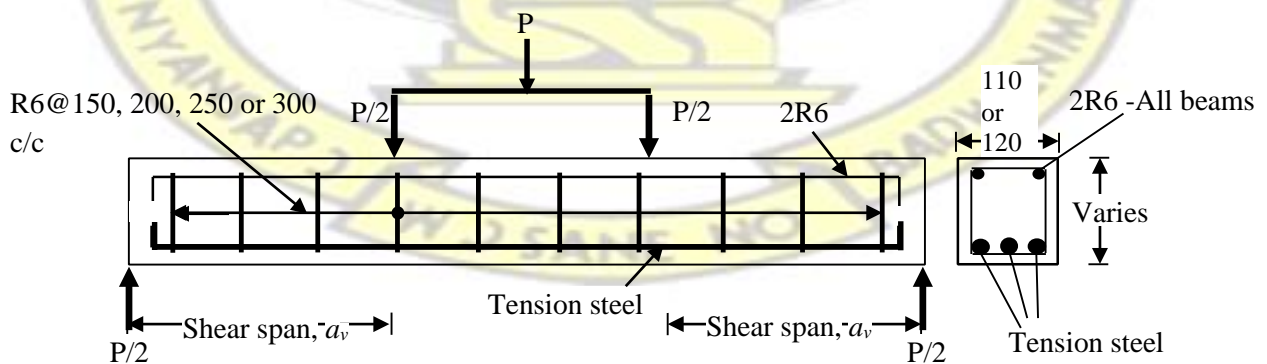


Fig. 3.5 Beams with shear reinforcement

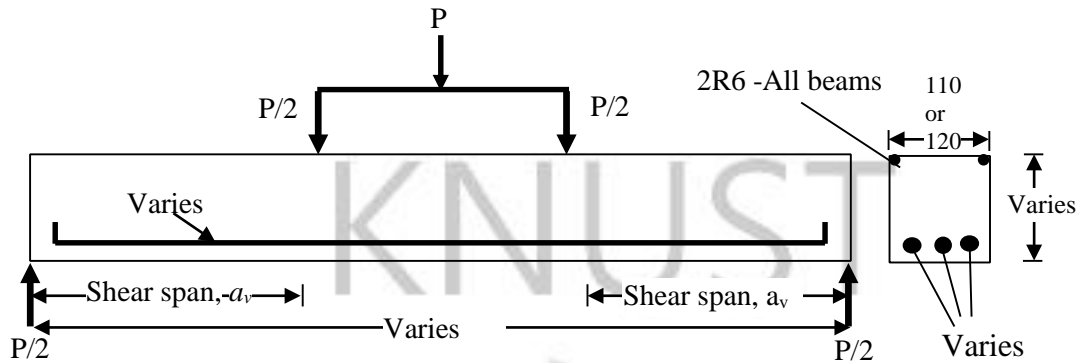


Fig. 3.6 Beams without shear reinforcement

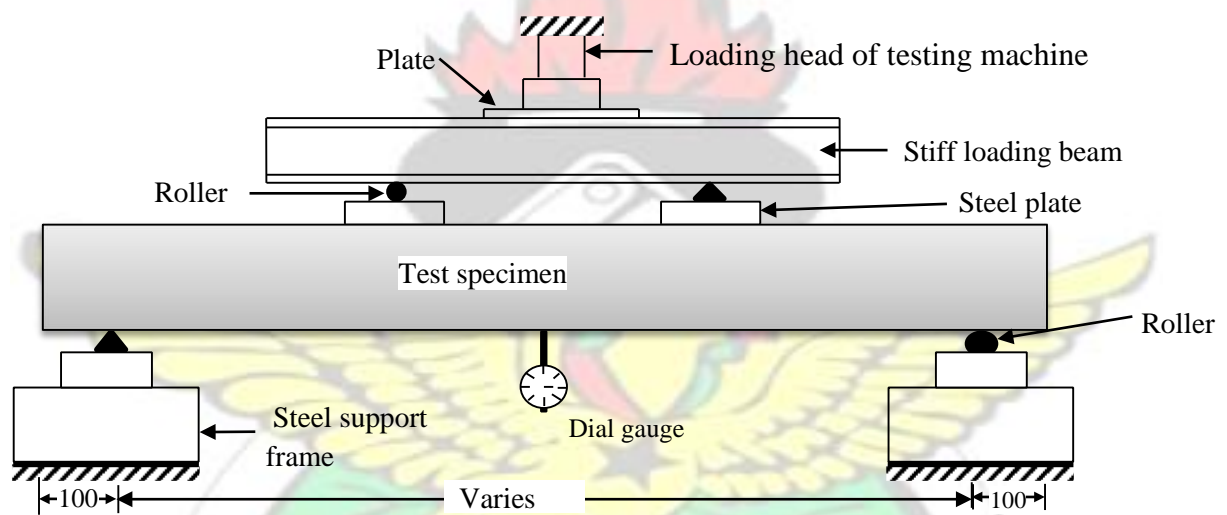


Fig.3.7 Schematic Diagram of experimental set-up

3.8.3 Reinforced Concrete Specimen Identification

The specimens were first identified according to concrete type as ‘P’ or ‘N’ denoting PKSC and normal weight concrete (NWC) beams respectively. Secondly, the beams were grouped into either beams without shear reinforcement (R-series) or beams with shear reinforcement (S-series). Considering the beams without shear reinforcement (R-series), each beam could be identified based on the amount of longitudinal reinforcement (first number), type of concrete (next letter ‘P’ or ‘N’), the depth of the beam (150 to 300) and shear span to depth ratio (last letter ‘a’ or ‘b’). A

typical beam identified without the last letter implies a default a_v/d_{eff} of 2.5. For instance, a beam identified as **1P150** is a PKSC beam with 1% longitudinal reinforcement, having a total depth 150 mm and a shear span to depth ratio of 2.5. Meanwhile a beam identified as **2.44P225a** is a PKS beam with 2.44% longitudinal reinforcement having a total depth of 225 mm and a shear span to depth ratio of 2.07. Other details of the specimens have been provided in Table 3.3.

Considering the beams with shear reinforcement (S-series), each beam was identified based on the type of concrete (first letter), spacing of shear reinforcement (150 mm to 300 mm), the shear span to depth ratio (last letter 'A' to 'D') and the type of loading ('f' or 'g'). All beams subjected to monotonic loading automatically omit the last letter 'f' or 'g'. The letters 'f' or 'g' denote 20 loading and unloading cycles at first crack loads and service loads respectively. A beam identified as **2P150A** implies a PKSC having a 2% longitudinal reinforcement, a shear reinforcement spacing of 150 mm, a shear span to depth ratio of 1.5 and subjected to monotonic loading. Similarly, a beam identified as **2N300E** denotes a NWC beam with 2% longitudinal reinforcement, a shear reinforcement spacing of 300 mm, a shear span to depth ratio of 3.11 under monotonic loading. On the other hand, a beam identified as **2P150Cf** is a PKS concrete beam with 150 mm shear reinforcement spacing, a shear span to depth ratio of 2.5 and subjected to 20 cycles of loading and unloading at first crack. The details of the specimens are presented in Table 3.4.

3.8.4 Types of Concrete

Normal weight concrete containing granite coarse aggregates were cast as a control material for both the S-series and R-series. The structural behaviour of this type of concrete is well established and understood worldwide by designers. Reinforced concrete codes of practice were developed

from extensive experimental works and the vast experience gained from using normal weight concrete. Thus normal weight concrete samples were limited in this study.

The main focus of this study was on PKS lightweight aggregate concrete. A comparatively lower concrete density is achieved by substituting the dense granite with PKS aggregates. This type of concrete with PKS aggregates is known to be completely different from other lightweight aggregate concretes since PKS is organic in nature. As an emerging product, the need to extensively understand the behaviour of large scale beam specimens produced from the PKS aggregates was necessary, especially its behaviour in shear compared to provisions in codes of practice.

3.8.4 REINFORCED CONCRETE SPECIMEN PREPARATIONS

3.8.4.1 Materials

The properties of the fine aggregate used in the study are presented in section 3.2.4. Ordinary Portland cement of strength class 42.5N was used in preparation of the beam specimens. The coarse aggregates used were crushed PKS with a maximum size of 14 mm (for the PKS concrete) and granite aggregates of 12 mm maximum size (for the normal weight concrete). PKS aggregates were pre-soaked in water for 24 hours prior to use. The aggregates were allowed to air dry for at least an hour to allow excess water to drain off. This ensured that batching of PKS aggregates was at saturated surface dry conditions. Superplasticizer (Sikament viscocrete) was used with the PKS concrete at a dosage of 5.5 kg/m^3 (representing 1% of the weight of cement) to obtain the required workability due to the relatively low w/c ratio. The mix design details are presented in Table 3.5.

Table 3.5 Mix proportions of the concrete

Mix designation	Target Compressive strength N/mm ²	Mix ratio			
		Cement content, Kg/m ³	w/c	Cement: sand: aggregate	Superplasticizer, %
PKSC, P series	30	550	0.40	1: 1.3: 0.7	1
	25	500	0.40	1: 1.3: 0.7	1
NWC, N series	30	440	0.50	1: 1.7: 2.5	0

3.8.4.2 Reinforced Concrete Beam Preparation

All beam specimens were cast in timber moulds of 37mm thick wawa boards. The timber moulds were coated with a layer of de-bonding oil prior to pouring concrete. Concrete was mixed mechanically with a concrete mixer until a uniform mix is obtained. The concrete was placed in two layers and vibrated with a shutter vibrator. After casting, all beam specimens were demoulded after 24-hrs and moist-cured under wet hessian mats in the open. These were regularly watered for 28-days.



Fig. 3.8 Samples of cast beams

Three cubes and three prismatic beams were cast simultaneously for each beam to study the compressive and flexural tensile strength of the beam specimens respectively. $150 \times 150 \times 150$ mm cubes were cast for compressive strength test while $100 \times 100 \times 500$ mm beams were cast for the modulus of rupture test.

3.8.4.3 Test Setup and instrumentation

The beams were simply supported on a stiff steel frame in the Civil Engineering Laboratory of the KNUST, Kumasi. A hydraulic actuator under crosshead displacement control was used to apply loads unto the beam specimens. The load from the hydraulic actuator was applied to two load point rollers through a stiff steel spreader beam onto the test specimen (Fig. 3.9). The spreader beam had sufficient bending capacity and stiffness to avoid excessive deformation and yielding before failure of the test specimens (Lim, 2007). After the beam was set up on the steel test frame, a preload of 2 kN was applied to ensure adequate contact of all the steel rollers and ball seats as well as to eliminate any settlement. A four-point loading configuration was used for the test (Fig. 3.9). The distance between two loading points was varied to obtain the required shear span to depth ratio for each test series. The observed sides of the beam were painted white to facilitate easy detection and observation of structural cracks as loads were applied.

Beam deflections at mid-span were measured with a dial gauge of 0.001 mm accuracy fixed at the bottom and midspan of each beam. The loading rate was kept at 0.2kN/s. Cracks were marked on the sides of the specimens as they developed, in order to assess the first flexural and shear cracks, and crack widths at tension steel level. Cracks were identified and observed visually while the crack propagation and crack patterns were marked by hand using a marker. Selected crack

widths were measured using a crack microscope of optical magnification X10 and reading to 0.02 mm. Initiation and propagation of both flexural crack and shear cracks were closely observed and recorded. After failure of each specimen, the crack patterns were photographed prior to the release of the actuator crosshead.



Fig. 3.9 Photograph of experimental set-up

3.9 REINFORCED CONCRETE TWO-WAY SLABS

3.9.1 Specimen details

Eight two-way concrete slabs reinforced with mild steel bars 1200 x 1200 mm and 75 mm thickness without any shear reinforcement were prepared in the laboratory. The slabs had a span to-depth ratio l/h of approximately 16. The slabs were reinforced in both directions with a clear concrete cover of 15 mm. Two grades of concrete strengths of 25 N/mm^2 and 30 N/mm^2 were used in this study. The percentage of total reinforcement was kept constant at 1.34. The details of the slabs are shown in Table 3.6. A uniform mixture for each mixing cycle was obtained using a concrete mixture, while adequate compaction was achieved by using a poker vibrator. The concrete consisted of ordinary Portland cement, river sand and either crushed granitic rock of 12

mm maximum size or PKS aggregates of 14 mm maximum size. Observed slumps of PKSC and NWC were 63 mm and 68 mm respectively. All slabs were cast and cured under similar conditions and tested after 28 days of curing. The properties of the concrete at 28 days have been presented in Table 3.6.

KNUST

3.9.2 Specimen Identification

The specimens were first identified according to the concrete type 'PS' or 'NS' denoting PKS concrete and normal weight concrete (NWC) beams respectively. Secondly, the slabs were identified as C25 and C30 depending on the compressive strength of the concrete. Lastly additional letters, 'a' or 'b' were used to identify the beams subjected to cyclic loads. For instance, a slab identified as PS25 is a PKSC with a compressive strength of 25 N/mm² subjected to monotonic loading. Meanwhile a slab identified as PS25a is a PKSC with a compressive strength of 25 N/mm² and subjected to 20 loading and unloading cycles.

3.9.3 Reinforced concrete specimen preparations

3.9.3.1 Materials

Ordinary Portland cement of strength class 42.5N was used to prepare the slabs. The coarse aggregates used were crushed PKS with a maximum size of 14 mm (for the PKS concrete) and granite aggregates of 12 mm maximum size (for the normal weight concrete). PKS aggregates were pre-soaked in water for 24 hours prior to use. The aggregates were allowed to air dry for at least an hour to allow excess water to drain off. This ensured that batching of PKS aggregates was at saturated surface dry conditions. Superplasticizer (Sikament visocrete) was used with the PKS concrete at a dosage of 5.5 Kg/m³ (representing 1% of the weight of cement).

3.9.4.2 Reinforced Concrete Slab Preparation

All slab specimens were cast in timber moulds of 37mm thick wawa boards. The timber moulds were coated with a layer of de-bonding oil prior to pouring concrete. The concrete was mixed manually in a mixing pan, placed in two layers and vibrated with a shutter vibrator. After casting, all slab specimens were de-moulded after 24-hrs and moist-cured under wet hessian mats for 28days. Samples of specimens are shown in Figures 3.10 and 3.11 for NWC and PKSC slabs respectively.

Three 150 mm × 150 mm × 150 mm cubes and three MOR beams measuring 100 mm × 100 mm × 500 mm were cast simultaneously for each slab to study the compressive and tensile strength of the slab specimens respectively.



Fig. 3.10 Sample of NWC slabs



Fig. 3.11 Sample of PKSC slabs

Table 3.6 Details of two-way slabs

Slab ID	Overall Depth, mm	Target Compressive strength, MPa	Effective depth, mm		Reinforcement details Area (mm ²)		
			X-	Y-	A _x	A _y	Total (%)
PS25	75	25	40	28	566	566	1.34
PS30	75	30	40	28	566	566	1.34
PS25a	75	25	40	28	566	566	1.34
PS30a	75	30	40	28	566	566	1.34
NS25	75	25	40	28	566	566	1.34
NS30	75	30	40	28	566	566	1.34
NS25a	75	25	40	28	566	566	1.34
NS30a	75	30	40	28	566	566	1.34

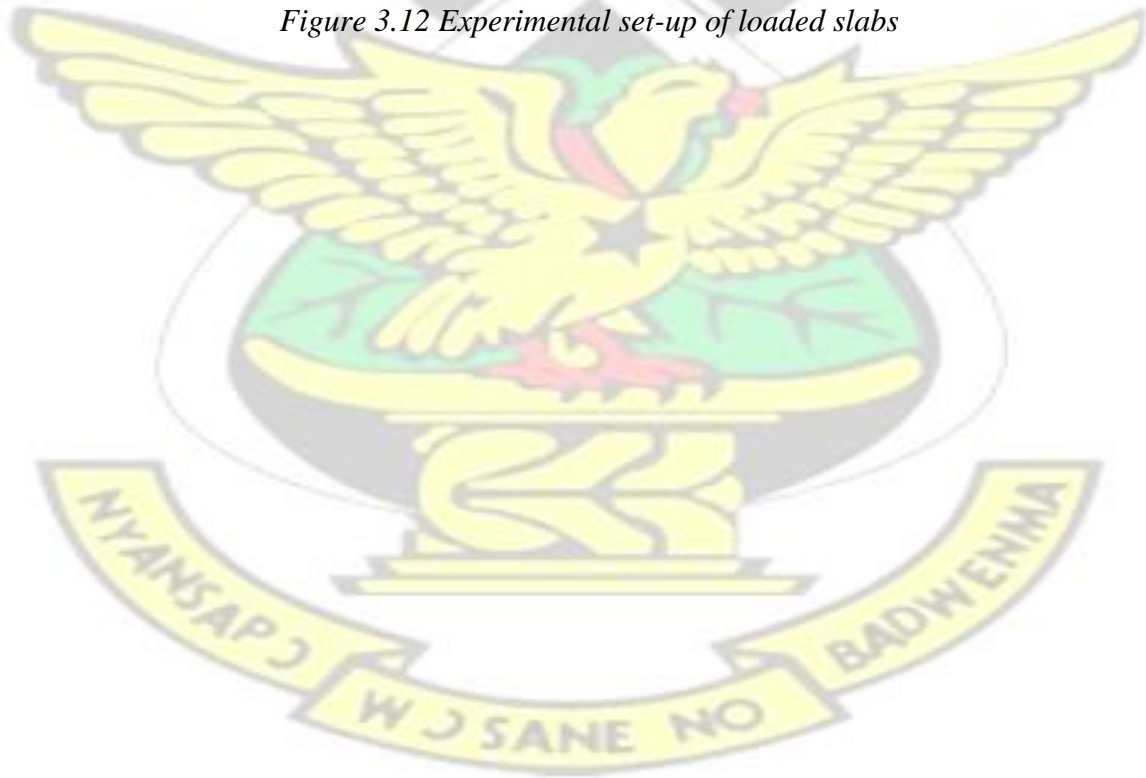
3.9.4.3 Test Setup and instrumentation

The slabs were painted white for easy detection and observation of structural cracks as loads are applied. During testing, the slabs were supported on a stiff steel frame and a hydraulic actuator under crosshead displacement control was used to apply loads. After setting up the slab on the steel test frame, a preload of 2 kN was applied to ensure adequate contact of all the steel rollers and ball seats as well as to eliminate any settlement.

Slab deflections at the mid-span were measured with a dial gauge of 0.001 mm accuracy fixed at the bottom and midspan of each slab. The loading rate was kept at 0.2kN/s. Cracks were marked on the sides and soffit of the specimens as they developed, in order to assess the first flexural, shear cracks, and crack widths at tension steel level. After failure of each specimen, the crack patterns were photographed prior to the release of the actuator crosshead. A photograph of the experimental set-up is shown in Figure 3.12.



Figure 3.12 Experimental set-up of loaded slabs



CHAPTER FOUR

RESULTS AND DISCUSSION

4.1 INTRODUCTION

In this chapter, the physical properties of the PKS, the compressive and tensile strengths of both PKS concrete and normal weight concrete (NWC) are presented and discussed. The shear behaviour of both reinforced PKS concrete and normal weight reinforced concrete beams are also discussed. The flexural behaviour of reinforced PKSC beams and slabs compared to normal weight reinforced concrete beams have been discussed based on the numerous parameters considered in the study. The provisions in the BS 8110-1(1997), ACI 318-08 and EC 2 for estimating concrete contribution to shear resistance have been discussed in relation to the results obtained. It is important to note that, all labeled shear loads at failure do not include the selfweight of the reinforced concrete beam specimen.

4.2 PHYSICAL PROPERTIES OF PKS AND NORMAL WEIGHT AGGREGATES

The physical properties of the normal granite aggregates and the PKS aggregates are presented in Table 4.1 and Figs. 4.2 and 4.3. The properties presented include particle size distribution, aggregate shape (flakiness index and elongation index), specific gravity, aggregate impact value, water absorption, aggregate crushing value, and Los Angeles Abrasion value.

4.2.1 Particle size distribution

The particle size distribution of fine aggregates and normal aggregates are presented in Figs. 4.1 and 4.2. Meanwhile, the particle size distribution of the PKS aggregates is shown in Fig. 4.3. The maximum aggregates size was 14 mm for the PKS aggregates and 12 mm for the granite

aggregates (Table 4.1). From the particle size distribution curves shown in Fig. 4.1 to Fig. 4.3, the grading of each aggregate type is observed to be within the upper and lower limit requirements of BS 882 (1992), indicating a uniformly graded particle size distribution of all the types of aggregates.

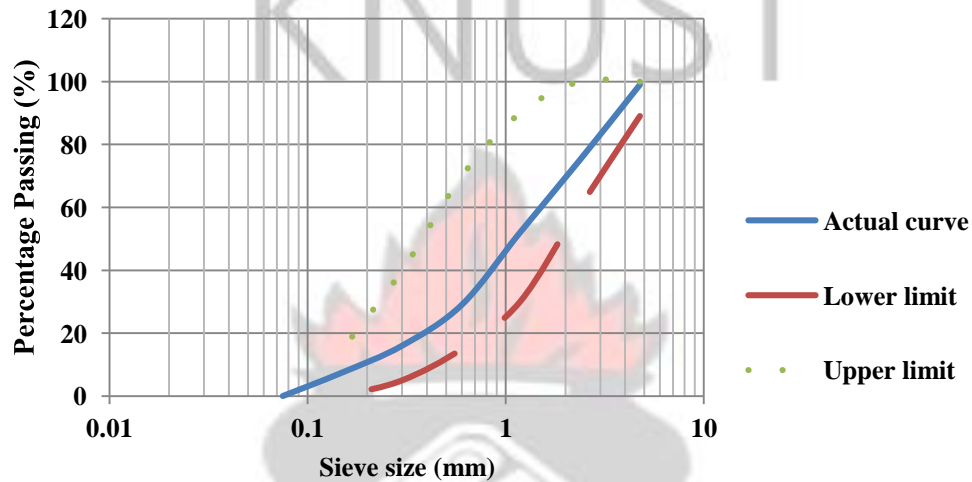


Fig. 4.1 Particle size distribution of fine aggregate

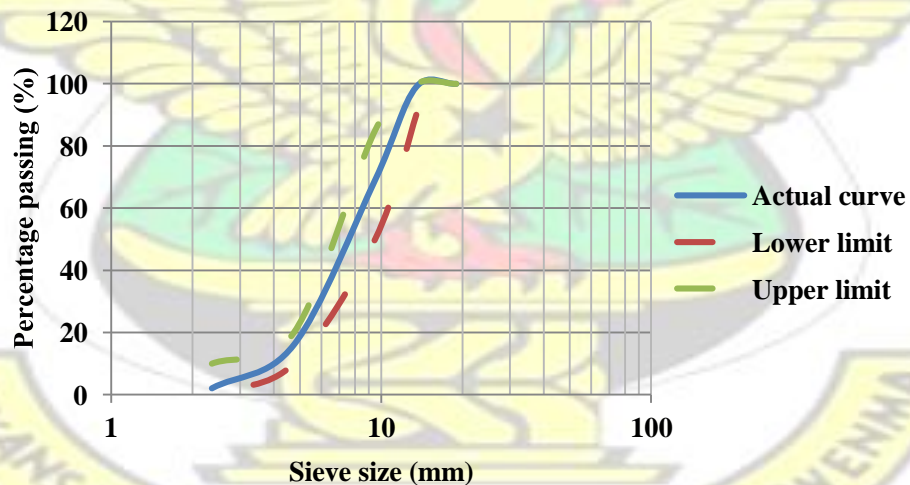


Fig. 4.2 Particle size distribution of granite coarse aggregate

In general, studies have shown that uniformly graded aggregate contribute more positively to the overall quality of concrete than gap-graded aggregates (Chandra and Berntsson, 2002; Glavind *et al.*, 1993), and desirable for efficient use of the paste. According to Golterman *et al.* (1997),

uniformly distributed aggregates lead to higher packing, resulting in concrete with higher density, less permeability, decreased cost of production, easy placement and enhanced overall quality of the concrete, and improved abrasion resistance (Mehta and Monteiro, 1993).

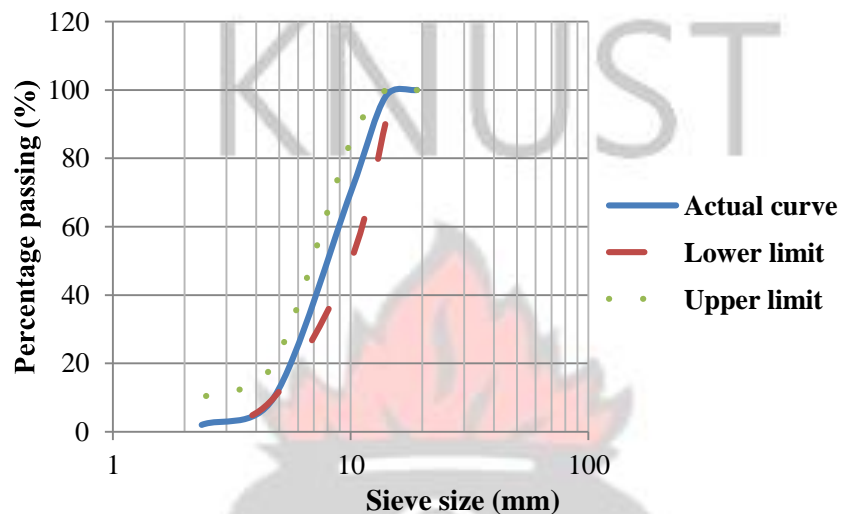


Fig. 4.3 Particle size distribution of PKS aggregate

Since the grading curves in Fig. 4.1 - 4.3 are indicative of well-graded aggregates, it can be inferred that a workable concrete with low void content can be produced from both types of coarse aggregates, resulting in concrete of high quality and strength.

4.2.2 Aggregate shape

The test results presented in Table 4.1 show that PKS and the granites have flakiness index of 63.2% and 31% respectively. The elongation index obtained for PKS and granite are 16.6% and 22% respectively. The shape of aggregate particles (whether flaky or elongated) influences water absorption, paste demand, placement characteristics such as workability, strength, void content, and packing density (Rached *et al.*, 2009). Legg (1998) and Shilstone (1990) also reported that flaky and elongated particles tend to produce harsh mixtures which affect the mobility of the resulting concrete.

Table 4.1 Physical properties of aggregates

Properties	PKS (LWA)	Granite (NWA)	Limits	References
Maximum aggregate size, mm	14	12	0	-
Shell thickness, mm	1 – 5.9	0	0	-
Specific gravity, saturated surface dry	1.35	2.65	< 2.4 - 2.8	Popovics, (1992)
Aggregate impact value (AIV), %	3.01	13.5	≤ 25	BS 882 (1992)
Aggregate crushing value (ACV), %	5.3	25.7		Neville and Brooks (2008)
	≤ 30	19.6	≤ 30 and ≤ 50	Shetty (2005)
Los Angeles Abrasion Value %	4.73 (AAV),			
24-hour water absorption, %	18	0.68	25	Kankam (2000)
Flakiness Index (%)	63.2	31	40 - 50	BS 882 (1992)
Elongation Index (%)	16.6	22	40 - 50	BS 882 (1992)
Moisture content (%)	9.7	0	-	Popovics, (1992)

Flaky and elongated aggregates increase void content in concrete mixes and water requirement, thereby reducing the strength of the concrete (Bouquety *et al.*, 2006; Jamkar and Rao, 2004). BS 882 (1992), therefore, specifies an upper limit of 50% for uncrushed gravels and 40% for crushed gravel. This means that the PKS, which is flakier than the granite, exceeds the upper limit specified in BS 882 (1992). This could be attributed to the method of cracking the shells for palm kernel extraction. The results indicate that water absorption and paste demand for the PKS concrete will be higher than that for the granite concrete, and this is likely to produce concrete of low strength, with flexural strength being more affected than compressive strength (Smith and Collis, 2001). This expectation is borne out of section 4.5.

4.2.3 Water absorption

The 24-hour water absorption obtained for PKS aggregates is 18% while that of granite aggregates is 0.68%, indicating a high porosity of PKS aggregates. In general, most lightweight aggregates have higher water absorption values than normal weight aggregates. According to the Concrete Society of the UK (1987), the water absorbed by LWAs may vary from 5% to 25% compared to about 2% for most normal weight aggregates. Generally, the 24-hour water absorption values of PKS have been reported to be high, ranging from 14% to 33% (Ndoke, 2006; Teo *et al.*, 2006b). The average 24-hour water absorption for PKS aggregate obtained in their study was about 23.4%.

Although, the water absorption of PKS aggregate is high compared to granites, higher water absorption values of 37% have been recorded for pumice aggregates (Hossain and Khandaker, 2004). The high water absorption properties of the PKS can be attributed to high porosity and large interconnecting pore structure of the aggregates. Since the water absorption of the PKS is high, it is reasonable to conclude that the PKS absorbs a greater amount of mixing water during concrete production. However, the high water absorption of PKS can be beneficial to the resulting hardened concrete as reported by Al-Khaiat and Haque (1998) that LWC with porous aggregates (i.e. high water absorption) is less sensitive to poor curing as compared to NWC, especially in the early ages due to the internal water stored by the porous lightweight aggregates (Browning *et al.*, 2011).

4.2.4 Specific gravity

The specific gravity obtained for PKS and granite were 1.35 and 2.65 respectively (Table 4.1). The high porosity of PKS is likely to have contributed to the low specific gravity value compared to that of the granite. Generally, aggregates with specific gravity less than about 2.4 are classified

as lightweight while normal weight concrete aggregates have specific gravity around 2.6 (Popovics, 1992). The specific gravities of 1.35 and 2.65 obtained from the study are considered representative of lightweight and normal weight aggregate respectively.

4.2.5 Aggregate impact value (AIV)

The Aggregate Impact Value (AIV) obtained for PKS and granite are 3.01% and 13.5% respectively. The aggregate impact value measures the toughness of the aggregates when impact loads are applied to the aggregates. The BS 882 (1992) sets the upper limiting value of AIV at 25%, for aggregates which are adequate for concrete of good impact resistance. This means that aggregates of higher impact values are weaker than aggregates with lower AIV. Therefore, both aggregates used in the study are adequate for the production of concrete of good impact resistance. Aggregate Impact Value also indicates the degree to which the aggregates absorb shock, indicating that the PKS has a greater degree of shock absorbance than the granite.

4.2.6 Aggregate crushing value (ACV)

The aggregate crushing values (ACV) obtained from the study were 5.3% and 25.7% for PKS aggregates and granite aggregates respectively. The ACV gives the relative measure of the resistance of an aggregate to crushing under a gradually applied compressive load. Aggregates with lower ACV have higher resistance to compressive loads. Therefore, PKS concrete is expected to possess better strengths under compressive loads than normal weight concrete. The recommended maximum ACV stipulated in BS 812 (1990) for aggregates for concrete production is 30%, indicating that the ACV of both PKS aggregates and the granites are within the recommended limit. This means that both aggregates are adequate for structural concrete production, especially for floors (where pedestrian traffic is high). Okpala (1990) obtained a

crushing strength of PKS as 12.06 N/mm^2 compared to about 181 N/mm^2 for granite aggregates. This indicates that the aggregate crushing value test may not be appropriate for PKS aggregates as observed for other weak aggregates by Neville (1981). It is likely that after crushing at the initial stage, the aggregates become compact with little or no crushing at later stages of loading, and thus the better ACV property than normal weight aggregates.

4.2.7 Aggregate Abrasion Value (AAV)

The results obtained for the AAV in the study were 4.73% and 19.6% for PKS aggregates and granites respectively. The Los Angeles Abrasion Value or Aggregate Abrasion Value (AAV) is a measure of an aggregate's ability to resist surface wear to due traffic. The lower the AAV, the higher the resistance to abrasion. Additionally, the level of wear in the Los Angeles Abrasion test indicates the potential increase in the amount of fines in the concrete when the fresh concrete is subjected to prolonged mixing (Popovics, 1992). This may increase the water requirement and require an increase in the water-cement ratio. According to Shetty (2005), the abrasion value of coarse aggregates should not be more than 30% for wearing surfaces and 50% for concrete other than wearing surfaces. Therefore, the AAV obtained for the PKS implies that concrete made from PKS aggregate will possess a high degree of resistance to wear as compared to the granite aggregates. It is therefore evident that PKS can be used in the production of concrete intended for floors and pavements where human traffic is expected to be heavy. Okpala (1990) reports that floors constructed with PKS in mud houses in Nigeria were still in good condition even after many years of use. The results of this study confirm the observation of high abrasion resistance of PKS aggregate concrete when used in the construction of floors.

4.3 DRY DENSITY OF CONCRETES

The average air dry densities of the concrete from the various mixes are presented in Table 4.2. The air-dry densities of the PKS concrete cubes were between 1809 Kg/m³ and 1985 Kg/m³ between 7 and 90 days. The densities of PKS concretes with Portland-limestone cement (PKSPL) varied from 1809 Kg/m³ to 1933 Kg/m³ at 7 days and from 1870 Kg/m³ to 1968 Kg/m³ at 28 days. The densities of PKS concretes with OPC (PKS-OPC) was in the range of 1860 Kg/m³ to 1942 Kg/m³ at 7 days and in the range of 1913 Kg/m³ and 1980 Kg/m³ at 28 days. It is seen that average air dry densities of the PKS concrete increased approximately proportional with age.

Table 4.2 Air dry density of various mix proportions

Type of concrete	Mix no.	Air dry Density (Kg/m ³)					
		7 days	14 days	21 days	28 days	56 days	90 days
PKSC with PL cement	MPL-1	1899	1901	1932	1946	1951	1958
	MPL-2	1897	1900	1908	1912	1922	1945
	MPL-3	1933	1944	1954	1968	1976	1979
	MPL-4	1809	1820	1837	1870	1910	1964
	MPL-5	1897	1870	1908	1901	1922	1877
PKSC with OPC	MOP-1	1889	1903	1903	1913	1922	1932
	MOP-2	1942	1954	1955	1915	1982	1985
	MOP-3	1874	1890	1911	1980	1935	1981
	MOP-4	1860	1898	1930	1947	1948	1951
	MOP-5	1922	1952	1964	1969	1971	1982
NWC	NPL	2318	2336	2360	2377	2380	2388
	NOP	2332	2348	2356	2376	2395	2409

The results show that PKS concrete can be classified as structural LWC as shown in the range of values of 1200-2000 Kg/m³ and 2400 Kg/m³ for lightweight and normal weight aggregate

concretes respectively, obtained in past studies (Chen and Liu, 2005; Clarke, 1993; BS EN 13055, 2002). The air-dry density of concrete is important for the weight of the structure and it defines the compactness, the amount of reinforcement and sizes of structural members in a particular structure. Lydon (1982) pointed out that for some lightweight aggregates, the compressive strength depends on the type of aggregates and increases with increase in density. The density of concrete depends on the specific gravity of the aggregates, sand content and the type of sand (Alengaram *et al.*, 2010b).

It is noted that, increasing the sand/cement ratio beyond 1.6 could result in higher density than the limit of 2000 Kg/m³ (Mahmud *et al.*, 2009). Given the low specific gravity of the PKS, the resultant density values close to the upper limit of 2000 Kg/m³ could be attributed to the use of river sand as fine aggregates which have a comparatively higher specific gravity of 2.66 (see section 3.5.1.1) and a sand/cement ratio close to 1.6. The relatively low weight of PKSC is brought about by the lightweight of PKS and low compactness of PKS concrete due to the highly irregular shapes of the shells (Teo *et al.*, 2007). Thus, the irregular aggregates are most likely to result in increased void content of the PKSC.

The normal weight concrete mix designs for NPL and NOP recorded densities ranging from 2318 Kg/m³ to 2377 Kg/m³ and 2332 Kg/m³ to 2376 Kg/m³ respectively between 7 and 28 days. These range of densities are characteristic of NWC. The higher densities of the NWC could be attributed to the higher specific gravity of the coarse and fine granite aggregates, higher sand to cement ratio and compactness (thus less voids) of the concrete mix.

According to Rossignolo *et al.* (2003) the density of LWC is often more important than the strength since LWC with the same compressive strength level may reduce the self-weight of resulting concrete as a result of a decreased density. From Table 4.2, the 28-day density of the optimum mix of PKS concrete made with Portland-limestone (MPL-3) is 1968 kg/m^3 . When compared to the 28-day density of NWC made with Portland-limestone cement (NWC-PL), which is 2377 kg/m^3 , there will be a saving in the self-weight of PKS-PL concrete by about 17%. Similarly, given the density of the optimum mix of PKS-OPC (MOP-3) as 1980 kg/m^3 , there will be a saving in the dead weight of the resulting structure by about 18% when compared to NWC – OPC with a density of 2376 kg/m^3 .

4.4 EFFECT OF SUPERPLASTICIZER (SP) ON THE WORKABILITY OF PKS CONCRETE

The effect of the superplasticizer (SP) on the slump and other properties of the concrete is presented in Fig. 4.4 and Table 4.3. It is observed that the workability of the concrete improved with increasing dosage of superplasticizer for both types of concretes. The slump of PKS concrete with Portland-limestone cement varied from 39 mm to 106 mm for 0% to 1.8% dosage of SP respectively. The slump of PKS-OPC concrete varied from 30 mm to 106 mm for 0% to 1.8% dosage respectively. Comparing the various mixes for the two types of PKS concrete, the dosage of SP appears to result in higher slumps for the PKS–PL concrete than the slump for PKS–OPC concrete. Given the low water/cement (w/c) ratios of the various mixes, the improved workability of the concrete could be attributed to the use of the superplasticizer (Collepari *et al.*, 2006). Hanna *et al.* (1989) reported that the fluidizing effect of superplasticizer is influenced by the type of cement used and the fineness of the cement.

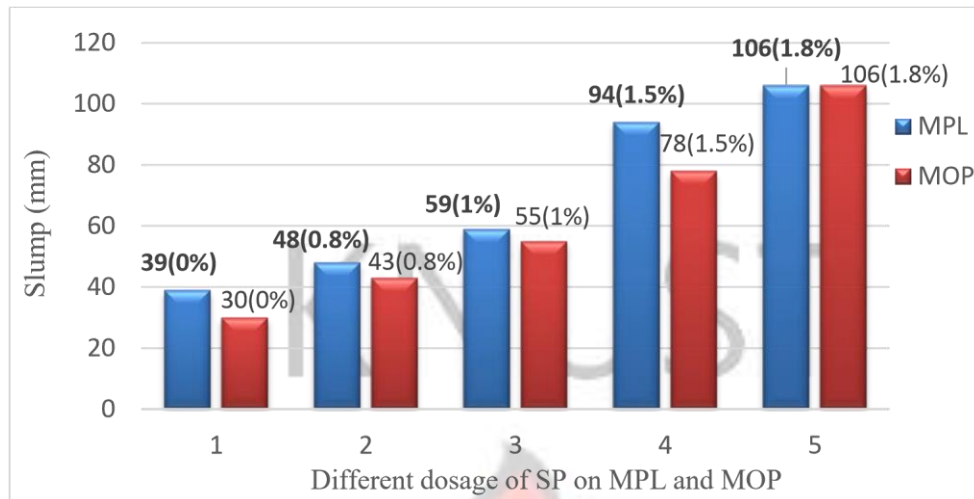
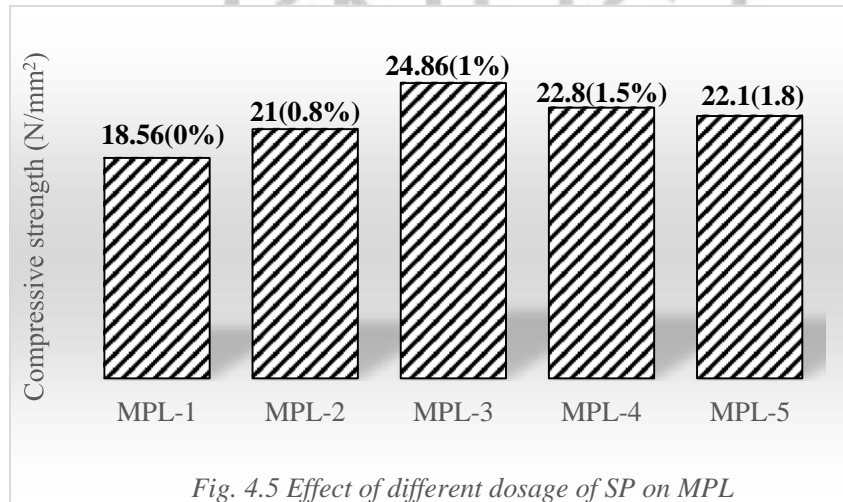


Fig. 4.4 Effect of SP dosage on slump of MPL and MOP

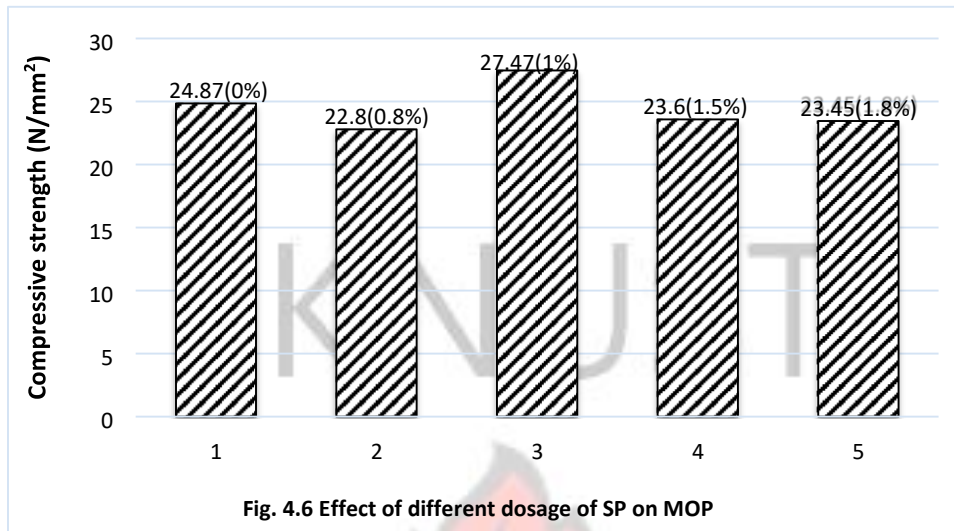
Though increase in dosage results in increase in slump, there is an optimum limit for the use of the SP. Alsadey (2012) reports that beyond this limit, the SP will cause bleeding and segregation, which will eventually affect the cohesiveness, initial set and uniformity of the concrete. This effect was observed in MOP-5 where 1.8% of SP was used. MOP-5 experienced bleeding and segregation which led to prolonged initial set.

The results of the 28-day compressive strengths for different dosage of SP using Portland limestone cement with PKS are presented in Fig. 4.5. Increasing the dosage of superplasticizer in PKS-PL concrete resulted in a corresponding increase in the 28-day compressive strength. The optimum SP content increase in compressive strength was 1% of the weight of cement. Beyond this SP content, the compressive strength decreases. This could be attributed to the high slump of the concrete associated with the increased SP content (see Fig. 4.4). In a given mix design with low water-cement ratio below 0.4, the workability of the concrete will almost totally depend on the amount of superplasticizer used (Neville, 2006). Thus from the results, it is reasonable to conclude that improvement in compressive strength can be related to the amount of superplasticizer. This is because addition of SP will provide more water from deflocculation of

cement particles for concrete mixing (Newman and Choo, 2003). Thus increasing the SP dosage will increase the entrapped water and promote hydration of the cement as long as the limit of SP dosage is not exceeded.



The results of the 28-day compressive strengths of PKS-OPC concrete for the different dosage of SP are presented in Fig. 4.6. The effect of the superplasticizer on compressive strength of PKSOPC concrete is, however, different from that of the PKS-PL cement concrete. PKS concrete with no superplasticizer had a higher 28-day compressive strength of 24.87 N/mm² than PKS concrete with 0.8%, 1.5% and 1.8% superplasticizer content. However, 1% superplasticizer improved the compressive strength of PKS concrete to 27.47 N/mm². Comparing PKS-OPC and PKS-PL concretes, the influence of the superplasticizer on the performance of PKS concrete depends on the type of cement. However, the optimum dosage of superplasticizer to result in improved compressive strength in PKS-OPC concrete appears to be 1% of the weight of the cement used.



The performance of SP in concrete production is known to depend on some factors such as the type of cement, aggregates, type and dosage of SP, mixing efficiency (Ozu *et al.*, 2001; Yamada *et al.*, 2006). The use of 1.8% dosage of SP resulted in a lower compressive strength compared to 1.5% dosage of SP. This could be attributed to the bleeding experienced at the mixing stage (see section 3.4).

Table 4.3 Effect of SP dosage on properties of PKS concrete

Type of concrete	Mix no.	SP (%)	w/c	Slump (mm)	28-day air dry density	28-day Compressive strength
PKS PL cement	MPL-1	0	0.40	39	1946	18.56
			0.35	48	1912	21.00
	MPL-2	0.8				
	MPL-3	1	0.40	59	1968	24.86
			0.35	94	1870	22.80
MPL-4	1.5					
MPL-5	1.8			106	1905	22.10

PKS concrete with OPC	MOP-1	0		30	1913	24.87
			0.35			
			0.40			
	MOP-2	0.8	0.35	43	1980	22.80
			0.40	55	1915	27.47
	MOP-3	1				
	MOP-4	1.5	0.35	78	1947	23.60
			0.35	106	1969	23.45
	MOP-5	1.8				
NWC	NPL	0	0.45	45	2377	33.29
			0.45	41	2376	37.62
	NOP	0				

4.5 COMPRESSIVE STRENGTH

4.5.1 Compressive strength with age of curing

The relationship between the compressive strength with age is shown in Figures 4.7 and 4.8. For all mixes, it was observed that the compressive strength increased rapidly with age until the 28th day after which strength development was gradual until 90 days. Generally, compressive strengths achieved at 28 days were in the range of 18.56 N/mm² to 24.86 N/mm² for PKS concrete made with Portland-limestone (PL) cement and 22.8 N/mm² to 27.42 N/mm² for the PKS concrete made with OPC.

The 7-day compressive strengths of PKS concrete using OPC varied from 12.3 N/mm² to 20.93

N/mm² (Fig. 4.7), and that of PKS concrete using PL cement varied from 11.4 N/mm² to 13.2 N/mm² (Fig. 4.7). The results of the study imply that OPC produce PKS concrete of higher compressive strength than Portland-limestone cement.

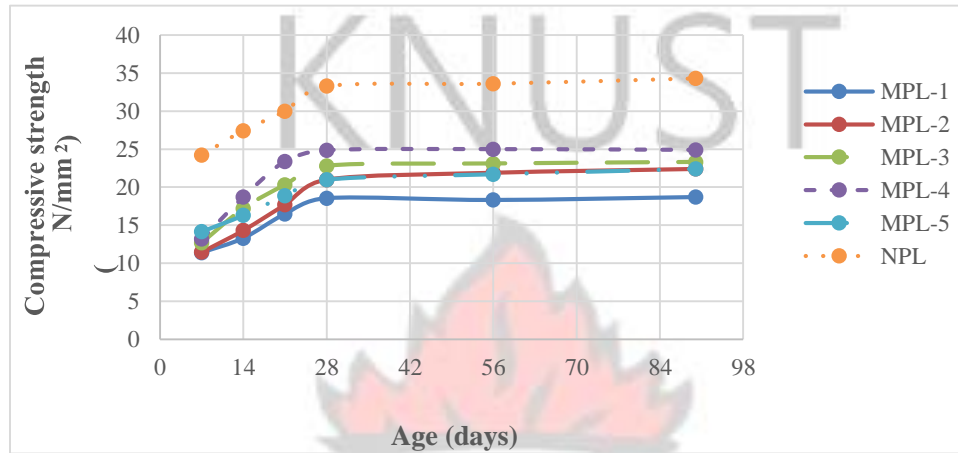


Fig.4.7 Comparison of compressive strength of PKS concrete and NWC using PL cement

Given the low water - cement ratios of PKS concrete mixes, the strength development during the first 7 days could be attributed to the higher hydration rate and thus strength of the cement paste. Beyond 7 days, the strength of the cement paste in the PKS concrete begins to approach the strength of the aggregates which limits further increase in compressive strength (Rossignolo *et al.*, 2003; Okpala, 1990). It is more likely that rather than strength of PKS aggregates, strength at higher curing periods will depend on the PKS-cement paste bond, as the hydration of cement paste will have run its course. The bond is low and thus lower gain in strength.

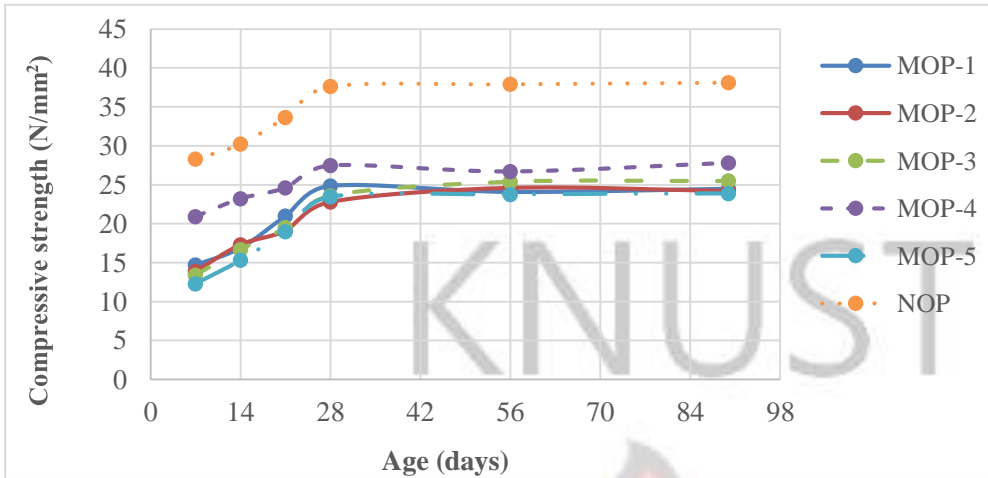


Fig.4.8 Comparison of compressive strength of PKS concrete and NWC using OPC

4.5.2 Comparison of PKS-OPC and PKS-PLC concrete

Figure 4.9 and Table 4.4 shows a comparison of the 28-day compressive strengths of PKS concretes using OPC and PL cements. The 28-day compressive strength varied from 18.56 N/mm² to 24.86 N/mm² for PKS concrete using Portland-limestone cement and from 22.10 N/mm² to 27.47 N/mm² for PKS concrete with OPC. Although the compressive strengths obtained using both types of cements are close, concrete made from OPC were higher in compressive strengths than those made with Portland-limestone cement. The results also show that, for the various mix proportions, the PKSC made with OPC had a faster hydration rate during the initial setting phase, reaching about 53% to 76% of the 28- day strength within 7 days and about 65 % to 85% of the 28-day strength within 14 days (Fig. 4.8). For the PKS concrete made with Portland-limestone cement, the hardening rate was about 53% to 61% of the 28- day strength within 7 days, and 68% to 75% of the 28- day strength within 14 days (Fig. 4.7).

Table 4.4 28-day compressive strength

Type of concrete	Mix ID	28- day strength	
		Mean	S. D.

PKS concrete with PL cement	MPL-1	18.56	2.16
	MPL-2	21	0.82
	MPL-3	24.86	3.56
	MPL-4	22.8	0.82
	MPL-5	22.1	1.1
PKS concrete with OPC	MOP-1	24.87	0.82
	MOP-2	22.8	1.73
	MOP-3	27.47	0.74
	MOP-4	23.6	2.16
	MOP-5	23.45	0.94
NWC	NPL	33.29	0.89
	NOP	37.62	1.67

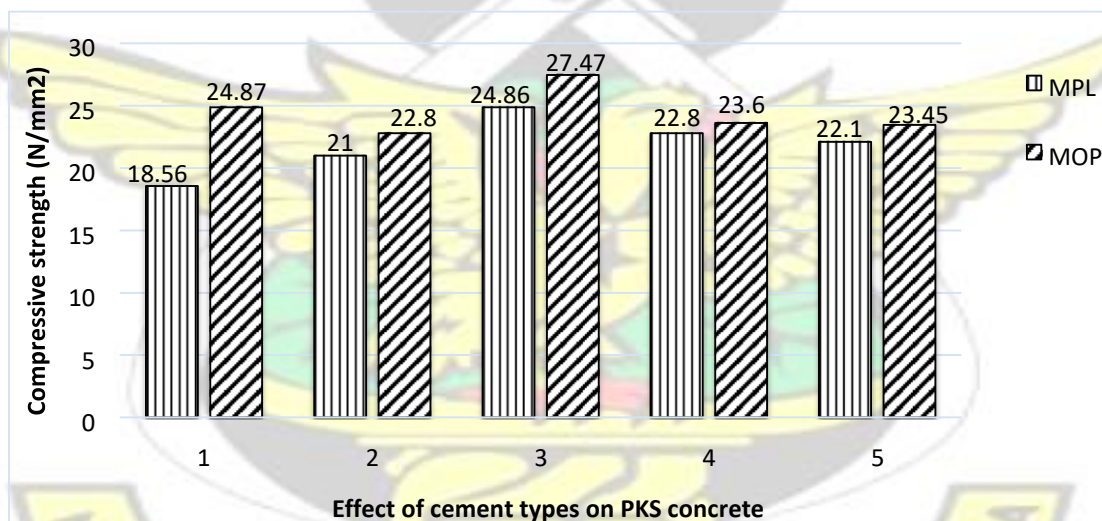


Fig. 4.9 Effect of cement types on compressive strength of PKS concrete

Based on the compressive strength classification given in BS 8110-1 (1997), PKSC made with Portland-limestone cement can be classified as C20 while that of PKS concrete with OPC can be classified as C25. The difference in the strengths of the two types of cement is clearly seen when comparing the 28-day compressive strengths of the NWC. Concrete made with Portlandlimestone cement was about 13% lower than concrete made with OPC (see Table 4.3). It can be concluded

from the results that the rate of strength development and the 28-day compressive strength of the PKSC are related to the strength of the cement used. Katz (2003) reported of a similar observation when the properties of concrete made with recycled aggregate from partially hydrated old concrete were investigated. It was reported that the compressive strength of concrete made using white Portland cement was 18% higher than the compressive strength of concrete made with Ordinary Portland Cement. Mannan and Ganapathy (2004) also reported that for a given workability, compressive strength increases with cement content, the characteristic strength of the cement and also with the type of aggregate employed.

4.5.3 Comparison of test results with minimum code provisions

The ASTM C330 (1999) recommends a minimum compressive strength of 17 N/mm² for structural LWC at 28-days. On the other hand, BS 8110 (1997) recommends a minimum compressive strength of 15 N/mm². The 28-day compressive strength of the PKS concrete produced from both OPC and Portland-limestone cements were higher than the minimum required strength recommended by both ASTM C330 and BS 8110. The 28-day compressive strength of the optimum mix (MPL-3) with Portland-limestone cement was 46% higher than the required 17 N/mm² recommended by the ASTM C330 (1999) and 66% higher than the required 15 N/mm² recommended by BS 8110 (1997). The 28-day compressive strength of PKS concrete mix (MOP-3) with ordinary Portland cement was about 62% higher than the required 17 N/mm² recommended by the ASTM C330 (1999), and 83% higher than the required 15 N/mm² recommended by BS 8110 (1997). This shows that PKS can be used to produce LWC for structural applications. The result compares favourably with findings of Liu (2005) who reported a 28-day compressive strength of 26.5 N/mm² for pumice aggregates.

4.5.4 Mode of failure of PKS concrete cubes

The PKS aggregates were parabolic, circular or semicircular, flaky and elongated (Table 4.1) and these are controlling factors for compressive strength (Chen *et al.*, 1999). The flaky and elongated shape of the PKS resulted in greater demand for cement-sand paste for a given mix as the total surface area of aggregate to be coated with the paste increased (Mindess *et al.*, 2003). The result is that corresponding concretes will have lower workability, be harsh, and be of lower strength where the cement paste is not sufficient to lubricate the aggregates for the necessary bonding. This property has the potential of contributing to concrete with a weaker mortar-aggregate interfacial bond (Abdullahi, 2012). Thus for a given PKSC mix, the cement-sand ratio needs to exceed the sand-PKS ratio in order to provide enough lubrication for an increased interfacial bond between the aggregates and the cement matrix, this bond having been contributed to by the beneficial effects of cement-sand bond. However, increasing the volume of paste is known to have detrimental effects on mechanical properties and time-dependent deformations such as increase in drying shrinkage (Roziere *et al.*, 2007; Bissonnette *et al.*, 1999). Thus crack formation of a given PKSC is expected to propagate from the aggregate-cement matrix.

In this study, failure of the PKSC cubes were observed to have been caused by a weak bond (Fig 4.10) between the PKS and the cement matrix. Failure was observed to be along the smooth convex surface of the PKS aggregates. The failure of the PKS concrete appears not to be as a result of failure of the PKS aggregates at least at early stages of hydration. This observation contradicts the findings of Mahmud *et al.* (2009) who reported that failure of PKS concrete in compression was as a result of the failure of the PKS aggregates. Mannan and Ganapathy (2002) indicated that failure of PKS concrete at 90 days is controlled more by the strength of PKS-cement paste bond than by the strength of PKS aggregate itself. Newman (2005) also reported that the

strength of lightweight aggregates was the primary factor controlling the upper strength limit of lightweight aggregate concrete (LAWC). The mode of failure of the PKSC observed in this study, however, suggests that the strength of PKSC depends on the strength of the mortar, and the interfacial bond between the PKS and the cement matrix at least at early stages of hydration.

The compressive strength of the optimum mix of PKS concrete with Portland-limestone cement (MPL-3) was 24.86 N/mm^2 and that for MOP-3 was 27.47 N/mm^2 at 28-days. The compressive strength of the PKS aggregate was found to be 12.06 N/mm^2 (Okpala, 1990), indicating that PKS concrete can achieve compressive strength higher than the compressive strength of the PKS aggregates.

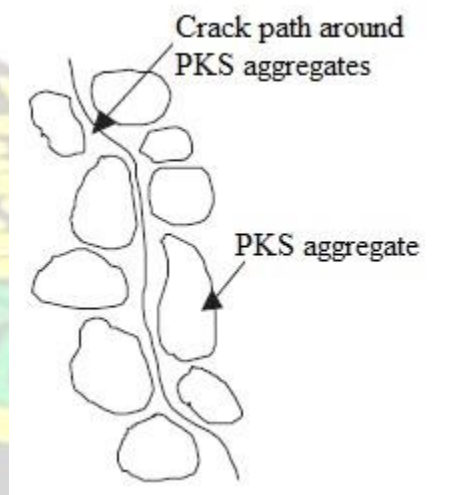


Fig. 4.10 Schematic sketch of crack pattern of PKS cubes

Bache and Nepper (1998) made a similar observation for angular sintered fly ash aggregates with compressive strengths between 17.5 and 20 N/mm^2 . However, the concrete produced from this aggregate had compressive strength of 46.3 N/mm^2 . Cui *et al.* (2012) also found that the compressive strength of lightweight aggregates such as expanded clay, shale and pulverished fuel ash, and expanded shale aggregates was not the only factor influencing the strength properties of

LWC. Other influencing factors such as flakiness and elongation indices of PKS aggregates coupled with the smooth convex surfaces of the PKS aggregates result in a weak bond between the PKS and the cement matrix. Even though, PKS aggregates have lower compressive strengths compared to granites (Okpala, 1990), improving the PKS-cement matrix bond would result in a corresponding increase in the compressive strength of PKS concrete. Alengaram *et al.* (2011b) reported that the use of mineral admixtures such as silica fume and fly ash with high silica content enhances the bond between PKS and mortar, which produced a higher compressive strength.



a) PKSC cubes

b) Granite concrete cubes

Fig. 4.11 Condition of PKS and granite cubes after failure

It was observed that for the normal weight aggregate concrete, failure of the concrete was explosive (BS EN 12390-3, 2009) which resulted in full disintegration of the test specimens (failure of the granite aggregates) (Fig. 4. 11). For the PKS concrete, however, failure was gradual and the specimens were capable of retaining the load even after failure without full disintegration. This may be attributed to the good energy absorbing quality of the PKS aggregates derived from the low AIV and ACV presented in Table 4.1 (Teo *et al.*, 2007). This behaviour of the PKS

aggregates is beneficial to concrete structures that require good impact resistance properties. The two kinds of failure modes are however consistent with provisions of BS EN 12390-3 (2009).

4.5.5 Compressive strength and density of the concrete cubes

Generally, the lower the density of concrete, the lower the compressive strength of the concrete (Orchard, 1979). The 28-day compressive strength of the PKS concrete with Portland-limestone cement, varied from 18.56 N/mm² to 24.86 N/mm². Meanwhile, the air-dry density of PKS concrete varied from 1912 Kg/m³ with a standard deviation of 1.25 to 1968 Kg/m³ with a standard deviation of 1.63 (Table 4.5). Similarly, the 28-day compressive strength and air-dry densities of PKS concrete with ordinary Portland cement varied from 22.1 N/mm² to 27.47 N/mm² while the density varied from 1903 Kg/m³ to 1981 Kg/m³ (Table 4.4). From Table 4.5, it can be inferred that the compressive strength of both PKS and normal weight concretes directly depend on the density of the corresponding concrete, the lower the density of concrete the lower the compressive strength and vice versa.

Table 4.5 28-day compressive strength vrs density

Type of concrete	Mix ID	28 – day density		28- day strength	
		Mean	S. D.	Mean	S. D.
PKS concrete with PL cement	MPL-1	1946	2.62	18.56	2.16
	MPL-2	1912	1.25	21	0.82
	MPL-3	1968	1.63	24.86	3.56

	MPL-4	1870	1.67	22.8	0.82
	MPL-5	1905	1.82	22.1	1.10
PKS concrete with OPC	MOP-1	1913	2.16	24.87	0.82
	MOP-2	1915	0.82	22.8	1.73
	MOP-3	1980	2.16	27.47	0.74
	MOP-4	1947	1.73	23.6	2.16
	MOP-5	1969	0.32	23.45	0.94
	NWC	NPL	2377	0.47	33.29
NOP		2376	0.82	37.62	1.67

4.6 TENSILE BEHAVIOUR OF THE CONCRETE

The trend of the flexural tensile strength and the age of curing the concrete is presented in Figures 4.12 and 4.13. The flexural tensile strength of PKS concrete made with Portland-limestone cement varied from 2.10 N/mm² to 3.83 N/mm² and from 2.16 N/mm² to 3.90 N/mm² with ordinary Portland cement. For all the mixes, the strength increased from 7 days to 90 days of curing. In general, the 28-day flexural tensile strengths of PKS-OPC concrete beams were higher than corresponding strengths of PKS-PL cement concrete. The flexural tensile strength of the normal weight concrete made with Portland-limestone cement varied from 3.50 N/mm² to 5.11 N/mm² and from 3.7 N/mm² to 5.21 N/mm² for NWC produced with ordinary Portland cement. Okpala (1990) reported the modulus of rupture of PKS concrete was in the range of 2.13 – 2.8 N/mm² which is about 14% of the compressive strength.

The modulus of rupture values of the NWC were higher compared to the PKS. This may be attributed to the higher roughness of the surface of granite aggregates and thus a better aggregate interlock and better bonding of the aggregates with the cement paste. This result agrees with the findings of Khaleel *et al.* (2011) and Mehta and Monteiro, (2006). The results also show that, the flexural tensile strength of the PKS concrete is directly related to the age of curing. That is, the

flexural tensile strength of PKS concrete beams increased with the period of hydration of the cement. The MOR for PKS appears to increase with increase in cement content and dosage of SP, except when the threshold is exceeded (as in MOP-5).

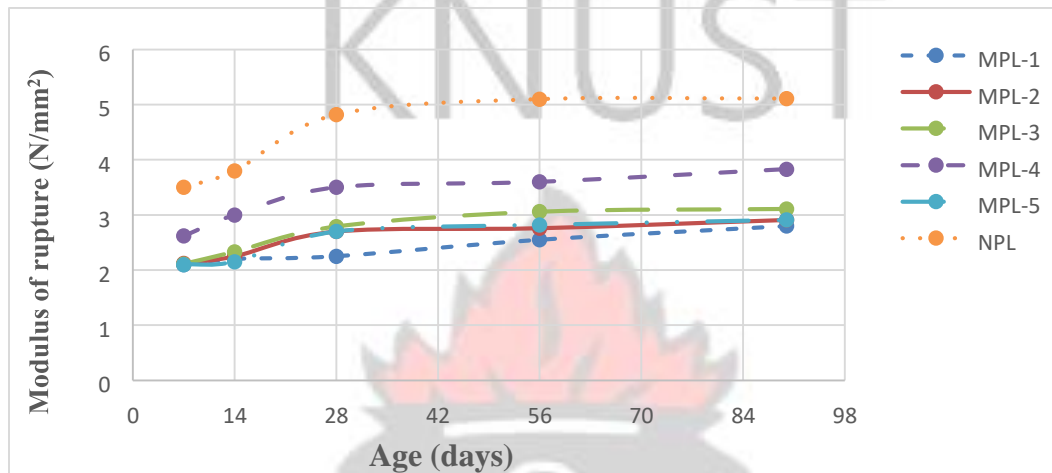


Fig. 4.12 Flexural tensile strength of PKS concrete using Portland-limestone cement

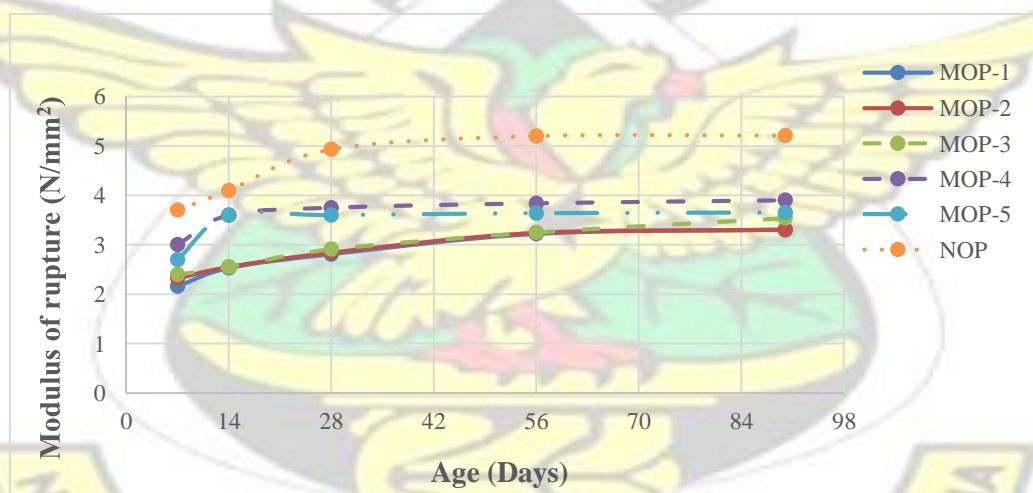


Fig. 4.13 Flexural tensile strength of PKS concrete using ordinary Portland cement

4.6.1 Tensile Failure beams

Generally, instantaneous failure of the beams in tension occurred as soon as induced bending stresses exceeded the tensile strength of the beams (Alengaram *et al.*, 2010a). Failure of the beams occurred as a result of failure of bond (in tension) between the cement matrix and the surface of the aggregates (see Fig. 4.10). Mehta and Monteiro (2006) have shown that concretes with rough textured or crushed aggregates have higher flexural tensile strengths, especially at early ages, than

smoother aggregates. Thus the higher MOR values obtained for NWC is attributable to the rough textured granite aggregates which enhanced the bond between the aggregates and the cement matrix. PKS aggregates have smooth convex surfaces which tend to reduce the strength of the bond between the aggregates and the mortar, hence the lower flexural strength.



4.7 BEHAVIOUR OF REINFORCED CONCRETE BEAMS IN FLEXURE

4.7.1 Details of PKS concrete and NWC (Control) Beams

The results of the densities, compressive and flexural tensile strengths of PKS concrete and normal weight concrete beams tested at the age of 28 days are presented in Table 4.6 and 4.7. The average air dry density of the PKSC (with target compressive strength of 25 N/mm²) was about 23.32 N/mm² which is 26% lower than that of the NWC. The average 28-day compressive strength obtained for the NWC was about 28.5 N/mm². This relatively low level of compressive strength value might be attributed to the use of high w/c ratio of 0.50. The 28-day average compressive strength of the PKS concrete was 23.6 N/mm² which was about 6% lower than the target strength of 25 N/mm². Meanwhile a compressive strength of 30.66 N/mm² was obtained for a target compressive strength of 30 N/mm² for the NWC. The tensile strengths of NWC beam specimens were greater than the corresponding tensile strengths of PKS concrete beams (Tables 4.6 and 4.7). The average tensile strength was about 3.63 N/mm² for PKS concrete beam specimens while the average tensile strength of NWC was about 4.22 N/mm². The results indicate identical mechanical properties of all tested beams. The lower tensile strength of PKS concrete beams may be due to the lower stiffness of the PKS concrete since it undergoes higher strains compared to crushed granite aggregate (Alengaram *et al.*, 2011). Moreover, the poor adhesion between PKS aggregate and cement matrix due to the smooth convex surface of PKS was one of the factors that affected the compressive and flexural tensile strengths of the concrete.

Table 4.6 Details of Test beams without shear reinforcement

Beam designation	Beam size B x D (mm)	Air dry density (Kg/m ³)	Age at testing (days)	Compressive strength, f_c (N/mm ²)	Flexural strength, f_r (N/mm ²)
1 P 150	120 x 150	1807	28	30.3	3.60
1.5 P 150	120 x 150	1833	28	31.1	3.70
2 P 150	120 x 150	1899	28	30.5	3.71
1 P 200	120 x 200	1875	28	29.8	3.45
1.5 P 200	120 x 200	1897	28	31.7	3.41
2 P 200	120 x 200	1885	28	29.5	3.64
1 P 225	120 x 225	1801	28	29.3	3.42
1.5 P 225	120 x 225	1811	28	30.9	3.70
2 P 225	120 x 225	1855	28	28.7	3.58
1 P 250	120 x 250	1904	28	32.3	3.66
1.5 P 250	120 x 250	1927	28	32.3	3.55
2 P 250	120 x 250	1875	28	30.4	3.74
1 P 300	120 x 300	1912	28	31.7	3.81
1.5 P 300	120 x 300	1895	28	31.1	3.73
2 P 300	120 x 300	1917	28	30.3	3.61
2.44P225a	110 x 225	1897	28	23.9	3.70
2.44P225b	110 x 225	1875	28	23.6	3.60
2.44N225a	110 x 225	2370	28	29.2	4.30
2.44N225b	110 x 225	2369	28	28.7	4.10

Table 4.7 Properties of Test beams with shear reinforcement

Beam designation	Beam size B x D (mm)	Air dry density (Kg/m³)	Age at testing (days)	Compressive strength, f_c (N/mm²)	Flexural strength, f_r (N/mm²)
2P150A	120 x 150	1817	28	30.3	3.60
2P200A	120 x 150	1843	28	31.2	3.61
2P250A	120 x 150	1899	28	30.5	3.71
2P150B	120 x 200	1875	28	29.7	3.55
2P200B	120 x 200	1907	28	31.7	3.31
2P250B	120 x 200	1875	28	29.5	3.64
2P150C	120 x 225	1821	28	29.3	3.32
2P200C	120 x 225	1811	28	31.9	3.70
2P250C	120 x 225	1855	28	30.7	3.66
2P300C	120 x 225	1951	28	29.4	3.48
2P150D	120 x 250	1904	28	30.5	3.66
2P200D	120 x 250	1917	28	32.1	3.55
2P250D	120 x 225	1941	28	30.4	3.50
2.44P200E	110 x 225	1902	28	22.6	3.70
2.44P250E	110 x 225	1911	28	23.4	3.71
2.44P300E	110 x 225	1888	28	23.1	3.45
2.44N200E	110 x 225	2342	28	29.2	4.10
2.44N250E	110 x 225	2395	28	30.3	4.30
2.44N300E	110 x 225	2375	28	29.8	4.30

4.7.2 BEHAVIOUR OF BEAMS WITHOUT SHEAR REINFORCEMENT

4.7.2.1 General load-deflection behaviour of the beams

The load-deflection curves for the various beams tested are presented in Fig. 4.14. The load-deflection curves could be identified by three distinct stages: pre-cracking stage, post cracking stage and the ultimate stage (steel yielding). The last two stages are not very distinct, however, they led to a significant reduction in the ultimate loads, depending on the amount of longitudinal reinforcement. At pre-cracking stages of loading, both steel and concrete behaved as a composite material and distributed the load throughout the specimen until the stress in concrete reached its tensile strength limit and the first crack appeared in the flexural zone.

The position of the first crack was, however, inconsistent and appeared to be random within the pure flexural zone. The flexural cracks began from the soffit of the beams and propagated vertically upward as the loading increased. The combination of bending and shear stress action within the shear zone led to the formation of flexural-shear cracks in most of the beam specimens. The cracks appeared as vertically oriented flexural cracks from the extreme bottom fibers which gradually propagated towards the load application point at the top of the beam (Appendix A). Various cracks initiated within the shear spans and the flexural zones with associated increase in applied loads. The PKS concrete beams at the pre-cracking stage behaved similarly as the normal weight concrete until the onset of flexural cracking which occurred comparatively earlier. It is seen from the load-deflection curves that PKS beams demonstrated larger deflections compared to the NWC beams.

First cracks appeared at loads of 12kN and 10kN (representing 17% and 20% of ultimate loads) for PKSC beam specimens 2.44P225a and 2.44P225b respectively in the pure bending zones

(Table 4.8). For the NWC beams, the first flexural cracks started at 18kN and 14kN (which represent 16% and 23.3% of ultimate loads), for specimens **2.44N225a** and **2.44N225b** respectively. Diagonal tension cracks were observed at about 56% of the ultimate load for the PKSC without shear reinforcement compared to 67% of ultimate loads for corresponding NWC beams. For specimen **2.44N225a**, the shear span to depth ratio, a/d , was 2.07. The shear transfers through dowel action and the intact concrete section within the compression zone therefore played significant role in resisting the applied shear force, which consequently resulted in increased ultimate failure load (He and Kwan, 2001). The higher shear strength of specimen **2.44N225a** could also be attributed to aggregate interlock mechanism of the granite aggregates due to high frictional forces that develop across the shear crack surface. This component of shear strength is more significant if the cracks are narrower (Ghannoum, 1998). Walraven and Al-Zubi (1995) reported that the irregular shape of crack surfaces enhances shear transfer mechanisms despite the fact that aggregates may fracture completely at cracking.

In all beams, first flexural cracks were observed at lower loads among the PKSC beams compared to NWC beams. This indicates a lower tensile strength of PKS concrete beams as shown by the results of the modulus of rupture test (see Fig. 4.13). For the NWC beams, the more linear behaviour of NWC in the pre-cracking stage could be attributed to the good aggregate bond of the granite aggregates in the concrete matrix and increased bending strength associated with concrete-steel bond. Considering the relatively short span beam (**2.44P225a** and **2.44P225b**), it is seen that both types of concrete exhibited closely related deflection values. Deflections and diagonal cracking were observed to vary considerably depending on the type of concrete and the associated beam properties. It was generally observed from the tests that ultimate failure loads obtained for PKSC beams are lower as shown in Fig. 4.14. It is seen that higher aggregate crushing

strength is provided by the gravel aggregates (see Table 4.1). This allows sufficient dowel action of longitudinal steel reinforcement to be mobilized and subsequently, leading to increase in the aggregate interlock capacity in NWC beams. Contrary to the lower impact strengths of PKS aggregates, the PKS aggregates can fracture easily in concrete. Therefore, this would lead to lack of dowel action of the tension reinforcement to be mobilized, leading to a lower ultimate failure load compared to the NWC beams.

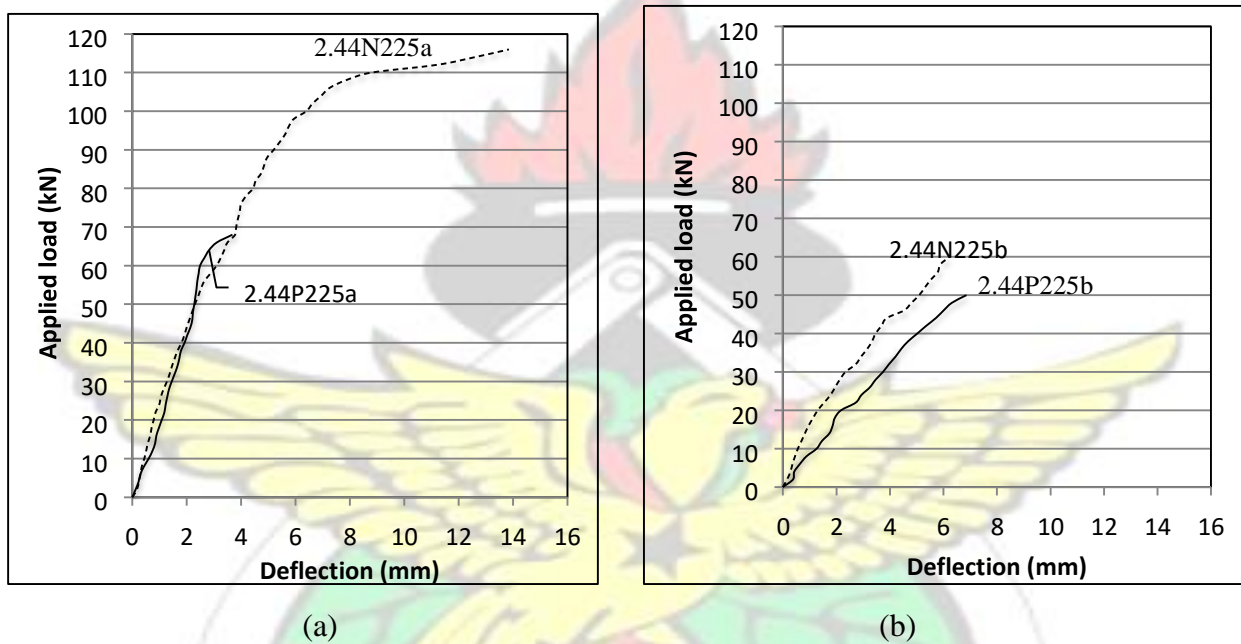


Fig. 4.14 Load-deflection behaviour of PKSC and NWC R-series beams

Table 4.8 Cracking loads of beams without shear reinforcement

Beam ID	Applied load, (P kN)	Ratio (%)
---------	----------------------	-----------

	First flexural crack, P_f	Diagonal crack, P_d	Ultimate failure load, P_u	$100P_f/P_u$	$100P_d/P_u$
1 P 150	10	30	52	19	58
1.5 P 150	12	32	60	20	47
2 P 150	14	36	62	23	55
1 P 200	12	32	62	16	52
1.5 P 200	14	38	68	21	56
2 P 200	18	42	82	22	51
1 P 225	12	40	72	17	56
1.5 P 225	14	46	78	18	59
2 P 225	18	54	88	20	61
1 P 250	14	44	80	18	53
1.5 P 250	18	52	84	21	62
2 P 250	30	64	92	33	70
1 P 300	18	68	102	18	67
1.5 P 300	30	72	104	29	69
2 P 300	40	78	106	38	74
2.44P225a	12	42	70	17	60
2.44P225b	10	28	50	20	56
2.44N225a	18	62	114	16	54
2.44N225b	14	40	60	23	67

Where P_f is first flexural crack; P_d is diagonal crack; P_u is ultimate failure load. The change in slope of the load deflection curve which is characteristic of the reduced stiffness of the cracked section, became dominant in all beam specimens after the first crack. At the postcracking stage, the properties of the longitudinal reinforcement were activated, leading to the utilization of the

tensile strength of the steel to achieve equilibrium in the composite section, and a change in slope of the load-deflection curve is observed. The associated failure was sudden for all types of beams with associated splitting of the concrete due to diagonal shear failure. All the series of beams tested failed as a result of diagonal tension cracks with wide cracks emanating from supports to loading points.

It is seen that, higher shear resistance of NWC beams compared to their PKSC counterparts were observed in the short spans, principally due to the formation of arch action. Since a greater proportion of the shear transfer occurs through aggregate interlock, which normally represents up to 50% of the total shear transfer, the reduced crushing strength of PKS aggregates could also account for the reduction in strength compared to the NWC. The shear forces in the cracked section at this stage was mainly resisted by the shear resistance of compression zone above the neutral axis, the interlocking action of the aggregates, and the dowel action of the longitudinal reinforcement (Kim and Park, 1996).

4.7.2.2 Crack Development Patterns of the Beams

First flexural cracks occurred in the pure bending zone of the beams. These cracks were soon joined by cracks in the shear spans of the beams and originated as flexural cracks. However, they quickly bent over and assumed the characteristics of diagonal tension cracks. One diagonal shear crack on each end of the beam developed more fully than the others. One of these fully developed shear cracks then led to failure. In some cases, two small cracks would combine to form the failure crack while independent cracks formed the failure cracks in some other beams, especially beams with 1% longitudinal reinforcement ratio. Shear transfer ran along one major diagonal crack,

which developed from one of the flexural cracks at one side of the beam in the shear-span of the support zone, when the load was close to the maximum in some beams.

The complete crack development in the beams is presented in Table 4.9. First flexural cracks appeared at loads of 10kN to 40kN (representing 19% to 38% of ultimate loads) for PKS concrete beam specimens in the pure bending zones. For the NWC beams, the first flexural cracks started at 18kN and 14kN (which represent 16% and 23.3% of ultimate loads), for specimens **2.44N225a** and **2.44N225b** respectively. As the loading increased, additional cracks appeared in the bending and shear spans, and the existing cracks extended and turned from vertical flexural cracks to inclined flexural-shear cracks (Fig. 4.15). The failure modes of both PKSC and NWC beams were sudden with virtually no warning, which is characteristic of reinforced concrete beams without shear reinforcement (Dinh, 2009; Angelakos, 1999).

The appearance of diagonal tension cracks was observed in all tested specimens at inclined angles ranging between 35° and 50° from the horizontal with steeper angles occurring at higher diagonal crack loads. In these beams, diagonal tension cracks evolved from previously formed flexureshear cracks where the inclined portion extended linearly down toward the soffit. This downward crack occurred because arch compression strut formed in the intact concrete above the flexureshear crack forcing the shear stresses in the bottom wedge to increase quickly and force the appearance of the diagonal crack. While flexure cracks tended to elongate progressively as the load was increased, diagonal tension cracks appeared quickly and were long and wide regardless of the manner with which they formed.

Table 4.9 Cracking behaviour of beams without shear reinforcement

Applied load, (P kN)	Max.

Beam ID	First flexural	Diagonal crack, Ultimate failure			Average crack spacing, mm	
	cracks	No. of	crack	crack, P_f	P_d	load, P_u
1 P 150	10	30	52	45	20	0.28
1.5 P 150	12	32	60	50	18	0.26
2 P 150	14	36	62	75	12	0.25
1 P 200	12	32	62	100	12	0.42
1.5 P 200	14	38	68	120	10	0.45
2 P 200	18	42	82	80	15	0.52
1 P 225	12	40	72	250	6	0.33
1.5 P 225	14	46	78	167	9	0.29
2 P 225	18	54	88	100	15	0.18
1 P 250	14	44	80	86	21	0.34
1.5 P 250	18	52	84	129	14	0.13
2 P 250	30	64	92	62	29	0.17
1 P 300	18	68	102	92	24	0.335
1.5 P 300	30	72	104	96	23	0.24
2 P 300	40	78	106	79	28	0.19
2.44P225a	12	42	70	100	15	0.30
2.44P225b	10	28	50	115	13	0.29
2.44N225a	18	62	114	164	11	1.76
2.44N225b	14	40	60	82	22	0.31

Where P_f is first flexural crack; P_d is diagonal crack; P_u is ultimate failure load

All PKSC beams without shear reinforcement failed as a result of diagonal tension shear as shown

by the diagonal cracks in Fig. 4.15. A close look at the values in Table 4.9 reveal that the formation

of flexural cracking is primarily controlled by the amount of tensile reinforcement and size of

beam; an increase in the former delayed cracking while an increase in the latter without corresponding increase in reinforcement facilitated the formation of the flexural cracks. Diagonal cracking loads increased at various loading levels depending on the amount of tension steel and the beam sizes (Appendix A). The average number of cracks in PKSC beams were lower than corresponding number of cracks in the NWC beams while the vice versa occurred for the maximum crack width at failure (Table 4.9). Cracking in reinforced concrete is a severe problem that may reduce the stiffness of structural members and the functional life of a structure (Carino and Clifton, 1995). Therefore, crack widths have to be controlled in reinforced concrete members to control deflection, corrosion, permeability, use of high grade steel, maintenance of integrity and appearance of the structure (Parghi *et al.*, 2008). To reduce the problems associated with cracking, BS 8110 (1997) limits crack widths for non-liquid containing structures to a maximum of 0.3 mm.

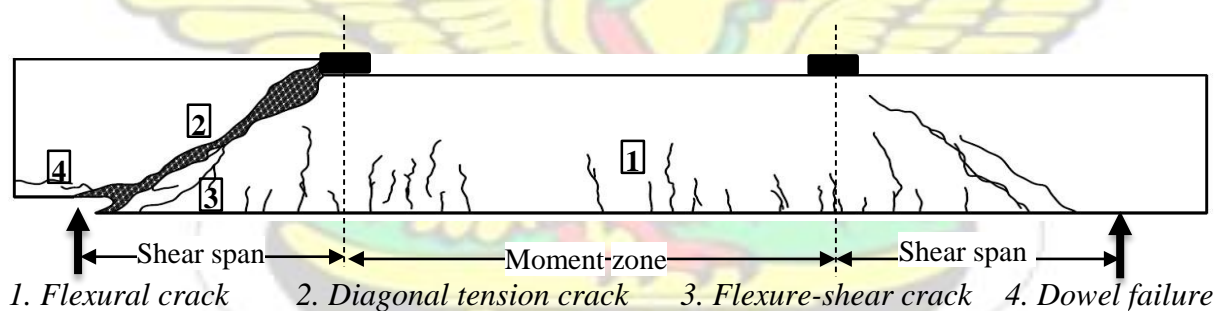


Fig. 4.15 Crack pattern for R-series specimen

4.7.2.3 Effect of longitudinal reinforcement, ρ_w on deflection and cracking of PKS beams

The amount of longitudinal steel has been shown to greatly affect the shear behaviour of a concrete beam (Figures 4.16). The important influence of the longitudinal steel ratio, ρ_w on the shear stress at failure is also confirmed as the beams with $\rho_w = 2\%$ were consistently stronger with associated increased failure loads. Generally, deflections decreased while shear stresses increased with increase in longitudinal steel ratios for all test specimens. It is reported that when the longitudinal

reinforcement ratios in beams decrease, the shear force carried by the dowel action of longitudinal steel reinforcement decreases (Kong and Evans, 1998). Thus, wider crack widths are observed in beams with lower longitudinal reinforcement ratios as shown in Appendix A.

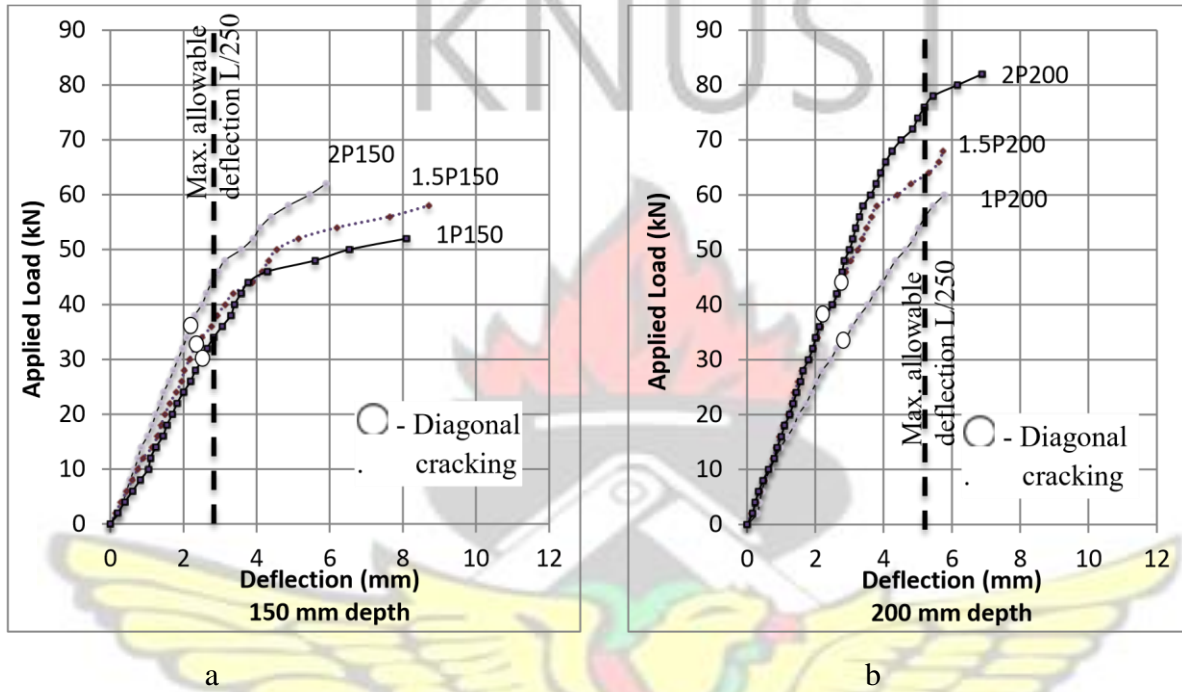
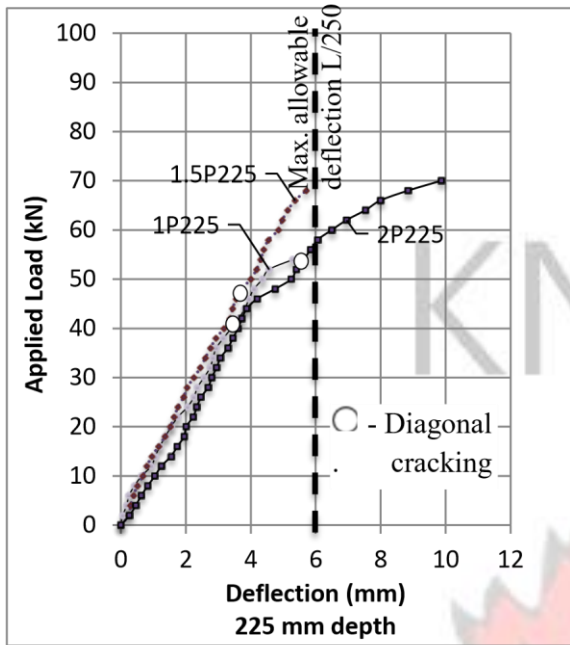
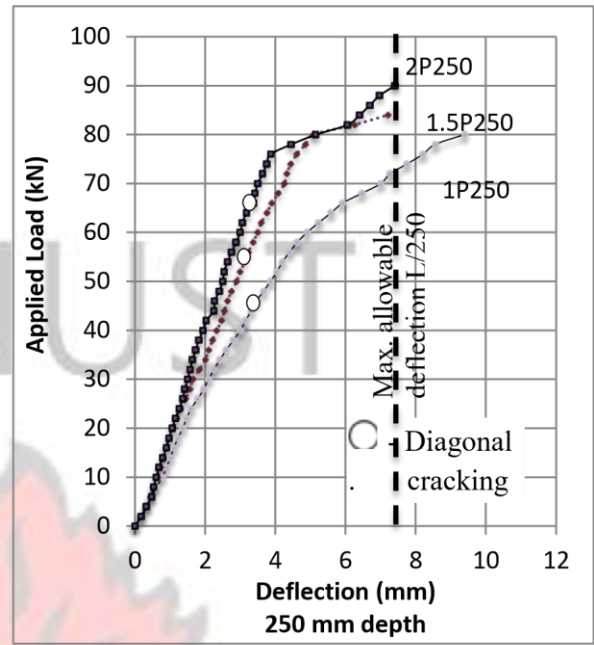


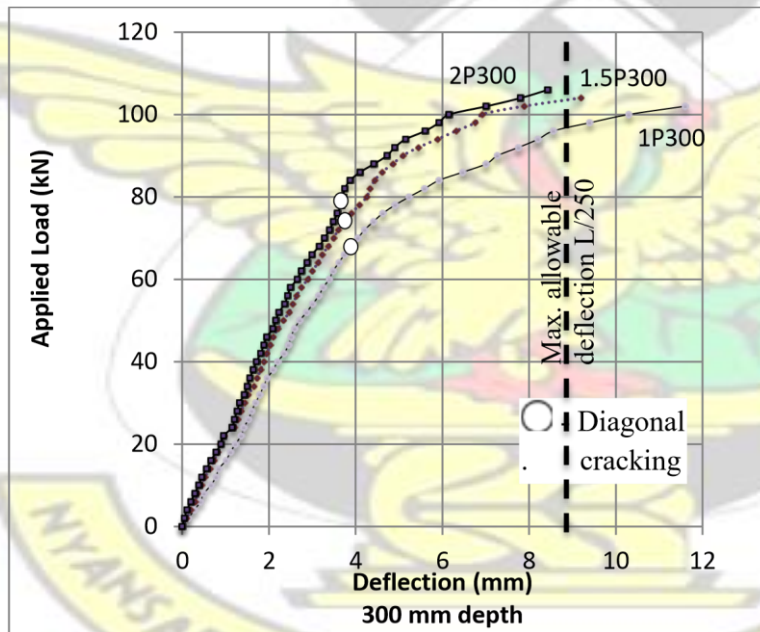
Fig. 4.16 (a-b) Load deflection behaviour of PKSC R-series beams



c



d



e

Fig. 4.16 (c-e) Load deflection behaviour of PKSC R-series beams cont'd The effect of the longitudinal steel on the shear strength of the beam can also be explained through the dowel action of the steel. A major component of shear strength in concrete arises from the friction forces that develop across the diagonal shear cracks by aggregate interlock and the dowel action of the

longitudinal reinforcement. This component of shear strength through aggregate interlock is more significant if the cracks are narrow (Ghannoum, 1998). Wider crack widths would reduce the aggregate interlock capacity, and result in lower ultimate failure loads (Kong and Evans, 1998). Subsequently, higher amount of longitudinal reinforcement which reduces the shear crack widths, would allow the concrete to resist more shear. The applied shear stress to initiate diagonal cracking increases with longitudinal reinforcement ratios. The increase in shear stress required is caused by the ability of the increased reinforcement bars through reduced stresses in them to control flexural cracking which disrupts the shear redistribution.

Given the same specimen geometry, the number, crack widths and their dispositions could be attributed to the amount of longitudinal reinforcement in the tested beam specimens. Crack lengths in specimens with a lower amount of longitudinal reinforcement are found to be longer compared to crack lengths in specimens with higher amount of longitudinal reinforcement. That notwithstanding, higher loads were needed to cause the same cracking in the specimens with higher amount of longitudinal reinforcement ($\rho_w = 1.5$ and $\rho_w = 2.0$). Increasing the amount of longitudinal reinforcement resulted in a corresponding increase in diagonal cracking loads for each beam series (see Table 4.9). This may be attributed to the fact that the longitudinal steel has a limited zone of influence in controlling the formation of diagonal crack widths over increased concrete cross sections. That is, smaller depth specimens will almost entirely be under the influence of the longitudinal reinforcement and have their shear crack widths controlled over most of their height. Meanwhile the cross-section of larger specimens is only partially influenced by the steel over only a limited region. Thus, the larger the specimen, the smaller the zone of influence with respect to the intact compression zone above the neutral axis in a given cross

section. Zararis and Papadakis, (2001) noted that this compression zone acts as a buffer for preventing any significant contribution of shear slip along the crack interface.

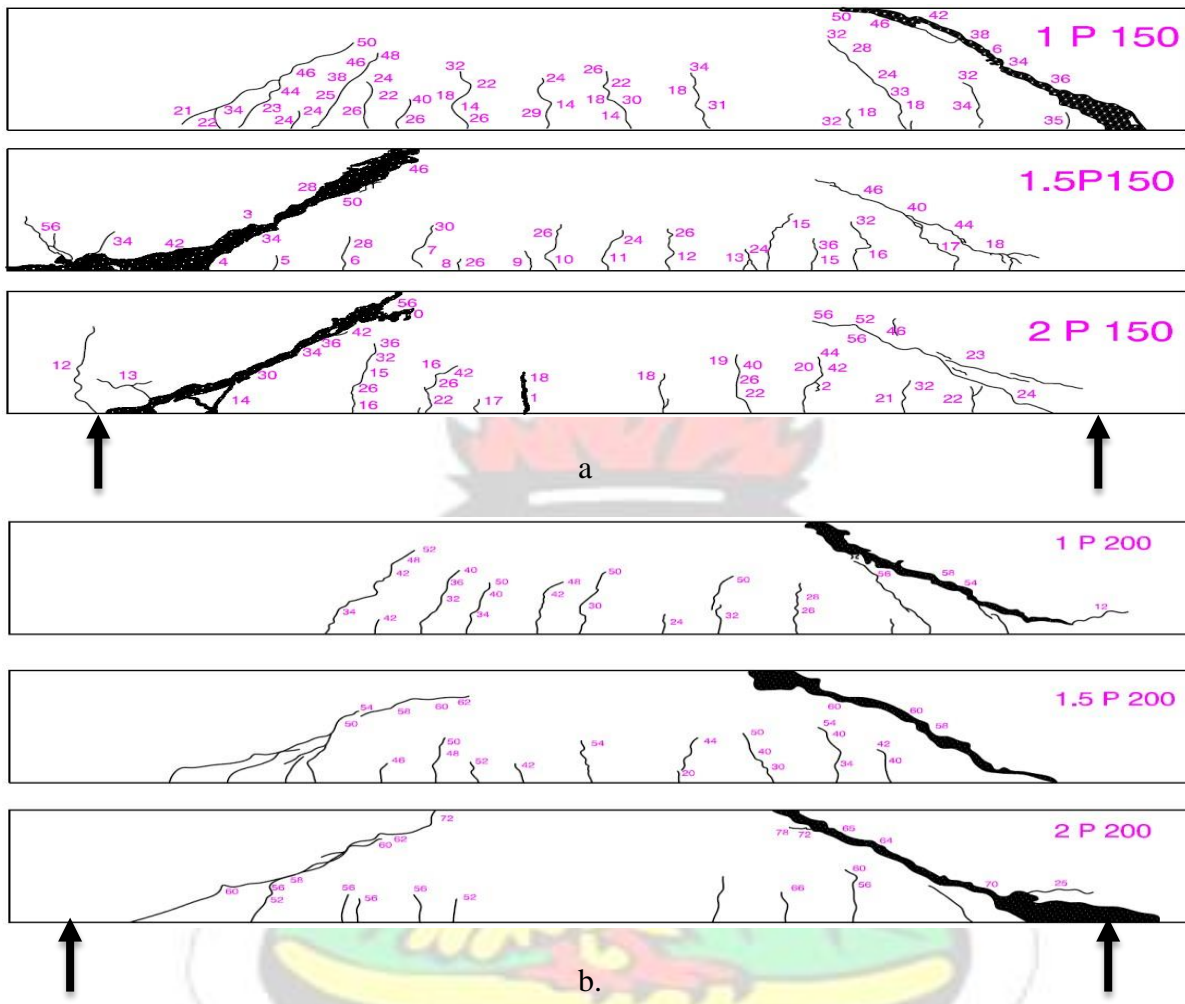
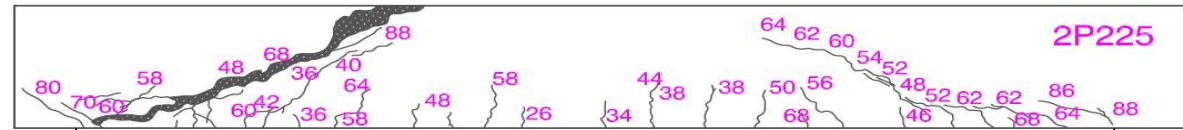
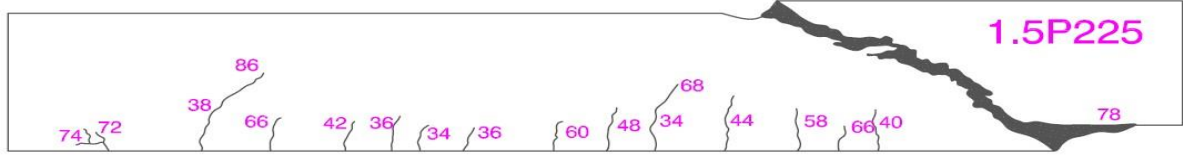
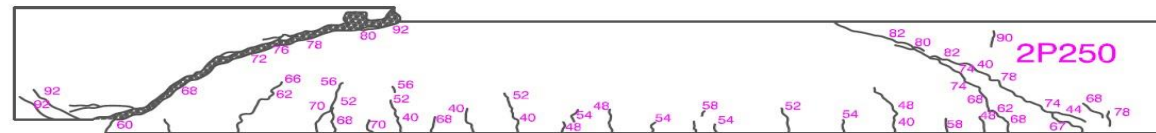
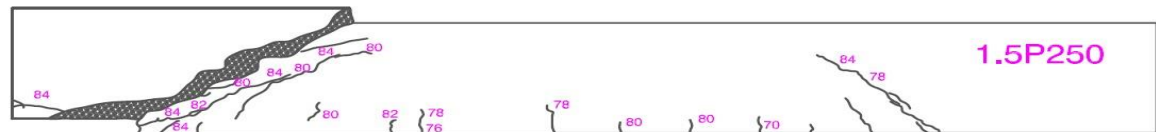
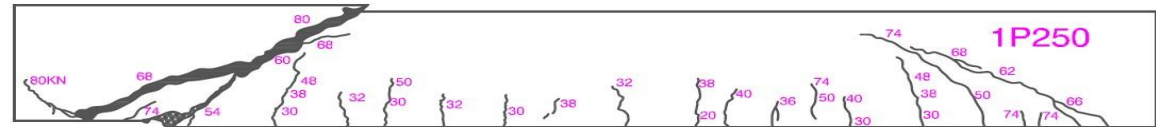


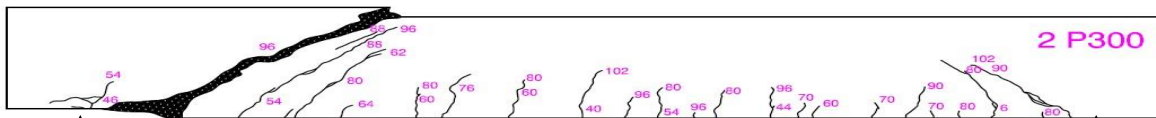
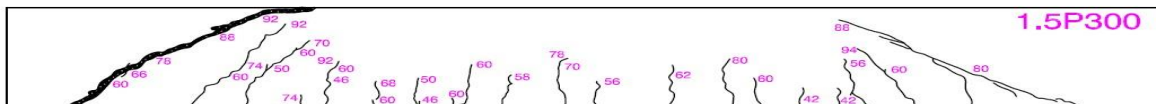
Fig. 4.17 (a-b) Effect of ρ_w on cracking of R-series Beams



c



d



e.

Fig. 4.17 (c-e) Effect of ρ_w on cracking of R-series Beams cont'd Considering specimens of depths 150 mm to 200 mm, the average crack width decreased with increasing longitudinal reinforcement while the average crack width increased with increasing amount of longitudinal reinforcement for specimens of depths 225 mm to 300 mm (Fig. 4.17a-e). The higher the beam size and amount of tension steel, the higher the ultimate failure loads. This may be attributed to the higher influence of the longitudinal reinforcement on smaller depth beams compared to the beams with increased depth. It is also obvious that the greater the number of cracks, the narrower the crack widths (Hassan *et al.*, 2008; Teo *et al.*, 2006; Lim *et al.*, 2006). This is clearly seen from the results in Table 4.11 where the maximum crack widths decreased with increasing number of cracks for a given beam series at various tension steel levels. As crack widths increased, their ability to transfer shear stresses by aggregate interlock were expected to decrease. This may have contributed to the reduced ultimate failure loads in beams with lower reinforcement ratios.

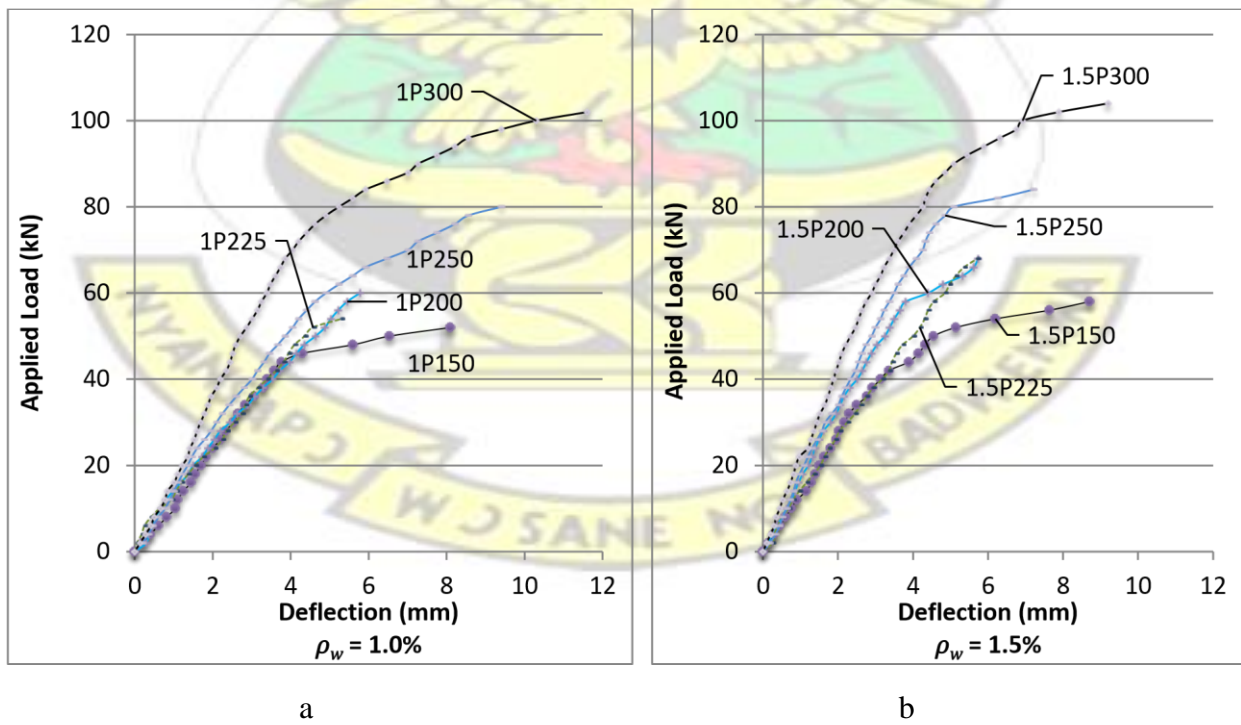
In Table 4.11, the average crack spacing shown is obtained by simply dividing the total length of the specimen by the number of cracks. Average crack spacings are found to be inconsistent with the amount of longitudinal reinforcement without following any specific pattern. A close look at the results in Table 4.11 reveals that for a given amount of longitudinal reinforcement, the number of cracks decreased with increasing amount of longitudinal reinforcement. This is because the increased longitudinal reinforcement ratio controlled the extent of flexural cracking for any given beam series.

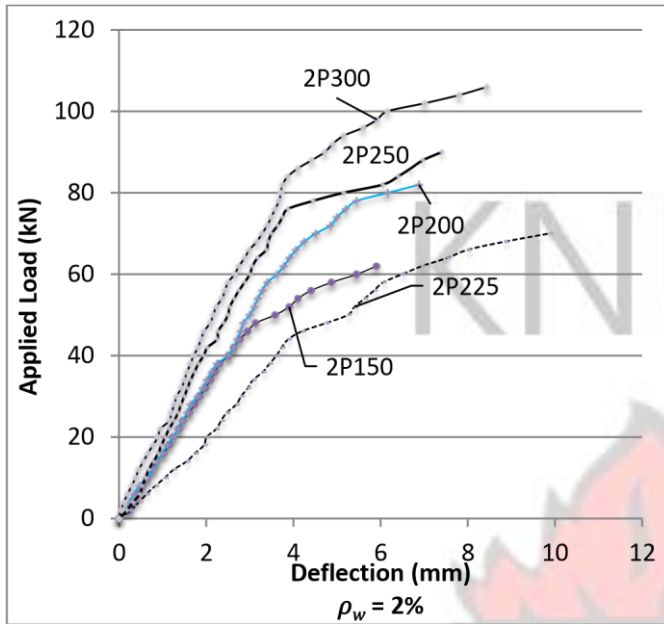
4.7.2.4 Effect of beam size on cracking patterns of PKS beams

Loading was applied monotonically to all beams, with the deflection, crack patterns and crack widths recorded at incremental loading. Considering the overall depth of the beams, five different

beam sizes could be identified, ranging from 150 mm to 300 mm. Meanwhile the effective spans of test beams were 900 mm, 1200 mm, 1500 mm, 1800 mm and 2200 mm. Considering Fig. 4.18 it is seen that deflections were identical for all dimensions of beams at the various tension steel ratios until the onset of first flexural cracks.

The ratio of diagonal cracking load to ultimate failure loads varied from 52% to 67% for beams depths varying from 150 mm to 300 mm at 1% longitudinal reinforcement ratio (see Table 4.9). This ratio varies from 47% to 69% and 51% to 74% for beams with $\rho_w = 1.5$ and $\rho_w = 2.0$ respectively. The average number of cracks varied from 6 to 24. However, the amount of variation was inconsistent with the size of the beam. A closer assessment of the results indicates an increase in the maximum crack widths at failure with increasing beam sizes. Figure 4.19 shows the variation of ultimate shear stress (V_n) of PKS concrete beams having varying depths at various longitudinal reinforcement ratios.





c

Figure 4.18 (a-c) Load-deflection behaviour of R-series beams

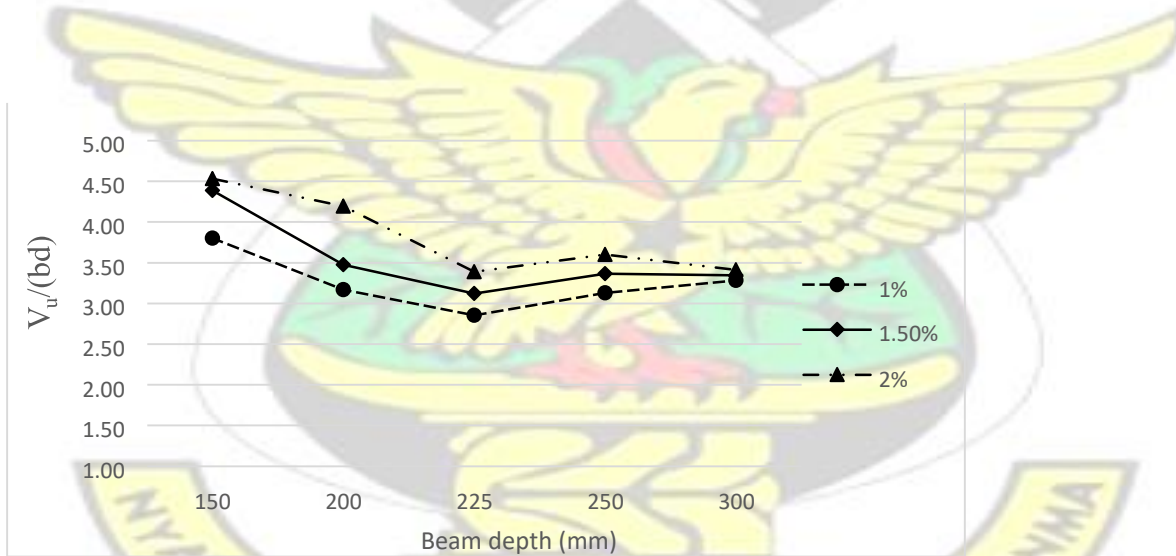


Figure 4.19 Effect of increasing beam depth on shear stress

It is observed that as the effective depth increases from 150 mm to 300 mm for beams without shear reinforcement, there is a reduction of cracking shear strength and ultimate shear strength, even though not very significant loss of strength as observed by other researchers for

comparatively large beam specimens (Arun and Ramakrishnan, 2014; Hassan *et al.*, 2008). This clearly indicates a size effect in diagonal cracking shear strength and ultimate shear strength of beams at various tension reinforcement.

4.7.2.5 *Ultimate failure modes*

Table 4.10 presents various modes of failure for the test specimens (see appendix A). The ultimate failure modes of all beams occurred either as flexural-shear, diagonal tension or concrete crushing. In some cases, anchorage failure was associated with either one of the former failure modes. It is observed that for short shear spans with a/d from 1 to 2.5, final failure of such beams is caused by a bond failure, a splitting failure, or a dowel failure along the tension reinforcement (Wight and Macgregor, 2012). Test specimens 2.44N225a and 2.44N225b showed anchorage failure in addition to the shear failure, which may be attributed to high stress concentration near the supports. Alengaram *et al.* (2011a) reasoned that anchorage failure is a sign of stronger bond between longitudinal reinforcement and the concrete.

Table 4.10 Modes of failure of R-series test specimens

Beam no.	Diagonal crack, P_d	Ultimate failure load, P_u	Failure mode
1 P 150	30	52	Flexural-shear/ diagonal tension
1.5 P 150	32	60	Flexural-shear/ diagonal tension
2 P 150	36	62	Flexural-shear/ diagonal tension
1 P 200	32	62	Flexural-shear/ diagonal tension
1.5 P 200	38	68	Flexural-shear/ diagonal tension
2 P 200	42	82	Flexural-shear/ diagonal tension
1 P 225	40	72	Flexural-shear/ diagonal tension

1.5 P 225	46	78	Flexural-shear/ diagonal tension
2 P 225	54	88	Flexural-shear/ diagonal tension
1 P 250	44	80	Flexural-shear/ diagonal tension
1.5 P 250	52	84	Flexural-shear/ diagonal tension
2 P 250	64	92	Flexural-shear/ diagonal tension
1 P 300	68	102	Flexural-shear/ diagonal tension
1.5 P 300	72	104	Flexural-shear/ diagonal tension
2 P 300	78	106	Flexural-shear/ diagonal tension
2.44P225a	42	70	Flexural-shear/ diagonal tension
2.44P225b	28	50	Flexural-shear/ diagonal tension
2.44N225a	62	114	Flexural-shear/ diagonal tension
2.44N225b	40	60	Flexural-shear/ diagonal tension

Beams without shear reinforcement typically failed as a result of diagonal tension or flexural shear with the beam rupturing either along a fresh diagonal crack or the union of two or more previously formed cracks. The behaviour of the PKSC beams was found to be similar to the ultimate behaviour of the NWC beam specimens. A critical diagonal crack formed that led to the rupture of the concrete section. This occurred when an inclined crack was wide enough to prevent stress redistribution to other shear resistance mechanisms. As such, diagonal tension failure did not occur immediately after the appearance of a dominant diagonal tension crack. Some level of tensile forces could still be transferred across the crack once they formed through interface shear. These cracks then increased in width until a stage where complete shearing of concrete at the compression zone caused ultimate failure. As expected, the diagonal crack formed independently and not as a result of flexural crack development (Kong and Evans, 1998). Diagonal cracks which were far from the mid-span of the test specimens resulted in splitting the bond between the

longitudinal reinforcement and the concrete from the support to the point of loading for all beam series (Fig. 4.20). The formation of cracks along tension steel levels was a sign bond failure between the longitudinal reinforcement and the concrete. The above modes of failure are characteristic of slender beams whose shear span to effective depth ratios are between 2.5 and 5.5 (Nawy, 1996).

It was observed that the initial diagonal tension cracking occurred at lower loads, which can be attributed to the low flexural tensile strength of the concrete. PKS concrete beams were able to develop sufficient shear capacity from other mechanisms to continuously resist the increasing load. Cracking of PKS beams was, generally, found to be along the convex surfaces of the shells and not failure of PKS (see Fig. 4.10). In weak members or sections that are heavily reinforced, stresses within the section may increase significantly to facilitate the formation of diagonal tension shear cracks (Juan, 2011). These cracks appear suddenly and without warning, simultaneously extending from the neutral axis towards the loading point and the support in a straight line.



a Beams with $\rho_w = 1.5\%$

b Beams with $\rho_w = 2\%$

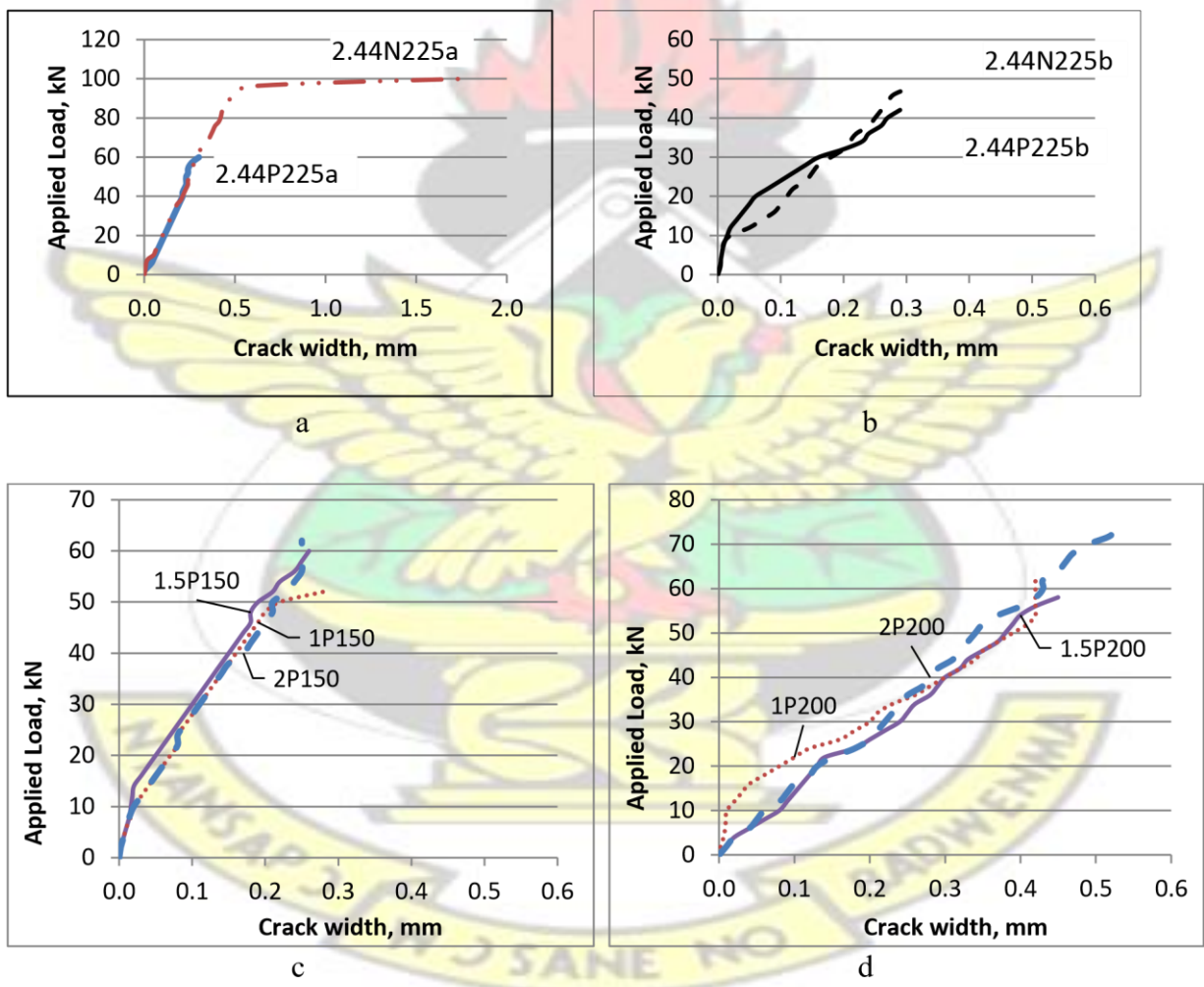
Fig. 4.20 Typical failure modes of test beams

The diagonal tension failure in the beams with high longitudinal reinforcement ratio indicates that the amount of longitudinal reinforcement contributed significantly to the shear failure modes of beams, either through dowel action or from an increased stiffness of the steel reinforcing bars. At higher longitudinal reinforcement ratios, the section developed larger flexural compression stresses to withstand higher loads. These higher loads also resulted in higher shear stresses at the tension steel levels. In the absence of shear reinforcement, it was observed that a shear compression failure mode occurred at intermediate longitudinal reinforcement ratios. It would be expected that as the longitudinal reinforcement ratio increased, with the additional compressive stresses, a similar shear compression failure would occur.

4.7.2.6 Crack spacing and crack width

In design, it is right to keep the maximum crack width at service load lower than the permissible values specified in Codes of Practice, depending on the type of structure and the conditions of its exposure. Service loads were determined based on the load factor method of BS 8110 (1997) for reinforced concrete beams (Adom-Asamoah and Afrifa, 2011). That is, service load is taken to be the ultimate load divided by a factor of 1.5. The maximum crack widths at service loads and failure are presented in Table 4.11. The applied load-crack width curves for the various specimens have been presented in Figure 4.21. It can be observed that at service loads, the average crack width for the reinforced PKS concrete beams without shear reinforcement (2.44P225a and 2.44P225b) are about 0.225 mm, and the maximum and minimum being 0.230 mm and 0.220 mm, respectively. For the NWC beams without shear reinforcement (2.44N225a and 2.44N225b), the average crack width was about 0.318 mm and the maximum and minimum being 0.390 mm and 0.245 mm respectively. However, wider crack widths appeared at comparatively higher loads. These values show that crack widths among PKS beam specimens were lower than corresponding NWC beam specimens.

The wide cracks in the NWC beams could be attributed to elongation of the reinforcement into the plastic region. It is also seen from Table 4.11 that diagonal shear cracks (first shear crack) occur before the beams' deflection exceeded the serviceability limits for all test specimens. However, the post-cracking behaviour of PKS concrete give a different behavior pattern. The PKS beams were able to sustain comparatively higher loads after cracking than the NWC beams before the ultimate failure occurred (Table 4.11).



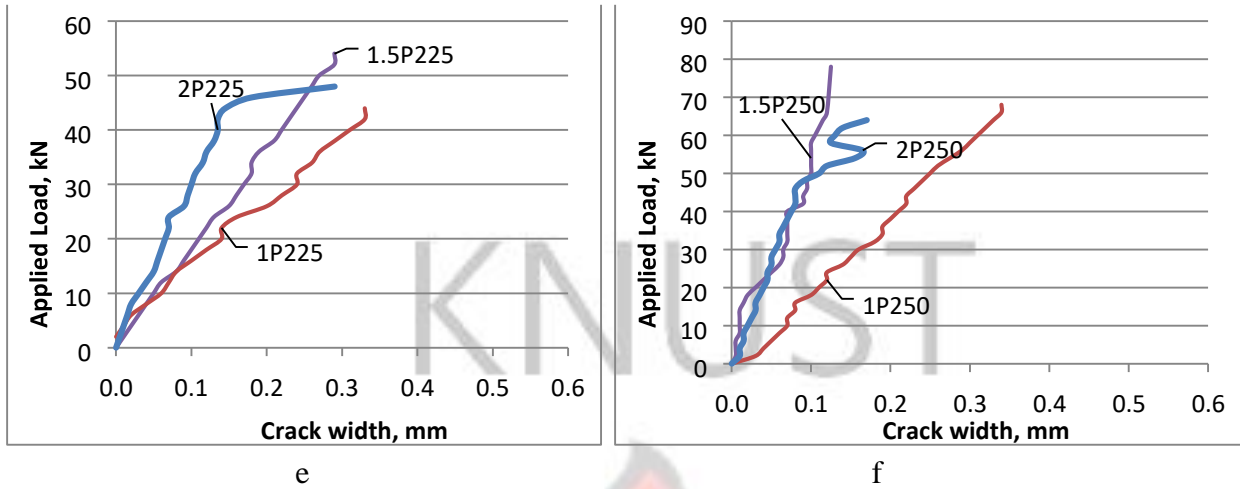


Fig 4.21(a-f) Cracking load versus crack width curves (a-g)

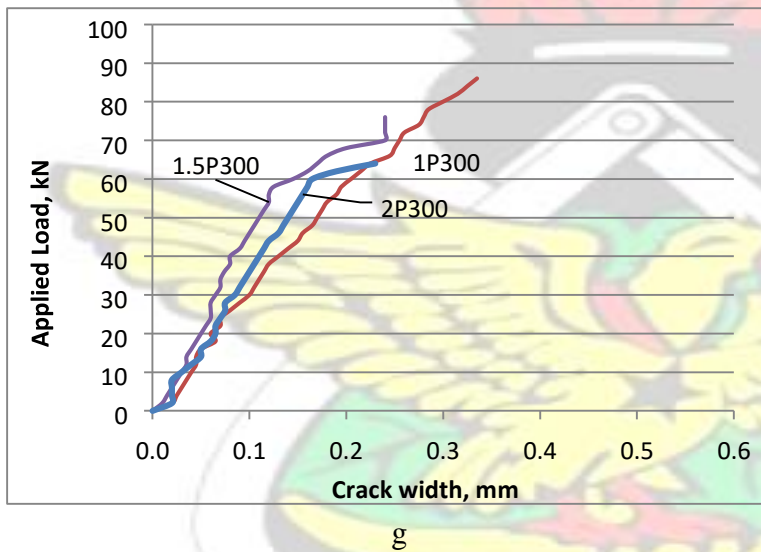


Fig 4.21g Cracking load versus crack width curves cont'd

4.7.2.7 Shear resistance characteristics of PKSC/NWC beams

To analyze and compare the shear strength of beams, the ultimate shear load (V_u) is normalized to account for the difference in compressive strength of the PKS concrete beams. Since the shear strength is proportional to the square root of the compressive strength of concrete (f_c), the normalized shear load (V_n) was determined as follows:

$$V_n = \frac{V_u}{\sqrt{f_c}} \quad (4.1)$$

The normalized shear stress (V_{ns}) is then calculated as:

$$V_{ns} = \frac{V_n}{bd} \quad (4.2)$$

Normalized shear load and stress for all experimental PKSC beams are tabulated in Table 4.12.

Table 4.11 Experimental cracking loads and deflections at service loads

Beam no.	First diagonal crack, P_d	Ultimate failure load, P_u	Crack width at failure (mm)	Number of cracks at failure	Service Loads, V_{st}	Crack width at service loads, mm	Deflections at service loads, mm
1 P 150	30	52	0.28	20	34.7	0.138	2.83
1.5 P 150	32	60	0.26	18	40.0	0.145	3.20
2 P 150	36	62	0.25	12	41.3	0.180	2.45
1 P 200	32	62	0.42	12	41.3	0.29	3.60
1.5 P 200	38	68	0.45	10	45.3	0.32	2.80
2 P 200	42	82	0.52	15	54.7	0.39	3.20
1 P 225	40	72	0.33	6	48.0	n/a	4.10
1.5 P 225	46	78	0.29	9	52.0	0.29	4.10
2 P 225	54	88	0.18	15	58.7	n/a	6.30
1 P 250	44	80	0.34	21	53.3	0.27	4.20
1.5 P 250	52	84	0.21	14	56.0	0.10	3.20
2 P 250	64	92	0.17	29	61.3	0.12	3.20
1 P 300	68	102	0.335	24	68.0	0.25	3.90
1.5 P 300	72	104	0.24	23	69.0	0.22	3.40
2 P 300	78	106	0.19	28	70.7	n/a	3.25
2.44P225a	42	70	0.30	15	46.67	0.21	0.230

2.44P225b	28	50	0.29	13	33.33	0.22	0.220
2.44N225a	62	114	1.76	11	76.00	0.40	0.390
2.44N225b	40	60	0.31	22	40.00	0.225	0.245

4.7.2.7.1 Effect of Longitudinal Reinforcement, ρ_w on shear characteristics

The load-deflection behaviour of the beams was elastic before the onset of first flexural cracks depending on the amount of longitudinal reinforcement (ρ_w). At pre-cracking stage, the combined action of the longitudinal reinforcement and the concrete was evident. It is seen that increasing the amount of longitudinal reinforcement (ρ_w) from 1% to 2% increased the amount of stress required to cause first flexural cracking of the beams for a given beam geometry (Fig. 4.22). It is also seen that increasing the amount of ρ_w increased the beams' stiffness of the various beam geometries as higher deflections were noted among beams with 1% longitudinal reinforcement compared to beams with 1.5% and 2.0% ρ_w . The increase in shear stresses required is caused by the ability of the longitudinal reinforcement to control flexural cracking. This is because the longitudinal reinforcing bars restrain the extent and width of flexural cracks which in turn causes less disruption to the shear distribution across the beam sections. This is demonstrated in beams with large cross sections which tend to have reduced shear strengths since the cracks in this type of beams tend to be wider and propagate higher into the beams (Wight and MacGregor, 2012; ASCE ACI 445 1998).

The ratio of the first flexural tensile crack load to the failure load increases with increase in beams having 1.5% and 2% tension reinforcements (see Table 4.8). First cracking loads ranged from 10kN to 18kN for specimens with $\rho_w = 1\%$, indicating 16% to 19% of the ultimate loads, while for the PKS specimens with $\rho_w = 1.5\%$ they varied from 12kN to 30kN, indicating a ratio of 18%

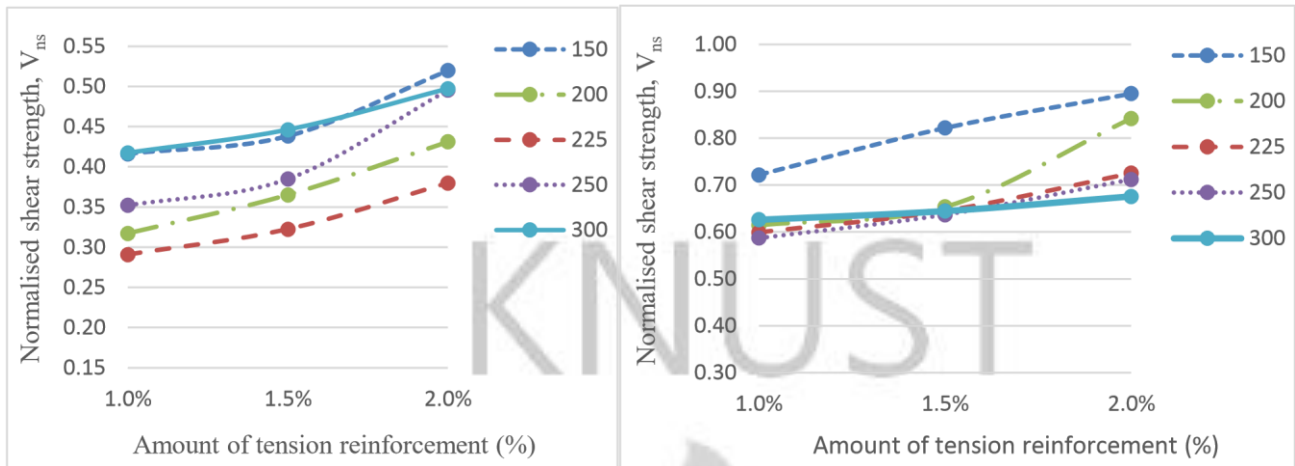
to 30% of the ultimate failure loads. The ratio of cracking loads to ultimate failure loads varied from 20% to 38% (14kN to 40kN) for beams with $\rho_w = 2\%$.

The onset of diagonal cracks within the shear zone were closely monitored and recorded with the corresponding cracking loads since shear failure only occurred once the concrete developed diagonal tensile cracks (Yap, 2012). It is seen that the applied shear force to initiate diagonal cracking increased with longitudinal reinforcement ratios just as observed at the first cracking. This increase in shear force required is caused by the ability of the increased reinforcement bars to control flexural cracking which interfered with shear distribution. After normalizing for the compressive strength of the concrete, it is noted that diagonal cracks initiated from 52% to 67% of ultimate failure loads for beams with $\rho_w = 1\%$. It is worthy of note that, the variation of the ratios was inconsistent with the sizes of the beam series. The ratio of diagonal cracking to ultimate failure loads varied from 47% to 69% for beams with $\rho_w = 1.5\%$ and 52% to 76% for beams with $\rho_w = 2.0\%$. This shows that the shear capacity of the concrete section to sustain additional loads after the diagonal cracking decreased significantly with increasing tension steel (Table 4.12).

Displacements at ultimate loads slightly decreased with an increase in longitudinal reinforcement (Fig. 4.22). It could be noted that the increase in shear transfer strength with longitudinal reinforcement is more for high reinforcement parameter. Generally, beams with lower tension reinforcement ratio of 1% developed wider crack widths during loading stages and at failure compared to beams with 1.5% and 2% longitudinal steel. This was expected as the presence of higher longitudinal steel ratio increases the resistance for the cracks to open wider and to extend vertically (Hassan *et al.*, 2008). According to El-Ariss (2006) for beams without shear

reinforcement, the shear capacity of beams' dowel action of reinforcing bars at the post-cracking stage of the loading process becomes very significant. As noted by Zararis (2003), the amount and disposition of the cracks for a given geometry of PKS beams were all affected by the amount of longitudinal reinforcement. Zakaria *et al.*, (2009) and Collins and Mitchell (1991) reported that the resistance of formation of diagonal cracking is a function of the ability of the longitudinal reinforcement to control vertical cracks. This was evident in all the tested beam specimens as the diagonal cracking loads increased in proportion to the amount of longitudinal reinforcement because of increased dowel action and a deeper compression zone (Ashour *et al.*, 1992 and Swamy *et al.*, 1993).

After normalizing for the compressive strength, it is seen from Figure 4.22 that the shear stress increases with increasing tension reinforcement as observed by Elzanaty *et al.* (1986). Comparing the stresses at diagonal cracking to the ultimate stresses at failure for the various beam depths, significant reduction in strength was noticed among beams with 300 mm depth. While the effect of increasing amount of longitudinal steel was significant (steep) in smaller depth beams, the effect is minimized, especially in beams with 300 mm depth. Contrary to the 300mm depth, beams with 150 mm depth maintained a consistent slope from the diagonal crack to the ultimate failure load. The effect of the longitudinal reinforcement on the shear strength can also be explained through the aggregate interlock mechanism which is obtained from the friction forces that develop across the diagonal shear cracks by aggregate interlock. This component of shear strength is more significant if the cracks are narrow (Ghannoum, 1998). Thus higher amount of longitudinal reinforcement which reduced the shear crack widths, would eventually allow the concrete to resist more shear stresses.



a. shear strength at diagonal cracking loads

b. Shear strength at ultimate loads

Fig. 4.22 Effect of ρ_w on normalized shear strength at diagonal and ultimate load

4.7.2.7.2 Effect of beam size on the behaviour of PKS concrete beams

Size effect is a phenomenon in reinforced concrete beams related to a relative reduction in shear strength due to increase in depth. The variations of diagonal cracking shear strength and ultimate shear strength of the PKS beams with effective depth have been explained.

The load-deflection behaviour of the various beam series at varying is shown in Figure 4.23. All tested specimens in this series failed as a result of flexure shear/diagonal tension with wide cracks irrespective of the size of the beam. Deflections decreased with increasing depth of the beam. It was observed that as the effective depth increase from 150mm to 300 mm for the beam series, there is a significant reduction in diagonal cracking load and ultimate failure loads.

After normalizing with the compressive strength, the ultimate shear stress decreased progressively with increase in beam depth (Table 4.12). When beam depth increased from 150 to 300 mm, the normalized shear stress of beams reinforced with 1% longitudinal steel decreased by 15%. Similarly, when beam depth increased from 150 to 300 mm, the shear stress of beams reinforced

with 1.5% and 2% longitudinal steel decreased by 25% and 26% respectively. Hassan *et al.* 2008 reported of a higher amount of decrease (32%) for self-compacting concrete with depths ranging from 150 mm to 750 mm and 1% longitudinal steel reinforcement. The effect of beam size is clearly demonstrated in Figure 4.23 where the shear stress decreases as the effective depth increases. The decrease in shear stress is almost 50% from **1P150** to **1P300**. The decreasing trend of the shear stress with increasing depth is consistent with the experimental results by Hassan *et al.* (2008).

This difference decreases as the specimen depth increases which confirms the effect of ρ_w on shear strength, with increased specimen depth. This may be attributed to the fact that the longitudinal reinforcement has a limited zone of influence in controlling the width of diagonal cracks over the concrete cross section (Ghannoum, 1998). Thus, the larger the specimen, the smaller the zone of influence with respect to the overall cross section. This effect indirectly contributes to the size effect in beams as well. Walraven and Al-Zubi (1995) reported that the irregular shape of crack surfaces enhances shear transfer mechanisms despite the fact that aggregates may fracture completely at cracking.

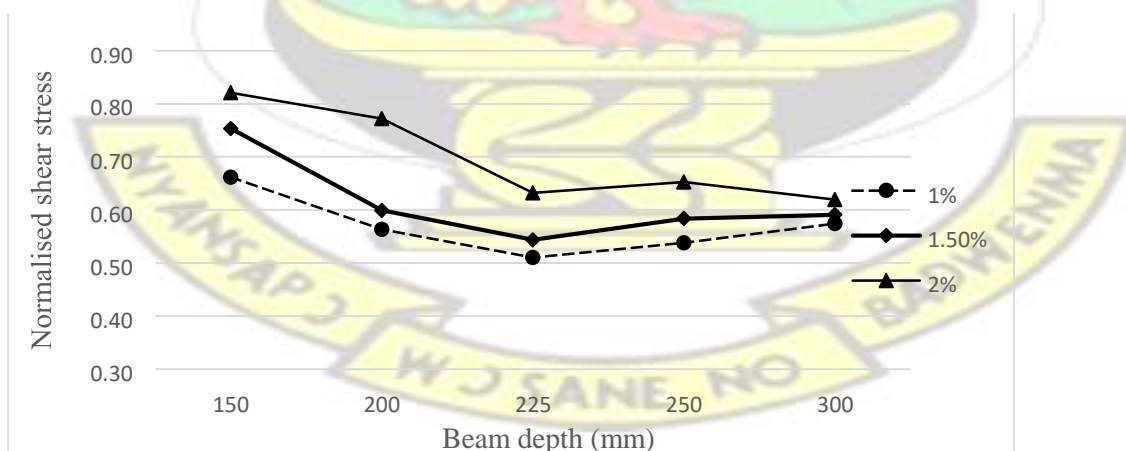


Figure 4.23 Effect of Normalised shear stress on beam size

4.7.2.7.3 Influence of parameters on reserve strength

Reserve shear strength index is taken as the ratio of the ultimate shear load to the diagonal cracking load (V_u/V_d). The diagonal-cracking stress is defined as the stress at which the first fully developed major diagonal tension crack appears in the shear span. The variation of decreasing reserve shear strength is shown in Figure 4.24. The reduction in reserve strength as beam depth increased from 150 mm to 300 mm varied from 1.73 to 1.50 for PKS beams with 1% steel reinforcement. The reserve strength varied from 1.88 to 1.44 and 1.72 to 1.36 for PKS beams with 1.5% and 2.0% steel reinforcement respectively (Table 4.12). It is seen that increasing the overall depth leads to a decrease in load carrying capacity after the diagonal cracking. This results in wider cracks and higher energy released rate at the interface of cracks due to reduction of shear strength (Arun and Ramakrishnan, 2014). The diagonal tension cracking stress was observed to be considerably less than the ultimate stress due to the interplay of different shear transfer mechanisms such as the beam arch action. A significant loss in reserve strength is found in beams with 2% longitudinal reinforcement ratio and a beam depth of 300 mm, indicating a size effect in the reserve strength of the beams (Fig. 4.25). Comparatively shallow specimens were consistently able to resist higher shear stresses after diagonal cracking than the deeper ones.

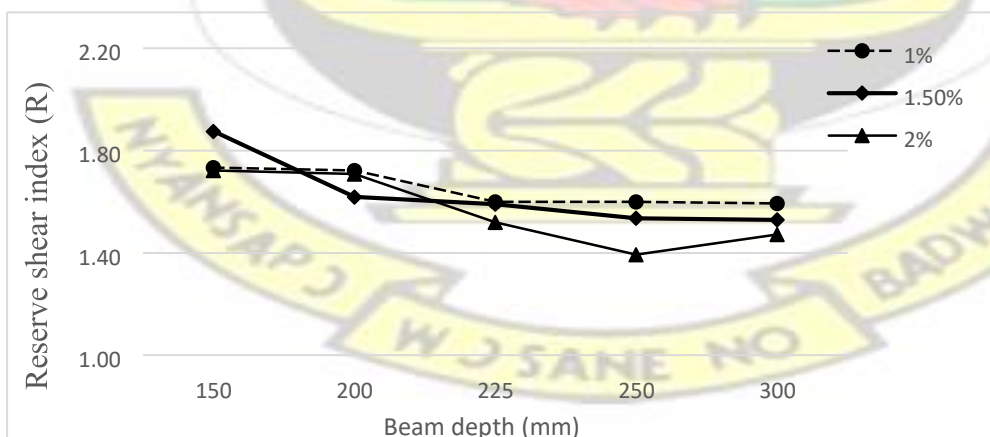


Fig. 4.24 Influence of reserve strength on beam size for varying ρ_w

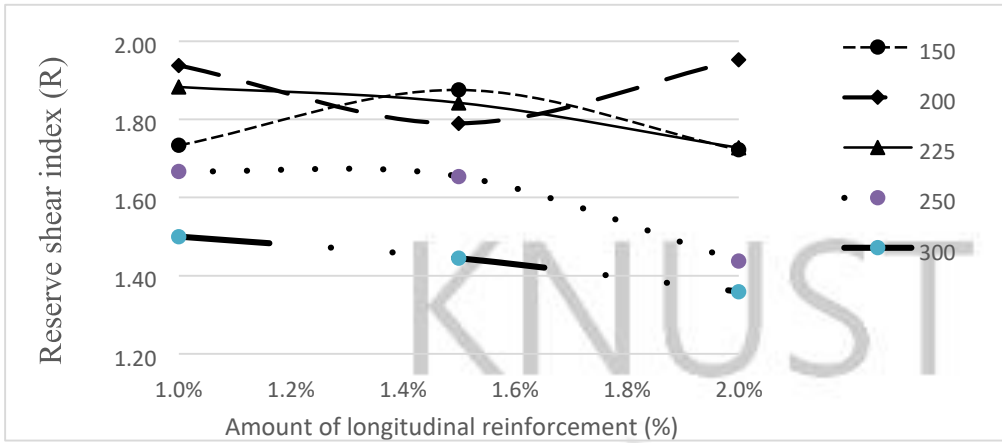


Fig. 4.25 Effect of Reserve shear strength on ρ_w for varying beam depths

Table 4.12 Normalized shear stress and reserve strength index of test specimens

Beam no.	Diagonal crack, P_a	Ultimate failure load, P_u	Stress at failure (N/mm ²)	Normalized stress at failure (N/mm ²)	Reserve strength, R (P_u/P_a)
1 P 150	30	52	3.64	0.52	1.73
1.5 P 150	32	60	4.20	0.60	1.88
2 P 150	36	62	4.53	0.62	1.72
1 P 200	32	62	3.08	0.47	1.94
1.5 P 200	38	68	3.37	0.50	1.79
2 P 200	42	82	4.19	0.63	1.95
1 P 225	40	72	2.76	0.44	1.88
1.5 P 225	46	78	3.02	0.47	1.84
2 P 225	54	88	3.39	0.53	1.73
1 P 250	44	80	3.06	0.47	1.67
1.5 P 250	52	84	3.32	0.50	1.65
2 P 250	64	92	3.60	0.56	1.44
1 P 300	68	102	3.23	0.50	1.50
1.5 P 300	72	104	3.30	0.52	1.44

2 P 300	78	106	3.41	0.53	1.36
2.44P225a	42	70	3.30	0.53	1.67
2.44P225b	28	50	2.36	0.42	1.79
2.44N225a	62	114	5.37	0.79	1.84
2.44N225b	40	60	2.83	0.45	1.50

4.7.3 BEHAVIOUR OF BEAMS WITH SHEAR REINFORCEMENT

Shear reinforcement performs the dual role of resisting shear stress as well as enhancing the ductility and strength of other shear transfer mechanisms. Provision of adequate amount of shear reinforcement can control the splitting cracks at the longitudinal reinforcement, increase the effect of the dowel action, and thereby enhance the shear capacity of the member (Angelakos, 1999; Yoon *et al*, 1996). Additionally, the shear reinforcement can limit crack propagation and crack widths in a structural member

4.7.3.1 Load-deflection Characteristics of Beams with Shear Reinforcement

The load-deflection characteristics of both PKS concrete and NWC beams with shear reinforcement are shown in Fig 4.26. The experimental shear capacities of the test specimens are tabulated in Table 4.13. In general, the load-deflection curves were similar for all three beams of PKS concrete (Fig. 4.26). The deflection curves were almost linear up to first cracking, beyond which nonlinearity began. Deflections at first crack loads were 2.5 mm, 1.40 mm and 0.84 mm for 2.44P200E, 2.44P250E and 2.44P300E at loads of 12 kN, 10 kN and 8 kN respectively. The deflections at first crack loads were 1.18 mm, 0.865 mm and 1.04 mm for 2.44N200E, 2.44N250E and 2.44N300E at loads of 16 kN, 14 kN and 12 kN respectively.

The ultimate failure loads obtained were 72 kN, 68 kN and 62 kN for 2.44P200E, 2.44P250E and 2.44P300E respectively. The presence and spacing of shear reinforcement increased the ultimate shear capacity of the beams by 44% for 2.44P200E, 36% for 2.44P250E and 24% for 2.44P300E when compared to the corresponding reinforced PKS beam without shear reinforcement. The results show that for a given load, the deflections of PKS concrete beams are higher than the corresponding NWC beam specimens (Fig. 4.26).

NWC beam specimens with shear reinforcement had ultimate failure loads of 74 kN, 72 kN and 66 kN for 2.44N 200 E, 2.44N 250 E and 2.44N 300 E beams (Table 4.13). Given the closeness of the values of flexural tensile strengths (MOR), the small but perceptible differences in the shear capacities of the beams would be due to the contribution of the shear reinforcement and particularly the spacing of stirrups.

From Fig. 4.26, the deflections of PKS concrete beams are higher than that of NWC beams. The results show that the contribution of shear reinforcement was marginal for both PKS concrete beams and NWC beams. It is evident that the amount of shear reinforcement is proportional to the shear capacity of both PKS concrete and NWC. That is, increasing shear reinforcement results in increased shear capacity of the beams. Ultimate deflections in both NWC and PKS concrete beams decreased with increasing spacing of shear reinforcement. This shows that the stirrups improved the ductility of the PKS concrete beams while brittle failure was greatly controlled. Lubell *et al.* (2009) concluded that the influence of the shear reinforcement decreases as the spacing of stirrups across the width of a member increases in NWC. Lubell *et al.* (2009) further concluded that the use of few shear reinforcement and widely spaced up to a distance of approximately $2d_{eff}$, decreased the brittleness of the failure mode compared with a geometrically similar member without web reinforcement.

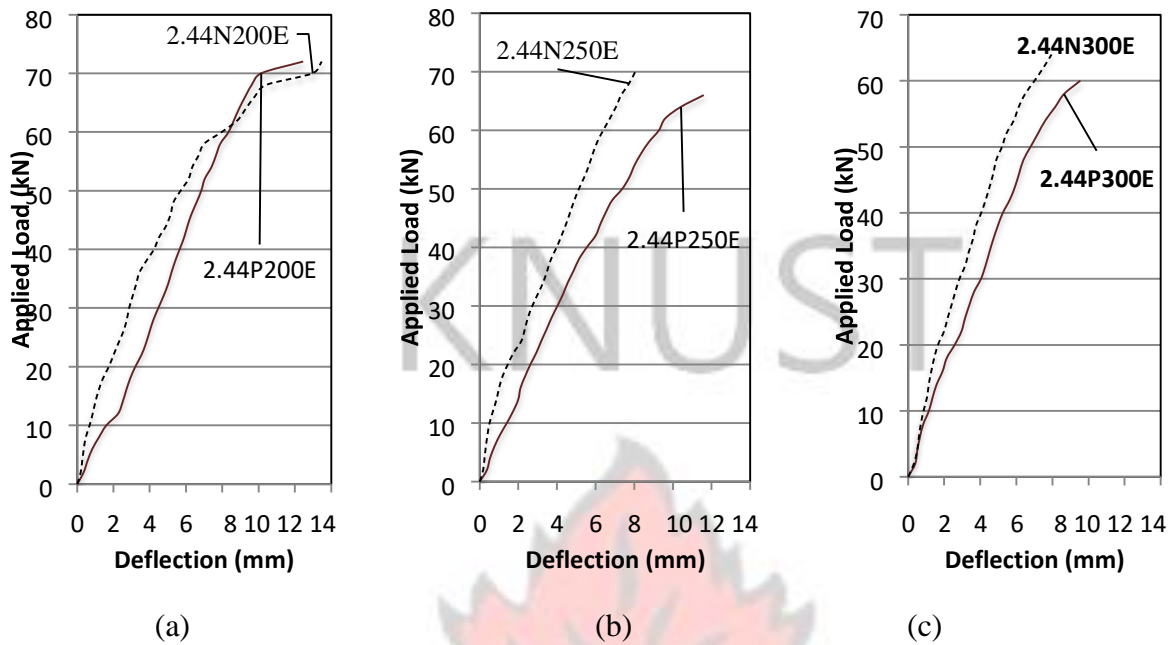


Fig. 4.26 Load/ Deflection behaviour of PKSC and NWC of S-series specimens

From this study, the amount of shear reinforcement is found to be proportional to the shear capacity of both PKSC and NWC. The results show a close relationship in the behaviour of the PKS and NWC beams under the influence of shear reinforcement. The amount of shear reinforcement is also found to influence the formation of diagonal cracking among the beams tested. This observation is in contrast to the observation by Lin and Lee (2003) who reports that increasing the quantity and the strength of shear reinforcement do not necessarily influence the formation of diagonal cracking strength of beams.

4.7.3.2 Cracking behaviour and crack width

Figures 4.27 and 4.28 depict a typical cracking pattern for PKS concrete and NWC beams with shear reinforcement while the cracking details of all beams have been presented in appendix A. Crack widths are found to be inconsistent with varying shear reinforcement spacing and shear span-to-depth ratio (Fig. 4.27a-d). The maximum measured crack width before failure varied from

0.28 mm to 0.51 mm depending on the amount of shear reinforcement and the shear span-to-depth ratio. However, no clear relationship could be established between the maximum crack width at failure and the shear span-to-depth ratio, a/d . Considering the effect of shear reinforcement, the crack width at failure were 0.38 mm, 0.40 mm and 0.44 mm (for beams with 150 mm, 200 mm and 250 mm spacing of stirrups respectively) for beams loaded with $a/d = 1.5$. The crack width at failure were 0.28 mm, 0.38 mm and 0.51 mm (for beams with 150 mm, 200 mm and 250 mm spacing of stirrups respectively) for beams loaded with $a/d = 2.0$. Meanwhile the maximum crack widths were 0.49 mm, 0.30 mm and 0.32 (for beams with 150 mm, 200 mm and 250 mm spacing of stirrups respectively) for beams loaded with $a/d = 2.5$. And the maximum crack width were 0.29 mm, 0.31 mm and 0.43 mm (for 150 mm, 200 mm and 250 mm respectively) for beams loaded with $a/d = 3.0$. The results show a close relationship between the cracking behaviour and the amount of shear reinforcement. This observation is expected since the number of cracks usually decreased with increasing shear reinforcement spacing.

Comparison between PKSC and NWC is also presented in Table 4.13 while the applied load versus crack width have been plotted in Fig. 4.28a-c. PKS concrete beams with shear reinforcement (2.44P200E, 2.44P250E and 2.44P300E), had average crack width of about 0.230 mm with the maximum and minimum being 0.240 mm and 0.215 mm respectively. For the NWC beams with shear reinforcement (2.44N200E, 2.44N250E and 2.44N300E), the average crack width is about 0.272 mm and the maximum and minimum being 0.320 mm and 0.240 mm. After cracking, shear is resisted by aggregate interlock, dowel action of the main reinforcing bars and the resistance of the uncracked concrete in the compression zone of the beam. If the cracks are wider, the aggregate interlock mechanism fails and may be rendered ineffective. Also, as the concrete strength increases the crack surfaces become smoother and consequently more dowel

action is required. Thus the shear capacity of lightly reinforced members may not increase for higher concrete strengths unless the cracks are contained, either by the addition of stirrups, or by increasing the percentage of longitudinal reinforcement.

During the crack propagation, a change in the nature of the crack was observed and a subsequent unstable crack branch began leading to the beam failure, called the diagonal tension failure. In the short span beams (shear span-to-depth ratios of 1.5-2.5), two major diagonal cracks formed symmetrically at opposite shear span zones of the beam when the load reached about 60% of the maximum loads. The dominant diagonal cracks within the shear span propagated towards the applied load and the support and their widths widened considerably up to 4.6 mm at failure.

When reinforced concrete beams are subjected to shear forces, shear cracks form diagonally with an inclination towards the neutral axis of the beam (Zakaria *et al.*, 2009). The width of a crack in a reinforced concrete member is partly contributed by the elastic recovery of the concrete at the formation of the crack and partly by relative slip between steel and concrete. As the concrete reaches its flexural strength, primary cracks form. The number and the length of these cracks depend on the depth of the member and placement of the longitudinal reinforcement (HyoGyoung and Filippou, 1990). Upon the initiation of the primary cracks, the concrete stress reduces to zero and the steel carries the entire bending stress.

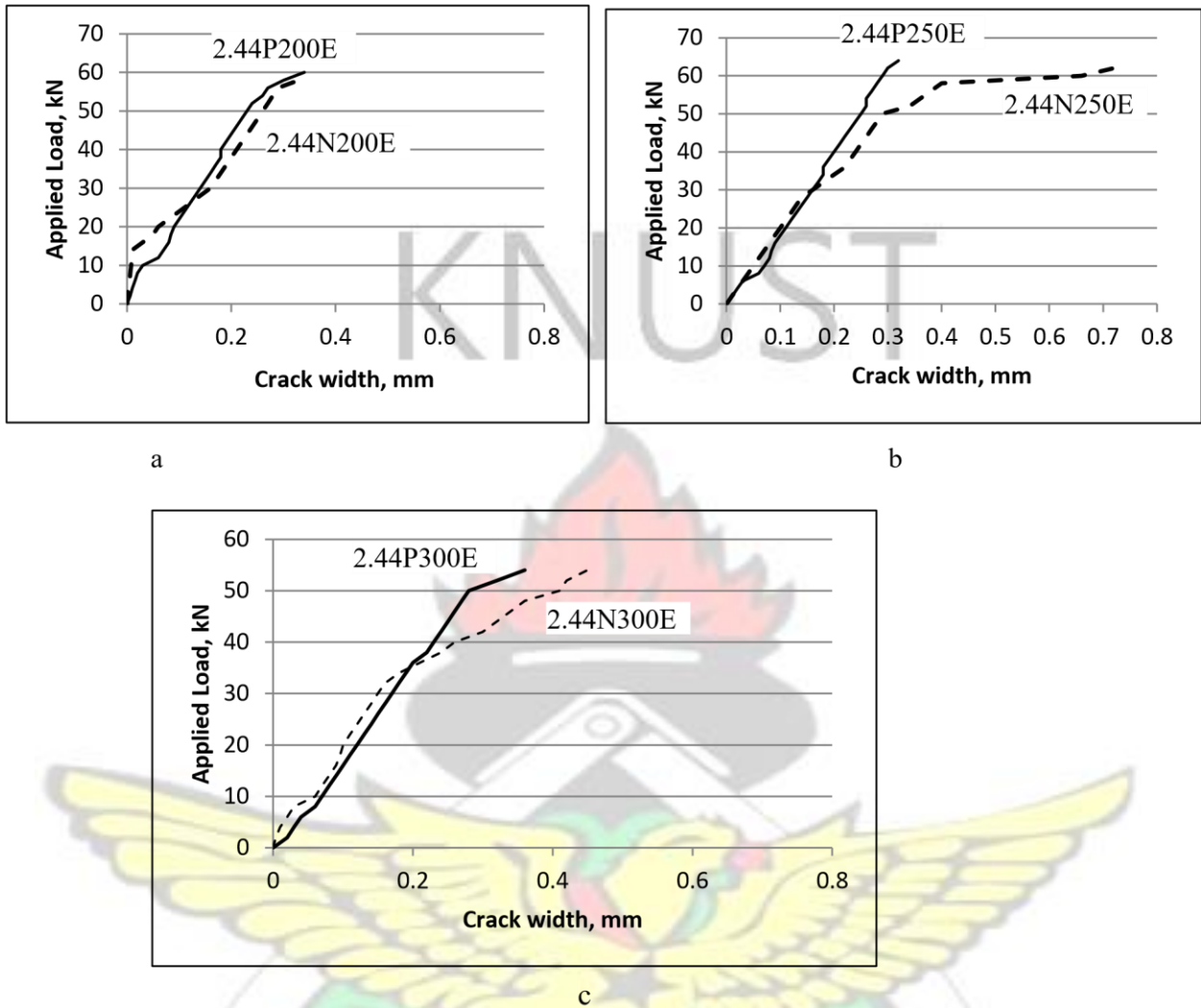


Fig. 4.27 Applied load versus crack width curves of PKSC and NWC S-series specimens

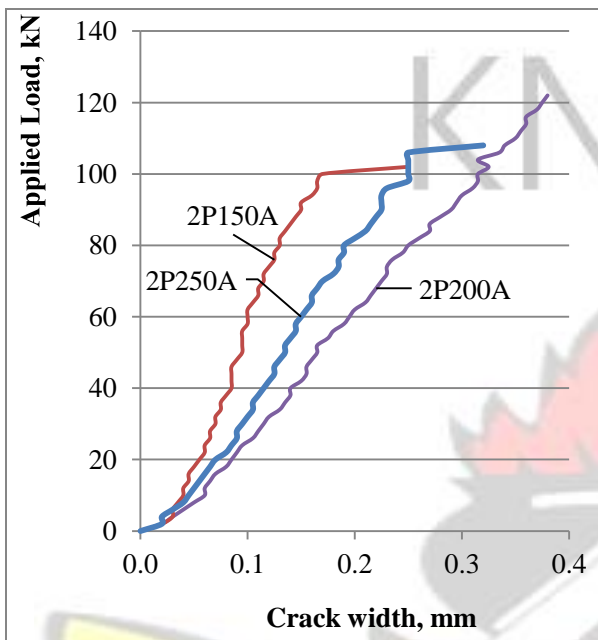
The concrete between the cracks, however, still carries some bending stresses, which decreases as the magnitude of applied load increases (Hyo-Gyoung and Filippou, 1990). This reduction in concrete bending stress with increasing load is associated with the breakdown of bond between reinforcing steel and concrete. A secondary system of internal cracks will develop around the reinforcing steel, which begins to slip in relation to the surrounding concrete (Hyo-Gyoung and Filippou, 1990).

Table 4.13 Cracking details of beams with shear reinforcement

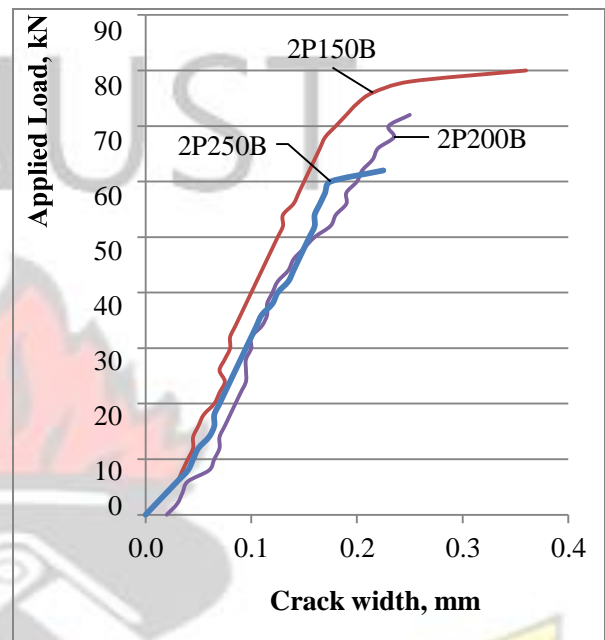
Beam no.	Diagonal cracking load, P_d (kN)	Ultimate failure load, P_u (kN)	Average crack spacing, mm	No. of cracks	Max. crack width, mm
2P 150 A	82	140	78	23	0.38
2P 200 A	76	132	86	21	0.40
2P 250 A	74	124	90	20	0.44
2P 150 B	80	132	72	25	0.28
2P 200 B	72	114	86	21	0.38
2P 250 B	62	94	90	20	0.51
2P 150 C	76	114	60	30	0.49
2P 200 C	64	96	78	27	0.30
2P 250 C	60	86	69	26	0.32
2P 150 D	74	108	67	27	0.21
2P 200 D	66	96	75	24	0.31
2P 250 D	58	82	72	25	0.43
2.44P 200 E	42	72	75	24	0.32
2.44P 250 E	38	68	78	23	0.34
2.44P 300 E	30	62	86	21	0.36
2.44N 200 E	50	74	95	19	0.33
2.44N 250 E	48	72	100	18	0.45
2.44N 300 E	42	66	113	16	0.72

The shear behaviour of reinforced lightweight pumice concrete and lightweight foamed concrete (LWFC) was studied by Lim (2007). The compressive strength of the lightweight aggregate concrete was between 20 to 90 MPa and density ranged from about 1500 to 2000 kg/m³. The study concluded that, the cracking performance of a LWC beam with respect to the number of

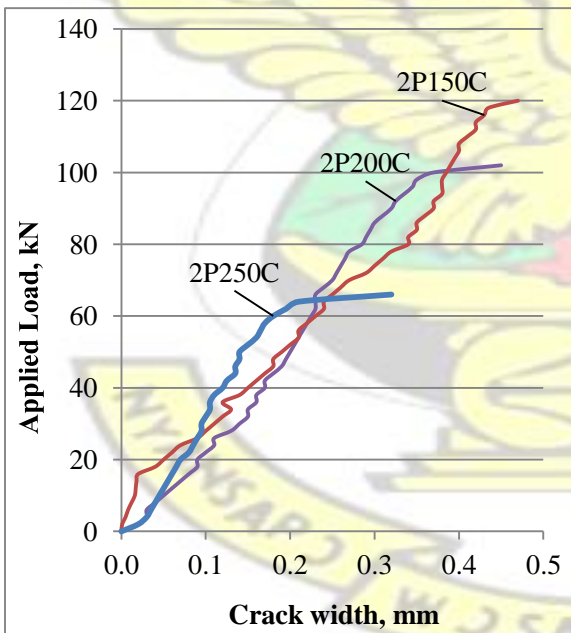
cracks and maximum crack width at anticipated service load was marginally better than its normal weight concrete counterparts.



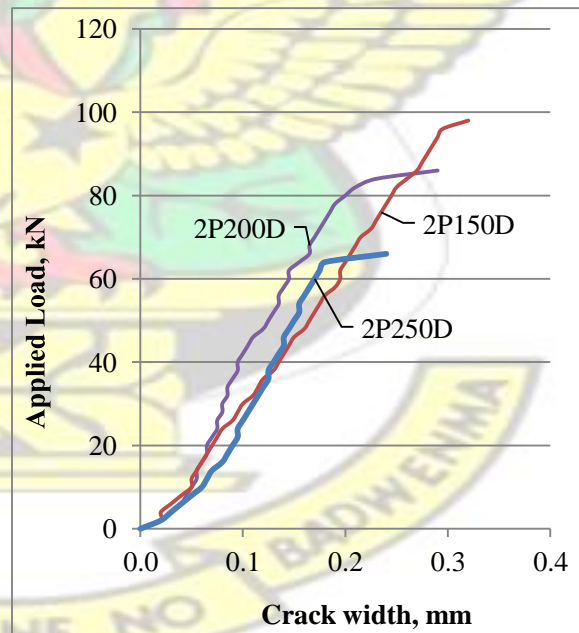
a



b



c



d

Fig. 4.28 Applied load versus crack width curves (a-d)

4.7.3.3 Ultimate failure modes

The failure modes identified during the testing process could be identified as diagonal tension, and flexure-shear compression failure, depending on the variables of the study. However, two or more types of failure was associated with one of these mode of failure. Diagonal tension failure is characterized by the sudden development of a critical diagonal tension crack and associated widening of it leading immediately to a brittle and sudden failure. The developed, inclined crack propagates quickly after its initiation and is accompanied by horizontal splitting (dowel cracks) along the tension reinforcement toward the end of the beam. Associated crushing of the concrete in the compression zone usually takes place within the constant moment region. Beams with stirrup spacing of 200 mm and 250 mm failed in this manner. For beams with a shear reinforcement spacing of 150 mm, flexure-shear compression and diagonal tension modes of failure occurred, leading to the yielding of the longitudinal steel and crushing of the concrete within the moment zone. However, several other cracks were formed along the span of the beams. This type of crack occurred in the region where the interaction of the flexural and shear stresses caused maximum compression.

In general, the observations made from the tests indicated that the ultimate shear loads increased as the span to depth ratio decreased (Table 4.14). Such observations are to be expected, because as the shear span reduces, the shear inclination angle increases, thereby, enhancing the contribution of the aggregate interlock towards the ultimate shear capacity. As a result, a higher shear resistance could be mobilized and transferred from one point to another. The formation of flexural cracks within the pure bending zone at varying loads was found to depend on the amount of shear reinforcement and the shear span-to-depth ratio. These cracks appeared due to the

reduced stiffness of the beams. The bond failure between steel bars and concrete was observed in the form of the horizontal cracks (dowel cracks) along the longitudinal reinforcement.

Table 4.14 Modes of failure of beams with shear reinforcement

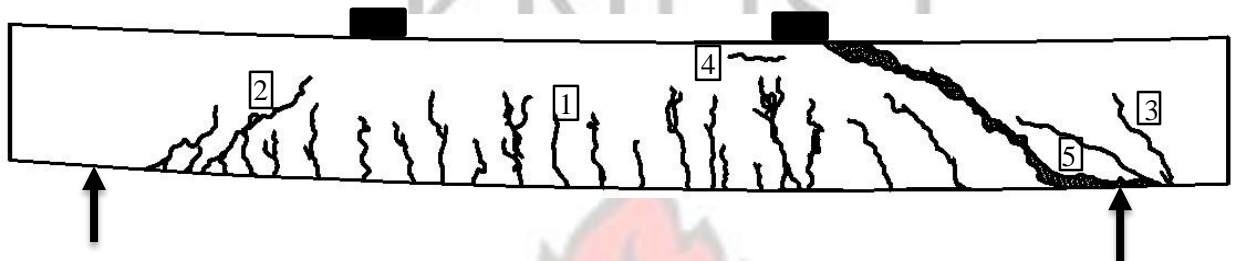
Beam no.	Diagonal crack, P_d (kN)	Ultimate failure load, P_u (kN)	Reserve strength, $R (P_u/P_d)$	Failure mode
2P 150 A	82	140	1.71	Flexural-shear/ Concrete crushing
2P 200 A	76	132	1.74	Flexural-shear/ diagonal tension
2P 250 A	74	124	1.88	Flexural-shear/ diagonal tension
2P 150 B	80	132	1.65	Flexural-shear/ Concrete crushing
2P 200 B	72	114	1.58	Flexural-shear/ diagonal tension
2P 250 B	62	94	1.42	Flexural-shear/ diagonal tension
2P 150 C	76	114	1.50	Flexural-shear/ Concrete crushing
2P 200 C	64	96	1.50	Flexural-shear/ diagonal tension
2P 250 C	60	86	1.54	Flexural-shear/ diagonal tension
2P 150 D	74	108	1.69	Flexural-shear/ Concrete crushing
2P 200 D	66	96	1.70	Flexural-shear/ diagonal tension
2P 250 D	58	82	1.78	Flexural-shear/ diagonal tension
2.44P 200 E	42	72	1.71	Flexural-shear/ Concrete crushing
2.44P 250 E	38	68	1.79	Flexural-shear/ diagonal tension
2.44P 300 E	30	62	2.07	Flexural-shear/ diagonal tension
2.44N 200 E	50	74	1.48	Flexural-shear/ diagonal tension
2.44N 250 E	48	72	1.50	Flexural-shear/ diagonal tension
2.44N 300 E	42	66	1.57	Flexural-shear/ diagonal tension

However, diagonal tension, resulting from development of a crack at a distance equivalent to the effective depth from the support resulted in failure. In some rare occasions diagonal compression occurred close to the support and contributed to the overall rupture of the beams.

Some specimens with 150 mm spacing of stirrups failed as a result of flexural shear/concrete crushing mode. This mode of failure differs from the failure modes of the remaining beams. Vertical flexural cracks propagated from the tension side of the beam to the compression zone (Fig. 4.29). On the other hand, cracks in the shear zones were diagonal, propagating from the tension side in the shear zone towards the loading positions. Additionally, few of the beam exhibited horizontal cracks at the level of the tension reinforcement, which indicated that there was bond failure.

It was observed that the crushing of the concrete in the compression zone started just after the appearance of shear crack at 42 kN for 2.44P225E. Therefore, the post diagonal cracking load could be attributed to the tension steel. Specimen 2.44P225E contained the greatest amount of shear reinforcement among the PKS concrete series in this study. This implies that the increased shear capacity (resulting from high shear reinforcement ratio) of the PKS beam offered by the increased shear reinforcement led to the concrete crushing in the compression zone before reaching its full shear capacity. Jumaat *et al.* (2009) observed that oil palm shell foamed concrete (OPSFC) beams with 150 mm centre to centre web reinforcement failed in flexure compared to OPSFC beams without shear reinforcement which failed in shear. Thus increasing shear reinforcement in reinforced PKS concrete beams is likely to results in flexural failure mode instead of shear mode. This can be attributed to the low compressive strength of the specimen

(see Table 4.7). The shear load of 42 kN is also seen to be lower than the corresponding service load of 48 kN (Table 4.15). This indicates that the beam specimen reached its full shear capacity before the flexural section reached service load, which is a sign of premature (over reinforced) failure (Juan, 2011).



1. Pure flexural cracks 2. Flexural-shear cracks 3. Anchor failure 4. Flexure compression cracks
5. Diagonal tension crack from dowel crack

Fig. 4.29 Crack pattern for PKSC beams with shear reinforcement

4.7.3.4 Influence of shear reinforcement

Twelve beams were cast to study the effect of shear reinforcement on the behaviour of PKS concrete beams in shear. These twelve PKS beams have been further subcategorized into four to take account of four different shear span-to-depth ratios. That is $a/d = 1.5; 2.0; 2.5$ and 3.0 .

In general, the curves exhibited similar load-deflection behaviour among all specimens (Fig. 4.30a-d). That is, a linear elastic behaviour even after diagonal cracking loads, and subsequently, the rate of change in the applied load with deflection decreases until ultimate failure occurs. The increase in the rate of deflection with load could be attributed to reduced stiffness as a result of the formation of flexural cracks at the bottom fibers of the beam specimens, especially beams with 150 mm stirrup spacing. The load-deflection curves show a little contribution from shear reinforcement to deflection values. However, ultimate deflections are found to increase with decreasing shear spacing of shear reinforcement.

From the test results in Fig. 4.32, it is seen that the ultimate loads decrease with increasing shear reinforcement spacing in both PKSC and NWC beam specimens. Additional shear strength to that of the concrete is provided by the transverse reinforcement upon its engagement once crossed by a diagonal crack. This observation is expected, because when the shear reinforcement spacing increases, the shear reinforcement ratio decreases. Consequently, a reduction in the shear force carried by shear reinforcement occurs, which leads to reduction in the ultimate shear stress. The amount of shear reinforcement is seen to control the formation of cracks (lower spacing of stirrup spacing results in lower crack spacing) which allows for a better aggregate interlock to be mobilized between the crack interfaces and subsequent increase in deflection. Consequently, higher ultimate shear stress results. That is, increasing shear reinforcement results in increased shear capacity of the beams as observed by Yoon *et al.* (1996).

After normalizing to account for the differences in the compressive strength by dividing the normalized shear loads by area of the cross-section, the variation of normalized shear stress (V_{ns}) of PKS/NWC beams with varying spacing of shear reinforcement: 200 mm, 250 mm and 300 mm has been plotted in Figure 4.31. The normalized shear stress, V_{ns} decreases with increasing spacing of shear reinforcement for both NWC and PKSC beams. That is, the shear resistance of PKSC beams (2.44P200E, 2.44P250E and 2.44P300E) are 11%, 8% and 6% higher compared to the NWC beam specimens (2.44N200E, 2.44N250E and 2.44N300E) for shear reinforcement spacing of 200 mm, 250 mm and 300 mm, respectively. This observation could be attributed to the higher aggregate interlocking provided by the PKS aggregates.

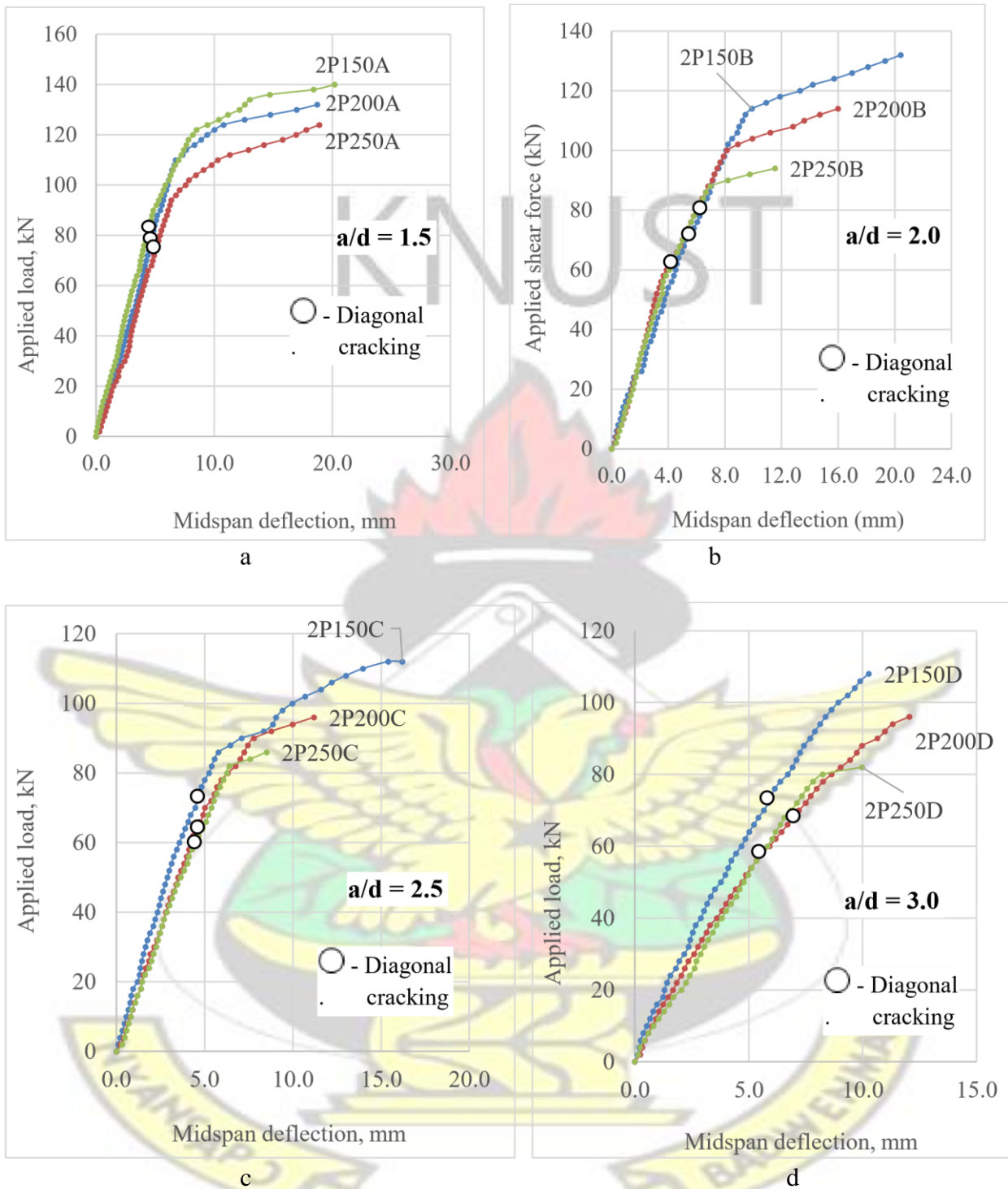


Fig. 4.30 Effect of shear reinforcement on applied load vrs midspan deflection

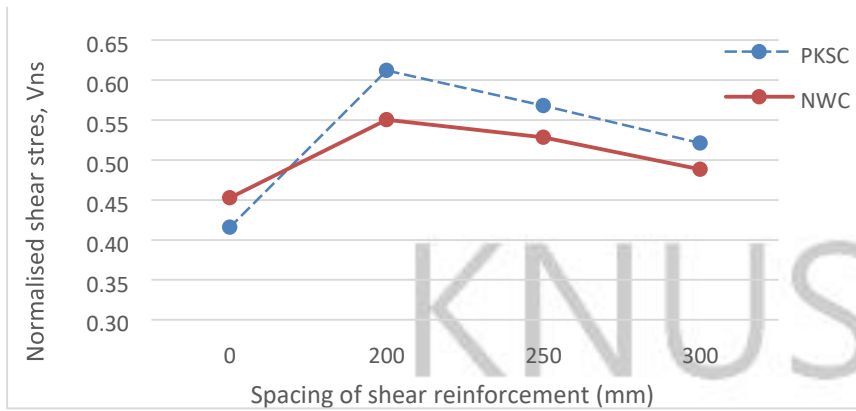


Fig. 4.31 Effect of normalized shear stress on stirrup spacing

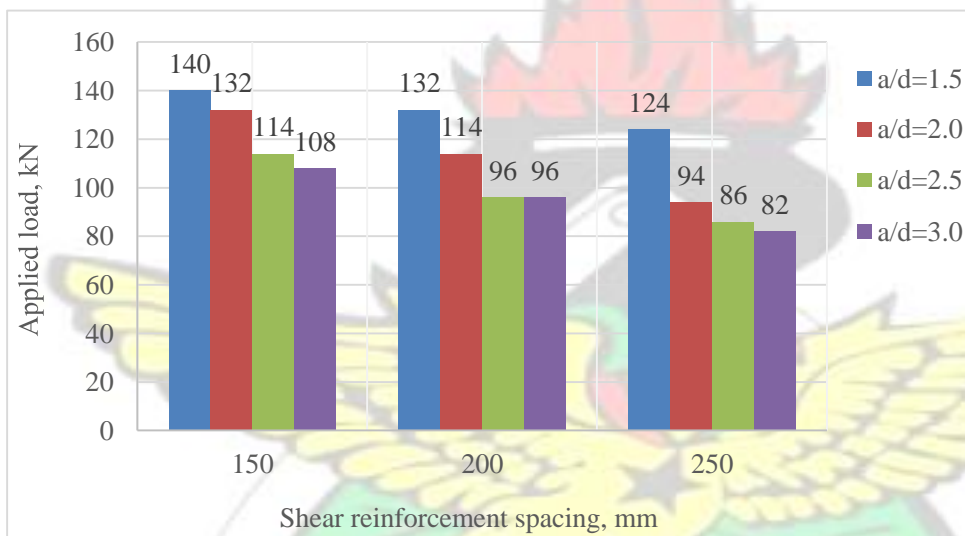
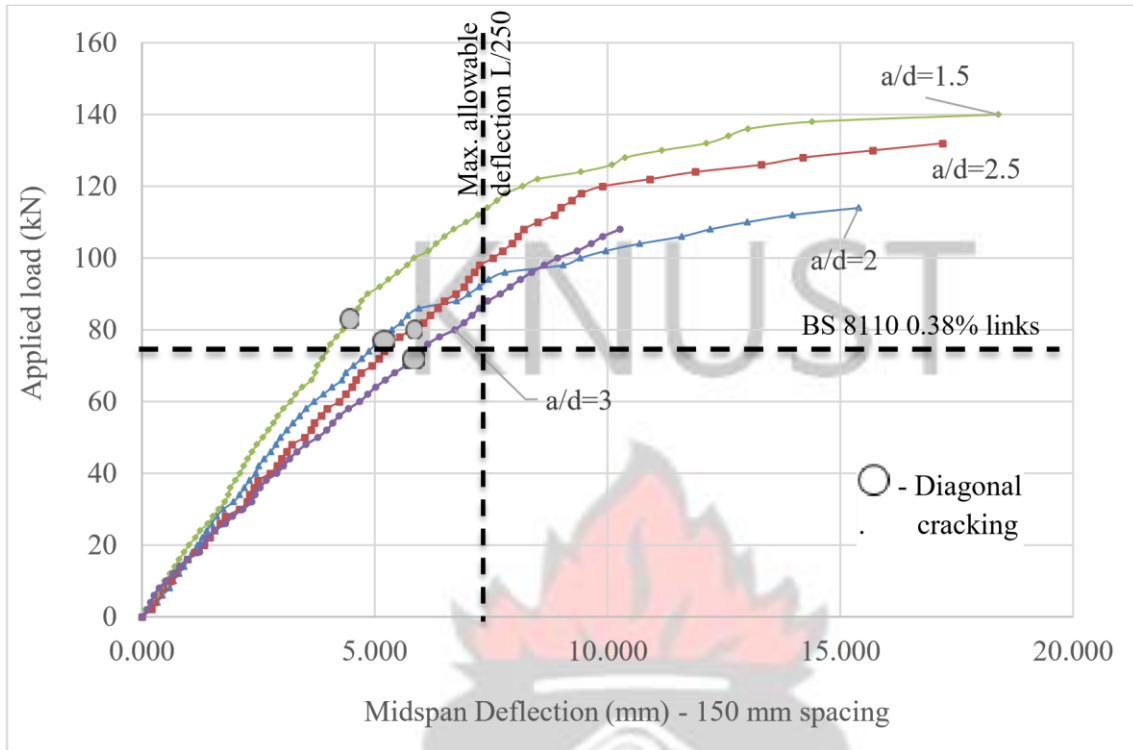


Fig. 4.32 Effect of stirrup spacing on applied loads and shear span to depth ratio

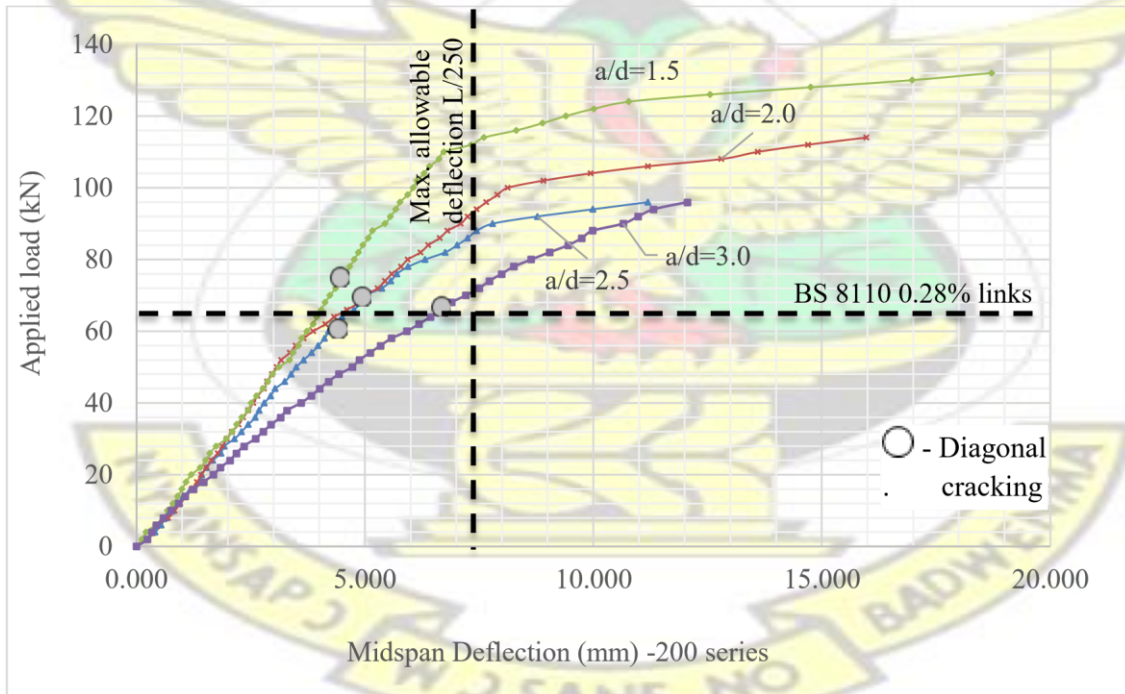
4.7.3.5 Effect of shear span-to-effective depth ratio on deflection and cracking behaviour The shear span-to-effective depth (a/d) ratios of specimens affect the crack development and failure modes. The load-deflection curves of the PKS concrete specimens show that shear span-to-effective depth ratios had no significant impact on the deflection values until post first cracking (Fig. 4.33a-d). Beyond the first cracking, deflection increased with increasing shear-span to depth ratio. First diagonal cracking loads initiated between 59% and 69% of ultimate loads for beams with 150 mm spacing of stirrups. The diagonal cracking loads initiated between 58% and 69% of

ultimate failure loads for beams with 200 mm stirrup spacing, and varied from 60% and 71% of failure loads for beams with 250 mm spacings of stirrups. It is worthy of note that beams loaded with high shear span-to-effective depth, a/d , ratio (2P250C, 2P150D, 2P200D and 2P250D) failed at comparatively lower ultimate loads compared with beams with low a/d ratios (2P150A, 2P200A, 2P250A, 2P150B) (Fig. 4.34).

It is noted that beams with higher a/d appeared to have their shear cracks formed at loads that are closer to their ultimate shear failure loads compared to beams with low a/d ratio where their shear cracks formed at loads far lower from their ultimate shear failure loads (Appendix A). This imply that the formation of shear cracks are dependent on the loading arrangement, that is, beams loaded with high shear span-to-effective depth ratio would have their shear cracks formed at loads closer to their ultimate capacities as compared to those loaded with a lower span to depth ratio. For a/d of between 1.5 to 2.5, the beams failed as a result of diagonal tension and shear-compression modes, which means the concrete crushed at the compression zone of specimens. During testing, it was observed that beams which failed in diagonal tension mode was the result of the diagonal cracks propagating from earlier formed flexural cracks in the shear span. On the other hand, beams that failed in as a result of concrete crushing, diagonal cracks initiated from the support reaction and propagated towards the loading position prior to the shear failure (Table 4.15).

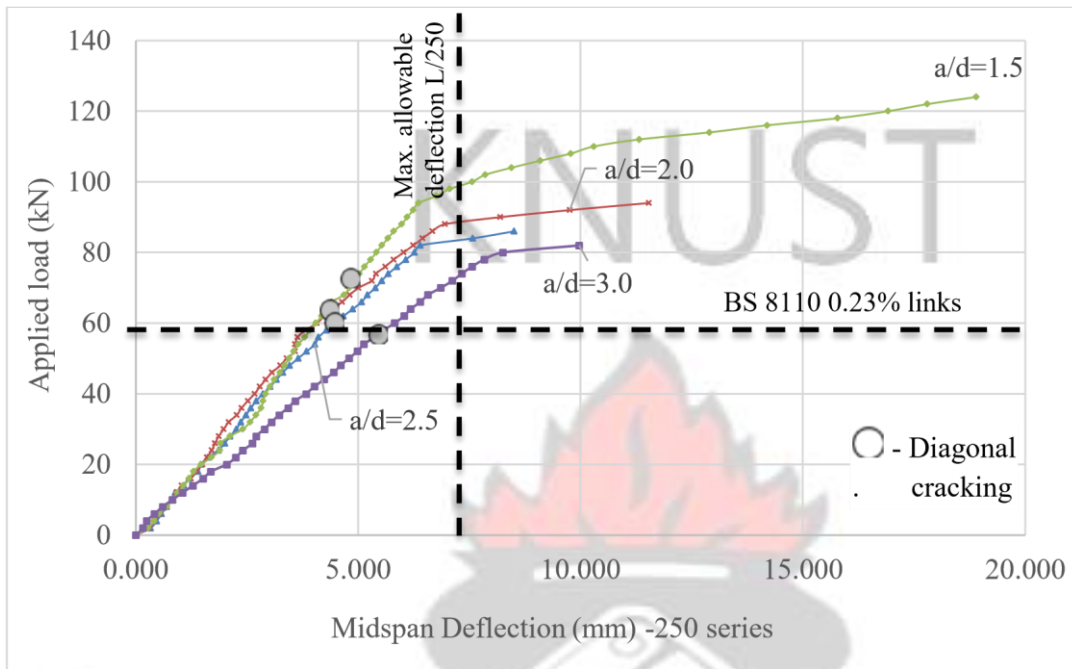


a



b

Fig. 4.33 (a-b) Load vrs midspan deflection for S-series beams



c

Fig. 4.33 c Load vrs midspan deflection for S- series beams

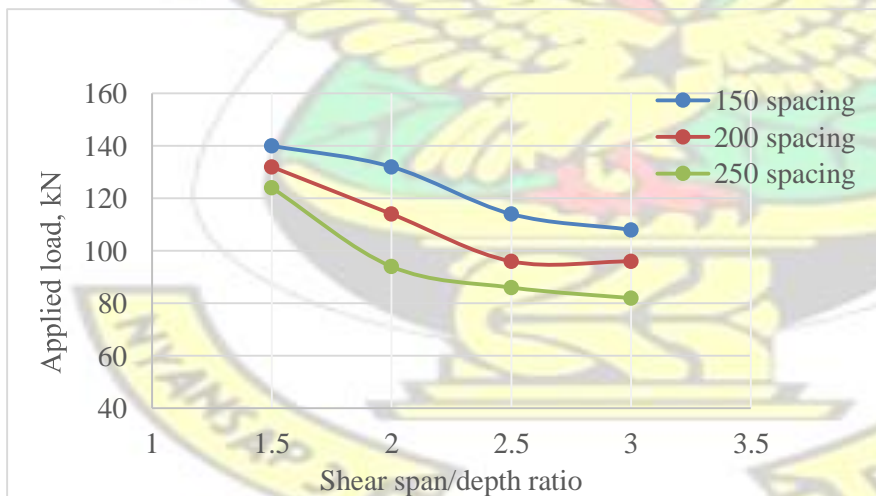


Fig. 4. 34 Applied load vrs shear span-to-depth ratio.

After the appearance of the first diagonal cracks at the supports, the inclined shear cracks were observed to propagate towards the loading positions through the specimen's section depth as the

applied load increases. The short span PKS concrete beams resisted more shear forces due to arch action, which is basically the direct transfer of the load to the support through a compressive strut.

This resulted in increased shear strength of the test specimens. For $a/d = 3.0$, the beam's failure occurred by producing splitting cracks along the tensile reinforcements in the shear span, which is known as shear-tension failure mode. It is worthy of note that the presence of the shear reinforcement controlled the failure modes of the beams without eliminating the effect of the shear span to depth ratio.

Generally, specimens loaded with span to depth ratio, $a/d < 2.5$ and stirrup spacing of 150 mm, failed as a result of shear compression by crushing of the concrete at the compression zone and the ultimate shear failure loads are higher than those specimens with $a/d \geq 2.5$. This has been expected since the beams were able to transfer the loads from the loading positions to the support reactions through the shorter shear span distance prior to the ultimate occurrence of shear compression failure. It was found that the ultimate shear load, P_u was considerably higher for the beams of $a/d = 1.5$ to 2.5 , as compared with other beams of $a/d > 3.0$, depending on the spacing of shear reinforcement (Table 4.15). The obtained experimental results have confirmed that the shear capacity of PKS beams is significantly affected by the shear span-to-depth ratio, a/d . However, significant loss in shear stress is noted among beams with shear span-to-depth ratio above 2.5.

Table 4.15 Cracking loads and ultimate deflection of S-series beams

Beam ID	Total load applied, P (kN)			Ratio		Service load, kN	Ultimate Deflection, δ_c (mm) (%)
	First flexural crack, P_f	Diagonal	Ultimate	$100P_f/P_u$ crack, P_d (%)	$100P_d/P_u$ failure load, P_u (%)		
2P 150 A	26	82	140	19	59	93.3	20.20
2P 200 A	22	76	132	17	58	88.0	18.72
2P 250 A	20	74	124	16	60	82.7	18.90
2P 150 B	24	80	132	18	61	88.0	20.40
2P 200 B	20	72	114	18	63	76.0	15.98
2P 250 B	18	62	94	19	66	62.7	11.54
2P 150 C	22	76	114	19	67	76.0	16.20
2P 200 C	18	64	96	19	67	64.0	11.20
2P 250 C	18	60	86	21	70	57.3	8.51
2P 150 D	16	74	108	15	69	72.0	10.27
2P 200 D	14	66	96	15	69	64.0	12.05
2P 250 D	10	58	82	12	71	54.7	9.97
2.44P 200 E	12	42	72	17	58	48.0	12.46
2.44P 250 E	10	38	68	15	56	45.3	11.60
2.44P 300 E	8	30	62	13	48	41.3	9.55
2.44N 200 E	16	50	74	22	68	49.3	13.48
2.44N 250 E	14	48	72	19	67	48.0	8.05
2.44N 300 E	12	42	66	18	64	44.0	7.95

4.7.3.6 Influence of parameters on reserve strength

The relationship between the reserve strength of the PKS concrete beams with shear reinforcement have been plotted in Fig. 4.35 in relation to the shear span to depth ratios. The reduction in reserve strength in relation to shear span to depth ratio (a/d) from 1.5 to 3.0 varied from 1.71 to 1.46 for PKS beams with 150 mm shear reinforcement spacing. The reserve strength varied from 1.74 to 1.50 and 1.68 to 1.41 for PKSC beams with 200 mm and 250 mm shear reinforcement spacings respectively. It is seen that increasing the shear reinforcement spacing leads to decrease in load carrying capacity after the diagonal cracking. This is expected because when the shear reinforcement spacing reduces, the amount of shear reinforcement increases. Thus the shear force carried by the dowel action of shear reinforcement increases. Considering the effect of shear span to depth ratio, considerable loss of strength is noticed as the shear span to depth ratio increases from 1.5 to 3.0 after the formation of diagonal cracking. This is because the activation of other shear transfer mechanisms depend on the span of the beams. Short span beams are able to transfer higher loads even after diagonal cracking due to arch action of the beams (Slobe, 2012).

Johnson and Ramirez (1989) also used the reserve shear strength index, to evaluate the effect of the amount of shear reinforcement. They observed that the reserve shear strength index increased as both the concrete compressive strength and the amount of shear reinforcement increased by almost 50%. Based on the limited samples tested in this study, the reserve strength varied from 41% to 74% of ultimate loads depending on the shear span to depth ratio.

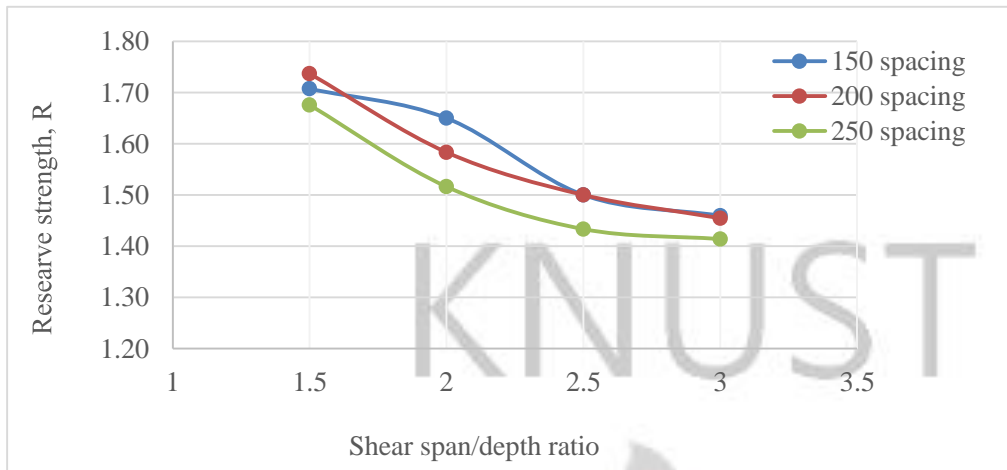


Fig. 4.35 Influence of shear-span-to-effective depth ratio on reserve strength

4.7.3.7 Effect of loading on the behaviour of PKS beams

The adoption of ultimate strength design procedures and the use of more durable materials require that structural concrete members perform satisfactorily under varying loading levels for a longer period of time (Al-Saraj, 2007). There is also a new recognition of the effects of repeated loading on a member, even if repeated loading does not cause a fatigue failure. Under reversed loading involving inelastic extension of the reinforcement, failure has been found to occur in a different manner from that of beams subjected to monotonic loading (Fenwick and Fong, 1979). Tests have shown that, the shear resisted by the concrete decreases under such conditions, and a diagonal tension type of shear failure usually occur unless adequate shear reinforcement is provided. Allowance should be made for the greater shear which may be sustained in the beam with the yield point of flexural reinforcement being greater than the specified minimum value (overstrength), and to its subsequent strain hardening. However, even in beams in which the web reinforcement meets these requirements a different form of shear failure may occur.

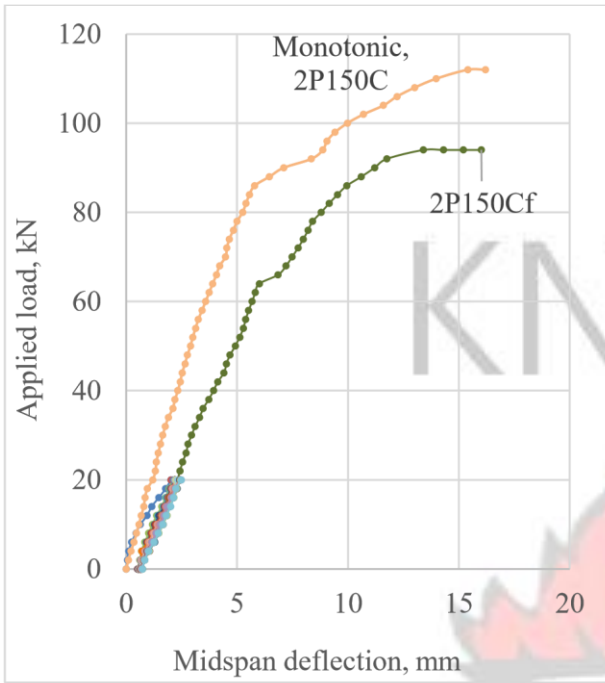
Eight PKS concrete beams with longitudinal reinforcement ratio of 2% were prepared and cast to study the effect of cyclic loading on the behaviour of the PKS concrete beams. The effect of

amount of shear reinforcement spacing, ranging from 150 mm to 300 mm were also studied in comparison with that of beams under monotonic loading. Figures 4.36 and 4.37 present the load-deflection behaviour of the beams subjected to loads at first crack and service loads respectively.

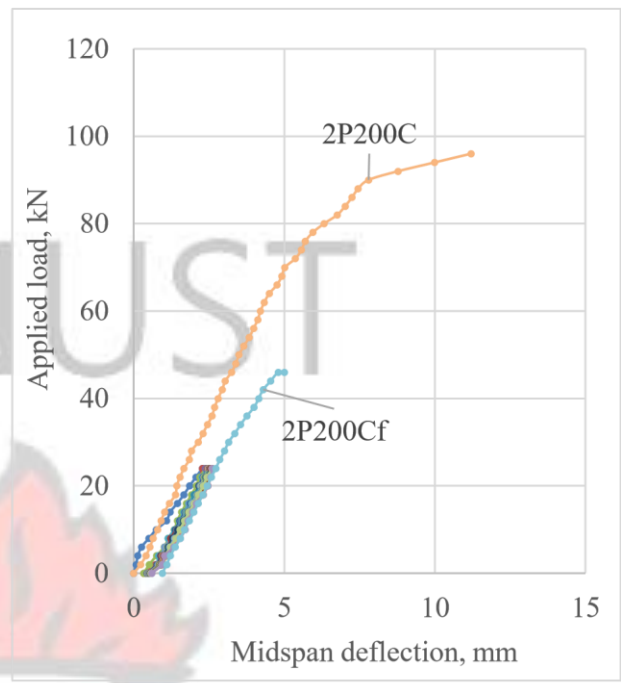
Failure modes for all beams were observed and failures of all beams have been presented in Appendix A. The load-carrying capacity of the beams under cyclic loading at different stages of loading is presented in Table 4.16. The load-deflection curves of the corresponding monotonically loaded beams have been superimposed on the curves for the cyclically loaded beams.

In all specimens, the initial stiffness remained constant until the appearance of first flexural cracks. Beyond this point the stiffness of the beam are significantly reduced compared to that of the uncracked section and the slope of load-deflection curve changed accordingly. Before cracking, deflection was directly proportional to the applied loads for all specimens irrespective of the stirrup spacing. After first crack though stiffness of the beam reduced, the load-deflection behaviour remained almost linear till yielding of reinforcement for both monotonic and cyclic loading (Figures 4.36 and 4.37). After yielding of the reinforcement, a significant loss in the stiffness of the beams was noted as a result of the excessive deep cracks into the concrete compressive zone. Ultimate deflections varied from 9.40 mm to 16.20 mm for the monotonically loaded beams, depending on the amount of shear reinforcement. The deflections varied from 4.81 mm to 16.01 mm and 11.4 mm to 15.4 mm for beams loaded up to the first crack and service loads respectively. Test specimens with higher amount of shear reinforcement demonstrated higher deflections, indicating a significant contribution of the shear reinforcement.

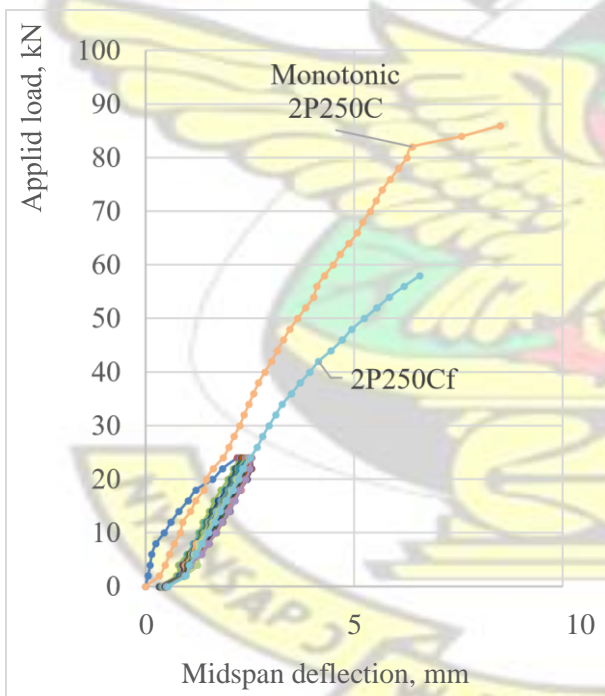
Critical diagonal cracks developed between 57% and 79% of the failure load for PKS concrete beams under cyclic loading up to first cracking (Table 4.16). Considering the beams subjected to cyclic loading at service loads, the critical diagonal cracks developed between 48% and 83% compared to 67% to 70% of ultimate loads under monotonic loads respectively. However, the diagonal shear cracks and their dispositions depend directly on the amount of shear reinforcement and mode of application of the load (whether monotonic or cyclic). The appearance of diagonal cracks varied depending on the number of cycles and the spacing of shear reinforcement (Table 4.16). A close assessment of the results in Table 4.16 indicates that the appearance of diagonal cracks varied from the first cycle of loading and unloading depending on the amount of stirrup spacing and the level of loading. For instance, the first diagonal crack in beam 2P150Cf appeared at the 14th loading cycle while the first diagonal crack in beam 2P150Cf appeared at the 6th cycle. The load-carrying capacities after maximum loads decreased gradually with increasing cycles. The amount of deterioration in the beams is, however, found to increase with increasing shear reinforcement spacing. As a result of hysteretic energy dissipation, beams subjected to cyclic loads failed at very low ultimate loads and deflections compared to the beams under monotonic loading (Fig. 4.37). It was thus observed that cyclic loading affected the stiffness, strength and deformation of the PKS beams with shear reinforcement, even at first flexural cracking. Meanwhile, beams under cyclic loading up to first flexural tensile cracking showed a strong resilience at failure, especially beams with 150 mm stirrup spacing (Fig. 4.36a). That notwithstanding, the increase in ultimate deflection could be attributed to the reduced stiffness and deterioration of bond between steel and concrete, and between aggregates and cement paste. These results contradict with the observations made by Adom-Asamoah and Afrifa (2013) for phyllite reinforced concrete beams under cyclic loading.



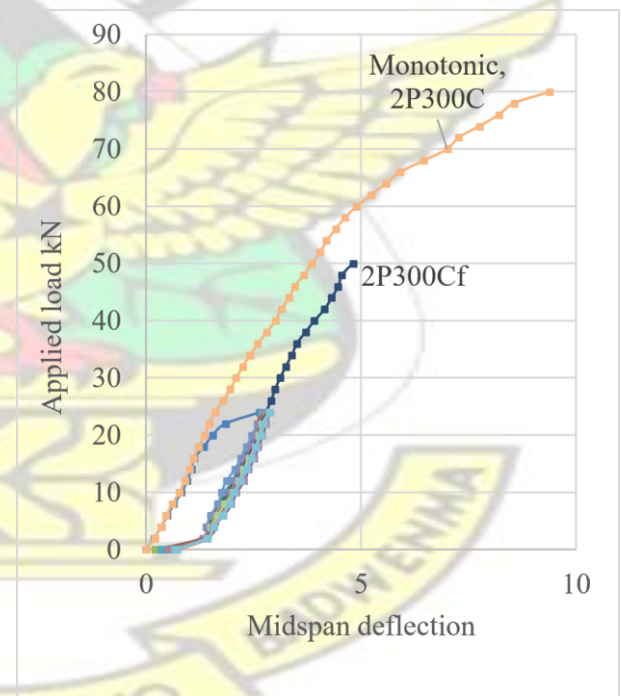
a



b



c



d

Fig. 4.36 (a-d) Applied load vrs Midspan deflection

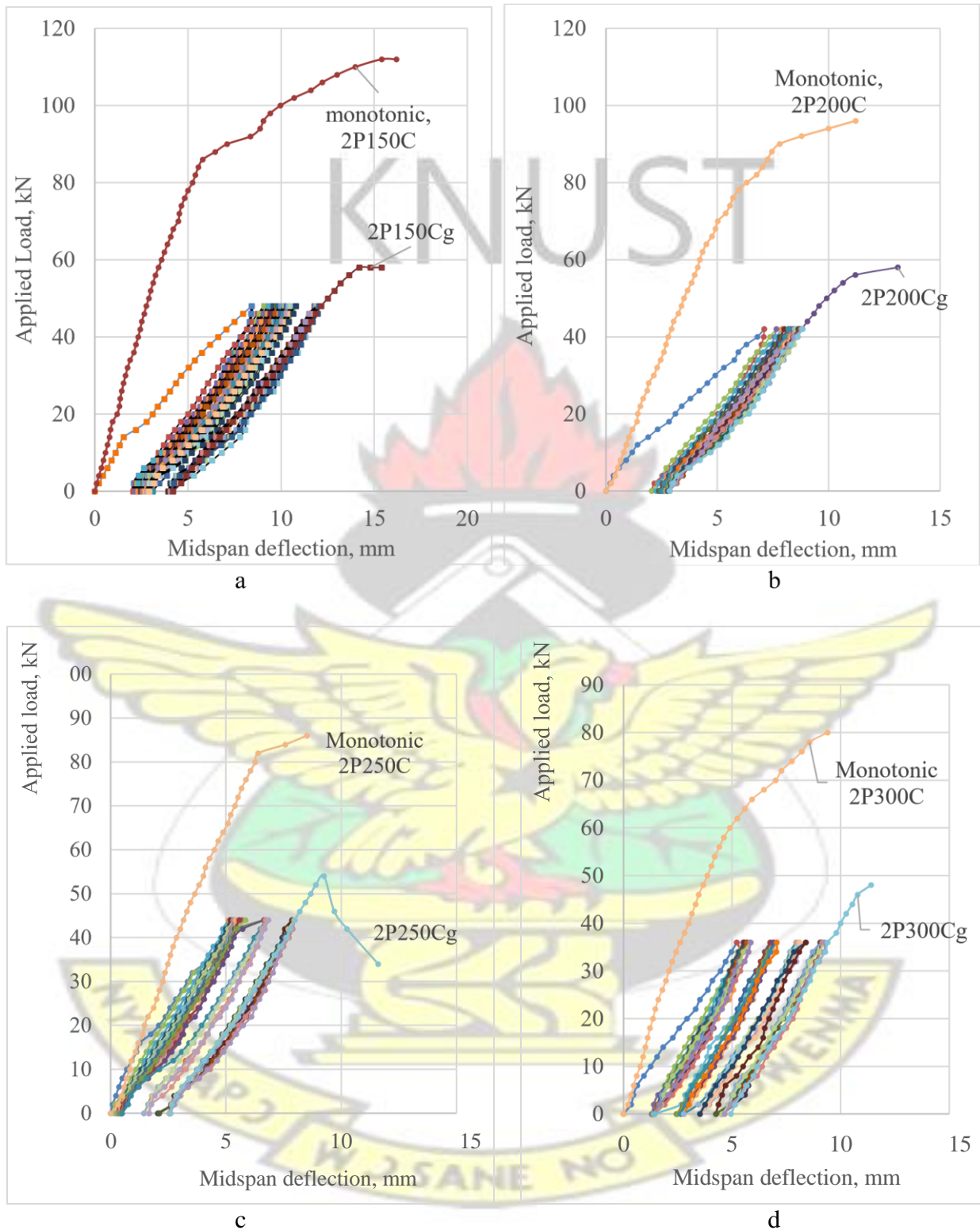


Fig. 4.37 Applied load vrs midspan deflection (a - d)

Table 4.16 Cracking behaviour and modes of failure of cyclically loaded beams

Beam ID	Total load applied, P (kN)		δ_c	Ultimate	Max.	V/bd	Mode of failure
	crack	Mode of failure		width, mm	N/mm ² crack, P _d		
2P 150 C	76	114	67	16.20	0.49	4.40	Flexural-shear/ Concrete crushing
2P 200 C	64	96	67	11.20	0.30	3.70	Flexural-shear/ diagonal tension
2P 250 C	60	86	70	8.51	0.32	3.30	Flexural-shear/ diagonal tension
2P 300 C	54	78	69	9.4	0.31	3.01	Flexural-shear/ diagonal tension
2P150Cf ¹⁴	54	94	57	16.01	0.30	3.63	Flexural-shear/ diagonal tension
2P200Cf ¹⁰	48	82	59	9.25	0.52	3.16	Flexural-shear/ diagonal tension
2P250Cf ⁸	44	56	79	6.58	0.65	2.16	Flexural-shear/ diagonal tension
2P300Cf ⁸	36	50	72	4.81	0.78	1.93	Flexural-shear/ diagonal tension
2P150Cg ⁶	50	60	83	15.40	0.28	2.31	Flexural-shear/ Concrete crushing
2P200Cg ⁴	36	58	62	13.10	0.58	2.24	Flexural-shear/ diagonal tension
2P250Cg ¹	44	54	81	11.60	0.72	2.08	Flexural-shear/ diagonal tension

1,4,6,8,10,14 Cycles at which diagonal cracks appeared

2P300Cg ⁴	24	50	48	11.40	0.89	1.93	Flexural-shear/ diagonal tension
----------------------	----	----	----	-------	------	------	-------------------------------------

4.7.4 COMPARISON OF TEST RESULTS AND EXISTING EQUATIONS

4.7.4.1 Introduction

Practically, the loads at first diagonal cracking is considered to be the shear failure load irrespective of the ultimate shear load which may be higher than the inclined cracking load (Juan, 2011). As a result, code provisions predict the shear capacity of a member as the onset of diagonal cracking of the beam. Diagonal cracking values are predicted because the extent to which a member continues to resist shear after the onset of diagonal cracking is uncertain and depends largely on the loading configurations and material properties (Juan, 2011). As stated earlier, shear stresses in reinforced concrete without shear reinforcement are resisted by the concrete compression zone, aggregate interlock, dowel action of the longitudinal reinforcement (Ramirez and Breen, 1991). Various codes of practice combine these shear transfer mechanisms to determine the capacity of the concrete section (V_c) and the contribution of the various mechanisms is influenced by a host of factors.

These contributions to shear are given by the equations 4.3 and 4.4. The BS 8110: Part-2 (1985), clause 5.4 considers a reduction factor of 0.8 for all LWC without any distinction between sandlightweight and all-lightweight aggregate concrete. However, the design concrete shear stress (V_c) of the NWC was calculated from the equations provided in Table 2.7 as specified in Table 3.9 of

BS 8110-1 (1997). For LWC, therefore, the design equations are;

$$V_c = 0.8 \times \frac{0.79}{\gamma} \left[\left(\frac{100A_s}{b_v d} \right)^{1/3} \times \left(\frac{400}{d} \right)^{1/4} \times \left(\frac{f_{cu}}{25} \right)^{1/3} \right] \quad (4.3)$$

$$V_s = \frac{A_{sv}}{S_v} \times 0.95 f_y d \quad (4.4)$$

The design for shear using the (ACI 318, 2008) is based on the computation of the shear strength, V_c , of the concrete beam cross-section and the maximum shear, V_u , that the beam will resist. A reduction factor of 0.85 is adopted for sand-lightweight aggregate concrete while a factor of 0.75 is assumed for all-lightweight aggregate concrete. The contributions of the concrete section without shear reinforcement, V_c and the shear reinforcement, V_s have been presented in equation 4.5 and 4.6 respectively, for sand-lightweight aggregate concrete which was used in the present study.

$$V_c = 0.85 \times \left[0.16\lambda\sqrt{f'_c} + 17\rho_w \frac{V_u d}{M_u} \right] b_w d \quad (4.5)$$

$$V_s = \frac{A_v f_{yt} d}{s} \quad (4.6)$$

Contrary to the design provisions of ACI 318, the provisions of the EC2 consider a semi-empirical equation for members which do not require shear reinforcement. This equation considers size effect of beams instead of the shear span to depth ratios. Values of C_{rdc} for LWC is also reduced from $0.18/\gamma_c$, for normal weight concrete to $C_{rdc} = 0.15/\gamma_c$ for LWC. Another reduction factor which depends on the density of the lightweight aggregate concrete used. The coefficient is then taken as 60% of the normal weight concrete by the ratio of the upper limit of the appropriate density class to the density of normal weight aggregate concrete (2200 kg/m^3). The reduction factor becomes $\eta_1 = 0.40 + 0.60\rho/2200$. The final equation for analyzing lightweight aggregate concrete is summarized into equation 4.7 while equation 4.8 depicts the contribution of the shear reinforcement.

$$V_{RD,C} = \left[0.15/\gamma_c \left(0.40 + 0.60\rho/2200 \right) \left(1 + \sqrt{200/d} \right) (100\rho_1 f_{ck})^{1/3} + \frac{0.1N_{ED}}{A_c} \right] bd \quad (4.7)$$

$$V_{RD,S} = \frac{A_{sw}}{s} Z f_{yd} \cot \theta \quad (4.8)$$

Where θ is the diagonal concrete strut angle which is set between 22° and 45° (the angle between inclined concrete struts and the main tension chord)

The BS 8110 uses cube compressive strength as compared to cylinder compressive strength used in both ACI and EC2 codes for computing the shear strength values. Thus, a reduction factor of 0.8 was used to convert cube compressive strength into cylinder compressive strength for estimating the shear strength values.

4.7.4.2 Beams without shear reinforcement

The PKSC and NWC beams exhibited similar failure mechanism, hence, the test results were compared with the predictions of the existing BS8110, ACI 318 and EC 2 models to determine the adequacy of these models in predicting the ultimate load-carrying capacity of PKSC beams without shear reinforcement. Table 4.17 presents the experimental failure loads and code based predictions. It can be noted that the existing model underestimated the ultimate loads of PKSC beams without shear reinforcement. Figures 4.38 to 4.40 compare the performance of code based equations (BS 8110, ACI 318 and EC 2) in predicting the diagonal shear load (P_u) of PKSC beams having 1%, 1.5% and 2% longitudinal reinforcement ratios. The results show that the predicted failure loads are much lower than the experimental loads especially for beams without shear reinforcement. It is seen that the BS 8110 predicted 52% and 40% of the ultimate applied load of PKSC (**2.44P225a**) and NWC (**2.44N225a**) beams with shear span-to-depth ratio of 1.5. However, the code predicted 73% and 76% of the ultimate applied loads of PKSC (**2.44P225b**) and NWC (**2.44N225b**) beams with shear span-to-depth ratio (a_v/d_{eff}) of 2.5. The ACI 318 predicted 54% and 40% of the ultimate applied load PKSC and NWC beams with a_v/d_{eff} of 1.5.

Meanwhile, the code predicted 69% and 70% of the ultimate applied load PKSC and NWC beams with a_v/d_{eff} of 2.5. The EC 2 predicted 64% and 48% of the ultimate applied load PKSC and NWC beams with a_v/d_{eff} of 1.5 while the code predicted 78% and 82% of the ultimate applied load PKSC and NWC beams with a_v/d_{eff} of 2.5. For relatively short span beams ($a_v/d_{eff} \leq 2.5$), the load is transferred directly from the loading points to supports owing to arch action (Kim and Park, 1996) after the formation of diagonal cracking. Once the formation of arch actions in the short span beam is enabled, redistribution of internal stresses allows the cracked beam to carry additional loads after the appearance of diagonal cracks.

Meanwhile, slender beams ($a_v/d_{eff} > 2.5$) without shear reinforcement becomes unstable and fails suddenly after the formation of the inclined cracks. Comparing the performance of the three codes of practices, the BS 8110 and ACI 318 predicted lower shear capacities of both PKSC and NWC beams compared to that of EC 2. This could be attributed to the fact that the ACI underestimates the effect of the a_v/d_{eff} (Rebeiz *et al.*, 2000) while the BS 8110 ignores this effect completely. Additionally, the increased ability of **2.44N225a** to carry the excessively higher loads could also be attributed to the effective transfer of loads through the intact concrete section in the compression zone and the dowel action of the longitudinal reinforcement. Thus NWC with a_v/d_{eff} of 1.5 showed anchorage and bond failure which resulted in the splitting of the concrete along the longitudinal steel level.

Considering the PKSC beams, BS 8110 under predicted the ultimate failure loads irrespective of the beam depth (150–300 mm) and amount of longitudinal reinforcement ratio (1%, 1.5% and 2%), as the ratio of BS 8110 prediction to experimental values ranges between 39% to 44% of the ultimate failure loads (Table 4.17 and Figures 4.38 to 4.40). The ratios varied from 36% to

44% for beams with $\rho_w = 1\%$, varied from 39% to 44% for beams with $\rho_w = 1.5\%$ and varied from 39% to 44% for beams with $\rho_w = 2\%$. However, the variation of these ratios were found to be inconsistent with the size of the beam considered. While the BS 8110 considers the effect of beam size on the shear capacity of the PKSC beams, the beam is found to be more conservative for 250 mm and 300 mm depth beams with $\rho_w = 1\%$ and $\rho_w = 1.5\%$. In general, BS 8110 is found to be more conservative than ACI and EC 2 (the conservativeness increases with increasing beam depth) and can be used safely for the prediction of ultimate shear resistance of PKSC beams as confirmed from this study. Rao *et al* (2007) made a similar observation in relatively large beams compared to the performance of the ACI 318 for the same beam geometry.

After normalizing for the compressive strength, the variation in the shear strength of the beams' strength could be attributed to the amount of longitudinal reinforcement. It is worth mentioning that the effect of beam size on BS 8110 predictions is greatly influenced by the amount of longitudinal reinforcement (Figs. 4.38 – 4.40). The degree of conservativeness of the BS 8110 is found to increase with increasing beam size and tension steel ratios. At lower reinforcement ratios, the effect of the beam size is greatly mitigated based on the tested specimens.

The ratio of ACI 318 predicted values to experimental values for PKSC beams with 1% reinforcement ratio varied from 45% to 55% of ultimate shear strength, although the variation was inconsistent with the beam depth. The ratio varied from 41% to 54% and varied from 45% to 52% of ultimate shear strength for beams with $\rho_w = 1.5\%$ and $\rho_w = 2.0\%$. The ACI equation which is reported to ignore the effect of beams' size is found to safely predict the behaviour of the PKSC beams even though it is conservative for all tested beam series. From the test carried out, the ACI code predictions is found to be very conservative in PKSC beams with higher

reinforcement ratios and unconservative in beams with lower reinforcement ratios as reported by other researchers (Hanafy *et al.*, 2012; Hong and Ha, 2001; Collins *et al.*, 1999; MacGregor, 1997). Comparing the performance of the three codes of practices, the ACI code gives a better prediction for beams with lower reinforcement ratios compared to beams with higher reinforcement ratios. The ACI predictions for smaller depth beams are conservative by as much as 60%, especially for beams with 2% longitudinal reinforcement. Stanik (1998) and Hassan *et al.* (2008) also indicated that the ACI code is conservative for smaller normal concrete and selfconsolidating concrete beams in shear respectively.

Similar to the predictions of the ACI, the EC 2 predicted 42% to 59% of ultimate loads of beams with 1% longitudinal reinforcement. The predicted values ranges from 46% to 58% of ultimate loads of beams reinforced with 2% longitudinal reinforcement. However, the amount of change was found to be inconsistent with the change in beam size for beams with $\rho_w = 1\%$ and $\rho_w = 1.5\%$ except for beams with $\rho_w = 2\%$ where the ratio increased with increasing beam depth. At higher longitudinal steel levels, the EC 2 gives an unconservative prediction.

After normalizing for the compressive strength, Figures 4.38 to 4.40 presents the relationship between the normalized shear stress at diagonal cracking for experimental and code predictions with varying beam depths and longitudinal reinforcement ratios. This is necessary since the design codes of practice limits the shear failures in beams to the diagonal cracking shear, principally due to the insufficient knowledge available on the redistribution of stresses at diagonal cracking and the ability of the section to reach equilibrium after stress redistribution.

Table 4.17 Experimental results of R-series beams and code predictions

Beam ID	Exp. Failure (kN), P_u	Code predictions – V_{code}			Shear force ratios, V_{code}/P_u load		
		BS 8110	EC 2	ACI 318	BS 8110 (%)	EC 2 (%)	ACI 318 (%)
1 P 150	52	20.18	21.90	23.48	39	42	45
1.5 P 150	60	23.12	26.10	24.59	39	44	41
2 P 150	62	24.97	28.74	24.61	40	46	40
1 P 200	62	28.31	31.70	33.22	46	51	54
1.5 P 200	68	30.11	38.47	34.82	44	57	51
2 P 200	82	32.73	43.24	35.33	40	53	43
1 P 225	72	31.9	35.51	37.84	44	59	55
1.5 P 225	78	33.23	45.07	39.92	43	58	51
2 P 225	88	34.66	47.59	40.23	39	54	46
1 P 250	80	33.57	39.25	43.94	42	51	55
1.5 P 250	84	36.80	46.31	45.18	44	55	54
2 P 250	92	40.28	52.86	46.71	44	57	51
1 P 300	102	36.3	52.88	53.50	36	52	52
1.5 P 300	104	41.2	55.44	54.21	40	53	52
2 P 300	106	44.29	61.74	55.41	42	58	52
2.44 P 225a	70	36.48	45.04	37.82	52	64	54
2.44 P 225b	50	36.48	38.95	34.65	73	78	69
2.44 N 225a	114	45.60	55.26	45.19	40	48	40
2.44 N 225b	60	45.60	49.05	41.90	76	82	70

The performance of all codes of practice is found to be satisfactory at the formation of diagonal cracking. The results show that EC 2 and BS 8110 underestimates PKSC beams with 1% longitudinal reinforcement compared to the ACI code. The trend however, changes to favour the EC 2 at increasing levels of longitudinal steel for the various beam sizes tested. With increased longitudinal steel reinforcement ratios, the PKSC beams are found to behave inconsistently with increasing beam depth which could be attributed to the improved redistribution of stresses within the intact compression zone above the neutral axis.

After the formation of the critical shear crack, shear transfer through aggregate interlock reduces significantly, giving way to dowel action, residual tensile stresses and the intact compression zone (Omar, 1998), especially in beams with higher longitudinal reinforcement. Since the dowel action of longitudinal reinforcement and the uncracked compression zone contribute to the prevention of excessive opening of the inclined shear cracks (Hong and Ha, 2001), it could be responsible for the lower crack widths recorded among the PKSC beams. This added advantage in the shear transfer behaviour of the PKSC beams is derived from the lower aggregate crushing value of the PKS aggregate (see Table 4.1).

It could be inferred that the reduction factor of 0.8 imposed on the PKSC by the BS 8110 is adequate for all tested beam dimensions and longitudinal steel ratios. At diagonal cracking, the reduction factor of 0.85 imposed on sand-lightweight aggregate concrete by the ACI 318 is overconservative for PKSC beams with higher longitudinal steel ratios.

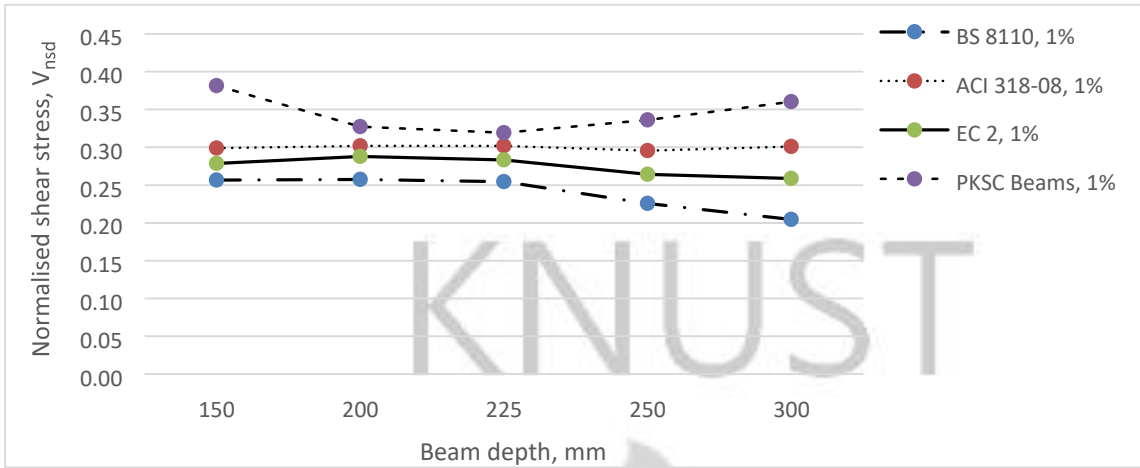


Fig. 4.38 Normalized shear strength (V_{ns}) at Exp. cracking and code predictions ($\rho_w = 1\%$).

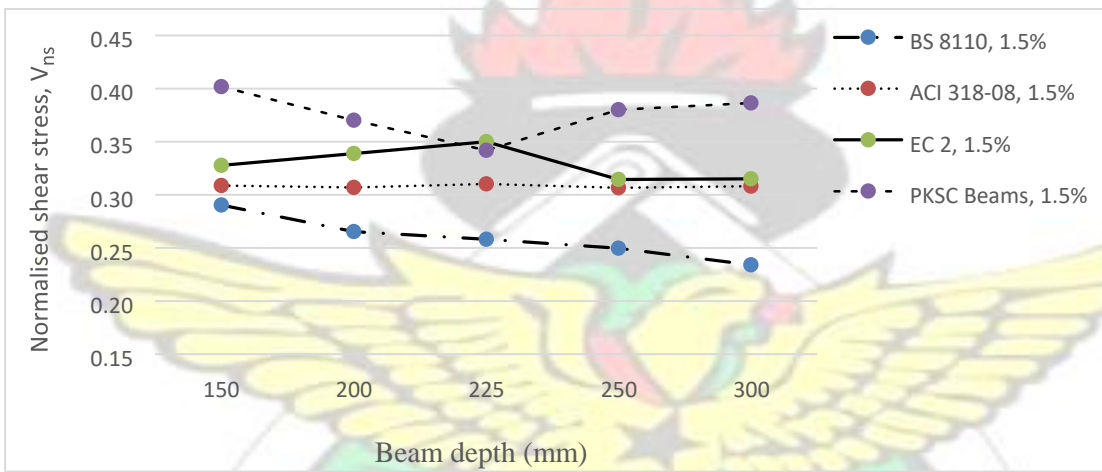


Fig. 4.39 Normalized shear strength (V_{ns}) at Exp. cracking and code predictions ($\rho_w = 1.5\%$).

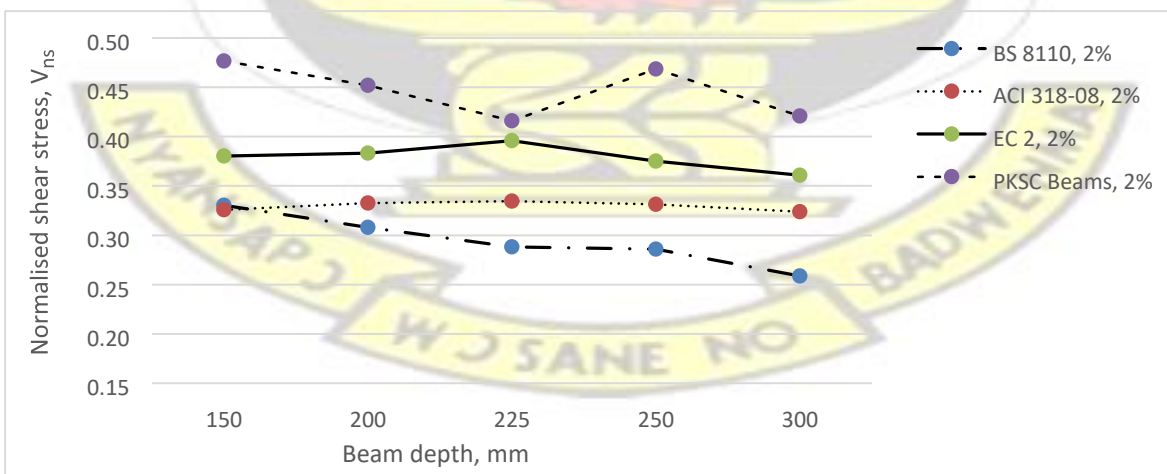


Fig. 4.40 Normalized shear strength (V_{ns}) at Exp. cracking and code predictions ($\rho_w = 2.0\%$).

4.7.4.3 Beams with shear reinforcement

The British Standard, BS 8110 uses an empirical approach to design the shear resistance of structural elements. This approach assumes the shear capacity of a beam is the sum of a concrete contribution and a contribution from transverse steel (See equation 4.3). The concrete contribution is derived from the shear carrying capacity of a beam without transverse reinforcement as discussed in section 4.7.2. That notwithstanding, it is now clear that the failure mechanism of beams with shear reinforcement is different from those without shear reinforcement. This means the code may be inappropriate for PKSC beams with shear reinforcement. Nevertheless, this approach has been used to yield design values that approximate the actual strength of a section through different underlying mechanisms.

Table 4.18 compares the experimental results and theoretical loads calculated using equations 4.3 to 4.8. The performance of BS 8110, EC 2 and ACI 318-08 in predicting the ultimate shear load of both PKSC and NWC beams with shear reinforcement have also been presented. Generally, all the assessed code models under predicted the ultimate capacity of the tested beam specimens. It is seen that ACI 318-08 under predicted the ultimate shear capacity of both PKSC and NWC beams irrespective of the amount of shear reinforcement. The ratio of $V_{(ACI318)}/P_u$ ranges between 67% to 71% and 72% to 76% for PKSC and NWC beams with shear reinforcement respectively. The study shows that the conservativeness of the ACI increases with decreasing amount of shear reinforcement, and can be used to safely to predict the ultimate shear resistance of both PKSC and NWC beams. The ratio of BS 8110 predicted values to experimental values ranges between 84% to 87% for PKSC beams with shear reinforcement and ranges between 81% and 97% for NWC beams with shear reinforcement. This shows that BS 8110 predictions compared to the normal weight concrete was reasonably accurate and able to produce economical and safe designs.

It is seen that, both ACI 318 and BS 8110 are conservative, especially the PKS concrete. However, the ACI is found to be more conservative than the BS 8110. The ratio of predicted EC 2 values to the experimental values ranges from 86% to 89% for the PKSC concrete beams and ranges from 95% to 99% for the NWC beams. EC 2 is found to closely predict the ultimate shear capacity of the PKSC and NWC beams compared to that of the ACI and the BS 8110. For NWC beams without shear reinforcement, the predictions are 70%, 76% and 82% of the shear capacity of the NWC beams for the ACI, BS 8110 and EC 2 respectively. The predictions of PKS beams without shear reinforcement are 72%, 73% and 80% of the shear capacity of the NWC beams for the ACI, BS 8110 and EC 2 respectively.

Considering the PKS concretes, the BS8110 produced calculated shear capacities that accurately predict the strength of the section. The reserve shear strength between the predicted value and the ultimate failure of the beams may be compromised especially in the short span beams, where the sections were able to develop only 10% of the reserve shear strength beyond the diagonal cracking (See Fig.4.34a-c). For beam specimens with 150 mm stirrup spacing, the ACI 318 predicted 59%, 48%, 55% and 57% of the ultimate shear capacity of PKS beams loaded with shear span to depth ratio, $a/d = 1.5, 2.0, 2.5$ and 3.0 respectively. The EC 2 predicted 69%, 62%, 72% and 76% of ultimate shear strength for PKS beams loaded with shear span to depth ratio, $a/d = 1.5, 2.0, 2.5$ and 3.0 respectively. Meanwhile the BS 8110 predicted 62%, 66%, 65% and 69% of the ultimate shear capacity of PKS beams loaded with shear span-to-depth ratio, $a/d = 1.5, 2.0, 2.5$ and 3.0 respectively. Considering beam specimens with 200 mm stirrup spacing, the ACI 318 predicted 52% to 60% of the ultimate shear strength for PKS beams loaded with shear span to depth ratios ranging from $a/d = 1.5$ to 3.0 . The EC 2 predicted 64% to 76% of the ultimate shear strength for

PKS beams loaded with shear span to depth ratios ranging from $a/d = 1.5$ to 3.0 . While the BS 8110 predicted 59% to 68% of the ultimate shear strength for PKS beams loaded with shear span to depth ratios ranging from $a/d = 1.5$ to 3.0 (Table 4.18). This indicates that the various codes of practices underestimate the strength of the PKS beams.

The variation of the shear stresses in relation to the amount of shear reinforcement was found to be non-proportional. That notwithstanding, the shear stresses decreased with decreasing amount of shear reinforcement. As seen from Fig. 4.41 to 4.43, the experimental failure stress results were higher than the code predictions, indicating that the codes are more conservative with the design of reinforced PKSC beams.

After normalizing the ultimate shear force to account for the difference in compressive strength (Table 4.19), the shear stress ratios of experimental values to BS 8110 predicted values range from 1.15 to 1.19 for PKSC beams with shear reinforcement while the ratio range from 1.04 to 1.23 for NWC beams with shear reinforcement. The shear stress ratios of the experimental values to EC2 predicted values range from 0.98 to 1.11 for PKSC beams without shear reinforcement. The variation of the shear stresses in relation to the amount of shear reinforcement was found to be non-proportional. That notwithstanding, the shear stresses decreased with decreasing amount of shear reinforcement. As seen from Fig. 4.34 and Fig. 4.35, the experimental shear stress results were higher than the code predictions, indicating that the codes are more conservative with the design of reinforced PKSC beams.

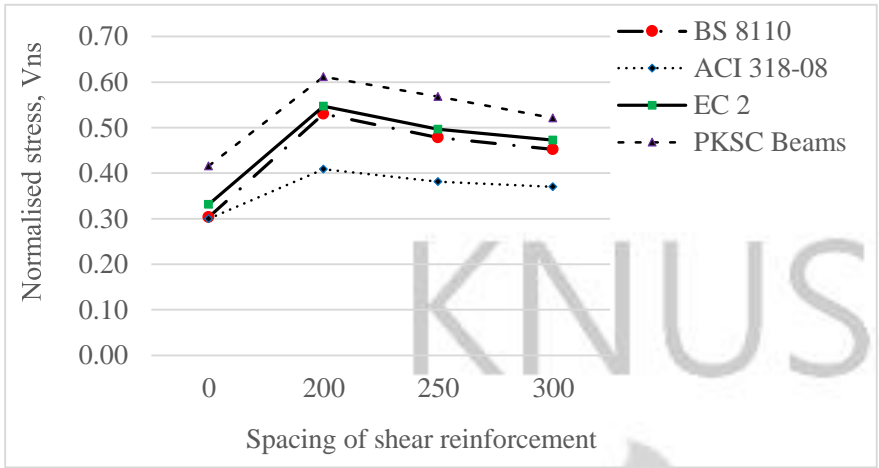


Fig. 4.41 Comparison of normalised stress (V_{ns}) with varying stirrup spacing for PKSC

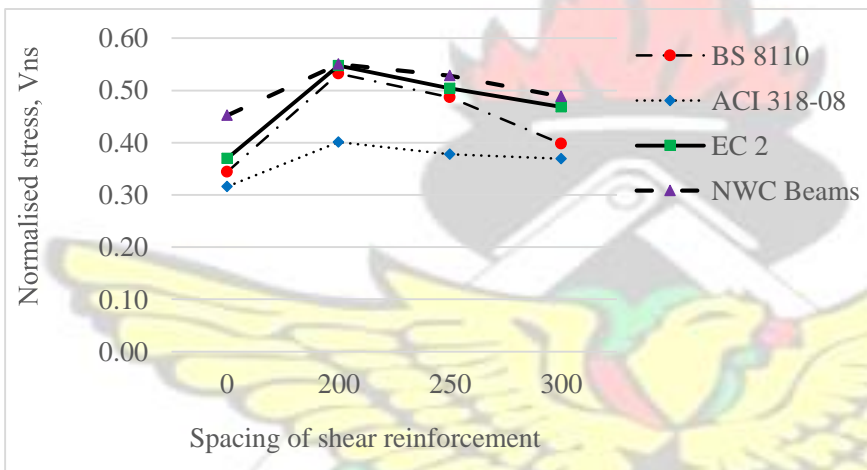


Fig. 4.42 Comparison of normalised stress (V_{ns}) with varying stirrup spacing for NWC

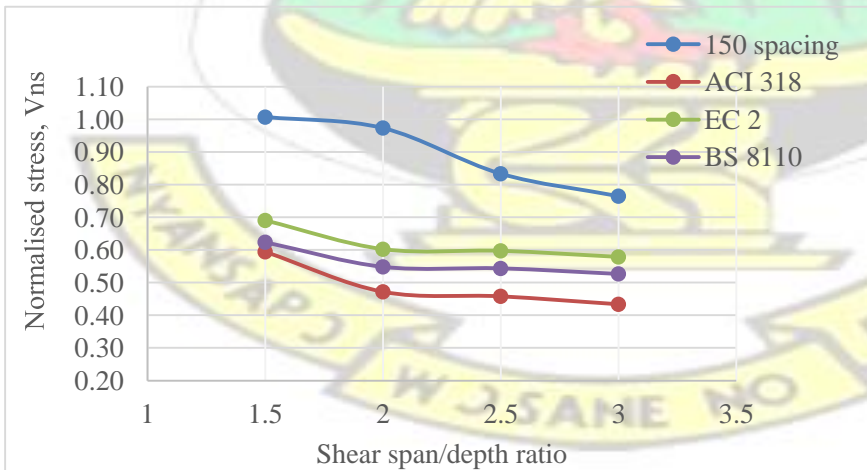


Fig. 4.43 Comparison of normalised stress (V_{ns}) with varying a/d – 150 mm

Table 4.18 Experimental results of S-series beams and code predictions

Beam ID	Exp. Failure load (kN), P_u	Code predictions – V_{code}			Shear force ratios, V_{code}/P_u		
		BS 8110	EC 2	ACI 318	BS 8110	EC 2	ACI 318
					(%)	(%)	(%)
2P 150 A	140	86.67	95.97	82.60	62	69	59
2P 200 A	132	77.40	87.19	77.91	59	66	59
2P 250 A	124	71.84	81.93	75.10	58	66	61
2P 150 B	132	74.36	81.72	64.01	66	62	48
2P 200 B	114	65.10	72.94	59.33	68	64	52
2P 250 B	94	59.54	65.92	56.52	76	70	60
2P 150 C	114	74.36	81.72	62.64	65	72	55
2P 200 C	96	65.10	72.94	57.95	68	76	60
2P 250 C	86	59.54	65.92	55.14	69	77	64
2P 150 D	108	74.36	81.72	61.25	69	76	57
2P 200 D	96	65.10	72.94	56.57	68	76	59
2P 250 D	82	59.54	65.92	53.76	73	80	66
Average:					67	71	58
2.44P 200 E	72	62.40	64.4	48.05	87	88	67
2.44P 250 E	68	57.22	59.48	45.65	84	86	67
2.44P 300 E	62	53.76	56.21	44.04	87	89	71
2.44N 200 E	74	71.52	73.60	53.90	97	99	73
2.44N 250 E	72	66.34	68.69	51.50	92	95	72
2.44N 300 E	66	53.76	63.28	49.90	81	96	76
Average:					90	97	74

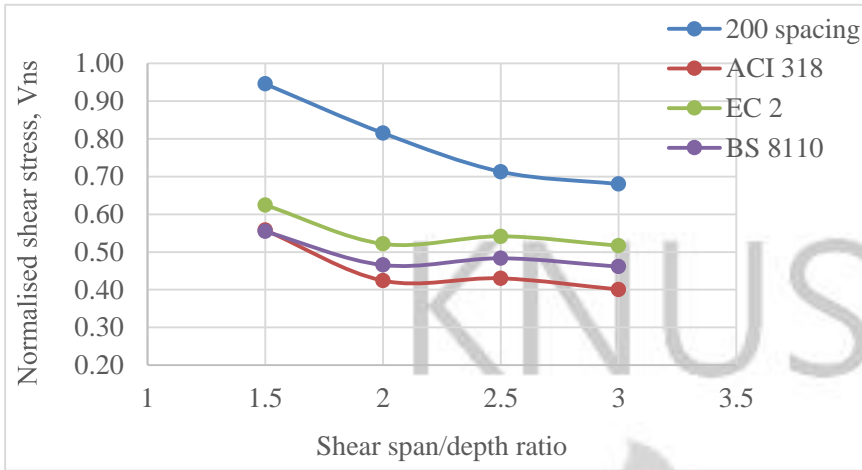


Fig. 4.44 Comparison of shear stress (V_{ns}) with varying a/d

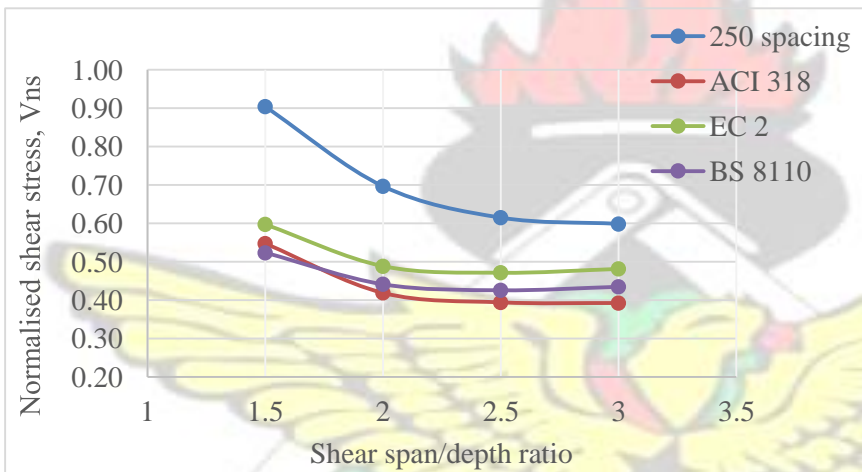


Fig. 4.45 Comparison of shear stress (V_{ns}) with varying a/d

4.7.4.4 Serviceability Limit State

Cracking in a reinforced concrete structure is inevitable, especially when the structure is in full service. In designing a reinforced concrete element, a designer is required to satisfy both serviceability and ultimate limit state conditions. To ensure serviceability requirements, it is necessary to accurately assess deflection and cracking loads of all structural elements. Due to the low tensile strength of concrete, cracking, which is primarily load dependent, can occur at service loads and reduce the flexural stiffness of the reinforced concrete element (Dundar and Kara,

2007). Cracking and resultant crack widths are of utmost concern especially under service load conditions because wide cracks are aesthetically unpleasant and may create serviceability problems such as water ingress leading to corrosion of steel reinforcement. It is therefore not surprising that, the design criterion with regard to cracking is limited to the maximum crack width at service loads (Lim *et al.*, 2007).

The maximum deflection limit under serviceability prescribed by BS 8110: part 2 (1985) (clause 4.2.1.1) is controlled by restricting the allowable deflection to the span of the beam, L divided by 250 (i.e. $L/250$). Without the need for a more rigorous determination of the deflection, the code provides a series of basic span-to-effective depth ratios within which the upper limit deflections do not exceed this serviceability limit. That is, deflection under service load becomes noticeable if it exceeds $span/250$ (Adom-Asamoah and Afrifa, 2011). Comparing the results of the study with the limit provided in the code, it is seen that experimental deflections are lower than the estimated deflection of about 7.2 mm using $L/250$.

From the study, it is seen that deflections at service loads for PKS concrete beams with shear reinforcement varied from 4.45 mm to 6.60mm. On the contrary, service load deflections for PKS concrete beams without shear reinforcement varied from 2.20 mm to 4.10 mm. These deflections are found to be lower than that of the predicted $span/250$ specified by BS 8110-1 (1997). It is also seen from Table 4.19 that service load deflections for NWC beams without shear reinforcement were 3.45 mm to 4.00 mm. However, service load deflections varied from 4.55 mm to 5.45 mm depending on the amount of shear reinforcement. It is observed that at service loads, the average

crack width for PKS concrete beam of 0.228 mm and 0.29 mm (Table 4.19) for NWC beams are both lower than the 0.3mm specified in BS 8110-2 (1985).

Table 4.19 Normalised shear stress prediction of various design codes

Beam ID	Normalized shear stress, V_{ns}							Deflections at service loads, mm	Crack widths at service loads
	Shear stress ratios (V_{exp}/V_{code})								
	V_{Exp}	V_{BS8110}	V_{ACI318}	V_{EC2}	V_{BS8110}	V_{ACI318}	V_{EC2}		
2P 150 A	1.01	0.62	0.59	0.69	1.63	1.71	1.46	5.20	0.12
2P 200 A	0.95	0.55	0.56	0.62	1.73	1.70	1.53	5.30	0.23
2P 250 A	0.90	0.52	0.55	0.60	1.73	1.64	1.50	5.60	0.20
2P 150 B	0.97	0.55	0.47	0.60	1.76	2.06	1.62	6.80	0.16
2P 200 B	0.82	0.47	0.42	0.52	1.74	1.95	1.58	5.50	0.18
2P 250 B	0.70	0.44	0.42	0.49	1.59	1.67	1.43	4.50	0.12
2P 150 C	0.83	0.54	0.46	0.60	1.54	1.80	1.38	5.30	0.32
2P 200 C	0.71	0.48	0.43	0.54	1.48	1.65	1.31	4.60	0.23
2P 250 C	0.61	0.43	0.39	0.47	1.42	1.56	1.30	4.40	0.17
2P 150 D	0.77	0.53	0.43	0.58	1.45	1.79	1.33	5.80	0.20
2P 200 D	0.68	0.46	0.40	0.52	1.48	1.70	1.31	6.50	0.13
2P 250 D	0.60	0.43	0.39	0.48	1.40	1.54	1.25	5.20	0.12
2.44P 200 E	0.42	0.30	0.30	0.33	1.40	1.40	1.27	6.60	0.240
2.44P 250 E	0.61	0.53	0.41	0.55	1.15	1.49	1.11	6.40	0.215
2.44P 300 E	0.57	0.48	0.38	0.50	1.19	1.50	0.98	4.45	0.235
2.44N 200 E	0.52	0.45	0.37	0.47	1.16	1.41	1.11	5.45	0.255
2.44N 250 E	0.45	0.34	0.32	0.37	1.32	1.41	1.22	4.92	0.240
2.44N 300 E	0.55	0.53	0.40	0.55	1.04	1.38	1.00	4.55	0.320

4.7.4.5 Summary

PKS were used as coarse aggregates in reinforced concrete beams and tested to failure. All the PKS LWC developed more extensive cracking than comparative normal weight concrete. Variations in the shear strength and crack propagation between the PKS LWC and the NWC can be attributed to the difference in compressive strengths between the concretes. From the results of the test on 19 rectangular beams without shear reinforcement, it was found that the BS8110, ACI 318 and Eurocode 2 produces safe conservative designs for LWC. However, when LWC was compared to normal weight concrete of this test, some loss in reserve shear strength beyond that calculated by the code was obvious. Nevertheless, this does not affect the design philosophy for shear critical LWC members.

4.8 FLEXURAL BEHAVIOUR OF REINFORCED CONCRETE TWO-WAY SLABS

4.8.1 Introduction

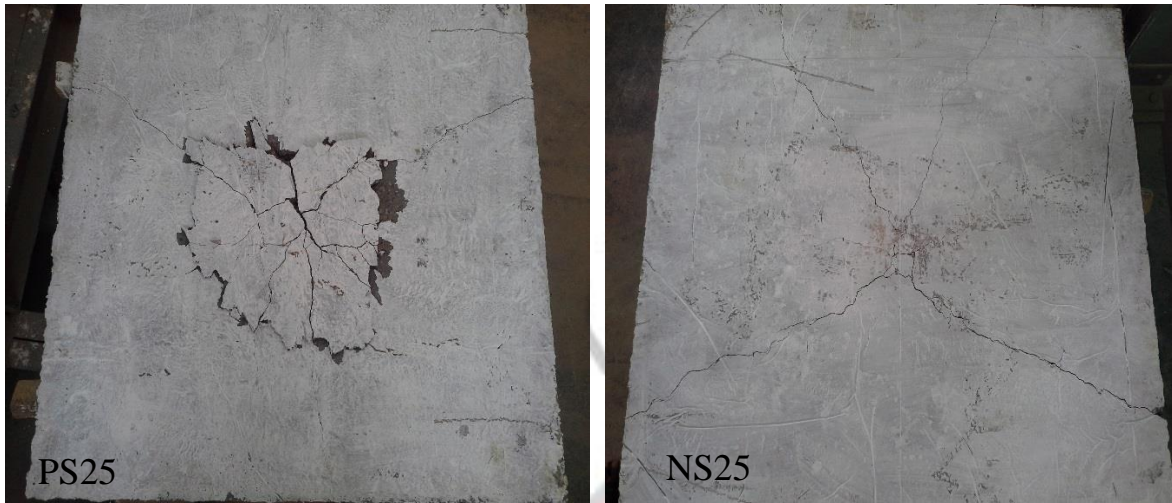
Structural systems involving reinforced concrete flat slabs are commonly used in practice. In such systems, the slabs are usually supported directly by columns without beams and that helps to reduce the building height and increase useable space (Nguyen-Minh *et al.*, 2011). However, this method of construction presents an important problem to the safety of such structures. That is, punching shear failure of the slabs is due to high concentration of stresses at the slab-column connections. The punching shear may also be associated with a slab supported by beams along its sides and subjected to a heavy point load, for example at its centre. This mode of failure is however very dangerous because of its brittle nature. The design of punching shear is to assume that the slab is subjected to hogging moments in both main directions above the column which

postulates that the slab is either continuous or that the slab-column connection is moment resisting. Once, the punching shear failure occurs, resistance of the structure is significantly reduced, which causes separation of the column and slab, and then lead to collapse of the whole structure.

This section simulates the flexural behaviour of reinforced two-way concrete slabs supported at their edges to study the structural behaviour of PKS concrete slabs. Thus the objective of this part of the study was to investigate the effect of concrete strength and the effect of loading on the behaviour of reinforced PKS concrete beams in shear. These were assessed by means of the measurement of shear capacity, deflection, cracking patterns, and modes of failure.

4.8.2 MODES OF FAILURE

The crack patterns for typical PKSC and NWC slab observed underneath the slabs are illustrated in Fig. 4.46 a-b. Bending cracks first developed underneath the slabs once the concrete tensile strength was exceeded due to the applied loads. From the figures it could be inferred that the yield line patterns did not always conform to the assumed patterns used in deriving the ultimate theoretical flexural failure loads (i.e. mechanisms of diagonal yield and circular fan patterns), especially the PKS concrete slabs. All PKS concrete slabs subjected to monotonic loading failed in punching shear (Table 4.20).



a. Crack pattern of PKSC slab

b. Crack pattern of NWC slab Fig. 4.46

Typical crack patterns underneath slabs

With increasing imposed loads, more flexural cracks formed in both directions along the tensile steel reinforcement grid (this being more visible in the control specimen) and diagonal cracks were generated propagating from the centre of the specimens to the corners. Collapse of the slabs always occurred through a combination of the crushing of the concrete after flexural cracks propagated extensively into the compression zone, and punching of concrete plug from the centre of the slabs. Punching was accompanied by immediate and significant drop in the applied load. The punched concrete plug was steeper (in the narrower direction) in the control specimen in comparison to the strengthened ones. After failure occurred the flatness of the slabs was maintained outside the load application area.

4.8.3 Load-deflection behaviour

Typical load–deflection curves of the two-way slabs, subjected to monotonic loadings are shown in Fig. 4.47. Loads do not include the dead load of the slabs while the deflection values do not include contribution from the dead load. The load deflection curves of the slabs generally

exhibited an elastic linear behaviour before cracking. It is seen that the slabs showed little loss in stiffness in the post-cracking stages during the monotonic loading. It was observed that the deflections in the PKS two-way slabs were higher than those observed in the NWC two-way slabs with the same concrete strength. This could be attributed to lower modulus of rupture of the PKSC specimens.

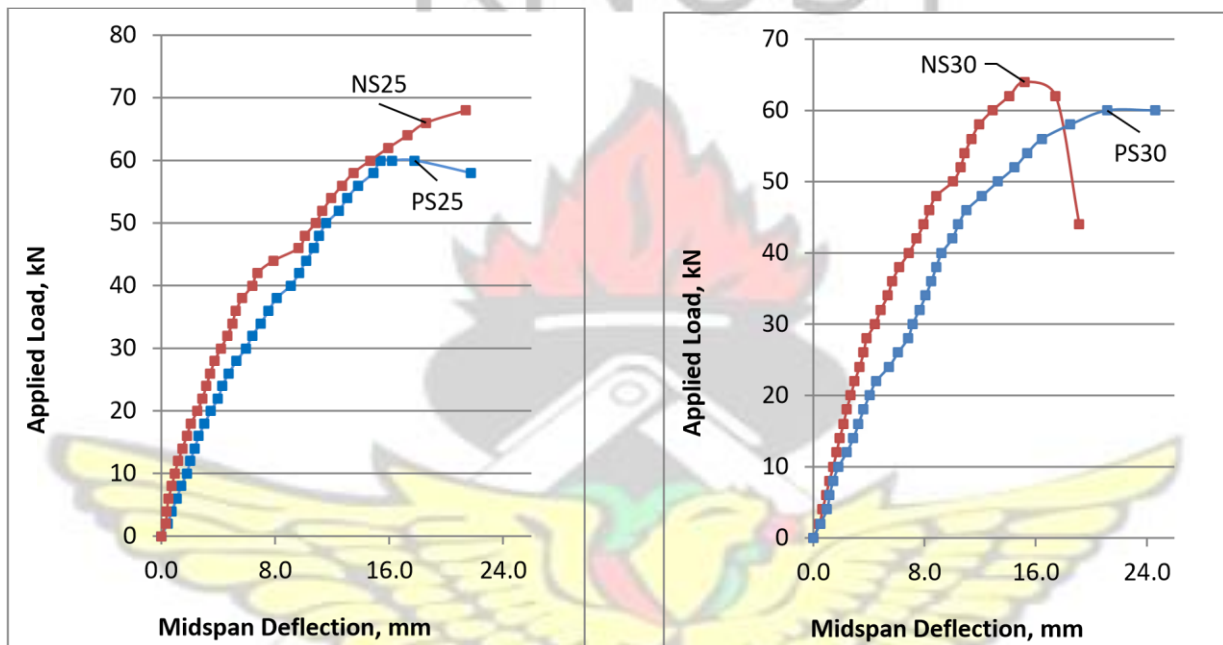


Figure 4.47 Load-deflection curves for PKS and NWC slabs

4.8.4 Cracking and failure loads

From Table 4.20, the experimental cracking loads (P_{cr}) of the slabs were 28% and 34% of the experimental failure load (P_{ult}) for PKS (PS 25) and NWC (NS 25) subjected to monotonic loading respectively. The experimental cracking loads of the slabs were 32% and 35% of failure loads for PS 30 and NS 30 respectively. These values were found to be dependent of the type of concrete tested. Final failure loads were found to increase with increasing concrete strengths.

However, first cracks were independent on the compressive strength of the slabs. The corresponding experimental failure loads (P_{ult}) to the theoretical failure loads (P'_{ult}) of the slabs

were 1.79 and 1.84 for PS25 and NS25 slabs subjected to monotonic loads, respectively. The experimental failure loads (P_{ult}) to the theoretical failure loads (P'_{ult}) were 1.53 and 1.57 for PS30 and NS30 slabs subjected to monotonic loads, respectively. The values were generally consistent with results for steel fibre reinforced concrete slabs (Nguyen-Minh *et al.*, 2011).

5.6.4 Effect of Cyclic loading

A typical load–deflection curve for the slabs under cyclic loading is illustrated in Figs. 4.48. It is seen that slabs NS and SP formed hysteresis loops. Loading–unloading to failure of the slabs varied from 1 to 20 cycles. It was observed that the load–deflection curves after load cycling were able to re-trace their initial curve paths for the loading cycles used in the investigation. The ability of the slabs to retrace their initial loading paths implies that very little deterioration in stiffness occurred. The gradients of the reloading curves were similar to those of the initial loading curves signifying that there was little or no stiffness degradation. In spite of this, the tensile reinforcement were not able to dissipate energy without permanent deformations at service loads (typically 30–35% of ultimate loads). The maximum deflection of slabs subjected to monotonic loading was slightly higher than those of corresponding slabs subjected to limited number of cyclic loading.

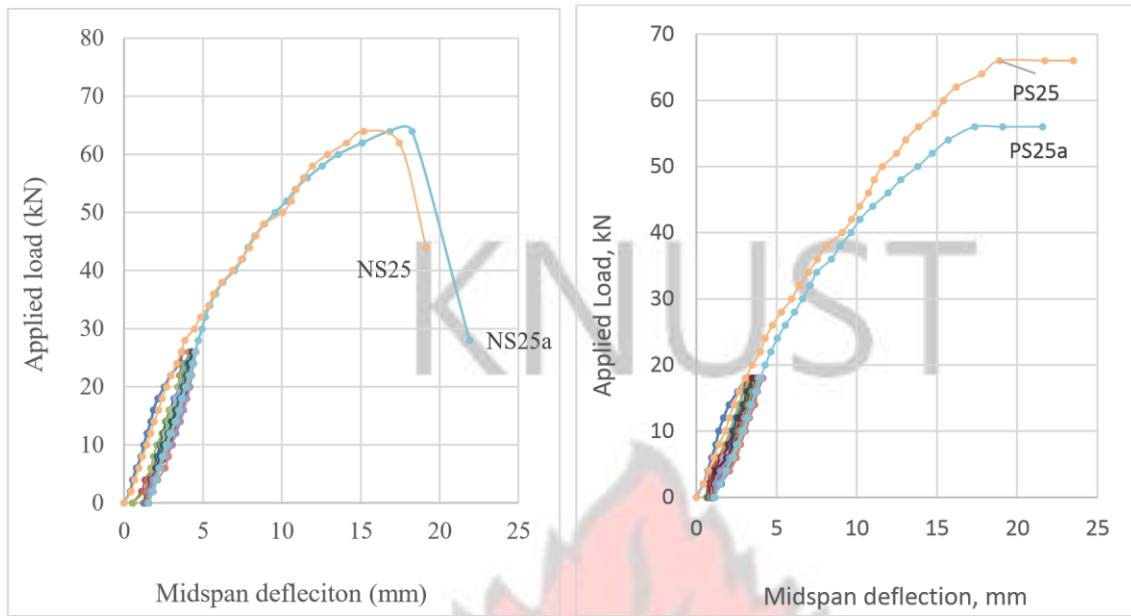


Figure 4.48 Load-deflection curves for PKS/NWC slabs under cyclic loading

Table 4.20 Failure crack loads and theoretical loads of two-way slabs

Slab Id	Target Compressive strength, MPa	Exp. cracking load (kN)		Theoretical		P_{cr}/P_{ult} (%)	P_{ult}/P'_{ult}
		First crack load, P_{cr}	Ultimate failure load, P_{ult}	failure load, P'_{ult}			
PS 25	25	16	58	32.3	28	1.79	
PS 30	30	22	64	34.7	34	1.84	
NS 25	25	20	62	40.4	32	1.53	
NS 30	30	24	68	43.4	35	1.57	
PS25a ¹	25	12	56	32.3	21	1.73	
PS30a ²	30	10	60	34.7	16	1.73	
NS25a ²	25	16	58	40.4	28	1.44	
NS30a ³	30	16	64	43.4	0.25	1.47	

^{1,2,3} Cycles at which first cracks appeared

CHAPTER FIVE

CONCLUSIONS AND RECOMMENDATIONS

5.1 SUMMARY

Lightweight concrete with and without shear reinforcement has potential to be used for lots of structures ranging from complex structures to simple low-cost housing and rapidly erected temporal structures. This study looked at the physical properties of PKS aggregates, the mechanical properties of PKS lightweight aggregate concrete (LWC) and the behaviour of reinforced PKS concrete beams in shear. The physical properties of the aggregates and the mechanical properties of fresh and hardened PKS concrete were also studied. For each study objective, comparisons between PKS concrete and normal weight concrete were made. Aggregate properties such as aggregate impact value (AIV), aggregate crushing value (ACV), Los Angeles abrasion value (AAV), water absorption and aggregate shape were estimated.

The second objective considered the properties of both fresh and hardened concrete specimens. The major parameters were to study the effect of cement types and aggregate types on the behaviour of PKS concrete and NWC in the fresh and hardened states. The mechanical properties studied were the compressive and flexural strength of both normal weight aggregate concrete and PKS aggregate concrete. The study employed a series of trial mixes to achieve an optimum compressive strength at 28-days of curing. Using the trial mixes, 216 cubes and 169 prisms were cast for compressive strength and modulus of rupture of the concrete.

The third stage involved the casting and testing of 46 reinforced concrete beams and 8 slabs to failure in flexure. The implications of the use of the two types of aggregates (PKS and granite aggregates) on the shear behaviour of reinforced PKS concrete and NWC beams as depicted by

cracking, ultimate strength and modes of failure have been discussed with reference to BS 8110, ACI 318 and EC 2 stipulations. Several parameters were considered at this stage. The two-way reinforced PKS concrete slabs behaved similarly to that of the NWC slabs.

Experimental tests and rigorous observations conducted and presented in this thesis indicate that design equations developed with normal weight concrete can be generalized and used in the design of PKS LWC. There also do not appear to be any weaknesses that can be considered as a significant material deficiency prohibiting PKS from structural use.

5.2 CONCLUSIONS

5.2.1 Physical Properties of Aggregate

The following conclusions are made from the results and the analysis thereof:

1. The physical and mechanical properties of the PKS aggregate are satisfactory, based on BS 882 (1992). Mechanical properties such as aggregate crushing, aggregate impact and Los Angeles abrasion values are found to be lower than corresponding values for the granite aggregates. PKS aggregates possess high abrasion resistance which suggests that PKS aggregates can be used as a floor finish, especially in areas of high pedestrian traffic. PKS aggregates have high water absorption (about 18%) compared to only 0.68% for granite aggregates. This can adversely affect the workability of the PKS concrete at the mixing stage with subsequent effect on the hydration of the cement and the creation of voids in finished concrete.
2. Based on the physical properties of PKS aggregate, PKS is a potential construction material and can be used as a complete replacement of granite aggregates for low applied

load situations. Its use in construction also solves the environmental problem of disposal of the agriculture waste material.

5.2.2 Mechanical Properties of Concrete with PKS aggregates

1. PKS aggregate concrete can be used to produce structural concrete with compressive strength of to 24.87 N/mm^2 using ordinary Portland cement (OPC) without the use of superplasticizers. The minimum cement content required is 500 Kg/m^3 with water/cement ratio of 0.4. Additionally, PKS can be used with Portland-limestone cement to produce LWC with compressive strengths up to 18.56 N/mm^2 without the use of superplasticizers. The required minimum cement content is 500 kg/m^3 with water/cement ratio of 0.4. To achieve a 28-day compressive strength of 27.47 N/mm^2 with OPC, a mix proportion containing PKS as coarse aggregate has been determined. The minimum cement content required is 500 kg/m^3 , water/cement ratio of 0.38 and superplasticizer content of 1% of the weight of the cement. Similarly, a 28-day compressive strength of 24.86 N/mm^2 has been produced using Portland-limestone cement with minimum cement content of 500 kg/m^3 , water/cement ratio of 0.38 and superplasticizer content of 1% of the weight of the cement.
2. PKS aggregates can be used to produce concretes with compressive strength higher than the minimum required strength of 17 N/mm^2 for structural LWC as given by the ASTM C330. The results of the study show that PKS has a good potential as a coarse aggregate for the production of structural LWC, especially where high strength is not of major objective in construction.

3. Ordinary Portland cement produced PKSC of higher strength compared to the Portlandlimestone cement. The 28-day compressive strength of PKS concrete using Portlandlimestone cement and the ordinary Portland cement was approximately 25% and 27% lower respectively compared to the granite (normal weight) concrete.

5.2.3 Reinforced Concrete Beams and two-way slabs

Comparisons between the ultimate shear failure capacities and the shear failure mechanisms of PKSC beams and NWC beams cast with and without shear reinforcement are comparable for the parameters considered in this study.

1. PKS LWC beams behaved similarly to the control normal weight concrete beams until onset of diagonal cracking. Thereafter, while normal weight concrete beams were able to continue resisting shear until a flexural failure occurred, the PKSC was unable to develop sufficient resistance and physically failed in a brittle shear mode.
2. The effect of shear reinforcement on the shear capacity of both PKS LWC and normal weight concrete was evident in the shear strength values obtained. Increasing the amount of shear reinforcement in both types of reinforced concrete specimens resulted in a corresponding increase in the shear capacity of the beams. The shear reinforcement in PKS beams increased the ultimate shear capacity of the PKS beams by about 35% when compared to corresponding PKS beams without shear reinforcement. Increasing the spacing of shear reinforcement (that is, reducing shear reinforcement) resulted in a decrease in the ultimate failure loads.

3. The amount of longitudinal reinforcement is found to affect the shear strength of PKSC beams. Increasing the amount of tension steel results in a corresponding increase in the shear strength of the PKSC beams.
4. The BS 8110-1, ACI 318 and EC 2 codes underestimate the experimental shear capacity of reinforced PKS concrete beams, especially PKSC beams without shear reinforcement and of a short span. However, the reduction factors imposed on LWC beams by the various codes are found to safely predict the ultimate shear capacity of PKSC beams with and without shear reinforcement. Similarly, the codes are found to safely predict the ultimate shear capacity of the NWC beams.
5. It was found that the three major codes BS 8110, ACI 318 and EC 2 design model, underestimates the ultimate shear failure loads of PKS beams with shear reinforcements.
6. Comparison of the ultimate limit state and serviceability limit state performance of the PKS LWC beams without shear reinforcement against design equations of the British Standards Institute show that the equations can be used with confidence.
7. The general load-deflection behaviour of PKS concrete beams with and without shear reinforcement were found to be similar to the behaviour of NWC beams. PKS concrete beams demonstrated higher deflection values at failure than that of the NWC beams. Deflections in PKSC beams were higher for a given load than those in NWC beams. The deflection of the PKSC beams with shear reinforcement at service loads were higher than the deflections of the NWC beams with shear reinforcement.

8. No noticeable difference in cracking patterns was observed between the different types of concretes tested.
9. Crack widths at service loads varied from 0.215 to 0.240 mm for PKS concrete specimens and these are below the maximum allowable crack width of 0.3 mm for durability requirements of BS8110 (1997) for non-liquid retaining structures. For the NWC, the crack widths varied from 0.245 to 0.39. This shows that crack widths of PKSC beam specimens were lower than corresponding NWC beam specimens. Greater number of cracks in PKS concrete resulted in lower crack widths compared to NWC concrete beams.
10. PKS two-way concrete slabs demonstrated higher deflections at various loading levels compared to corresponding NWC slabs. Collapse of the slabs occurred through a combination of concrete crushing in flexure and punching shear. The 20 cycles of loading/unloading of the two-way slabs revealed that, a very little deterioration in stiffness occurred.
11. The experimental failure loads to theoretical failure loads, based on the BS 8110-1, varied from 1.53 and 1.84 for the PKS and NWC two-way slabs. This indicates that the code can be used to safely design PKS concrete slabs

5.3 RECOMMENDATIONS FOR INDUSTRY

The following recommendations are made for the industry:

1. PKS can be used in the production of both single storey and low height multi-story structures for accommodation. Specifically, PKS concrete can be used in the production

of reinforced concrete elements such as beams and two-way slabs, and sustain loads as in mass concrete, blinding, partition walls, concrete floors, stairs, lintels and beams.

2. The use of *Dura* and *Tenera* species are highly recommended for construction purposes due to the thickness of the shells.
3. The use of superplasticizer is recommended to produce PKS concrete of higher compressive strength. The limit of SP dosage must however be strictly adhered to. In the absence of a superplasticizer, it is recommended that the PKS be produced with OPC for concrete production.
4. Even though the three codes of practice are found to be satisfactorily predict the behaviour of PKS concrete beams, designs using the EC 2 is highly recommended since it gives a safer and closer prediction irrespective of the beam dimensions and tension steel.
5. Palm kernel shell concrete beams with a maximum depth of 300 mm, with compressive strengths up to 30 MPa and 1.5% longitudinal steel is recommended.
6. Adequate shear reinforcement should be provided in PKSC slabs, especially slab-tocolumn connection to mitigate the appearance of punching shear.

5.4 RECOMMENDATIONS FOR FURTHER RESEARCH

The following studies are recommended to carry the research forward

1. This study considered compressive and flexural strengths up to 90 days of curing. The experimental and analytical investigations of longer-term flexural response of PKS concrete is recommended.
2. Experimental investigations of reinforced concrete deep beams using PKS aggregates is recommended to fully understand the effect of size of beams on PKS concrete.
3. Since this study was carried out on only rectangular PKS beams with and without shear reinforcements, and two-way slabs, it would be appropriate to carry out further studies on structural elements, for example other forms of T beams, columns, one-way slabs and other concrete elements to expand the use of PKS aggregates as coarse aggregates in concrete. With these studies, new design equations specifically for the structural concrete elements can be proposed if required.
4. This study holistically considered the structural applicability of PKS aggregates. Sustainability assessment such as Life Cycle Assessment (LCA) is recommended for further studies to consider the variability and consistency of PKS as an aggregate.
5. It is also recommended that further studies should be carried out to investigate the performance of PKS concrete specimens in times of fire.

5.5 LIMITATIONS OF STUDY

In spite of numerous efforts to ensure a controlled research work activity in the laboratory, there were a host of limitations encountered in the laboratory. A major problem encountered was the

influence of the weather conditions which could affect the quality of the concrete produced, especially at the mixing stage. While efforts were made to cast samples at consistent times of the day, the weather conditions varied considerably. Secondly, the hydraulic actuator was manually operated, some inconsistent readings were recorded whenever there was fatigue. This problem was often observed at the time of testing beams and slabs subjected to the cyclic loading.

For the range of variables investigated, the PKS concrete beams and two-way slabs performed adequately well in the face of the three major codes of practice. Readers should therefore approach the current findings and conclusions with caution. Other influencing parameters, especially increasing the overall cross section of the beams could result in a significant variation in the results.

REFERENCES

- Abdullah, A. A. A. (1996), Palm oil shell aggregate for lightweight concrete. Waste material used in concrete manufacturing, Noyes Publication, pp. 624-636.
- Abdullahi, M. (2012), Effect of aggregate type on Compressive strength of concrete, *International Journal of Civil and Structural Engineering*, Vol. 2(3), pp. 791- 800.
- Abdullahi, M., Al-Mattarneh, H. M. A. and Mohammed, B.S. (2009), Equations for Mix Design of Structural Lightweight Concrete, *European Journal of Scientific Research*, Vol. 31(1), pp. 132-141.
- Abrams, D.A, (1927), Water-cement Ratio as a Basis of Concrete Quality, *Journal of American Concrete Institute*, 1927, Vol. 23, pp. 452-457.
- ACI Committee 211.2 (2004), Standard Practice for Selecting Proportions for Structural Lightweight Concrete, American Concrete Institute Committee, pp. 1-18.
- ACI Committee 213R-03, (2003), Guide for Structural Lightweight-Aggregate Concrete, American Concrete Institute Committee, pp. 1-34.
- ACI Committee 304.5R (1991), Batching, Mixing, and Job Control of Lightweight Concrete, American Concrete Institute, pp. 1-9.

- ACI 318-08 (2008), Building Code Requirements for Structural Concrete (ACI 318M-08) and Commentary, American Concrete Institute, pp. 103- 202.
- Adeagbo, D. O. (1999), Effect of water cement ratio on the properties of sandcrete cubes when partially replaced with sawdust, *Journal of Environmental Sciences*, Vol. 3(2), pp. 187-192.
- Adewuyi, A. P. and Adegoke, T. (2008). Exploratory Study of Periwinkle Shells as Coarse Aggregates in Concrete Works, *ARPJ Journal of Engineering and Applied Sciences*, Vol. 3(6), pp. 1-5.
- Adom-Asamoah, M. and Afrifa, R. O. (2013), Shear behaviour of reinforced phyllite concrete beams, *Materials and Design*, Vol. 43, pp. 438-446.
- Adom-Asamoah, M., Afrifa, R.O. and Ampofo, J.W. (2012), Comparative study on shear strength of reinforced concrete beams made from phyllite and granite aggregates without shear reinforcement, In: Badu, E., Dinye, R., Ahadzie, D. and Owusu-Manu, D. (Eds.), In Proceedings of 1st International Conference on Infrastructural Development in Africa (ICIDA 2012), Kumasi, Ghana, Pp. 684 – 697, ISBN: 2026 – 6650.
- Adom-Asamoah, M. and Afrifa, O. A. (2011), Investigation on the flexural behaviour of reinforced concrete beams using phyllite aggregates from mining waste, *Materials and Design*, Vol. 32, pp. 5132-5140.
- Adom-Asamoah, M. and Afrifa, O. A. (2010), A study of concrete properties using phyllite as coarse aggregates, *Materials and Design*, Vol. 31(9), pp. 4561-4566.
- Adom-Asamoah, M. and Kankam, C. K. (2008), Behaviour of reinforced concrete two-way slabs using steel bars milled from scrap metals, *Materials & Design*, Vol. 29(6), pp. 1125–1130.
- Adzimah, S. K. and Seckley, E. (2009), Modification in the design of an already existing palm nut-fibre separator, *African Journal of Environmental Science and Technology*, Vol. 3(11), pp. 387-398.
- Agbodeka, F. (1992), An economic history of Ghana: from the earliest times, Accra, Ghana Universities Press.
- Ahn, N., (2000), An Experimental Study on the Guidelines for Using Higher Contents of Aggregate Microfines in Portland Cement Concrete, Ph.D. Thesis, University of Texas at Austin.
- Ahn, N.S. and Fowler, D.W. (2001), An Experimental Study on the Guidelines for Using Higher Contents of Aggregate Microfines in Portland Cement Concrete, *International Center for Aggregates Research Report 102-1F*, Austin TX, USA.
- Akhras, G. and Foo, H.C., (1994), A knowledge-based system for selecting proportions for normal concrete, *Expert systems with applications*, Vol. 7(2), pp. 323-335.
- Alengaram, U.J., Abdullah, B A. M., Jumaat, M. Z. (2013), Utilization of oil palm kernel shell as lightweight aggregate in concrete – A review, *Construction and Building Materials*, Vol. 38, pp. 161-172.
- Alengaram, U.J., Jumaat, M.Z, Mahmud, H. and Fayyadh, M. M. (2011a), Shear behaviour of reinforced palm kernel shell concrete beams, *Construction and Building Materials*, Vol. 25, pp. 2918–2927.

- Alengaram, U.J., Mahmud, H. and Jumaat, M.Z, (2011b), Enhancement and prediction of modulus of elasticity of palm kernel shell concrete, *Materials and Design*, Vol. 32, pp. 2143-2148.
- Alengaram, U. J., Mahmud, H., Jumaat, M. Z. and Shirazi, S. M. (2010a), Effect of aggregate size and proportion on strength properties of palm kernel shell concrete, *International Journal of Physical Science*, Vol. 5(12), pp. 1848–1856.
- Alengaram, U.J., Mahmud, H. and Jumaat, M. Z. (2010b), Comparison of mechanical and bond properties of oil palm kernel shell concrete with normal weight concrete, *International Journal of the Physical Sciences* Vol. 5(8), pp. 1231-1239.
- Alengaram, U.J., Jumaat, M.Z. and Mahmud, H. (2008a), Influence of cementitious materials and aggregate content on compressive strength of palm kernel shell concrete, *Journal of Applied Sciences*, Vol. 8(18), pp. 3207-3213.
- Alengaram, U. J., Jumaat, M. Z. and Mahmud, H. (2008b), Ductility behaviour of reinforced palm kernel shell concrete beams, *European Journal of Scientific Research*, Vol. 23(3), pp. 406-420.
- Alexander, M. G. and Mindness, S. (2005), *Aggregates in Concrete*, Taylor and Francis Publication, Abingdon, Oxfordshire, UK.
- Al-Khaiat, H. and Haque, M. N. (1998), Effect of internal curing on early strength and physical properties of a lightweight concrete, *Cement and Concrete Research*, Vol. 28(6), pp. 859-866.
- Al-Saraj, W. K. A. (2007), Fatigue Behaviour of Reinforced Concrete Beams Strengthened with GFRP Sheets, *Journal of Engineering and Development*, Vol. 11(2), 1-18.
- Alsadey, S. (2012), Influence of Superplasticizer on Strength of Concrete, *International Journal of Research in Engineering and Technology (IJRET)*, Vol. 1(3), pp. 164-166.
- Amankwah, E. O., Kankam, C. K., Bediako, M. (2014), Influence of calcined clay pozzolana on strength characteristics of Portland Cement Concrete, *Material Science and applications*, Vol. 3(6), pp. 410-419.
- Andaleeb, S. M. (2005), Concrete mix design for lightweight aggregates and an overview on high strength concrete, MSc. Thesis, Department of Civil Engineering, Bangladesh University of Engineering and Technology.
- Angelakos, D. (1999), The Influence of Concrete Strength and Longitudinal reinforcement Ratio on the Shear Strength of Large-Size Reinforced Concrete Beams with and without, Transverse Reinforcement, MSc. Theses, Department of Civil Engineering University of Toronto, USA.
- Arun, M. and Ramakrishnan, S. (2014), Size Effect on Shear Behavior of High Strength RC Slender Beams, *IJRET: International Journal of Research in Engineering and Technology*, Vol. 03 (08), pp. 113-118.
- ASCE-ACI Committee 426, (1973), The shear strength of reinforced concrete members, *Journal of Structural Division, ASCE*, Vol. 99, pp. 1091–187.
- ASCE-ACI Committee 445 on Shear and Torsion (1998), Recent approaches to shear design of structural concrete, *Journal of Structural Engineering*, Vol. 124, pp. 1375–417.
- ASTM C125-07 (2007), Standard Terminology Relating to Concrete and Concrete Aggregates, American Standard for Testing Materials (ASTM) International, West Conshohocken, PA, www.astm.org.

- ASTM C127-07 (1993), Standard test method for specific gravity and absorption of coarse aggregate, American Standard for Testing Materials (ASTM) International, West Conshohocken, PA, www.astm.org, pp. 1-5.
- ASTM C330, (1999), Standard Specification for Lightweight Aggregates for Structural Concrete, American Standard for Testing Materials (ASTM) International, West Conshohocken, PA, www.astm.org, pp. 1-4.
- ASTM C494, (1999), Standard Specification for Chemical Admixtures for Concrete, American Standard for Testing Materials (ASTM) International, West Conshohocken, PA, 2003, DOI: 10.1520/C0033-03, www.astm.org.
- Ashour, S. A., Hasanain, G. S., and Wafa, F. F. (1992). "Shear Behavior of High-Strength Fiber Reinforced Concrete Beams." *ACI Structural Journal*, 89(2), 176- 184.
- Atiemo, E., Kankam, C. K. Momade, F. Appiah-Boakye, K., (2014), Hydration properties of calcined clay pozzolan and limestone mineral admixtures in binary and ternary cement, *Journal of Physical Science and Application*, Vol. 4(5), pp. 323-327.
- Bache, H and Nepper, H. (1998), Christensen observation on strength and fracture in Lightweight concrete, Proceedings of the 1st International Congress on Lightweight Concrete, pp 93108, Cement and Concrete Association, London.
- Babu, K. G. and Babu, D. S. (2003), Behaviour of lightweight expanded polystyrene concrete containing silica fume, *Cement and Concrete Research*, Vol. 33(5), pp. 755–762.
- Bai, Y., Ratiyah, I. and Basheer, P.A. M. (2004), Properties of lightweight concrete manufactured with fly ash, furnace bottom ash, and lytag, Wang, K. (Ed.), In Proceedings of the International Workshop on Sustainable Development and Concrete Technology, Beijing, China, pp. 77-88.
- Bambang, I. S., Kariantoni, G. and Liliani, T. S., (2005), Workability and Resilient Modulus of Asphalt Concrete Mixtures Containing Flaky Aggregates Shape, *Journal of the Eastern Asia Society for Transportation Studies*, vol. 6, pp. 1302 – 1312.
- Basri, H.B., Mannan, M.A. and Zain, M. F. M. (1999), Concrete using oil palm shells as aggregate, *Cement and Concrete Research*, Vol., 29(4), pp. 619-622.
- Balendran, R. V., Zhou, F. P., Nadeem, A. and Leung, A. Y. T. (2002), Influence of steel fibres on strength and ductility of normal and lightweight high strength concrete, *Building and Environment*, Vol., 37, pp. 1361-1367.
- Bazant, P. Z. and Sun, H. H. (1987), Size Effect in Diagonal Shear Failure: Influence of Aggregate Size and Stirrups, *ACI Materials Journal*, paper no. 84-M2 pp. 259-269.
- Bazant, P. Z. and Kim, J. K. (1984), Size Effect in Shear Failure of Longitudinally Reinforced Beams, *ACI Materials Journal*, vol. 81, pp. 456-467.
- Bhikshma, V. and Annie, F. G. (2013), Studies on effect of maximum size of aggregate in Higher grade concrete with high volume fly ash, *Asian Journal of Civil Engineering (BHCR)*, Vol. 14(1), pp. 101-109.
- Bissonnette, B., Pierre, P. and Pigeon, M. (1999), Influence of key parameters on drying shrinkage of cementitious materials, *Cement and Concrete Research*, Vol. 25(5), pp. 1075-1085.
- Boison, K. B. (2002), Environmental and Institutional Sustainability of Regimanuel Gray's East Airport Estate, Accra, Ghana, MSc. Theses, Infrastructure Department.

- Bouquety, M. N., Descantes, Y., Barcelo, L., DeLarrard, F. and Clavaud, B. (2006), Experimental study of crushed aggregate shape, *Construction and Building Materials*, Vol. 21(4), pp. 695-920.
- Browning, J., Darwin, D., Reynolds, D. and Pendergrass, B. (2011), Lightweight aggregate as Internal curing agent to limit concrete shrinkage, *Materials Journal of American Concrete Institute*, Vol. 108(6), pp. 638-644.
- BS 812, (1990), Testing aggregates, British Standards Institution, London, UK.
- BS 882, (1992), Specification for aggregates from natural sources for concrete, British Standards Institution, London, UK.
- BS 1348-2, (1980), Test of Water for making Concrete, British Standards Institution, London, UK.
- BS 8110-1, (1997), Structural use of concrete: Code of practice for design and construction, British Standards Institution. London, UK.
- BS 8110-2, (1985), Structural use of concrete: Code of practice for special circumstances, British Standards Institution. London, UK.
- BS EN 197-1, (2000), Cement - Part 1: Composition, specifications and conformity criteria for common cements, British Standard Institution, London, UK.
- BS EN 1097-6, (2000), Test for mechanical and physical properties of Aggregates-Part 6: Determination of particle density and water absorption, British Standard Institution, London, UK.
- BS EN 12390-1 (2000), Testing hardened concrete — Part 1: Shape, dimensions and other requirements for specimens and moulds, British Standard Institution, London, UK.
- BS EN 12390-2 (2009), Testing hardened concrete- Part 2: Making and curing specimens for strength tests, British Standard Institution, London, UK.
- BS EN 12390-3 (2009), Testing hardened concrete- Part 3: Compressive strength of test specimens, British Standard Institution, London, UK.
- BS EN 12390-5 (2000), Testing hardened concrete- Part 5: Flexural strength of test specimens, British Standard Institution, London, UK.
- BS EN 13055-1 (2002), Lightweight aggregates-Part 1: Lightweight aggregates for concrete, mortar and grout, British Standard Institution, London, UK.
- Carino, N. J. and Clifton, J. R. (1995), Prediction of Cracking in Reinforced Concrete Structures, National Institute of Standards and Technology, Department of Commerce, USA, pp. 230.
- Chandra, S. and Berntsson, L. (2002), Lightweight Aggregate Concrete, *Building Materials series*, William Andrew Publishing, Norwich, New York, U.S.A.
- Chen, B. and Liu, J. (2005), Contribution of hybrid fibers on the properties of the high-Strength lightweight concrete having good workability, *Cement and Concrete Research*, Vol., 35, pp. 913-917.
- Chen, H. J., Yen, T., Lia, T. P. and Huang, Y.L. (1999), Determination of the dividing strength and its relation to the concrete strength in lightweight aggregate concrete, *Cement and Concrete Composites*, Vol. 21, pp. 29-37.
- Clarke, J. L. (1993), Structural lightweight aggregate concrete, Blackie Academic and Professional - an Imprint of Chapman and Hall, London.

- Cho, J. S., Lundy, J. and Shih-Ho, C. (2009), Shear Strength of Steel Fiber Reinforced Prestressed Concrete Beams, Griffis, L., Helwig, T., Waggoner, M. and Hoit, M. (Eds.), *In Proceedings of Structures Congress 2009: Don't Mess with Structural Engineers: Expanding Our Role*, ASCE, pp. 1058-1066.
- Colak, A. (2006), A new model for the estimation of compressive strength of Portland cement concrete, *Cement and concrete research*, Vol. 36, pp.1409-1413.
- Colleparadi, S., Coppola, L., Troli, R. and Colleparadi, M. (2006), Mechanisms of Actions of Different Superplasticizers for high performance concrete.
- Collepradi, M. (1995), *Concrete Admixtures Handbook*, 2nd ed, Noyes Publication, pp. 359.
- Collins, M.P., Bentz, E.C. and Sherwood, E.G. (2008), Where is Shear Reinforcement Required? Review of Research Results and Design Procedures, *Structural Journal of American Concrete Institute*, Vol. 105(5), pp. 590-600.
- Collins, M.P. and Mitchell, D. (1997), *Pre-stressed Concrete Structures*. Response Publications. Canada, pp. 766.
- Concrete Society of UK, (1987), *Guide to the Structural use of Lightweight Aggregate Concrete*, Licensed copy of University of Northumbria (01/2012), The Institution of Structural Engineers, UK.
- Cui, H.Z., Tommy, Y.L., Shazim, A.M. and Weiting, X. (2012), Effect of lightweight aggregates on the mechanical properties and brittleness of lightweight aggregate concrete, *Construction and Building materials*, 35, pp. 149-158.
- Danyo, D. (2013), Oil Palm and Palm Oil Industry in Ghana: A Brief History, *International Research Journal of Plant Science*, Vol. 4(6), pp. 158-167.
- De-Pauw, P., Taerve, L. and Desymyter, J. (1995), Concrete and Masonry Rubble as aggregates for Concrete, Something in between Normal and Lightweight Concrete, 2nd *International Symposium on Structural Lightweight Aggregate Concrete 2000*, Kristiansand, Norway, pp. 660–669.
- Department for Communities and Local Government, (2013), *Mineral extraction in Great Britain 2011*, Business Monitor PA1007, pp. 1-29.
- Department of Environment (DOE), (1988), *Concrete mix design*, UK.
- Dinh, H. H. (2009), Shear behaviour of steel fiber reinforced concrete beams without stirrup reinforcement, PhD Thesis, University of Michigan, USA.
- Dundar, C. and Kara, F. I. (2007), Three dimensional analysis of reinforced concrete frames with cracked beam and column elements, *Engineering Structures*, Vol. 29, pp. 2262-2273.
- El-Ariss, B. (2006), Shear mechanism in cracked concrete, *International Journal of Applied Mathematics and Mechanics*, Vol. 2(3), pp. 24-31.
- Elzanaty, A.H., Nilson, A.H, Slate, F.O., (1986), Shear Capacity of Reinforced Concrete Beams Using High-Strength Concrete, *ACI Structural Journal*, Vol. 83(2), pp. 290-296.
- Emiero, C. and Oyedepo, O. J. (2012), An Investigation on The Strength and Workability of Concrete Using Palm Kernel Shell and Palm Kernel Fibre as a Coarse Aggregate, *International Journal of Scientific & Engineering Research*, Vol. 3(4), pp. 1-5.
- EuroLightCon (1998), *Definitions and International Consensus Report, Economic Design and Construction with Lightweight Aggregate Concrete*.

- Fenwick, R.C and Fong, A. (1979), The Behaviour of Reinforced Concrete Beams Under Cyclic Loading, Bulletin of the New Zealand National Society for Earthquake Engineering, Vol. 12(3), pp. 158-167.
- Ferguson, P. M., Breen, J. E. and Jirsa, J.O. (1988), Reinforced concrete Fundamentals, John Wiley and Sons, NY, USA, pp.143-160.
- FIP manual (1983), Manual of Lightweight Aggregate Concrete, 2nd Edition, Surrey University Press.
- FIP Manual of Design and Technology (1977). Lightweight Aggregate Concrete. First publication, Great Britain.
- Fold, N. and Whitefield, L. (2012), Developing a Palm Oil Sector: The Experiences of Malaysia and Ghana Compared, DIIS Working Paper, pp. 43.
- Galloway, J. E. Jr. (1994), Grading, Shape, and Surface Properties ASTM Special Technical Publication No. 169C, Philadelphia, pp. 401-410.
- Gao, J., Sun, W. and Morino, K. (1997), Mechanical properties of steel fiber-reinforced, high strength, lightweight concrete, *Cement and Concrete Research*, Vol., 19(4), pp. 307-313.
- Ghaffar, A., Javed, A., Rehman, H., Kafeel, A. and Ilyas, M. (2010), Development of Shear Capacity Equations for Rectangular Reinforced Concrete Beams, *Pakistan Journal of Engineering & Applied Science*, vol. 6, pp. 1-8.
- Ghannoum, W. M. (1998), size effect on shear strength of reinforced concrete beams, MSc. Thesis, Department of Civil Engineering and Applied Mechanics, McGill University, Canada
- Glavind, M., Olsen, G.S. and Munch-Petersen, C., (1993), Packing Calculations and Concrete Mix Design, *Nordic Concrete Research*, Publication No. 13.
- Golterman, P., Johansen, V., and Palbfl, L. (1997), Packing of Aggregates: An Alternative Tool to Determine the Optimal Aggregate Mix, *Materials Journal of American Concrete Institute*, Vol. 94(5), pp 435.
- Graves, R.E. (2006), Grading, Shape, and Surface Texture, Significance of Tests and Properties of Concrete and Concrete-Making Materials, ASTM Special Technical Publication No. 169D, 337-345.
- Guduz, L. and Ugur, I. (2005), The effects of different fine and coarse pumice aggregate/cement ratios on the structural concrete properties without using any admixtures, *Cement and Concrete Research*, Vol. 35(9), pp.1859–1864.
- Haktanir, T. and Altun, F. (2002), Structural Lightweight Concrete with Pumice Aggregate of Erciyes Region, *Innovations and Development in Concrete Materials and Construction*, Dhir Hewlett Csetenyi.
- Halit, Y., (2008), The effect of silica fume and high-volume Class C fly ash on mechanical properties, chloride penetration and freeze–thaw resistance of self-compacting concrete, *Construction and Building Materials*, Vol. 22, pp. 456–462.
- Hamadi, Y. D. and Regan, P. E. (1980), Behaviour of normal and lightweight aggregate beams with shear cracks. *The Structural Engineer* 58B(4), pp. 71–79.
- Hanafy, M. M., Hatem, M. M. and Yehia, N. A. B. (2012), On the Contribution of Shear Reinforcement in Shear Strength of Shallow Wide Beams, *Life Science Journal*, Vol. 9(3), pp. 484-498.

- Hanna, E., Luke, K., Perraton, D. and Aitcin, P.C. (1989), Rheological Behavior of Portland Cement in the Presence of a Superplasticizer, Proceedings of the 3rd International Conference on Superplasticizers and Other Chemical Admixtures in Concrete, Malhotra, V. M. (Ed.), American Concrete Institute, pp. 171-188.
- Harimi, M., Hrimi, D., Kurian, V.J. and Nurmin, B. (2007), Evaluation of the thermal performance of metal roofing under tropical climatic performance of metal roofing under tropical climatic conditions, *Malaysian Construction Research Journal (MCRJ)*, Vol. 1(1), pp. 72-80.
- Hartmann TH, Kester DE, Davis FT (1993). Plant Propagation Principles and Practice, 5th edition, New Delhi pp. 105 - 210.
- Hassan, A. A. A., Hossain, K. M. A. and Lachemi, M. (2008), Behavior of full-scale self-consolidated concrete beams in shear, *Cement and Concrete Composites*, Vol. 30, pp. 588–596.
- Hawkins, N. M., Kuchma, D. A., Mast, R. F., Marsh, M. L. and Karl-Henz, R. (2005), Simplified Shear Design of structural concrete members, National Cooperative Highway Research Program (NCHRP), Report 549, pp. 1-49.
- He, X.G. and Kwan, A.K.J. (2001), Modeling dowel action of reinforcement bars for finite element analysis of concrete structures, *Computer and Structures*, 79, pp. 595-604.
- Higginson, G., Wallace, B. and Ore, E. L. (1963), Effect of maximum size of aggregate on compressive strength of mass concrete, Symposium on Mass Concrete, American Concrete Institute, Special Publication, No. 6, pp. 219-256.
- Hossain, K.M.A. (2003), Properties of volcanic pumiced based cement and lightweight concrete, *Cement and Concrete Research*, Vol. 24(78).
- Hossain, A. and Khandaker, M. (2004), Properties of volcanic pumice based cement and lightweight concrete, *Cement and Concrete Research*, Vol. 34(2), pp. 283–291.
- Hyo-Gyoung, K. and Filippou, F. C. (1990), Finite element analysis of reinforced concrete structures under monotonic loads, Structural Engineering, Mechanics and Materials, Department of Civil Engineering University of California, Berkeley, Report No. UCB/SEMM-90/14
- Jamkar, S.S. and Rao, C.B.K. (2004), Index of aggregate particle shape and texture of coarse aggregate as a parameter for concrete mix proportioning, *Cement and Concrete Research*, Vol. 34(11), pp. 2021-2027.
- Jo, B.W., Kim, C. H. Tae, G. and Park, J. B. (2007), Characteristics of cement mortar with nano SiO₂ particles, *Construction and Building Materials*, Vol. 21(6), pp. 1351-1355.
- Johnson, M. and Ramirez, J. A. (1989) Minimum shear reinforcement in beams with high strength concrete, *Structural Journal of American Concrete Institute*, Vol. 86(4), pp. 376-82.
- Juan, K. Y. (2011), Cracking Mode and Shear Strength of Lightweight Concrete Beams, PhD Theses, Department of Civil and Environmental Engineering, National University of Singapore.
- Jumaat, M. Z., Alengaram, U. J. and Mahmud, H. (2009), Shear strength of oil palm shell foamed concrete beams, *Materials and Design*, Vol., 30(6), pp. 2227–2236.
- Jung, S. and Kim, K. S. (2008), Knowledge-based prediction of shear strength of concrete beams without shear reinforcement, *Engineering Structures*, Vol. 30, pp. 1515–1525.

- Kan, A. and Demirbog, R. (2009), A novel material for lightweight concrete production, *Cement and concrete Composite*, Vol., 31, pp. 489-495.
- Kankam, C.K. (2000), Potential for using palm kernel shell as aggregates in Portland cement concrete. *In Proceedings of 25th Conference Our World in Concrete and Structure: 23 – 24 August, 2000*, Singapore.
- Karthik, O., Haejin, K. and Colin, L. (2007), Effect of Continuous (Well-Graded) Combined Aggregate Grading on Concrete Performance Phase A: Aggregate Voids Content (Packing Density), National Ready Mix Concrete Association (NRMCA), Project D340 Report, pp. 1-32
- Katz, A. (2003), Properties of concrete made with recycled aggregate from partially hydrated old concrete, *Cement and Concrete Research*, Vol. 33, pp. 703-711.
- Kayali, O. A. and Haque, M.N., (1999), Status of structural lightweight concrete in Australia as the new millenium dawns, *Concrete in Australia*, pp. 22 – 25.
- Kerali, A.G., (2001), Durability of Compressed and Cement-Stabilised Building Blocks, PhD Theses, University of Warwick, School of Engineering.
- Khaleel, O. R., Al-Mishhadani, S.A. and Razak, H. A. (2011), The Effect of Coarse Aggregate on Fresh and Hardened Properties of Self-Compacting Concrete (SCC), *Procedia Engineering*, Vol. 14, pp. 805–813.
- Kilic, A., Atis, C. D., Yasar, E. and Ozcan, F. (2009), High strength Lightweight concrete made with scoria aggregate containing mineral admixtures, *Cement and Concrete Research*, Vol. 32, pp. 1595-1599.
- Kim, J. K. and Park, Y. D. (1996), Prediction of Shear Strength of Reinforced Concrete Beams without Web Reinforcement, *ACI Materials Journal*, Technical paper, Title no. 93-M24.
- Kong, F.K. and Evans, R.H., (1998), *Reinforced and Prestressed Concrete*. 3rd Edition; Cambiridge: E & FN Spon.
- Kosmatka, H. S., Kerkhoff, B. and Panarese, W. C. (2003), *Design and Control of Concrete Mixtures*, EB001, 14th edition, Portland Cement Association, Skokie, Illinois, USA.
- Ksenija, J., Nikolic, D., Bojovic, D., Loncar, L., Romakov, Z. (2011), The estimation of compressive strength of Normal and recycled aggregate concrete, *Architecture and Civil Engineering*, Vol. 9(3), pp. 419-431.
- Lamond, J. F. and Pielert, J. H. (2006), Significance of Tests and Properties of Concrete and Concrete- Making Materials, American Society for Testing and Materials, Philadelphia, PA, 337-354.
- Legg, F.E. Jr., (1998), Aggregates, *Concrete Construction Handbook*, Dobrowolski, J. (Ed), McGraw-Hill, 4th ed.
- Lim, L. H. (2007), Structural Response of LWC Beams in Flexure, PhD Theses, Department of Civil Engineering, National University of Singapore.
- Lin, C.H., and Lee, F.S. (2003), Shear Behaviour of High Workability Concrete Beams, *ACI Structural Journal*, V. 100, N. 5, Sep.-Oct., pp. 599-608.
- Liu, X., (2005), Structural Lightweight Concrete with Pumice Aggregate, MSc. Thesis, National University of Singapore. Available at

<http://scholarbank.nus.edu.sg/bitstream/handle/10635/17014/Meng%20thesis%20submitted%20by%20Liu%20Xiaopeng%20HT026202E.pdf?sequence=1> [Date assessed 12th September, 2011].

- Lo, T.Y., Cui, H.Z. and Li, Z.G. (2004), Influence of aggregate pre-wetting and fly ash on mechanical properties of lightweight concrete, *Waste Management*, Vol. 24(4), pp. 3333-38.
- Lubell, A.S, Evan, C.B. and Michael, P.C. (2009), Shear reinforcement spacing in wide members, *ACI Structural Journal*, vol. 106, pp. 2–25.
- Lydon, F. W. (1982), *Concrete Mix Design*, 2nd edition, Applied Science Publishers.
- MacGregor, J. G., (1997), *Reinforced Concrete: Mechanics and Design*, Prentice-Hall Inc., Upper Saddle River, N.J.
- Maekawa, K. and Shawky, A. A. (1997), *Collapse Mechanism of Hanshin RC Bridge Piers*, EASEC-5, Australia
- Mahmud, H. Jumaat, M. Z. and Alengaram, U. J. (2009), Influence of sand/cement ratio on Mechanical properties of palm kernel shell concrete, *Journal of Applied Sciences*, Vol., 9(9), pp. 1764 – 1769.
- Mannan, M. A., Alexander, J., Ganapathy, C., Teo, D. C. L. (2006), Quality improvement of Oil Palm Shell (OPS) as coarse aggregate in lightweight concrete, *Building Environment*, Vol., 41(9), pp. 1239–1242.
- Mannan, M.A. and Ganapathy, C. (2004), Concrete from an agricultural waste oil palm shell (OPS), *Building Environment*, Vol., 39(4), 441-448.
- Mannan, M.A. and Ganapathy, C. (2002), Engineering properties of concrete with oil palm shell as coarse aggregate, *Construction and Building Materials*, Vol. 16(1), pp. 29-34.
- Mannan, M.A., Basri, H. B., Zain, M. F. M. and Islam, M. N. (2002), Effect of curing Conditions on the properties of OPS – concrete, *Building and Environment*, Vol., 37, pp. 1167-1171.
- Mannan, M. A. and Ganapathy, C. (2001), Mix design for oil palm shell concrete, *Cement and Concrete Research*, Vol. 31, pp. 1323–1325.
- Mansour, M.Y., Dicleli, M., Lee, J.Y. and Zhang, J. (2004), Predicting the shear strength of reinforced concrete beams using artificial neural networks, *Engineering Structures*, vol. 26, pp. 781–799.
- Mehta, P.K., and Monteiro, P.J.M. (2006), *Concrete: Microstructure, Properties, and Materials*. 3rd Edition, McGraw-Hill, Inc. New York, USA.
- Mehta, P. K. and Monteiro, P. J., (1993) *Concrete: Structure, Properties, and Materials*, 2nd ed., Prentice-Hall, Englewood Cliffs, N.J.
- Mehta, P.K. (1986), *Concrete: Structure, Properties, and Materials*, Prentice Hall, Englewood Cliffs.
- Mindess, S., Young, J. F. and Darwin, D. (2003), *Concrete*. 2nd ed. Pearson Education, Inc. New Jersey, USA.
- Mphonde, A. G., Frantz, G. C. (1984), Shear tests of high and low strength concrete beams without stirrups. *ACI Journal*, pp. 350–357.
- Muttoni, A. and Fernandez, M. R. (2008), *Shear Strength of Members without Transverse*

- Reinforcement as Function of Critical Shear crack width, *Structural Journal of American Concrete Institute*, Vol., 105(2), pp. 163-172.
- Nawy, E. G. (2008), *Concrete Construction Engineering Handbook*, 2nd Edition, CRC Press, USA.
- Nawy, E.G. (1996), *Reinforced concrete: a fundamental approach*. New Jersey: Prentice- Hall Inc., pp. 155–207.
- Ndoke, P. N. (2006), Performance of palm kernel shells as a partial replacement for coarse aggregate in asphalt concrete, *Leonardo Electronic Journal of Practices and Technologies*, Vol. 5(9), pp. 145-52.
- Neville, A. M. and Brooks, J. J. (2008), *Concrete Technology*, Pearson Education Asia Pte Ltd.
- Neville, A.M. (2006), *Concrete, Neville's Insights and Issues*, Thomas Telford Publishing, Thomas Telford Ltd, 1 Heron Quay, London, pp. 1-302.
- Neville, A.M. (1997), Aggregate bond and modulus of elasticity of concrete, *Material Journal of American Concrete Institute*, Vol. 94(1), pp. 71-74.
- Neville, A.M. (1981), *Properties of Concrete*, 3rd ed, Pitman, New York.
- Newman, J. B. (2005), Properties of structural lightweight aggregate concrete, *In Structural lightweight aggregate concrete*, 1st Edition, Clarke, J. L. (Ed.), Blackie Academic and Professional, pp. 10-23.
- Newman, J. and Choo, B. S. (2003), *Advanced concrete Technology-Constituent Materials*, Replika Press Pvt Ltd, India.
- Nguyen-Minh, L., Rovňák, M., Tran-Quoc, T. and Nguyenkim, K. (2011), Punching Shear Resistance of Steel Fiber Reinforced Concrete Flat Slabs, *Procedia Engineering*, vol. 14, pp. 1830–1837
- Novak, D., Bazant, Z. P. and Vitek, J. L. (2002), Experimental-analytical size-dependent prediction of modulus of rupture of concrete, *Non-Traditional Cement & Concrete*, Bilek, V. and Kersner, Z. (Eds), pp. 387-392.
- O'Flynn, M. L. (2000), Manufactured Sands from Hardrock Quarries: Environmental Solution or Dilemma for Southeast Queensland, *Australian Journal of Earth Sciences*, Vol. 47, pp. 65-73.
- Okafor, F. O. (1988), Palm kernel shell as a lightweight aggregate for concrete, *Cement and Concrete Research*, Vol. 18(6), pp. 901–910.
- Okpala, D. C. (1990), Palm kernel shell as a lightweight aggregate in concrete, *Building Environment*, Vol. 25(4), pp. 291–296.
- Okamura, H. and Maekawa, K. (1991), *Nonlinear Analysis and Constitutive Models of Reinforced Concrete*, University of Tokyo.
- Olanipekun, E.A., Olusola, K.O. and Ata, O. (2006), A comparative study of concrete properties using coconut shell and palm kernel shell as coarse aggregates, *Building Environment*, Vol. 41(3), pp. 297-301.
- Olutoge, F. A. (2010), Investigations on Sawdust and Palm Kernel Shells as Aggregate Replacement, *Asian Research Publishing Network (ARPN) Journal of Engineering and Applied Sciences*, Vol. 5(4), pp. 7-13.

- Omange, G. N. (2001), Palm kernel shells as road building materials, *Technical Transactions of the Nigerian Society of Engineers*, Vol. 36(1), pp. 17-25.
- Omar, W. (1998), The shear assessment of concrete beams with a honeycombed zone present in the high shear region, PhD Thesis, Faculty of Engineering, University of Birmingham, UK.
- Orchard, D.F. (1979), *Concrete Technology*, 4th Ed. Applied Science Publishers, London.
- Oreta, A. W. C. (2004), Simulating size effect on shear strength of RC beams without stirrups using neural networks, *Engineering Structures*, Vol. 26, pp.681-691.
- Owens, P. L. (1993), Lightweight aggregates for structural concrete, In *Structural Lightweight Aggregate Concrete*, Clarke, J. L (Ed.), Blackie Academic & Professional, Glasgow, London, pp. 1-9
- Ozu, H., Yamada, K., Yano, M. and Toriiminami, K. (2001), The fluidity relationship among concrete, mortar, and paste containing different kinds of cement, *In Proceedings of the Japan Concrete Institute*, Vol. 23(2), 283-288.
- Parghi, A., Modhera, C.D. and Shah, D.L. (2008), Micro mechanical crack and deformations study of SFRC deep beams, *33rd Conference on Our World in Concrete & structures*, 2527 August, 2008, CI-Premier PTE Ltd, Singapore.
- Poku, A. (2002), Small-scale palm oil processing in Africa, *FAO Agricultural services bulletin*, 148, ISSN 1010-1365.
- Polat, R., Demirboga, R., Karakoç, M.B. and Türkmen, I. (2010), The influence of lightweight aggregate on the physico-mechanical properties of concrete exposed to freeze–thaw cycles, *Cold Regional Science Technology*, Vol., 60, pp. 51-56.
- Popovics, S. (1992), *Concrete Materials Properties, Specifications and Testing*, 2nd Edition, Noyes Publications, New Jersey, USA.
- Punkki, J. and Gjörv, O.E. (1995), Effect of Water Absorption by Aggregate on Properties of High strength Lightweight Concrete, *CEB/FIP International Symposium on Structural Lightweight Aggregate Concrete*, Sandefjord, Norway, pp. 604-616.
- Punkki, J. and Gjörv, O. E. (1993), Water Absorption by High-strength Lightweight Aggregate, *Proceedings of the Symposium of Utilization of High Strength Concrete*, Lillehammer, Norway 20-23 June, pp. 713-721.
- Quiroga, P. N. and Fowler, W. D. (2004), The effects of aggregates characteristics on the performance of Portland cement concrete. International Center for Aggregates Research, University of Texas, Austin, USA.
- Rached, M., Moya, D. M. and Fowler, D.W. (2009), Utilizing Aggregates Characteristics to Minimize Cement Content in Portland Cement Concrete, *International Center for Aggregates Research (ICAR 401)*, University of Texas, Austin, USA.
- Ramazan, D. (2001), Effect of Expanded Perlite Aggregate and Mineral Admixture on the Compressive Strength of Low-Density Concretes, *Cement and Concrete Research*, Vol. 31, pp. 1627-1623.
- Ramirez, J.A. and Breen, J.E. (1991), Evaluation of a modified truss-model approach for beams in shear, *Structural Journal of American Concrete Institute*, Vol. 88(5), pp. 562-571.
- Rebeiz, K. S., Fente, J. and Frabizzio, M. (2000), New Shear Strength for Concrete Members Using Statistical and Interpolation Function Techniques". The 8th International Specialty Conference on Probabilistic Mechanics and Structural Reliability. PMC2000-279.

- Regan, P. E.; Kennedy-Reid, I. L.; Pullen, A. D.; and Smith, D. A., (2005), The Influence of Aggregate Type on the Shear Resistance of Reinforced Concrete, *The Structural Engineer*, V. 83(23), pp. 27-32.
- Ries, J. P., Speck, J. and Harmon, K. S. (2010), Lightweight Aggregate Optimizes the Sustainability of Concrete, *Concrete Sustainability Conference*, pp. 1-15.
- Robert, J. F. (2000), Behavior of Large-Scale Reinforced Concrete Beams with Minimum Shear Reinforcement, *Structural Journal of American Concrete Institute*, Vol. 97 (6), pp. 814-820.
- Rossignolo, J. A., Agnesini, M.V.C. and Morais, J. A. (2003), Properties of high-performance LWC for precast structures with Brazilian lightweight aggregates, *Cement & Concrete Composites*, Vol. 25, pp. 77-82.
- Roziere, E., Granger, S., Turcry, P. and Loukili, A. (2007), Influence of paste volume on shrinkage cracking and fracture properties of self-compacting concrete, *Cement and Concrete Composites*, Vol., 29(8), pp. 626-636.
- Sacramento, P. V. P., Ferreira, M. P., Oliveira, D. R. C. and Melo, G. S. S. A. (2012), Punching strength of reinforced concrete flat slabs without shear reinforcement, *Ibracon Structures and Materials Journal*, Vol. 5(5), pp. 659-691.
- Sagaseta, J. and Vollum, R. L. (2011), Influence of beam cross-section, loading arrangement and aggregate type on shear strength, *Magazine of Concrete Research*, Vol. 63(2), pp. 139-153
- Saha, P. (1999), Lightweight aggregates for advanced civil engineering, *Fly Ash Utilisation for Value added Products*, Chatterjee, B., Singh, K. K. & Goswami, N. G. (Eds.), NML, Jamshedpur, pp. 159-163.
- Sarfo-Ansah, J. (2010), Enhancing the Reactivity of Clay Pozzolona through Mechanical Activation, MPhil. Thesis, Department of Materials Engineering, KNUST, Kumasi, Ghana.
- Sarsam, K. F. and Al-Musawi, J. M S. (1992), Shear Design of High- and Normal Strength Concrete Beams with Web Reinforcement, *ACI Structural Journal*, 89(6), pp. 658-664.
- Shamsai, A., Rahmani, K., Peroti, S. and Rahemi, L. (2012), The Effect of Water-Cement Ratio in Compressive and Abrasion Strength of Nano Silica Concretes, *World Applied Sciences Journal*, Vol. 17(4), pp.540-545.
- Shafigh, P., Jumaat, M. Z., Mahmud, H. B. and Anjang, N. A. H. (2012), Lightweight concrete made from crushed oil palm shell: Tensile strength and effect of initial curing on compressive strength, *Construction and Building Materials*, Vol. 27, pp. 252-258.
- Shafigh, P., Mahmoud, H. M., Vahid, R. S. and Mohsen, K. (2011), An investigation of the flexural behavior of reinforced lightweight concrete beams, *International Journal of the Physical Sciences*, Vol., 6(10), pp. 2414-2421.
- Shafigh, P., Jumaat, Z. M., and Mahmud, H. (2010), Mix design and mechanical properties of oil palm shell lightweight aggregate concrete: A review, *International Journal of the Physical Sciences*, Vol. 5(14), pp. 2127-2134.
- Shanmugasundaram, S., Jayanthi, S., Sundararajan, R., Umarani, C. and Jagadeesan, K. (2010), Study on Utilization of Fly Ash Aggregates in Concrete, *Journal of Modern Applied Science*, Vol. 4(5), pp. 44-57.
- Shetty, M. S. (2005), *Concrete technology theory and practice*, India, S. Chand & Company Ltd., India.

- Shilstone, J. M. S., (1990), Concrete Mixture Optimization, *Concrete International: Design and Construction*, Vol. 12(6), pp. 33-39.
- Short, A, and W. Kinniburgh, (1978), *Lightweight Concrete*, 3rd ed. London: Applied Science.
- Slobe, A.T., Hendriks, M.A.N. and Rots, J.G. (2012), sequentially linear analysis of shear critical reinforced concrete beams without shear reinforcement, *Finite Elements in Analysis and Design*, 50, pp. 108–124.
- Smith, M.R. and Collis, L. (2001), Aggregates: Sand, gravel and crushed rock aggregates for purposes, Geological Society, London, Engineering Geology Special Publication, 17, pp. 199-220
- Song, J., Won-Hee, K., Kim, K. S. and Jung, S. (2010), Probabilistic shear strength models for reinforced concrete beams without shear reinforcement, *Structural Engineering and Mechanics*, Vol. 34(1), pp. 15-38.
- Subasi, S., (2009), The effects of using fly ash on high strength lightweight concrete produced with expanded with expanded clay aggregate, *Science Resource Essays*, Vol., 4(4), pp. 275-288.
- Sundram, K., Ravigadevi, S. and Yew-Ai, T. (2003), Palm fruit chemistry and nutrition, *Asia Pacific Journal of Clinical Nutrition*, Vol., 12(3), pp. 355-362.
- Swamy, R. N., Jones, R. and Chiam, A. T. P. (1993). "Influence of Steel Fibers on the Shear Resistance of Lightweight Concrete I- Beams." *ACI Structural Journal*, 90(1), 103-114.
- Swamy, R.N. and Lambert, G.H. (1981), Microstructure of Lytag Aggregate, *Journal of Cement Composite and Lightweight Concrete*, Vol 3(4), pg. 273-282.
- Teo, D.C.L., Mannan, M.A. and Kurian, V.J. (2010), Durability of lightweight OPS concrete under different curing conditions, *Materials and Structures*, Vol. 43, pp. 1-13.
- Teo, D.C.L., Mannan, M.A., Kurian, V.J. and Ganapathy, C. (2007), Lightweight concrete made from oil palm shell (OPS): Structural bond and durability properties, *Building and Environment*, Vol. 42(7), pp. 2614–2621.
- Teo, D.C.L., Mannan, M. A. and Kurian, J. V. (2006a), Flexural Behaviour of Reinforced Lightweight Concrete Beams Made with Oil Palm Shell (OPS), *Journal of Advanced Concrete Technology*, Vol. 4(3), pp. 1-10.
- Teo, D. C. L., Mannan, M. A. and Kurian, V. J. (2006b), Structural Concrete Using Oil Palm Shell (OPS) as Lightweight Aggregate, *Turkish Journal of Engineering and Environmental Science*, Vol. 30, pp. 1–7.
- Teoh, B. K., Mansur, M. A. and Wee, T. H. (2002), Behavior of High-Strength Concrete I-Beams with Low Shear Reinforcement, *Journal of American Concrete Institute*, Vol., 99(3), pp. 299-307.
- Topcu, I.B. (1997), Semi-lightweight concretes produced by volcanic slags, *Cement and Concrete Research*, Vol., 27, pp. 15– 21.
- Troxell, G.E., Davis, H. E. and Kelly, J.W. (1968), *Composition and properties of Concrete*, 2nd Ed. McGraw-Hill Book Company, New York, USA.
- Vecchio, J. F. and Collins, M. P. (1988), Predicting the response of reinforced concrete beams subjected to shear using modified compression field theory, *Structural Journal of American Concrete Institute*, no. 85-S27, pp. 258-267.

- Walraven, J.C. and Al-Zubi, N. (1995), Shear capacity of lightweight concrete beams with shear reinforcement. *Proceedings of Symposium on Lightweight Aggregate Concrete*, Sandefjord, Norway. Vol. 1, pp. 91–104.
- Waner, R.F., Rangan, B.V., Hall, A.S., and Faulkes, K.A. (1999), Concrete structures. 1st ed. South Melbourne: Addison Wesley Longman Australia Pty Ltd.
- Washa, G. W. (1998), Permeability and Absorption, Concrete Construction Handbook, McGraw-Hill, 4th ed., New York, USA.
- Waziri, B.S. Mohammed, A. and Bukar, A.G. (2011), Effect of water-cement ratio on the strength properties of quarry-sand concrete (QSC), *Continental Journal of Engineering Sciences*, Vol. 6(2), pp. 16-21.
- Wight, J. K. and MacGregor, J. G. (2012), Reinforced Concrete: Mechanics and Design, 6th Edition, Pearson Higher Education, 1 Lake Street, Upper Saddle River, NJ 07458.
- Woo, K. and White, R. N. (1991) Initiation of Shear Cracking in Reinforced Concrete Beams with No Web Reinforcement, *ACI Structural Journal*, V. 88(3), pp. 301-308.
- Xuan, H. V., Yann, M., Daudeville, L. and Buzaud, E. (2009), Effect of the water/cement ratio on concrete behavior under extreme loading, *International Journal for Numerical and Analytical Methods in Geo-mechanics*, Vol. 33, pp. 1867-1888.
- Yamada, K., Sugamata, T and Nakanishi, H. (2006), Fluidity performance evaluation of cement and superplasticizer, *Journal of Advanced Concrete Technology*, Vol. 4(2), pp. 241-249.
- Yaqub, M. and Bukhari, I. (2006), Effect of size of coarse aggregate on compressive strength of high strength concretes, *In Proceedings of 31st Conference on Our world in Concrete and Structures*, Singapore. Available online: <http://cipremier.com/100031052>
- Yasar, E., Atis, C. D., Kilic, A., and Gulsen, H. (2003), Strength properties of lightweight concrete made with basaltic pumice and fly ash, *Material Lett.*, Vol., 57, pp. 2267-2270.
- Yoon, Y., Cook, W.D. and Mitchell, D. (1996), Minimum Shear Reinforcement in Normal, Medium and High-Strength Concrete Beams, *Structural Journal of American Concrete Institute*, Vol. 93(5), pp. 576-584.
- Yap, W. T. (2012), Strut and Tie modelling of reinforced concrete short span beams, 1st Civil and Environmental Engineering Student Conference, 25-26 June, 2012, Imperial College, London
- Zakaria, M., Ueda, T., Zhimin, Wu. And Liang, M. (2009), Experimental Investigation on shear cracking behaviour in reinforced concrete beams with shear reinforcement, *Journal of Advanced Concrete Technology*, Vol. 7(1), pp. 79-96.
- Zami, M. S. and Lee, A. (2008), Using earth as a building material for sustainable low cost housing in Zimbabwe, *The Built & Human Environment Review*, Vol. 1, pp. 40-55.
- Zararis, P. D. (2003), Shear strength and minimum shear reinforcement of RC slender beams, *ACI Structural Journal*, 100, pp. 203-214.
- Zararis, P. D. and Papadakis, G. C. (2001), Diagonal Shear Failure and Size Effect in RC Beams Without Web Reinforcement *Journal of Structural Engineering*, pp. 733-742.
- Zayed, A.M., Brown, K. and Hanhan, A. (2004), Effect of Sulfur trioxide content on concrete structures using Florida materials, Florida Department of Transportation, Florida, USA.

Zhang, M. H. and Gjørsv, O. E. (1995), Properties of High-strength Lightweight Concrete, *CEB/FIP International Symposium on Structural Lightweight Aggregate Concrete*, Sandefjord, Norway, pp. 683-693.

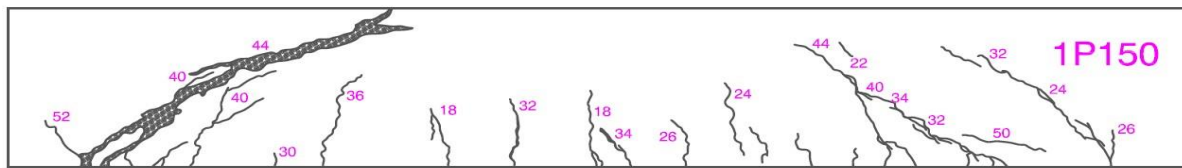
Zhang, M. H. and Gjørsv, O. E. (1991), Characteristics of Lightweight Aggregates for High-Strength Concrete, *ACI Materials Journal*, Vol. 88(2), pp. 150-158.

Zhang, M. H. and Gjørsv O.E. (1990). Microstructure of the interfacial zone between lightweight aggregate and cement paste, *Cement and Concrete Research*, Vol. 20(4), pp. 610-618.

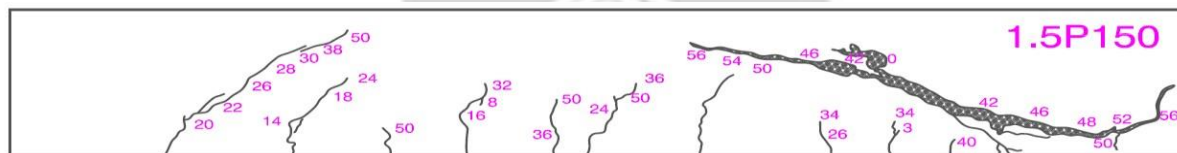
APPENDICES

APPENDIX A: FAILURE MODES AND CRACK PATTERNS OF TEST SPECIMENS

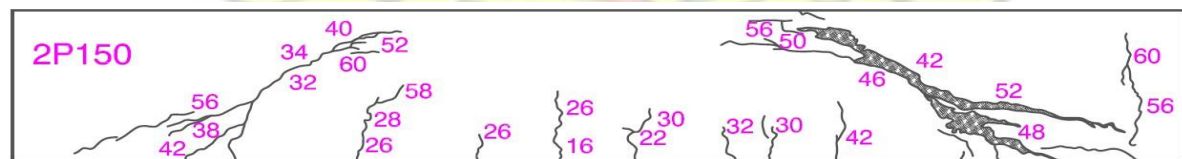
R-SERIES (*Note: The numbers are the loads (kN) at which the cracks appeared*)



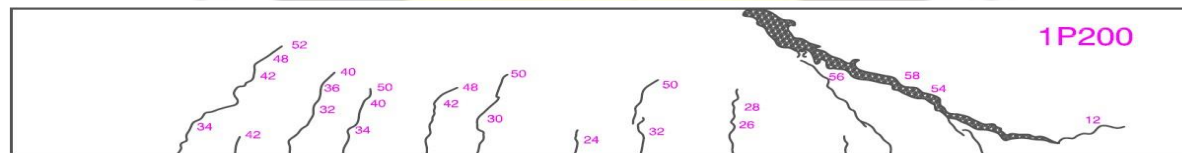
BEAM 1 ($P_u = 52$ kN)



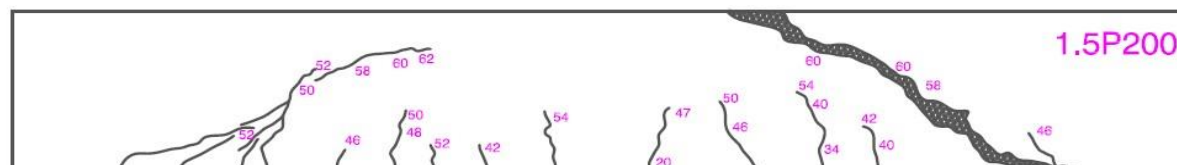
BEAM 2 ($P_u = 60$ kN)



BEAM 3 ($P_u = 62$ kN)



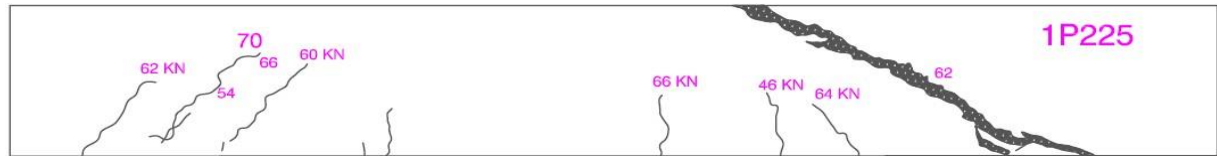
BEAM 4 ($P_u = 62$ kN)



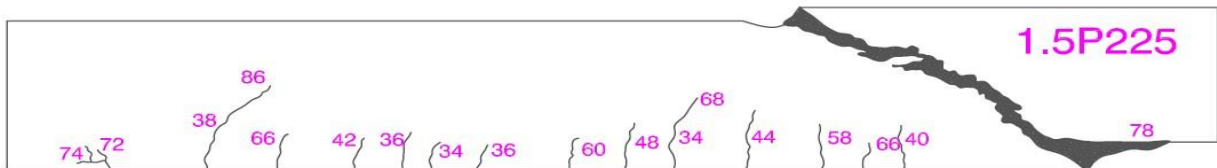
BEAM 5 ($P_u = 68$ kN)



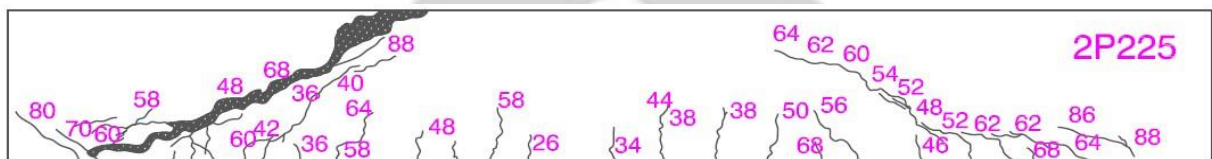
BEAM 6 ($P_u = 82 \text{ kN}$)



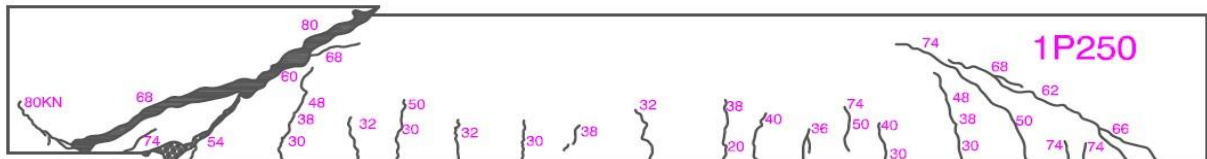
BEAM 7 ($P_u = 72 \text{ kN}$)



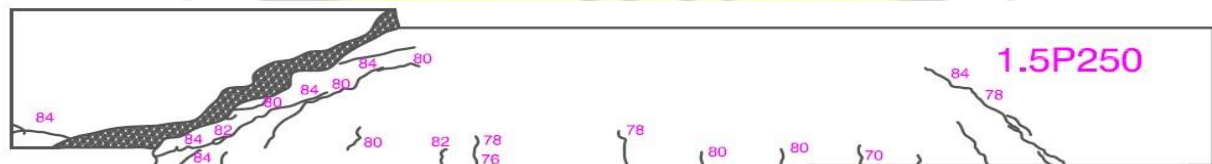
BEAM 8 ($P_u = 78 \text{ kN}$)



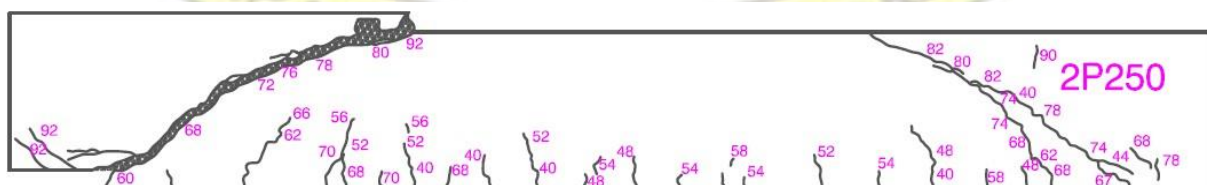
BEAM 9 ($P_u = 88 \text{ kN}$)



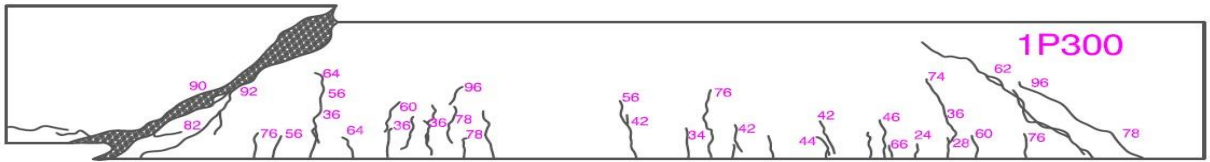
BEAM 10 ($P_u = 80 \text{ kN}$)



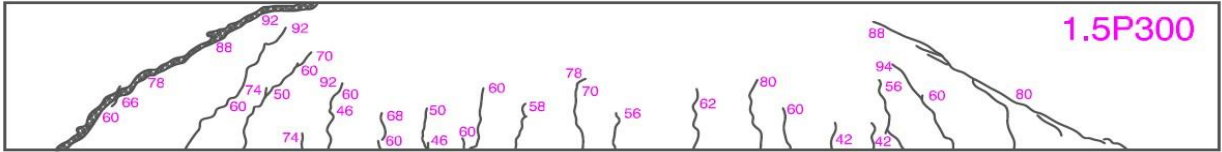
BEAM 11 ($P_u = 84 \text{ kN}$)



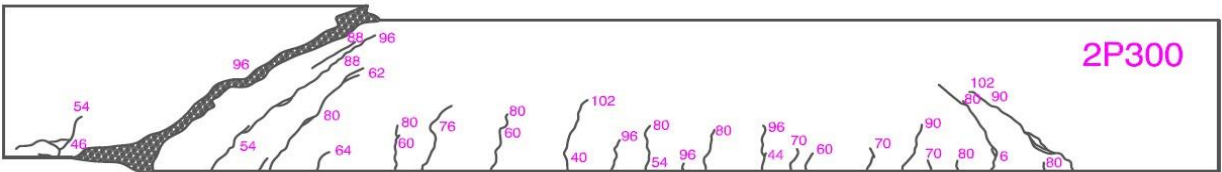
BEAM 12 ($P_u = 92 \text{ kN}$)



BEAM 13 ($P_u = 102$ kN)

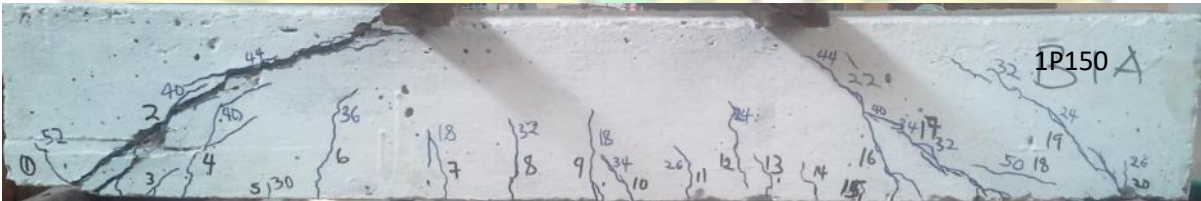


BEAM 14 ($P_u = 104$ kN)

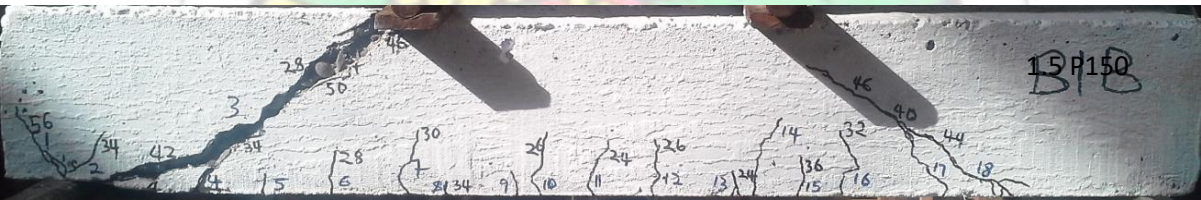


BEAM 15 ($P_u = 106$ kN)

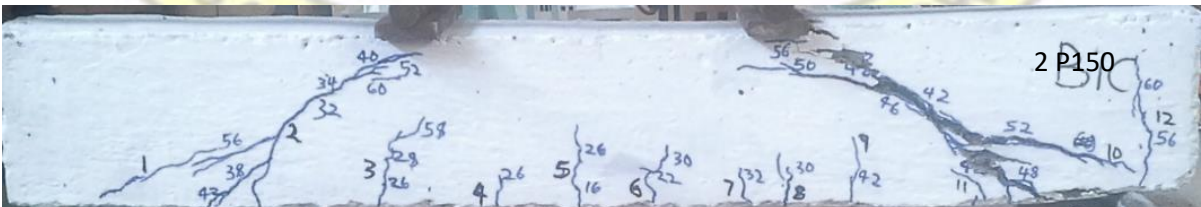
R-SERIES (*The numbers are the loads (kN) at which the cracks appeared*)



BEAM 1 ($P_u = 52$ kN)



BEAM 2 ($P_u = 60$ kN)



BEAM 3 ($P_u = 62$ kN)



BEAM 4 ($P_u = 62$ kN)



BEAM 5 ($P_u = 68$ kN)



BEAM 6 ($P_u = 82$ kN)



BEAM 7 ($P_u = 72$ kN)



BEAM 8 ($P_u = 78$ kN)



BEAM 9 ($P_u = 88$ kN)



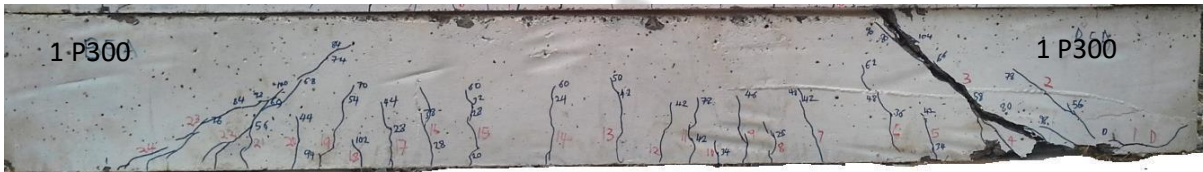
BEAM 10 ($P_u = 80$ kN)



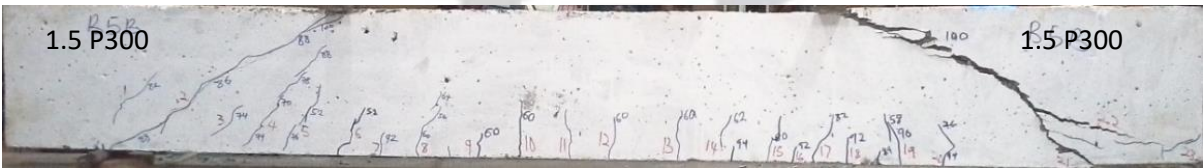
BEAM 11 ($P_u = 84$ kN)



BEAM 12 ($P_u = 92$ kN)



BEAM 13 ($P_u = 102$ kN)



BEAM 14 ($P_u = 104$ kN)



BEAM 15 ($P_u = 106$ kN)

S-SERIES – BEAMS WITH SHEAR REINCEMNT

(Note: The numbers are the loads (kN) at which the cracks appeared)



BEAM 1 ($P_u = 140$ kN)



BEAM 2 ($P_u = 132$ kN)



BEAM 3 ($P_u = 124$ kN)



BEAM 4 ($P_u = 132$ kN)



BEAM 5 ($P_u = 114$ kN)



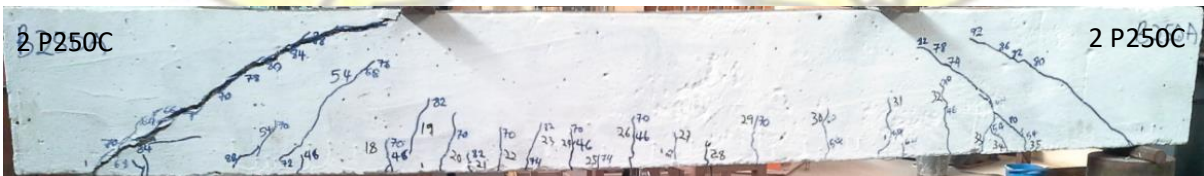
BEAM 6 ($P_u = 94$ kN)



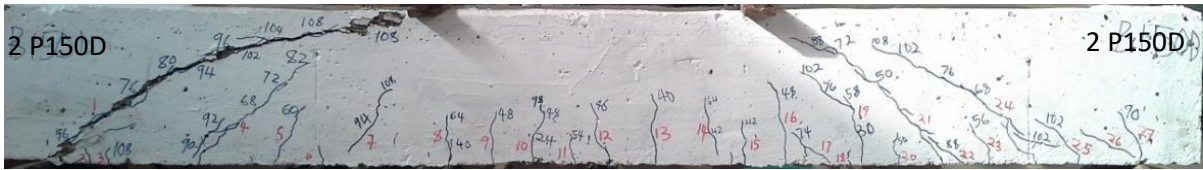
BEAM 7 ($P_u = 114$ kN)



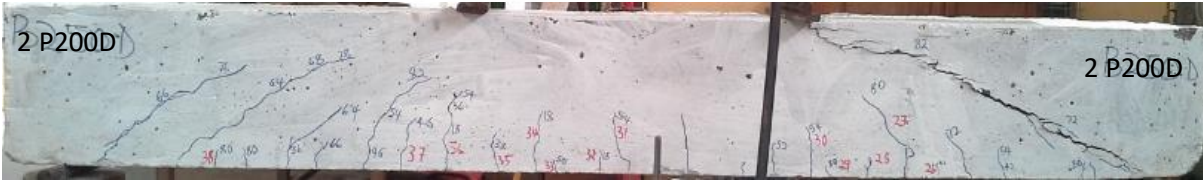
BEAM 8 ($P_u = 96$ kN)



BEAM 9 ($P_u = 86$ kN)



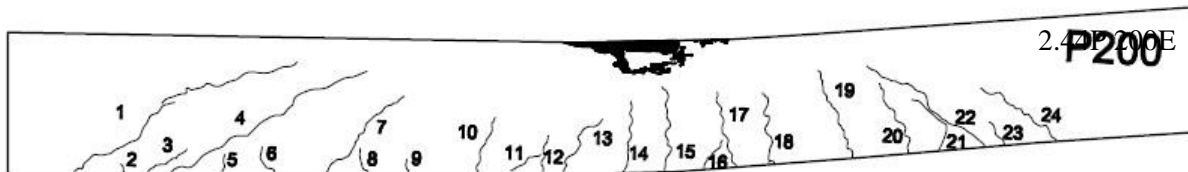
BEAM 10 ($P_u = 108$ kN)



BEAM 11 ($P_u = 96$ kN)



BEAM 12 ($P_u = 82$ kN)



BEAM 13 ($P_u = 72$ kN)

S-SERIES-CYCLICALLY LOADED BEAMS

(Note: The numbers are the loads (kN) at which the cracks appeared)

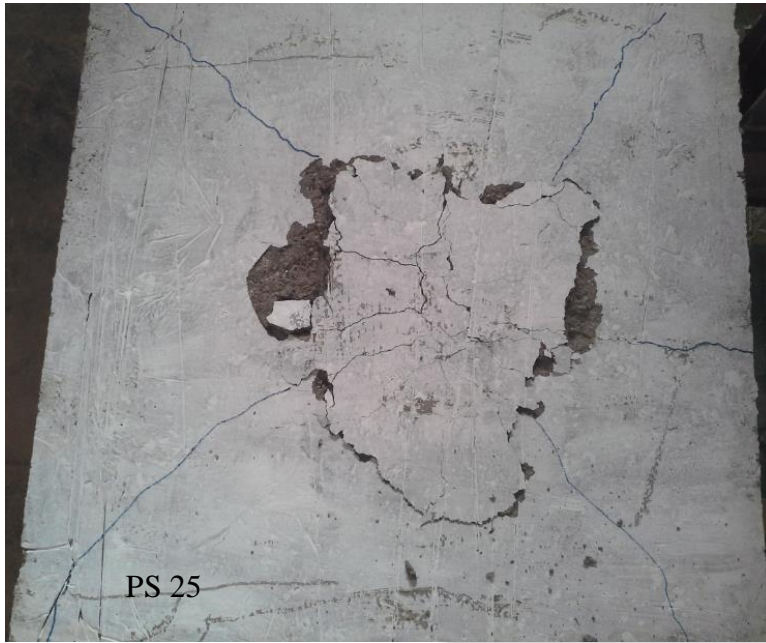


BEAM 1 ($P_u = 94$ kN)

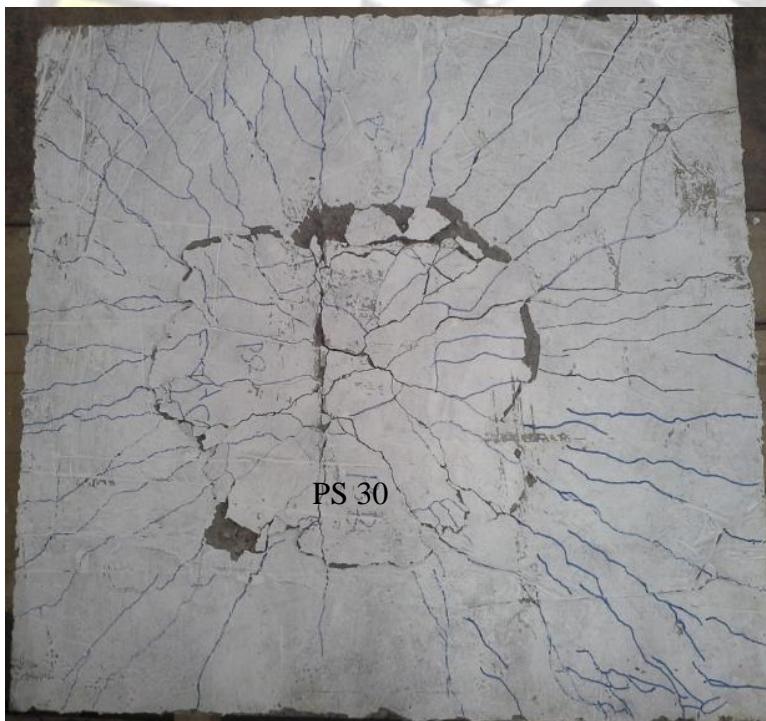


BEAM 2 ($P_u = 82$ kN)

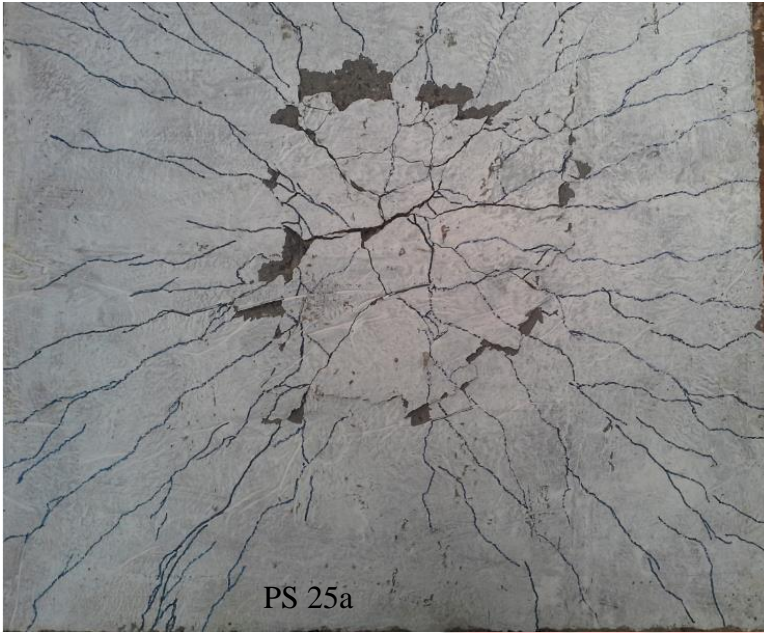
SLABS (*Markings denote the cracking patterns*)



SLAB 1 ($P_u = 60$ kN)



SLAB 2 ($P_u = 66$ kN)



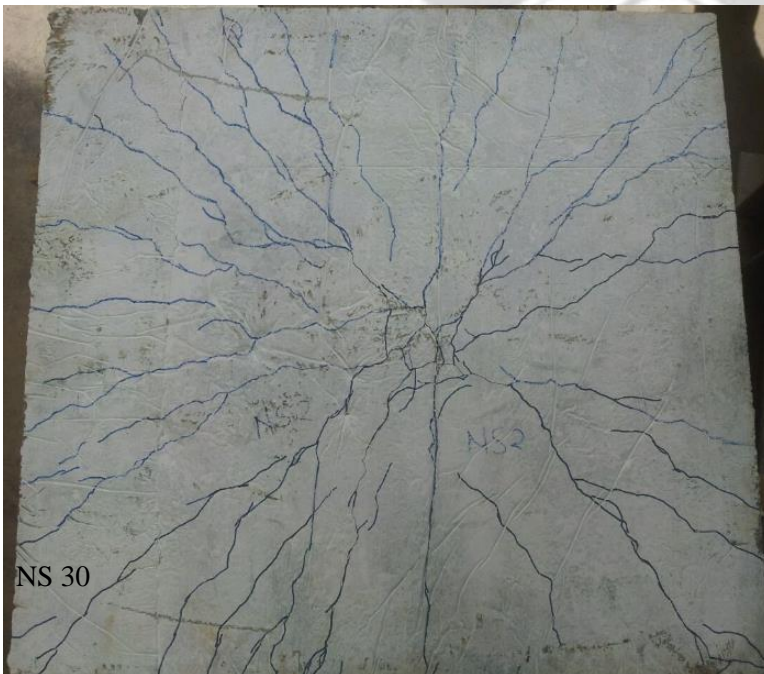
SLAB 3 ($P_u = 56$ kN)



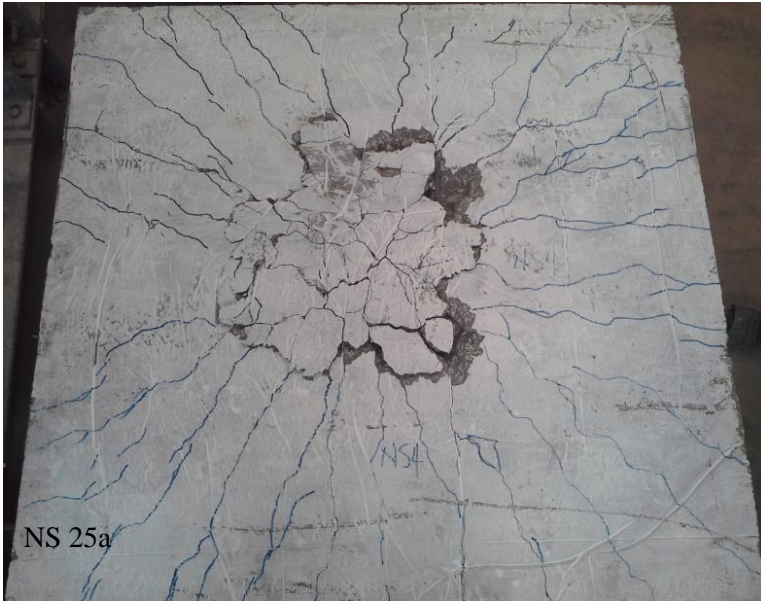
SLAB 4 ($P_u = 64$ kN)



SLAB 5 ($P_u = 64$ kN)



SLAB 6 ($P_u = 68$ kN)



SLAB 7 ($P_u = 68$ kN)



SLAB 8 ($P_u = 68$ kN)

APPENDIX B: DETERMINATION OF THEORETICAL LOADS

(Sections 3.4.5.4 of BS 8110-1 and 5.4 of BS 8110-2)

1.0 Estimation of Shear Failure Load Using BS 8110 Approach

Sample Calculation for Specimen for beam **P1** (Lightweight Concrete)

Density: 1890 Kg/m³

Weight of concrete = $1890 \times 9.81 = 18.54 \text{ kN/m}^3$

$b = 110 \text{ mm}$, $D = 225 \text{ mm}$ and $d = 225 - 20 - \frac{1}{2} \times 12 - 6 = 193 \text{ mm}$

The total shear resistance of the beam depends on the design concrete shear stress, V_c and the dowel action of the stirrups, V_s .

That is $V_{ult} = V_c + V_s$

From BS 8110-2, Table 5.3,

$\frac{100A_s}{bd} = 1.5968$, this implies that the actual values of V_c should be interpolated from Table 5.3

Interpolation

$$\begin{array}{r} 1.5 \text{ -----} 0.53 \\ 1.5968 \text{ -----} x \\ 2.0 \text{ -----} 0.59 \\ \hline \frac{1.5968 - 1.5}{2 - 1.5} = \frac{x - 0.53}{0.59 - 0.53} \\ \gggg 0.5x - 0.265 = 5.808 \times 10^{-3} \\ \gggg x = 0.542 \text{ N/mm}^2 \end{array}$$

The shear resistance due to concrete, $V_{conc} = V_c b d$

$V_{code} = 0.549 \times 110 \times 193 = 11506.7 \text{ N}$ or 11.51 kN

There is no shear resistance from the steel since there is no transverse shear, ie $V_s = 0$.

$P/2 = V_{ult}$; that is $P = 2 \times 11.51 = 23.01 \text{ kN}$

Thus the theoretical failure load in shear for beam P1 is **23.01kN**

2.0 Estimation of Failure Loads Using BS 8110-2 Approach

Sample Calculation for Specimen for beam **P0** (Lightweight Concrete)

Density: 1890 Kg/m³

Weight of concrete = $1890 \times 9.81 = 18.54kN/m^3$

$b = 110mm$, $D = 225mm$ and $d = 225 - 20 - \frac{1}{2} \times 12 - 6 = 193mm$

The total shear resistance of the beam depends on the design concrete shear stress, V_c

That is $V_{ult} = V_c$

The shear resistance due to concrete, $V_{code} = V_c b d$

$V_c = 0.542N/mm^2$

$V_{code} = 0.542 \times 110 \times 193 = 11506.7N$ or $11.51kN$

There is no shear resistance from the steel since there is no transverse shear, i.e. $V_s = 0$.

$P/2 = V_{ult}$; that is $P = 2 \times 11.51 = \mathbf{23.01kN}$